CENTRO INTERNACIONAL DE ESTUDOS
DE DOUTORAMENTO E AVANZADOS
DA USC (CIEDUS)

TESIS DE DOCTORADO

HUMAN iPSCs USE AS A PRECLINICAL MODEL FOR DRUG STUDY IN CEREBROVASCULAR DISEASES

Héctor Fernández Susavila

ESCUELA DE DOCTORADO INTERNACIONAL

PROGRAMA DE DOCTORADO EN MEDICINA MOLECULAR

SANTIAGO DE COMPOSTELA

2019

USC
UNIVERSIDADE
DE SANTIAGO
DE COMPOSTELA

DECLARACIÓN DEL AUTOR DE LA TESIS

"Human iPSCs use as a preclinical model for drug study in cerebrovascular diseases"

D. Héctor Fernández Susavila

Presento mi Tesis, siguiendo el procedimiento adecuado al Reglamento, y declaro que:

1) *La Tesis abarca los resultados de la elaboración de mi trabajo.*
2) *En su caso, en la Tesis se hace referencia a las colaboraciones que tuvo este trabajo.*
3) *La Tesis es la versión definitiva presentada para su defensa y coincide con la versión enviada en formato electrónico.*
4) *Confirmo que la Tesis no incurre en ningún tipo de plagio de otros autores ni de trabajos presentados por mí para la obtención de otros títulos.*

En Santiago de Compostela., 20 de Septiembre de 2019..

Fdo.

Héctor Fernández Susavila

AUTORIZACIÓN DE LOS DIRECTORES DE LA TESIS

"Human iPSCs use as a preclinical model for drug study in cerebrovascular diseases"

D. José Castillo Sánchez
D. Tomás Sobrino Moreiras
D. Francisco Campos Pérez

INFORMAN:

Que la presente Tesis, corresponde con el trabajo realizado por D. Héctor Fernández Susavila, bajo mi dirección, y autorizo su presentación, considerando que reúne los requisitos exigidos en el Reglamento de Estudios de Doctorado de la USC, y que como director de ésta no incurre en las causas de abstención establecidas en Ley 40/2015.

En Santiago de Compostela, 20 de Septiembre de 2019

Fdo. Director	Fdo. Director	Fdo. Director y tutor
José Castillo Sánchez	**Tomás Sobrino Moreiras**	**Francisco Campos Pérez**

Funding

This study has been partially supported by grants from Instituto de Salud Carlos III (P17/0054), Spanish Research Network on Cerebrovascular Diseases RETICS-INVICTUS (RD12/0014), the Ministry of Economy and Competitiveness of Spain (SAF2014-56336-R), Xunta de Galicia (Consellería de Educación, GRC2014/027), and the European Union program FEDER.

During the development of this Thesis, the doctoral candidate Héctor Fernández Susavila benefited from a predoctoral contract "IIS-Empresas en Ciencias y Tecnologías de la Salud (i-PFIS) from the Instituto de Salud Carlos III (IFI14/00031). This contract included funds for a 6 months stay.

During this period, Dr. Francisco Campos, Director of the Thesis, has been the beneficiary of the Miguel Servet contract, of the Instituto de Salud Carlos III (CP14/00154 and CPII19/00021). Dr. Tomás Sobrino, Director of the Thesis, has been the beneficiary of the Miguel Servet contract, of the Instituto de Salud Carlos III (CPII17/00027).

Conflict of interest

The author and the directors of the work agreed to present the results in this Thesis and declare no conflict of interests.

Publications

During the development of this Thesis the PhD student took part in the following publications:

- Vieites-Prado A, Iglesias-Rey R, **Fernández-Susavila H**, da Silva-Candal A, Rodríguez-Castro E, Gröhn OH, Wellmann S, Sobrino T, Castillo J, Campos F. Protective Effects and Magentic Resonance Imaging Temperature Mapping of Systemic and Focal Hypothermia in Cerebral Ischemia. Stroke. 2016 Sep; 47(9): 2386-96.
- **Fernández-Susavila H**, Iglesias-Rey R, Dopico-López A, Pérez-Mato M, Sobrino T, Castillo J, Campos F. Inclusion criteria update for the rat intraluminal model ischaemic model for preclinical studies. Dis Model Mech. 2017 Dec; 10(12): 1433-1438.
- **Fernández-Susavila H**, Rodríguez-Yáñez M, Dopico-López A, Arias S, Santamaría M, Ávila-Gómez P, Doval-García JM, Sobrino T, Iglesias-Rey R, Castillo J, Campos F. Heads and Tails of Natriuretic Peptides: Neuroprotective Role of Brain Natriuretic Peptide. J Am Heart Assoc. 2017 Dec; 6(12). pii: e007329.
- Pérez-Mato M, Iglesias-Rey R, Vieites-Prado A, Dopico-López A, Argibay B, **Fernández-Susavila H**, da Silva-Candal A, Pérez-Díaz A, Correa-Paz C, Günther A, Ávila-Gómez P, Isabel Loza M, Baumann A, Castillo J, Sobrino T, Campos F. Blood glutamate $EAAT_2$-cell grabbing therapy in cerebral ischemia. EBioMedicine. 2019 Jan; 39: 118-131.

From the development of this Thesis the following articles have been published:

- **Fernández-Susavila H**, Mora C, Aramburu-Núñez M, Quintas-Rey R, Arias S, Collado M, López-Arias E, Sobrino T, Castillo J, Dell'Era P, Campos F. Generation and characterization of the human iPSC line IDISi001-A isolated from blood cells of a CADASIL patient carrying a NOTCH3 mutation. Stem Cell Res. 2018 Apr; 28: 16-20.
- **Fernández-Susavila H**, Bugallo-Casal A, Castillo J, Campos F. Adult Stem Cells and Induced Pluripotent Stem Cells for Stroke Treatment. Front Neurol. 2019 Aug; 10(908).

Agradecimientos

A los que me conocen, a estas alturas sabrán bien que no soy un hombre dado a expresar muchas emociones. Sin embargo, aunque probablemente estas líneas de agradecimiento que siguen a continuación seguramente no estén a la altura de lo que realmente siento, querría expresar mi más profundo y sentido agradecimiento colectivo antes de empezar a todos los que apareceréis a continuación. Para mí, personalmente, es un orgullo haber conseguido un objetivo propuesto hace ya tantísimos años (más de los que llevo en el LINC), pero sin todas las personas que me habéis ayudado/guiado/apoyado a lo largo de este arduo y a veces descorazonador camino, no estaría ahora mismo escribiendo esta Tesis.

Si tengo que empezar por alguien es por el Dr. Francisco "no-me-cuentes-tu-vida" Campos. Fran, gracias por saber entenderme (no es tarea fácil) y haberme dado siempre el espacio y tiempo que necesitaba. Gracias por toda la confianza que has depositado en mí a lo largo de la Tesis incluso cuando las cosas no salían. Eso es algo que no se olvida. Para mí siempre será un orgullo presumir de director de Tesis. Y a pesar del sobrenombre, no engañas a nadie, algo siempre te preocupas.

Muchísimas gracias también al Profesor José Castillo, Pepe. Por ser el artífice del LINC, ese laboratorio que para muchos ha sido, es y será lugar de trabajo pero también una segunda familia y por abrirme sus puertas y dejarme formar parte de él. También por "meterme caña" en los seminarios cuando hacía falta para hacerme pasar del chico que presentaba "como si tuviera un caramelo en la boca" a… dejémoslo en algo entendible de momento. Bromas aparte, gracias por toda la ayuda prestada a lo largo de la Tesis y por tener siempre la puerta del despacho abierta para lo que queramos.

Al Dr. Tomás Sobrino, por el apoyo brindado desde el momento en que entré en el laboratorio (¡y por el correo diciéndome que era uno de los elegidos para entrar!), por tener siempre palabras de amabilidad hacia mí, y por la ayuda y los muchos consejos que nos brindas a todos cuando lo necesitamos.

A toda la planta de la unidad de ictus del Hospital Universitario de Santiago de Compostela, por haber estado siempre dispuestos a prestarme su opinión y ayuda como clínicos cuando era necesario. En especial a la Dra. Susana Arias por facilitarnos el contacto con los pacientes diagnosticados con CADASIL.

Y por supuesto, al resto del LINC, a mi segunda familia durante tantos años. Tanto a los que siguen como a los que ya no están, no quiero agradecer uno por uno a todos vosotros porque el ambiente único y que sería la envidia de cualquier otro lugar de trabajo es fruto de una combinación de generosidad, amabilidad y buen rollo por parte de todos. Todos, desde los más veteranos a los más nuevos, habéis participado en mayor o menor medida de esta Tesis, y por ello, aunque incluso hasta en las mejores familias pueden surgir rencillas pasajeras, todos tenéis mi más profundo y sincero agradecimiento. El recorrido diario hasta la puerta del LINC siempre ha sido mucho más ligero sabiendo que al otro lado de la puerta estabais vosotros.

Pero también hay vida más allá del LINC, y por ello también me gustaría agradecer a la Fundación Galega de Medicina Xenómica, concretamente a la investigadora Rita Quintas por ser el enlace y la persona que "sufrió" mis prisas por querer tener siempre los resultados de los análisis cuanto antes.

Of course, I would like to thanks Prof. Patrizia Dell'Era and the FRU laboratory at Brescia. Without you this Thesis would have not even started. I owe you 6 amazing and unforgettable months, where I fell in love with Italy and its people.

A todos los colegas de Los Tilos, con vosotros se podría decir que este viaje empezó ya hace 20 años (y más) y aquí seguimos. La Tesis es una amiga muy jodida y que me ha exigido muchos periodos de tiempo sin poder estar todo lo que quisiera con vosotros y es una espina que me llevaré siempre de esta Tesis. Pero aunque probablemente no vayáis a leer esto jamás (y menos mal) y si lo hacéis yo negaré ser el autor de estas líneas, gracias por no dejar que esos periodos de aislamiento debilitasen nuestra amistad. Gracias por hacerme olvidar las preocupaciones cada vez que nos juntamos y por estar tan rematadamente locos.

Y llega el momento de la familia, la de verdad, la que te hace ser lo que eres. Tanto a mi familia de Narón como a mi familia de Imo, os debo ser mi vía de escape. De todos vosotros he adquirido mi filosofía de vida, la que me ha hecho avanzar en los momentos más difíciles de ésta Tesis.

Y dentro de mi familia de Narón, hay dos personas que son uno de los principales motores de esta Tesis, mis abuelos. Abuelos, esta Tesis es vuestra, por hacerme el nieto más afortunado del mundo. A ti abuela por tener siempre un plato de filloas preparado cada vez que iba a tu casa, yo creo que incluso cuando no sabías que iba a ir, cosa de abuelas supongo. Con tu sencillez y bondad te ganaste mi corazón y devoción para siempre. Y a ti abuelo, para ti no hay palabras en el mundo que hagan justicia al cariño y respeto que tu nieto te profesa, aunque nunca tenga el valor de decirlo abiertamente. La mente almacena recuerdos, pero los míos contigo están grabados por siempre en el alma. Los días de pesca, las tardes de dominó y cartas, los chistes de abuelo… Si esta Tesis existe es en buena parte por querer que os sintáis orgulloso de vuestro nieto, porque él no podría estar más orgulloso de vosotros.

A mi hermano y a Silvia. Aparte de ser hermano y cuñada, a lo largo de estos 5 años habéis sido amigos, de lo mejor que se puede soñar con tener al lado. Gracias por hacerme reír cada vez que estoy con vosotros. Cada semana, la perspectiva de pasar la tarde del

viernes con vosotros me hacía olvidar las preocupaciones diarias del trabajo. Si todavía sigo cuerdo es en gran parte a vosotros (a pesar de ciertas canciones…).

A la razón de mi existencia, mis queridos padres. A mi madre por su amor incondicional, que aunque no se vea, siempre está ahí. De ti he aprendido lo que es la moderación, el respeto y sobre todo lo importante que es la unidad familiar. A mi padre…por ser mi padre, único e irrepetible, con tus peculiaridades que han hecho que de ti aprenda a ser yo mismo (lo que me lleva inquietante y peligrosamente a parecerme cada vez más a ti), a ser consciente del maravilloso mundo que nos rodea, a apreciar y saborear cada momento de la vida. En definitiva, gracias padres por todo. De vosotros dos juntos he aprendido que no hay recompensa sin esfuerzo y sobre todo he aprendido de vuestros valores. Si todo el mundo los siguiera, el mundo sería un lugar muchísimo mejor.

Y por último, de la razón de mi existencia pasamos a mi razón de vivir desde hace ya más de 6 años. A ti Elena, que mientras escribo estas líneas ya has querido hacerme el hombre más feliz del mundo aceptando casarte conmigo, para ti sí que no hay palabras que puedan expresar ni una mínima parte de hasta qué punto te estoy agradecido. Por aguantarme (esos inicios…), por la paciencia infinita que muestras en mis días malos (y en los excesivamente buenos), por ser tan feliz cuando eres feliz, por sacarme del pozo en el que caigo cuando las cosas no salen (bien por las buenas o bien por las malas). Gracias por ser mi constante en la vida, esa persona que sé que siempre estará ahí para lo bueno y para lo malo.

Y sobre todo, gracias por aparecer en mi vida.

"Always look on the bright side of life"

Monty Python (Life of Brian)

USC
UNIVERSIDADE
DE SANTIAGO
DE COMPOSTELA

Resumo

O ictus é a principal causa de mortalidade e morbilidade nos países desenvolvidos. Unha porcentaxe relevante de ictus débese a diversas patoloxías cerebrovasculares con trasfondo xenético. Mentres que o estudo destas enfermidades con modelos animais segue tendo moitas limitacións, co desenvolvemento da tecnoloxía da reprogramazón celular creouse un novo e prometedor enfoque para superar as barreiras existentes nos modelos animais.

Nesta Tese recóllese por primeira vez a creazón dun modelo celular *in vitro* para unha destas enfermidades cerebrovasculares, a enfermidade de CADASIL, con células do propio paciente xeradas a partires desta tecnoloxía de reprogramazón celular.

Resumen

El ictus es la principal causa de mortalidad y morbilidad en los países desarrollados. Un porcentaje relevante de ictus son debidos a diversas patologías cerebrovasculares con trasfondo genético. Mientras que el estudio de estas enfermedades en modelos animales está resultando ineficiente, con el desarrollo de la tecnología de la reprogramación celular se creó un nuevo y prometedor enfoque para superar las barreras existentes en los modelos animales.

En esta Tesis se recoge por primera vez la creación de un modelo celular *in vitro* para una de estas enfermedades cerebrovasculares, el CADASIL, con células del propio paciente generadas a partir de esta tecnología de reprogramación celular.

Abstract

Stroke is the main cause of mortality and morbidity in developed countries. A relevant percentage of strokes are due to several cerebrovascular pathologies with genetic background. While the study of these diseases in animal models is proving inefficient, with the development of the cellular reprogramming technology in 2006, a new approach appeared to overcome the existing barriers found in these models.

The current Thesis supposes the first time that an *in vitro* cellular model with the patient's own cells is achieved for the study of one of these cerebrovascular pathologies, CADASIL, thanks to the cellular reprogramming technology.

Index

USC
UNIVERSIDADE
DE SANTIAGO
DE COMPOSTELA

Resumen

El ictus es la principal causa de mortalidad y morbilidad en los países desarrollados, con un incremento en la incidencia debido al envejecimiento de la población. A pesar del considerable esfuerzo que ha llevado a un mejor entendimiento de esta patología, la traslacionalidad de este conocimiento, en forma de terapias efectivas, solamente ha resultado de momento en el tratamiento con activador del plasminógeno tisular o rtPA, el cual presenta una ventana de administración limitada. Aunque los principales factores de riesgo en la enfermedad cerebrovascular son ambientales, existen factores genéticos que son causa única de la aparición de estas patologías. Hasta la fecha, la experimentación con modelos animales (principalmente ratas y ratones) modificados genéticamente han permitido mimetizar estas alteraciones cerebrovasculares de forma satisfactoria y avanzar de forma significativa en el conocimiento de los mecanismos asociados. Sin embargo, su utilidad para traducir estos conocimientos al desarrollo de estrategias protectoras no ha tenido, por el momento, resultados en los pacientes.

En los últimos años, el desarrollo de las células pluripotentes inducidas humanas ha surgido como una técnica novedosa que permite generar células humanas afectadas por una enfermedad genética, con las que posteriormente poder estudiar la enfermedad e incluso buscar nuevas formas terapéuticas. Ésta técnica es conocida como "disease-in-a-dish" y consiste en extraer una muestra de células somáticas de un paciente con una determinada enfermedad para reprogramarlas a

células pluripotentes inducidas humanas y de ahí diferenciarlas al tipo celular de interés para poder realizar los estudios que sean requeridos y/o un screening de fármacos directamente sobre una línea celular humana. En el campo de las patologías cerebrovasculares, la arteriopatía cerebral autosómica dominante con infartos subcorticales y leucoencefalopatía (CADASIL) constituye una enfermedad cuyo abordaje mediante esta técnica resulta muy prometedor.

La enfermedad de CADASIL se engloba dentro de las enfermedades de pequeño vaso, tratándose de la forma más compleja dentro de dichas enfermedades. Esta enfermedad presenta una degeneración de las células musculares lisas vasculares de la túnica media, estrechamiento del lumen y engrosamiento de las paredes de los vasos pequeños, lo que lleva a una reducción del flujo sanguíneo y afectando de forma significativa y principalmente al tejido cerebral en forma de cambios de la sustancia blanca, microsangrados, aparición de espacios perivasculares dilatados y atrofia cortical y subcortical. En consecuencia, los pacientes con CADASIL desarrollan leucoencefalopatías, migrañas con aura, ataques isquémicos recurrentes, demencia y discapacidad motora como principales síntomas. Se trata además de una enfermedad autosómica dominante, lo que implica un 50% de probabilidades de ser transmitida a la descendencia. Actualmente no existe tratamiento alguno para esta enfermedad más allá de tratamientos paliativos, y la esperanza de vida para los pacientes se sitúa en torno a los 60-65 años.

A nivel etiopatológico, la enfermedad de CADASIL se debe a una mutación en alguno de los exones que codifican para el dominio

extracelular de la proteína NOTCH3. Esta mutación siempre da lugar a una pérdida o ganancia de un residuo de cisteína en alguna de las repeticiones de factores de crecimiento epidérmicos de los que se compone este dominio extracelular. Esta mutación provoca que el residuo extra o de menos de cisteína de lugar a un mal plegamiento de la proteína, lo que conlleva a que cuando alguno de los ligandos interaccione con el dominio extracelular de NOTCH3, éste se quede acumulado en la membrana celular formando depósitos de material osmiofílico granular que llevarían en última instancia al engrosamiento y alteración de la actividad de las células musculares lisas vasculares.

Para el estudio del CADASIL se han empleado principalmente modelos knockout y con diferentes mutaciones para *Notch3* en ratón. A pesar de su valor como herramienta de estudio para esta enfermedad, hoy en día existe una ausencia de estudios más traslacionales y centrados en el desarrollo de tratamientos potenciales para esta enfermedad. A este respecto, los modelos animales suponen una barrera filogenética donde los potenciales fármacos desarrollados fallan. Por ello, la tecnología de reprogramación celular a células pluripotentes inducidas humanas aparece como una solución prometedora a este problema. El modelaje de una enfermedad bien definida y monogenética como el CADASIL mediante la reprogramación de células somáticas a partir de pacientes con CADASIL y su posterior diferenciación a los tipos celulares afectados [las células musculares lisas vasculares y posiblemente también células endoteliales vasculares, aunque su implicación todavía no haya sido demostrada] puede suponer una plataforma *in vitro* adecuada para el estudio de esta enfermedad y el ensayo con fármacos potenciales ya que la barrera filogenética quedaría superada. Además, el desarrollo de

esta plataforma permitiría abrir nuevas vías de estudio a otras enfermedades neurovasculares con afectación genética.

Por ello en este proyecto se propuso el desarrollo de la técnica de reprogramación celular con el fin de conseguir los tipos celulares envueltos en la enfermedad de CADASIL. Así, el conseguir estos tipos celulares a partir de células somáticas del propio paciente supondría un salto cualitativo a la hora de poder acercarnos al desarrollo de un fármaco que realmente ejerciera funciones neuroprotectoras.

Como objetivo principal de esta Tesis, se propuso desarrollar por primera vez la técnica de reprogramación celular en nuestro laboratorio, con el fin de poder aplicarla al estudio del CADASIL y generar un modelo *in vitro* humano de CADASIL que permitiera el estudio, entre otros, de la acumulación patogénica del dominio extracelular de NOTCH3 en las células musculares vasculares.

Los objetivos principales de la Tesis se resumen a continuación:

1) La generación y caracterización de una línea humana de células pluripotentes inducidas a partir de células mononucleares de sangre periférica de un paciente con una mutación asociada a la enfermedad de CADASIL previamente diagnosticada.

2) La obtención y caracterización de células musculares lisas de vasculatura y células endoteliales vasculares derivadas a partir de la línea generada de células pluripotentes inducidas humanas de un

paciente con CADASIL mediante la puesta a punto e implementación de protocolos de diferenciación pre-existentes.

3) El estudio de los niveles del dominio extracelular e intracelular de NOTCH3 así como sus patrones de expresión tanto para las células musculares lisas de vasculatura como para las células endoteliales vasculares derivadas de la línea de células pluripotentes inducidas humanas de uno de los pacientes con CADASIL.

Para alcanzar éstos objetivos se obtuvieron muestras de sangre periférica procedentes de dos pacientes previamente diagnosticados con una mutación asociada a la enfermedad de CADASIL. Previa a la extracción, a los pacientes se les presentó un documento de consentimiento informado con todos los detalles concernientes a la investigación para que lo leyeran, hicieran todas las preguntas sobre el estudio y firmasen en caso de estar de acuerdo.

La reprogramación a células pluripotentes inducidas humanas se realizó concretamente a partir de células mononucleares de sangre periférica. Para ello, las células mononucleares de sangre periférica se extrajeron mediante una solución de Ficoll-Hypaque y su posterior centrifugación. Para el cultivo de las células mononucleares de sangre periférica, éstas se sembraron en 3 pocillos de una placa de 12 pocillos, con $5x10^6$ células en cada uno. Se cultivaron las células mononucleares de sangre periférica durante 4 días en un medio compuesto por StemPro-34 SFM más una combinación específica de citoquinas recombinantes humanas (Flt3L, SCF, IL-3 e IL-6).

Para la generación de células pluripotentes inducidas humanas a partir de células mononucleares de sangre periférica se empleó un protocolo de reprogramación de células mononucleares de sangre periférica con el CytoTuneTM -iPS Reprogramming Kit, el cual emplea la utilización de virus Sendai, que son virus no integrativos y que se replica en el citoplasma de la célula sin entrar al núcleo . El kit se compone de tres vectores virales diferentes: un vector policistrónico que contiene *Klf4-Oct3/4-Sox2* (KOS), otro vector que contiene *c-Myc* y otro vector que contiene más *Klf4*.

Para la transfección, se utilizaron dos muestras con un total de $3x10^5$ de células mononucleares de sangre periférica cada una. Uno de los tubos se utilizó para la reprogramación mientras que el otro se sirvió como control positivo una vez infectado. Para la infección se siguió la multiplicidad de infección (MOI) sugerida por el fabricante de los vectores para cada uno de ellos (MOI vector con *Klf4* + *Sox2* + *Oct3/4* = 5; MOI vector con *c-Myc* = 5; MOI vector con *Klf4* = 3).

Una vez realizada la infección vírica se procedió a la selección positiva de las colonias emergentes. Durante la primera semana después de la infección viral, se realizó una transición suave a lo largo de los días en la cual se pasó del medio de cultivo propio de células mononucleares de sangre periférica con el kit de citoquinas al medio propio de las células pluripotentes inducidas humanas. Una vez comenzaron a aparecer las colonias emergentes, la selección positiva consistió en el aspirado y resembrado de las regiones de las colonias emergentes que presentaban las características morfológicas propias de células pluripotentes

inducidas. Éste proceso de selección positiva se extendió hasta el pase número 4 para cada clon generado. A partir del pase 4, cada clon se empezó a manejar según las guías básicas de manejo y manipulación de células pluripotentes inducidas.

Para el cultivo de células pluripotentes inducidas humanas se utilizó siempre el medio comercial específico mTeSR1. Al cultivo de células pluripotentes inducidas humanas se le cambió el medio todos los días, proceso que incluyó la eliminación mecánica e individual de cada colonia en proceso de diferenciación para que no desestabilizara al resto de colonias de cada placa. Este proceso de eliminación se realizó siempre en el medio comercial DMEM-F12. El proceso de expansión celular para las células pluripotentes inducidas humanas consistió en el levantamiento mecánico (cell lifter) y/o enzimático (dispasa) de las colonias cortadas en "clusters" para su redistribución en varias placas Petri de 35 mm^2. El proceso de congelado y almacenaje de las células pluripotentes inducidas humanas se realizó siempre con el medio de congelación comercial BAMBANKER.

El proceso de caracterización de las diferentes líneas de células pluripotentes inducidas humanas obtenidas a lo largo de la Tesis implicó una amplia batería de pruebas exigidas por la comunidad internacional para el registro oficial de una nueva línea de células pluripotentes inducidas humanas.

La primera prueba para determinar que las colonias obtenidas presentaban capacidad pluripotente consistió en una tinción de diversos

clones con fosfatasa alcalina. La tinción se aplicó directamente sobre la placa Petri con las colonias a analizar. Después de lavados previos, un total de 3 µL de fosfatasa alcalina se diluyeron en la placa Petri y se dejó incubar durante media hora a temperatura ambiente antes de llevar la muestra a un microscopio de fluorescencia invertido y observar la placa. Se comprobó satisfactoriamente que los diferentes clones que fueron sujetos a un análisis por fosfatasa alcalina eran positivos para este enzima, lo que sugería una primera demostración de la existencia de un estado de pluripotencia. Al tratarse de una enzima relacionada con niveles de pluripotencia, este test es una buena primera prueba para establecer la posibilidad de que efectivamente una colonia esté constituida por células pluripotentes inducidas humanas.

La siguiente prueba para caracterizar las nuevas líneas de células pluripotentes inducidas humanas consistió en el análisis por inmunofluorescencia para una serie de marcadores relacionados con pluripotencia. Dichos marcadores eran tanto nucleares (OCT4, SOX2, NANOG) como de membrana (TRA-1-60 y SSEA4). El marcaje fue positivo para todos los marcadores y en ambas líneas de células pluripotentes inducidas humanas.

Otro análisis molecular y crítico en la demostración de que las nuevas líneas celulares eran efectivamente células pluripotentes inducidas humanas fue la formación de cuerpos embrionarios. Para ello se indujo su formación a partir de "clusters" celulares mediante la utilización de un medio rico en nutrientes en placas no adherentes y al que se le añadía *rock inhibitor* para favorecer las uniones intercelulares. Una vez

formados los cuerpos embrionarios, había que demostrar que éstos eran capaces de diferenciarse en tipos celulares de las tres diferentes capas germinales embrionarias para demostrar su capacidad pluripotente. Para ello se sembraron cuerpos embrionarios en placas de adherencia y en un medio de cultivo rico en nutrientes durante 14 días. Pasados los 14 días, se sometieron a los cuerpos embrionarios a análisis por inmunofluorescencia de diversos marcadores específicos para las tres capas germinales. Aunque fue imposible obtener un triple marcaje positivo para un solo cuerpo embrionario, sí se pudo demostrar la presencia de tipos celulares procedentes de las tres capas germinales de forma individual.

A mayores, periódicamente, se fueron proporcionando muestras de las dos líneas de células pluripotentes inducidas humanas generadas a un laboratorio externo para analizar una posible contaminación por *Mycoplasma.* Además, cada día se observaron todos los cultivos celulares uno por uno en busca de posibles contaminaciones por bacterias u hongos. Brevemente, durante un momento concreto de la Tesis ocurrió una contaminación por *Mycoplasma* que por desgracia provocó la pérdida de la segunda línea de células pluripotentes inducidas humanas generada. Esta segunda línea pudo ser caracterizada pero los procesos de diferenciación a células musculares lisas vasculares y células endoteliales vasculares así como el análisis de los dominios de NOTCH3 sólo pudieron ser llevados a cabo a partir de la primera línea de células pluripotentes inducidas humanas generada.

También se realizaron diferentes pruebas y análisis genéticos para la correcta caracterización de las nuevas líneas de células pluripotentes inducidas humanas. Se midió la expresión génica de algunos genes relacionados con pluripotencia. Estos genes fueron *SOX2* y *OCT4*. Para ello, primero se extrajo el RNA de diferentes clones procedentes de las dos líneas de células pluripotentes inducidas humanas generadas. Una vez realizada la extracción, se realizaron retrotranscripciones para generar el cDNA necesario a partir del cual se llevaron a cabo diversas PCRs en tiempo real para analizar dichos genes. Los resultados obtenidos para cada gen se relativizaron en base a los niveles de expresión de *GAPDH*. Además, los resultados obtenidos para cada clon se relativizaron también en comparación a los niveles de expresión de cada gen en una línea control negativa (fibroblastos humanos en este caso). Para ambas líneas de células pluripotentes inducidas humanas, se pudo observar una expresión de estos genes relacionados con pluripotencia. También se realizaron análisis de cariotipado para las dos líneas de células pluripotentes inducidas humanas generadas, con el fin de determinar si las células mostraban algún tipo de alteración cromosómica, siendo los resultados negativos. Por otra parte, al tratarse de una línea celular generada por primera vez y portadora de una mutación, se llevó a cabo la secuenciación del segmento donde se diagnosticó inicialmente la mutación en los pacientes para todos los tipos celulares obtenidos a partir de las células mononucleares de sangre periférica originales (es decir, las células pluripotentes inducidas humanas y las células musculares lisas vasculares y células endoteliales vasculares derivadas de estas), con el fin de probar que la mutación no hubiera sido eliminada. Por último, también se realizaron análisis de una combinación de *short-tandem repeats* para todos los tipos celulares

obtenidos a partir de cada muestra de células mononucleares de sangre periférica.

Una vez caracterizadas por completo y demostrado que las líneas celulares obtenidas eran efectivamente líneas de células pluripotentes inducidas humanas portadoras de una mutación asociada a la enfermedad de CADASIL se procedió al registro de la nueva línea en diversas instituciones nacionales ("Banco Nacional de Líneas Celulares del Instituto de Salud Carlos III") e internacionales (Human Pluripotent Stem Cell Registry). Dicha línea recibió el nombre oficial IDISi001-A, mientras que la línea obtenida a partir de la segunda reprogramación, al no tener que ser registrada, recibió el nombre no oficial de CAD02.

El siguiente paso consistió en el desarrollo y optimización de los protocolos experimentales para la diferenciación de células pluripotentes inducidas humanas en células musculares lisas vasculares y células endoteliales vasculares así como su posterior caracterización. Para la diferenciación a células musculares lisas vasculares se realizó siguiendo un protocolo optimizado y adaptado de un artículo publicado en la revista *Biochemistry Journal* en Enero de 2015 (Dash BC et al. *Biochem J,* 2015). Básicamente, el proceso consistió en el corte de las colonias de hiPSCs en pequeños "clusters" (10-20 células/cluster) de forma que la suspensión final fuese prácticamente monocelular. Ésta suspensión se repartió en diversos pocillos a diferentes densidades para encontrar la correcta combinación a la cual las células eran capaces de crecer y diferenciarse. Las células se sembraron y cultivaron durante los primeros 10-14 días en un medio de diferenciación específico. Una vez

alcanzada la confluencia, las células se expandían 1:2 y se cultivaban con el mismo medio pero añadiendo dos factores de crecimiento (PDGF-BB y TGF-β). Además, el primer día de diferenciación se añadió a los cultivos *rock inhibitor* para favorecer la supervivencia celular. A partir de la expansión, cada cultivo era mantenido hasta el momento deseado para la realización de diversas pruebas y experimentos (caracterización de la línea, extracción de proteína, extracción de RNA).

La caracterización de la línea celular obtenida así como de su control celular, que consistió en una línea de células musculares lisas aórticas humanas consistió en el análisis por inmunofluorescencia de diversos marcadores específicos para célula muscular (vimentina, desmina y α-SMC-actina) así como en el análisis de la capacidad contráctil de las células mediante la adición de carbachol a 10 µmol/L.

Para la diferenciación a célula endotelial vascular se siguió un protocolo publicado en la revista *Stem Cells Journal* en Abril de 2017 (Harding A et al. *Stem Cell*, 2017). Brevemente, las hiPSCs en estado de confluencia se cortaron para formar "clusters" de tamaño normal. Éstos "clusters" se sembraron sobre sobre Petris de 35mm^2 recubiertas con Matrigel™ con un medio de cultivo específico (STEMdiff™ APEL™2-LI) y suplementadas con FGF2. Al día siguiente se cambió el FGF2 y se sustituyó por CHIR99012. Dos días después, se sustituyó CHIR99012 por una combinación de FGF2, BMP4 y VEGF. Finalmente, a los dos días, se cambió el medio STEMdiff™ APEL™2-LI por un medio de cultivo comercial (EC Growth Medium MV2) y se añadió al cultivo más VEGF. A

partir de ahí, las células se cultivaron solamente con el medio comercial, sin necesidad de añadir más factores de crecimiento ningún día más.

La caracterización de la línea celular obtenida así como de su control celular (células endoteliales aórticas humanas) consistió en el análisis por inmunofluorescencia de diversos marcadores específicos para célula endotelial (CD34 y von Willebrand factor) así como en el análisis de la capacidad de formación de vasos mediante el sembrado de estas células a diferentes densidades en Matrigel™ con factores de crecimiento reducidos.

Una vez caracterizadas las líneas de células endoteliales vasculares y células musculares lisas vasculares se procedió al análisis tanto del dominio intracelular de NOTCH3 como del dominio extracelular en ambas líneas celulares, con el fin de validar la presencia de la acumulación de la proteína NOTCH3, descrita en la enfermedad. Para analizar los patrones de expresión de NOTCH3, se realizaron análisis por inmunofluorescencia a diferentes tiempos (10, 16 y 30 días para las células musculares lisas vasculares y cultivos en pase 3 o más, equivalente a 30 días o más para las células endoteliales vasculares). Los resultados obtenidos permitieron demostrar una acumulación del dominio extracelular de NOTCH3 en células musculares lisas vasculares a partir de los 20 días de cultivo y la presencia de depósitos en la membrana celular que podrían tratarse de material osmiofílico granular. En el caso del dominion intracelular de NOTCH3, encontramos una ligera acumulación tanto en las células musculares lisas vasculares como en

las células endoteliales vasculares, aunque los resultados con éstas úiltimas son todavía preliminares.

En definitiva, los resultados obtenidos a lo largo de esta Tesis permiten concluir que:

1) Se ha generado por primera vez una línea de células pluripotentes inducidas humanas a partir de células mononucleares de sangre periférica de un paciente con una mutación asociada a la enfermedad de CADASIL previamente diagnosticada.

2) Se ha conseguido obtener tanto una línea celular de células musculares lisas vasculares derivada de células pluripotentes inducidas humanas procedentes de un paciente con CADASIL como una línea de células endoteliales vasculares a partir de la implementación de protocolos de diferenciación.

3) Se pudo realizar con éxito el estudio tanto del dominio extracelular de NOTCH3 como del dominio intracelular en células musculares lisas vasculares derivadas de células pluripotentes inducidas humanas procedentes de un paciente con CADASIL así como en las células endoteliales vasculares derivadas también de esta línea de células pluripotentes inducidas humanas. De ahí se desprende que se ha podido conseguir por primera vez un modelo de "disease-in-a-dish" para la enfermedad de CADASIL.

4) Para el dominio extracelular de NOTCH3, no se encontró presencia de este dominio en WB, pero sí se encontró acumulación de la proteína NOTCH3 entera en células musculares lisas vasculares derivadas de células pluripotentes inducidas humanas procedentes de un paciente con CADASIL a partir de los 20 días después de su diferenciación, en comparación con los niveles encontrados en las células de musculatura lisa aórtica humanas y las células endoteliales vascualres derivadas de esta misma línea celular. Además, por immunofluorescencia se observó acumulación de NOTCH3/dominio extracelular en forma de depósitos en zonas concretas de la membrana celular de las células musculares lisas vasculares derivadas de células pluripotentes inducidas humanas procedentes de un paciente con CADASIL. Para el dominio intracelular de NOTCH3, se apreció un ligero incremento de este dominio tanto en las células musculares lisas vasculares derivadas de células pluripotentes inducidas humanas procedentes de un paciente con CADASIL como en las células endoteliales vasculares, aunque en el caso de estas últimas los resultados todavía sean preliminares.

Para finalizar, en esta Tesis se concluye que se ha podido generar por primera vez un modelo de "disease-in-a-dish" para la enfermedad de CADASIL en el que, al menos, se observa una acumulación de NOTCH3/dominio extracelular.

Abbreviations & acronyms

ADAM	A disintegrin and metalloproteinase enzyme
ADMSC	adipose tissue-derived mesenchymal stem cell
ALS	amyotrophic lateral sclerosis
AP	alkaline phosphatase
APS	ammonium persulfate
BCA	bicinchoninic acid assay
bFGF	basic fibroblast growth factor
BM-MNC	bone marrow-derived mononuclear cell
BMP4	bone morphogenetic protein 4
BMSC	bone marrow stem cell
BSA	bovine serum albumin
CAD02	unofficial name given to the second CADASIL-hiPSC line
CADASIL	cerebral autosomal dominant arteriopathy with subcortical infarcts and leukoencephalopathy
Cas9	CRISPR associated protein 9
CD31	cluster of differentiation 31
cDNA	complementary deoxyribonucleic acid
CIU	cell infectious units

c-Myc	c-Myc proto-oncogene protein
CRISPR	clustered regularly interspaced short palindromic repeats
CSL	CBF1, Suppressor of Hairless, Lag-1 transcription factor
CTX0E03	a type of neural stem cell line
DM1	differentiation medium 1 for vSMC differentiation
DM2	differentiation medium for vSMC differentiation
DMEM-F12	Dulbecco's modified eagle medium with nutrient mixture F12
DNA	deoxyribonucleic acid
DNAse	deoxyribonuclease
EAAT2	excitatory amino-acid transporter-2
EB	embryoid bodies
EBM	embryoid bodies medium
ECL	enhanced chemiluminescence
EGF	epidermal growth factor-like protein repeat
ESC	embryonic stem cell
FBS	fetal bovine serum
Flt3L	Feline McDonough Sarcoma-like tyrosine kinase 3 ligand
FOXA2	forkhead box A2

GAPDH	glyceraldehyde 3-phosphate dehydrogenase
gDNA	genomic deoxyribonucleic acid
GOM	granular osmiophilic material
HAoEC	human aortic endothelial cell
HAoSMC	human aortic smooth muscle cell
Hek	human embryonic kidney cell
hESC	human embryonic stem cell
HFF	human foreskin fibroblast
hiPSC	human induced pluripotent stem cell
i.a	intra-arterial
i.v	intravenous
IL-3	interleukin 3
IL-6	interleukin 6
iPSC	induced pluripotent stem cell
Klf4	Kruppel-like factor 4
KOS	combination of Klf4, Oct4 and Sox2 in the same vector
Kv1	voltage-gated potassium channels
LNG	Lin-12/Notch/GLP repeats
MAML	mastermind like protein

MAPC	multipotent adult progenitor cell
MEM	minimum essential medium
mESC	mouse embryonic stem cell
miRNA	micro ribonucleic acid
MOI	multiplicity of infection
MRI	magnetic resonance imaging
mRNA	messenger ribonucleic acid
MSC	mesenchymal stem cell
NECD	NOTCH3 extracellular domain
NICD	NOTCH3 intracellular domain
NPC	neural progenitor cells
NRR	negative regulatory region
NSC	neural stem cell
NT-hESC	nuclear transferred-human embryonic stem cell
Oct4	octamer-binding transcription factor
P/S	penicillin/streptomycin
PBMC	peripheral blood mononuclear cell
PBS	phosphate-buffered saline
PCR	polymerase chain reaction

PDGF-BB	platelet-derived growth factor with two B chains
PEST	peptide sequence rich in proline (P), glutamic acid (E), serine (S) and threonine (T).
PFA	paraformaldehyde
PROBE	prospective randomized open blinded end-point trial
qPCR	quantitative polymerase chain reaction
RCT	randomized controlled trial
RIPA	radioimmunoprecipitation assay buffer
RNA	Ribonucleic acid
RNAse	ribonuclease
RT	room temperature
S1	first cleavage that suffers NOTCH3 in its metabolic pathway
S2	second cleavage that suffers NOTCH3 in its metabolic pathway
S3	third cleavage that suffers NOTCH3 in its metabolic pathway
SCF	stem cell factor cytokine
SCNT	somatic cell nuclear transfer
SDS	sodium dodecyl sulfate
SeV	Sendai virus

Sox2	sex determining region Y-box 2 factor
SSEA1	stage-specific embryonic antigen 1
SSEA4	stage-specific embryonic antigen 4
STR	short-tandem repeat
SVD	small vessel disease
TAE	tris-acetate-EDTA
TALEN	transcription activator-like effector nuclease
TBS	tris-buffered saline
TBS-T	tris-buffered saline with tween
TEMED	tetramethylethylenediamine
TGF-β	transforming growth factor beta
Thy1	thymocyte differentiation antigen 1
TIMP3	metalloproteinase inhibitor 3
UV	ultraviolet
vEC	vascular endothelial cell
VEGF	vascular endothelial growth factor
vSMC	vascular smooth muscle cell
vWF	von Willebrand factor
WB	western blot

USC
UNIVERSIDADE
DE SANTIAGO
DE COMPOSTELA

INTRODUCTION

HYPOTHESIS

OBJECTIVES

MATERIALS & METHODS

RESULTS

DISCUSSION

CONCLUSIONS

USC
UNIVERSIDADE
DE SANTIAGO
DE COMPOSTELA

The aim of the introduction of this Thesis is to trace a path showing the way followed from a field as broad as stem cells to a field as specific as cerebrovascular diseases (Fig. 1). Thus, we will start with a brief introduction about stem cells and continue with the aim of this Thesis, the induced pluripotent stem cells (iPSCs). Then it will continue with a deeper review of iPSCs describing, at the end, their potential applications in cell therapy. Later, it will be provided the state of the art for both adult stem cells and iPSCs in cell therapy, specifically in stroke, to finally enter into a review of the cerebral autosomal dominant arteriopathy with subcortical infarcts and leukoencephalopathy (CADASIL) disease and how iPSCs can be used to study this disease.

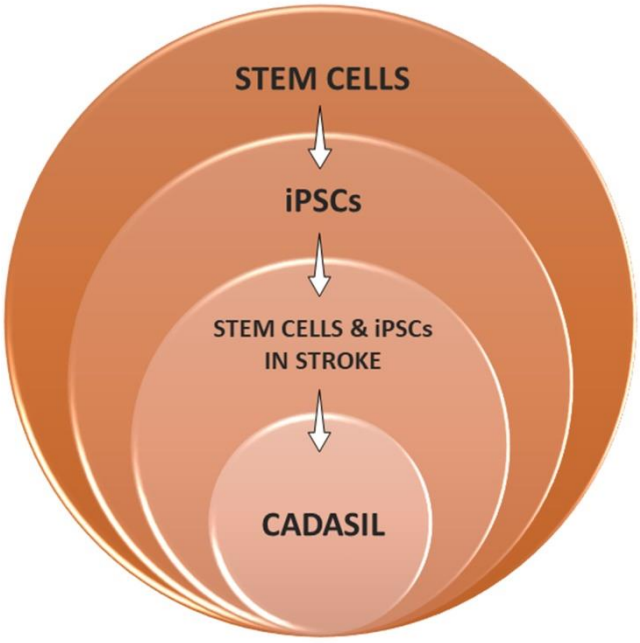

Figure 1. Representation of the scheme that will be followed throughout the introduction. Self-created image.

1. STEM CELLS

1.1. Introduction

Universally, stem cells are defined as cells that have the capability of self-renew virtually limitlessly *in vitro* and *in vivo,* and the ability, to different extents, to differentiate into various lineages[1]. Given that an endless capacity of self-renewal and proliferation is literally impossible to prove, it is commonly stated that a cell has this capability once is proved that is able to undergo more than twice the amount of population doublings that a somatic adult cell is able to undergo *in vitro* (70-90 population doublings)[2].

There is quite a consensus that points to the scientists Ernest McCulloch and James Till as the first researchers that rigorously define the key properties of a stem cell. They did it on their pioneering work in mice in the 1960s, when they discovered the blood-forming stem cells, the hematopoietic stem cells[3, 4]. It is important to highlight this fact since it is a common thought that the embryonic, pluripotent stem cells (ESCs) were the first stem cells on being isolated and cultured since they are the "most-known" stem cells. In fact, it was not until 1981 that Martin Evans and Matt Kauffman identified, isolated and successfully cultured mouse embryonic stem cells (mESCs) for the first time[5] (Fig. 2). This discovery opened the doors to the beginning of the "murine genetic models" creation, that is, mice with one or several genes deleted or modified in order to study their function in the disease[6, 7]. These mice were achieved by genetic modification of mESCs that are later injected into an early mouse blastocyst, so when the blastocyst develops into an adult mouse, every cell of its body will have the genetic modification.

However, the term ESC was defined 25 years before the experiments of Evans and Kauffman, by Stevens and Little in 1954 in their paper "Pluripotential embryonic cells appear to give rise to both rapidly differentiating cells and others which like themselves, remain undifferentiated", which was the first definition of an ESC[8, 9]. On the following decade, the pathologist Barry Pierce deeply studied the behavior of these teratoma cells, and in 1964 he demonstrated the ability of one single teratoma cell to create a new teratocarcinoma. This way, it was unequivocally that these cells had pluripotent capabilities. These cells were named as embryonic carcinoma cells (ECs)[10].

On 1974 it was reported for the first time that scientists successfully transferred ECs to a blastocyst and participate in embryonic development[11]. This fact made the scientific community suspect that these ECs may be homologous to those cells of the early blastocyst. In 1981, Evans and Kauffman finally isolated these early blastocyst cells, the mESCs, as previously mentioned. After that, it was not until 1998 that the next and awaited step was achieved. For the first time, scientists were able to isolate and culture human embryonic stem cells (hESCs)[12]. This discovery highly intensified the desire of using the unique properties of the ESCs in medicine. This way, since 1981 and 1998, scientists of all over the world has been able to work with mESCs and hESCs respectively, but experiments with multipotent stem cells are being carried out since the early 1960s.

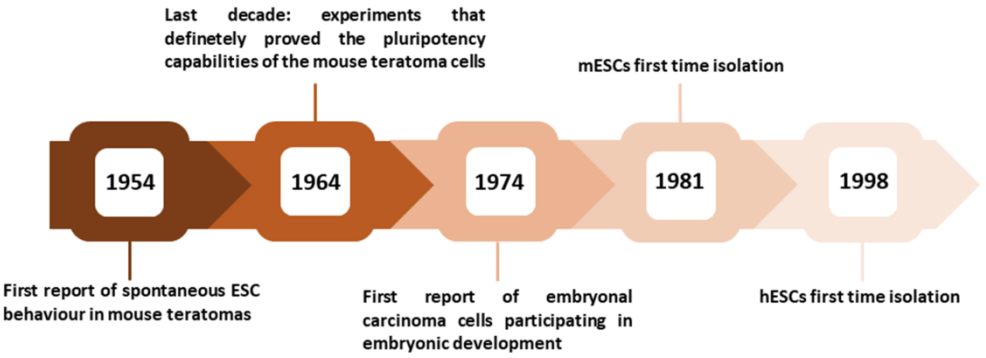

Figure 2. Timeline showing the main discoveries that led to final isolation of hESCs. Self-created image.

1.2. Classification of stem cells

Stem cells can be classified based on two parameters: their differentiation potential and their origin (Fig. 3).

1.2.1. ESCs CLASSIFICATION BASED ON THEIR DIFFERENTIATION POTENTIAL

Totipotent stem cells: able to generate all type of cells, including extraembryonic cell types, e.g. zygote.

Pluripotent stem cells: able to generate all body cells including germ cells but not extraembryonic cell types, e.g. ESCs, induced pluripotent stem cells, inner cell mas of the blastocyst-stage embryo.

Multipotent stem cells: able to generate all cell types from a specific tissue so their differentiation potential is committed to a specific lineage, e.g. tissue stem cells like hematopoietic stem cells.

Unipotent stem cells: able to generate just a single cell type, but have the property of self-renewal, e.g. spermatogonial cells.

It has to be highlighted that this hierarchy is not unidirectional, as in certain circumstances a cell can dedifferentiate to form cells with higher potency[13]. However, in mammals, particularly humans, regeneration is highly restricted and differentiation during embryonic and postnatal development is normally considered to be irreversible, although a recent work has demonstrated the capacity for dedifferentiation in some mammalian cells following tissue ablation or injury[14, 15].

1.2.2. ESCs CLASSIFICATION BASED ON ORIGIN

Early/embryonic stem cells: These cells are pluripotent stem cells existing in the early blastocyst stage. Specifically, they form the inner cell mass of the blastocyst. In a normal embryonic development, this population of cells would produce the epiblast that would give rise to all adult tissues but, if isolated, they can be cultured and maintained as ESCs[2].

Mature/adult stem cells: Multipotent stem cells located within different tissues/organs that give rise to the specific cell lineages that form that tissue/organ. In embryonic and fetal stages these cells conform dynamic populations of precursor cells and some of them, as the embryonic and fetal stages progress, are sequestered into the different tissue/organ niches and their potentiality become committed to the cell lineages that conform that tissue/organ [16, 17].

Induced pluripotent stem cells: First created in 2006 by Takahashi and Yamanaka[18], iPSCs are pluripotent stem cells derived from different

somatic cells by introducing inside them the four factors of Yamanaka (*Klf4, Sox2, Oct3/4* and *c-Myc*). However, nowadays is not necessary to reprogram by using the four factors, and just a combination of them can make it possible depending on several variables. These iPSCs cells highly mimic the properties and behavior of the ESCs, so their creation supposed a revolution in order to avoid the ethical issues concerning the use of hESCs[19, 20], since the derivation and culture of hESCs require the destruction or manipulation of *ex utero* embryos[12, 21].

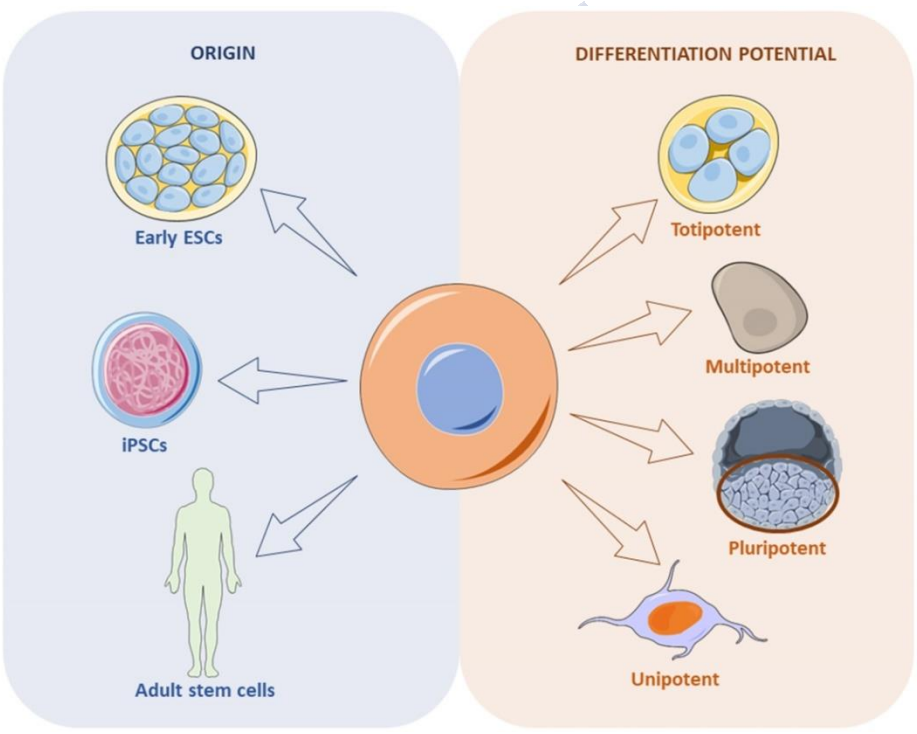

Figure 3. Classification of stem cells based on their origin and their differentiation potential. Self-created image (using elements with Creative Common license).

2. INDUCED PLURIPOTENT STEM CELLS

2.1. Introduction

We can define iPSCs as pluripotent stem cells that come from "pushing" a given type of somatic adult cell through a process where they suffer several genotypic and phenotypic changes in order to become a pluripotent stem cell[2, 22]. Theoretically, they can be obtained from any type of adult somatic cell with nucleus, and there is, in fact, an extended bibliography reporting multiple cell sources[18, 23, 24].

Regarding their behavior, proliferation rate and morphology, iPSCs are similar if not identical to the ESCs, although they present small genotypic differences that make them not fully identical to hESCs. These genotypic differences fall mainly in the fact that iPSCs may retain the epigenetic[25] and gene expression of donor cells[26].

The history of the iPSCs begins as a logic evolution step after the consolidation of the hESCs in basic science. Experimentation with hESCs, despite its value, has two major limitations: destruction of human embryos (with the ethical issues that implies) and the limited source they are obtained from. Thus, the great breakthrough happened in 2006, when Yamanaka and Takahashi were able for the first time to induce mouse fibroblasts into iPSCs[18]. With 24 candidate genes for generation of pluripotency as starting point, they fine-tuned the process until achieving a final combination formed by just 4 of them: the four factors of Yamanaka. By introducing these 4 factors inside mouse fibroblasts using integrative virus as vectors, they were able to obtain iPSCs. On the next year, they reported the same process but for adult human fibroblasts[27]. The development of these human induced

pluripotent stem cells (hiPSCs) supposed the way of bypassing the ethical concerns associated to hESCs. Also, hiPSC were presented as a way to obtain pluripotent stem cells in a theoretically infinite way.

But prior to this discovery, several different reprogramming approaches were developed in order to achieve this iPSCs and to study all the underlying mechanisms that led a somatic cell to become an iPSC. Historically, experiments with some of that approaches paved the way to the development of iPSCs by Yamanaka and Takahashi.

2.2. Approaches to induce reprogramming

2.2.1. SOMATIC CELL NUCLEAR TRANSFER

The somatic cell nuclear transfer (SCNT) was the first attempt to reprogram a somatic cell into a pluripotent stem cell. Basically, it consists on the insertion of a somatic cell nucleus inside an enucleated oocyte (Fig. 4).

SCNT is one of the main methods for the production of cloned animals. To this regard, the first experiments were assayed on amphibians, and later with Dolly the sheep. The success of these experiments proved that the somatic cell genomes maintained their capability of generating viable cloned animals, thus indicating that the genome restrictions imposed during development and changes throughout cell differentiation were reversible and caused by epigenetic modifications and not by permanent changes in the genome[28, 29].

Despite its low efficiency and the intrinsic methodological difficulties when performing this method, this technique had its importance on the

first years after the development of the iPSCs by Yamanaka. This was because it had not been discovered yet the non-integrative mechanisms of reprogramming. By that time, the reprogramming techniques entailed the risk of inserting transgene copies, which could cause insertional mutations and break the normal endogenous gene pattern expression. Also, these transgenes could be continuously overexpressed or be spontaneously reactivated[30].

However, the efficiency of SCNT is also quite low, and even more, the cell that reach pluripotency tend to maintain the genome of pluripotent cells, which may lead to genetic instability. But regarding low efficiency, many studies have reported that a treatment with histone deacetylase inhibitors and DNA methyltransferase inhibitors improve the chances of successful reprogramming, since histone methylation, acetylation and DNA methylation are the main epigenetic mechanisms that act as barriers in the donor cells that want to be reprogrammed[31].

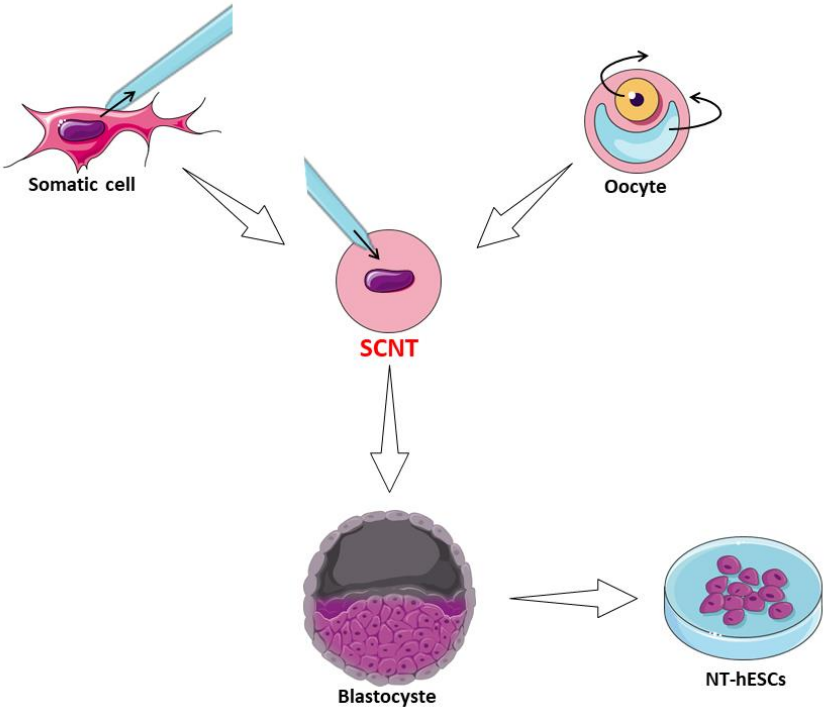

Figure 4. Somatic cell nuclear transfer procedure. NT-hESCs: nuclear transferred-human embryonic stem cells. Self-created image (using elements with Creative Common license).

2.2.2. EXTRACT OF PLURIPOTENT STEM CELLS

Given the aforementioned epigenetic barriers that act as a "defense" against reprogramming, an initial solution was to reprogram somatic cells with extracts of pluripotent stem cells. Embryonic stem cells, embryonic germ cells and/or embryonic stem cell-like cells are the most used for this purpose, since they have high presence of demethylating and deacetylating enzymes. The crude extract obtained from these cells is directly inserted into somatic cells, generally by using chemicals to

permeabilize the membrane (Fig. 5)[32]. Once reprogrammed, pluripotent stem cells have shown to be able to differentiate to several cell types, although this has only been achieved in animal cells. In human cells, cell extracts have been applied but with partial success. Cells were just partially reprogrammed and they were not able to differentiate *in vivo*. Transdifferentiation was not possible either[33]. Regarding efficiency, this technique requires of high amount of ECS cells in order to achieve a small amount of extract. Also, there is no information about imprinting genes which would lead to genetic instability. Furthermore, this technique has not been proved yet in primary cells of adult individuals.

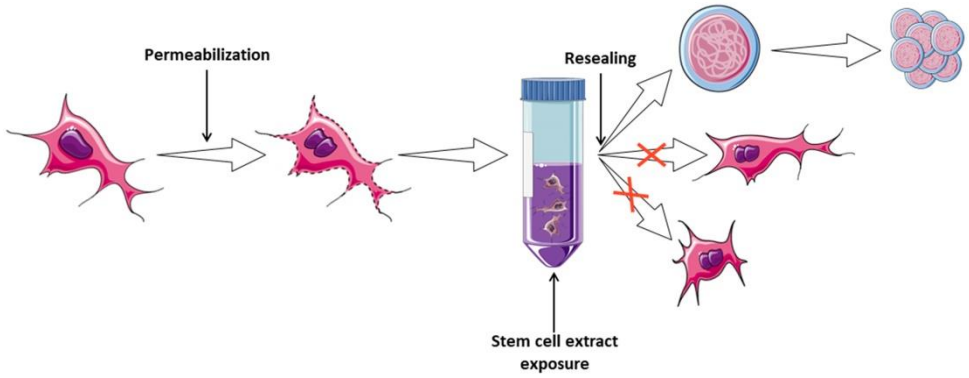

Figure 5. Generation of pluripotent stem cells by exposing permeabilized somatic adult cells to an extract of stem cells. Self-created image (using elements with Creative Common license).

2.2.3. CELL FUSION

Cell fusion relies on the fusion of the same or different type of cells, forming entities known as homokaryions or heterokaryons respectively. In these structures, the parental nuclei remain discrete although within a single cell body, sharing the same cytoplasm. This normally give rise to stable proliferating hybrid cells that contain an increase in chromosome content (tetra- or polyploid cells) as a result of the fusion

of nuclei. On the other hand, when fusing certain type of cells like myocytes, it may also occur that this fusion generates a stable non-dividing multinucleated state that begin to express muscle-related genes in a sequence resembling a normal muscle differentiation[34, 35]. Regarding reprogramming processes, somatic adult cells like fibroblasts may be fused with ESCs to form tetraploid reprogrammed cells that, when dividing, will form diploid reprogrammed cells (Figure 6). To this regard, SCNT as well as cell fusion reprogramming are good tools to study and elucidate the first steps developed in the reprogramming process. To this regard, although iPSCs reprogramming has supposed a revolution in the field of stem cells, it still presents some issues in order to study the early events of the first stages of reprogramming: the low rate of successful iPSC conversion or the late identification and selection of real iPSC clones. On the opposite, SCNT supposes a more direct route to study these stages, although the requirement for expertise handling, the limitation in oocyte availability and the low efficient rate make them not the best option either. In contrast, cell fusion guarantees a cheap and accessible technique with which the early events of reprogramming can be studied while the conversion of somatic cell towards an ESC-like state occurs[34].

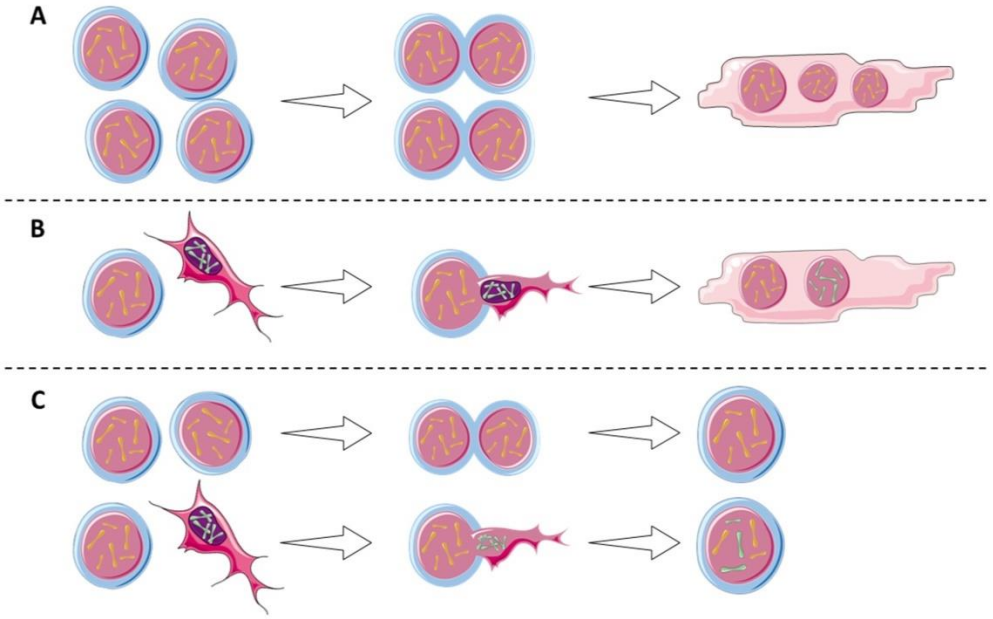

Figure 6. Cell fusion possibilities. A) Fusion of cells of the same type may result in syncityum, where the nuclei of the fused cells remain discrete inside a common cell body. B) Fusion of cells from different types may result in heterokaryons, where the nuclei remain discrete inside a common cell body, thus having the genetic composition of both original cells. C) Cell fusion may also give rise to synkaryons, where nuclei from the original cells fuse, giving rise to tetraploid cells. Self-created image (using elements with Creative Common license).

2.2.4. REPROGRAMMING FACTORS

Despite the undeniable value of the techniques mentioned above, due to their historical meaning or their value as study tools, from the moment iPSCs were developed by Yamanaka and Takashi in 2006, the most employed method for reprogramming nowadays all over the world is the reprogramming by addition of the four (or a combination of) Yamanaka´s factors *Oct4, Sox2, Klf4* and *c-Myc* inside a population of a given somatic cell type. It has already been more than a decade since that discovery was made, and a lot of several methods regarding the

induced expression of these factors have been developed. These methods not only refer to a viral transfection of the factors as it was performed in the beginnings (Figure 7), but also non-viral transfection like reprogramming by mRNAs or episomal plasmids among others (Figure 8).

- **Viral transfection methods**

    - **Lentivirus:** lentiviruses belong to a subclass of retrovirus, the first viral vectors used for reprogramming. But unlike retroviruses, lentiviruses are able to infect both non-dividing and proliferating cells, becoming in the beginning the preferred delivery vector to introduce the Yamanaka´s factors inside somatic cells. However, difficulties on achieving the correct stoichiometry for infection as well as concerns about the incorporation of DNA sequences of the own virus within the iPSCs genome supposed two important issues to take into account[36]. Both problems were solved at once with the development of a single cassette reprogramming vector carrying all factors but separated by a self-cleaving peptide signal. Also, these vectors are engineered with *loxP* sites so the integrated transgenes may be excised by overexpression of *Cre*-recombinase. These vectors were tested for the first time in patients with Parkinson´s disease. It was proved that after excision of the transgenes sequences, patient´s iPSCs retained pluripotency[37].

    - **Adenovirus:** with the use of adenoviruses, the problem of possible mutagenesis produced by the integration of the virus

genome within the DNA of the iPSCs was overcome. Also, thanks to that, it was proved for the first time that this mutagenesis was not necessary for the generation of iPSCs. One of the objectives of using adenoviruses was to prove if the efficiency of reprogramming was higher than with integrative viruses (around 0.1-0.01%); what it was found, in fact, is that it is lower: around 0.001-0.0001% in mouse cells[38] and 0.0002% in human cells[39].

- **Sendai Virus** (SeV)**:** this paramyxovirus is probably the most used viral vector for inducing reprogramming. SeV has a broad cellular trophism, wider than adenovirus, englobing hematopoietic stem cells, macrophages or dendritic cells, neuronal cells…[40] This is because it uses ubiquitous sialic acid as cellular receptor, which allows it to quickly infect many tissues and cell types. Also, it has never been associated to any human disease, being a really safe choice to work with. Importantly, it is a non-integrating RNA virus that does not enter inside the nucleus of the cell. Although SeVs are harder to produce and work with than lentiviruses, SeVs are sold as commercial vectors for induction of pluripotency, so it is not necessary to produce them[41]. However, one disadvantage that SeVs may present is that although they do not integrate within the iPSCs genome, it may take up to 10 passages to fully remove them from inside the cell. Another problem regarding SeVs is that apparently, infected cells may need to be cultured at 39°C, but there are studies where this was not needed[42].

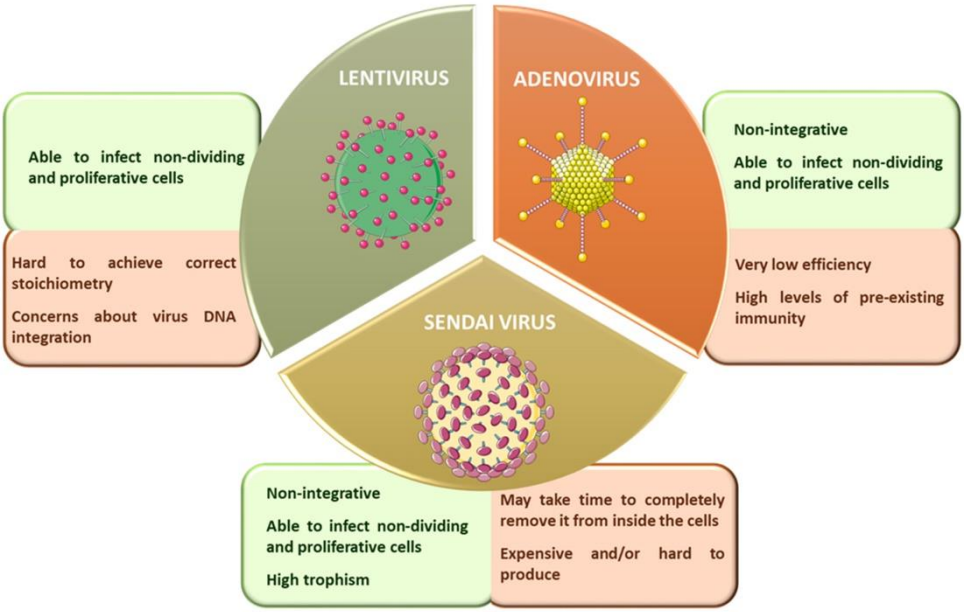

Figure 7. Scheme with the three main viral vectors used for reprogramming.. Self-created image (using elements with Creative Common license)

- **Non-viral transfection methods**

  - **mRNA transfection:** since 2010, when Warren et al. generated for the first time iPSCs just by transfecting synthetic mRNA coding for the four Yamanaka's factors[43], it was set the possibility of generating iPSCs without the need of using virus as vectors. Although this process has been improved with the years by discovering several compounds that improve the efficiency of the process, it still presents some drawbacks. It is labor-intensive and requires daily addition of mRNAs over time to keep the transgenes levels up time enough so cells may have the time to reach a stable iPSC phenotype[41].

- **miRNA:** miRNAs play a key role as regulators of the expression of genes that establish and maintains cellular fate. Some of these miRNAs were found uniquely in ESCs and were regulated by *Oct4, Sox2* and *Klf4*. This fact lead researchers to successfully try to generate iPSCs by transfecting these miRNAs into somatic cells[44, 45]. Although it can be improved with the addition of other several compounds, the reprogramming efficiency with miRNAs is quite low, mainly due to the half-life of miRNAs (declines in few days) and their delivery method, requiring an intensive labor, which implies the daily addition of the reprogramming molecules. However, miRNAs have also attracted the attention for direct differentiation or transdifferentiation. These miRNAs could be used in order to suppress repressors of specific transcriptional factors, guiding the cells to another phenotype[46].

- **Episomal plasmids:** an alternative to RNAs transfection systems as non-viral transfection method are the episomal plasmids. Portions of the Epstein-Barr human herpesvirus were used to create the first non-viral episomal vectors able to be transfected without viral packaging. Combinations of reprogramming factors that in previous reprogramming experiments with lentivirus had proved a higher efficiency than average were cloned into the episomal vector and then transfected into somatic cells. However, iPSCs generation efficiency was quite low (3 to 6 colonies/10^6 input cells)[47], although there have been efforts to improve this efficiency, rising it to 1 colony/10^{-5} – 3 colonies/10^{-4} input cells[48].

Apart from being a non-integrative method, episomal vectors are easily removable from cells by a drug selection method, freeing the cell from any exogenous agent/molecules.

- **Small molecules and chemical compounds:** the idea of using small molecules and chemicals is to enhance reprogramming efficiency. In some cases, the addition of specific molecules avoids the use of some of the Yamanaka´s factors and potentiate the process[49, 50]. Also, the use of some compounds may avoid the need of using the problematic *c-Myc* reprogramming factor without compromising the reprogramming process[51]. There are a huge number of groups working in this promising field nowadays. There is a strong belief that the use of these molecules may be the final solution to produce genuine and stable iPSCs free of integrations and undesirable mutations. Furthermore, this technology seems to be very safe, since the way of action of the molecules is interacting through discrete pathways rather than through modifications to reprogram cells. Nonetheless, regarding efficiency, the substitution of some transcription factor for a small molecule or chemical decreases the efficiency of the process[52]. This fact strongly suggests that these compounds may not be able to entirely replace the role of a functioning transcription factor.

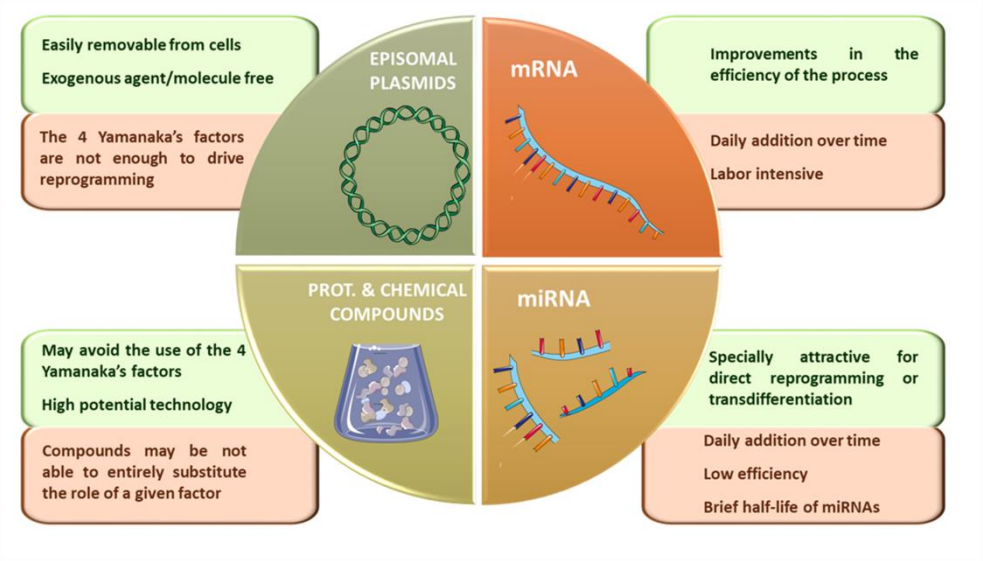

Figure 8. Scheme with the four main non-viral reprogramming methods. Self-created image (using elements with Creative Common license).

2.3. Possible mechanisms underlying the reprogramming

Reprogramming is a highly complex process that involves the removal of the entire transcriptional and epigenetic signature from the donor somatic cells and the establishment and constant preservation of the epigenome in iPSCs. Since the first creation of iPSCs, many researchers have focused they attention in trying to fully unravel the mechanisms underlying reprogramming. A complete comprehension of these mechanisms would be translated into more efficient and safer reprogramming techniques that would guarantee a better and safer translationality into clinical practice, which could be the key difference between a failed trial and a successful one. Although there have been a lot of advances regarding these underlying mechanisms, there is still so

many issues to understand and study. But basically, what it is known until now is reflected in Figure 9. It should be pointed that experiments to elucidate these mechanisms have been carried out mostly in mouse fibroblasts[53]. Briefly, after the first 1-3 days when the fibroblast-associated surface marker *Thy1* is downregulated and the alkaline phosphatase is upregulated, it comes an intermediate phase where SSEA1 gets activated and upregulated. Finally, what seem the main core factors for pluripotency, *Oct4* and *Nanog*, are activated and at the same time, telomerase and silent chromosome X reactivate. All over middle/final stages of reprogramming, exogenous transgenes begin to disappear, meanwhile the activation of *Oct4* and *Nanog* starts a stabilizing circuit that keeps the expression of the endogenous genes/factors of pluripotency constant[53-55]. Interestingly, during the first 12-14 days of reprogramming, there are two waves of major gene activity; one at the beginning, on day 0-3, followed by a quieter phase, and other one after day 9. While in the early wave proliferation and pluripotency related genes are upregulated, in the second wave genes related with embryonic development and stem cell maintenance are activated. Furthermore, it has been shown that the first transcriptional wave is due to *c-Myc*, one of the Yamanaka's factors. This wave occurs in almost all cells whereas the second is more restricted to reprogrammable cells, involving a gradual increase in the expression of *Oct4* and *Sox2* targets. While *c-Myc*, *Oct4* and *Sox2* are inducing all the initial and last mechanisms for reprogramming, *Klf4* seems to be constantly supporting the process by repressing somatic genes at the beginning, and facilitating the expression of pluripotency genes later[56]. Also, *Oct4*, *Sox2* and *Klf4* are the pioneers that open the chromatin in the regions of genes that are essential for the establishment and

maintenance of pluripotency. In fact, it has been shown that these pioneer factors bind to more regions than those in which they appear to bound later in ESCs[57]. Following this initial binding, *Oct4*, *Sox2*, *Klf4* and also *Nanog* begin to interact with chromatin modifiers, mainly demethylases and acetylases that reset the epigenomic of the somatic cell[56].

As can be seen, direct reprogramming is dependent in the correct amount, balance, continuity and silencing of the transgene expression of the four Yamanaka's factors. Also, it should be taken into account that some of these four factors are already expressed in some cell lines, for example *Klf4* in fibroblasts, although its level is not enough for iPSCs generation[58]. This way, the multiplicity of infection (MOI) should be pondered independently for each cell lineage, being a crucial step since an incorrect balance of the factors would result in an unsuccessful reprogramming or directly in cell death[59].

Figure 9. Timeline with the expression over the first 16 days of several key agents for the transition from somatic adult cell to iPSCs. Horizontal timeline is expressed in days. Self-created image (using elements with Creative Common license).

There is an important part of the reprogramming process that still remains elusive and that presents two well defined hypotheses that tries to solve it: why just a small proportion of cells subjected to reprogramming gets successfully reprogrammed whereas the majority of them failed? Or in other words, what makes a cell to be reprogrammed? As curious as it may be, given all those specific and molecular mechanisms that are already known during reprogramming, something apparently as global as what makes a cell to be successfully reprogrammed is yet on debate. As mentioned above, there are two main hypotheses that would explain it: the so called "elite model" and the "stochastic model" (Figure 10).

2.3.1. ELITE MODEL

In the elite model, it is assumed that just small subpopulations of the cells that are going to be reprogrammed are capable of it. This model is subdivided in two. In one of them, called the "predetermined elite model", just a small number of cells are competent for reprogramming even before they are infected with the Yamanaka's factors. This theory is supported by the presence of tissue stem cells and other undifferentiated cells located in regenerative tissues. These cells would be the "elite" cells that would be already predisposed to be reprogrammed. Furthermore, in some cases the reprogramming process efficiency results in nearly the same percentage that the presence of some multipotent stem cells in some tissues[60]. However, nowadays the efficiency of the process has improved. For fibroblasts for example, there are reports suggesting a 10% of efficiency, and it seems unlikely that among the fibroblast population there are a 10% of multipotent "elite" stem cells. Also, there are studies that have already shown the

capability of the four Yamanaka's factors to reprogram terminally differentiated cells[61], indicating that the factors are able to reprogram lineage-committed cells.

The second model within the "elite model" is the "induced elite model" in which more than the four factors must be activated by viral integration in the host genome. As it can be deducted, this model is not supported anymore since the first reprogramming experiments without retroviruses were performed, clearly indicating that virus integration is not needed for iPSCs generation.

Nowadays, studies that support the "elite model" goes more in the way that they proved the existence of cells that become "elite cells" in the very beginning of the process, either because they are already predisposed to overcome the first reprogramming barrier and after that all the iPSCs obtained would be their progeny[62, 63], or because a previous treatment with some proteins force somatic cells to behave as elite cells[64].

2.3.2. STOCHASTIC MODEL

In opposite to the "elite model", in the "stochastic model" is assumed that all adult somatic cells have the capability of becoming iPSCs once they have been transfected with the four factors. Before the discovery of iPSCs, the pluripotency state seemed just a transient state, where cells quickly passed to more committed lineages. However, ESCs presented the ability of self-renewal and maintenance of their current state for long periods of time. Thus, it seems like the four factors worked together to force cells to go back to their pluripotency state and as suppressors of their natural tendency to lineage commitment. But in

order to achieve that, there are some barriers that cells may overcome. These barriers would play the stochastic role that just few cells would definitely pass to become iPSCs. The first barrier is constituted by the need of the four factors to be expressed in a specific pattern that guarantees that the cells take the "right direction" to reprogramming. This barrier supposes a stochastic one since there are no technologies yet that control 100% the expression levels of the four transgenes. There are protocols provided by companies that suggest different MOIs for each viral vector carrying each factor; they are just a tested approximation that guarantees the reprogramming but, in general, with low efficiency. Second, cells must suffer an epigenetic erase, and, beyond that, they need to be maintained stable so iPSCs may remain as they are. To this regard, the four reprogramming factors cannot act as such epigenetic roadblock; they just turn on the first mechanisms that lead to that epigenetic erase but they cannot assure that the process follows the right steps. Thus, a second stochastic process is established for generation of iPSCs.

In the same way as for elite model, there are studies that support the stochastic model. Some of them, apart from proving this, also suggest metabolic targets to improve the chances of reprogramming success.

Also, there are studies defending a mixture of both stochastic and a more deterministic model[65]. For example, Buganim et al. analyzed the profile of 48 genes in single cells at different stages of the reprogramming process and found that after an initial stochastic gene expression, if this step is overcome, the next steps would follow a hierarchical phase, being *Sox2* the upstream factor that regulates it[66].

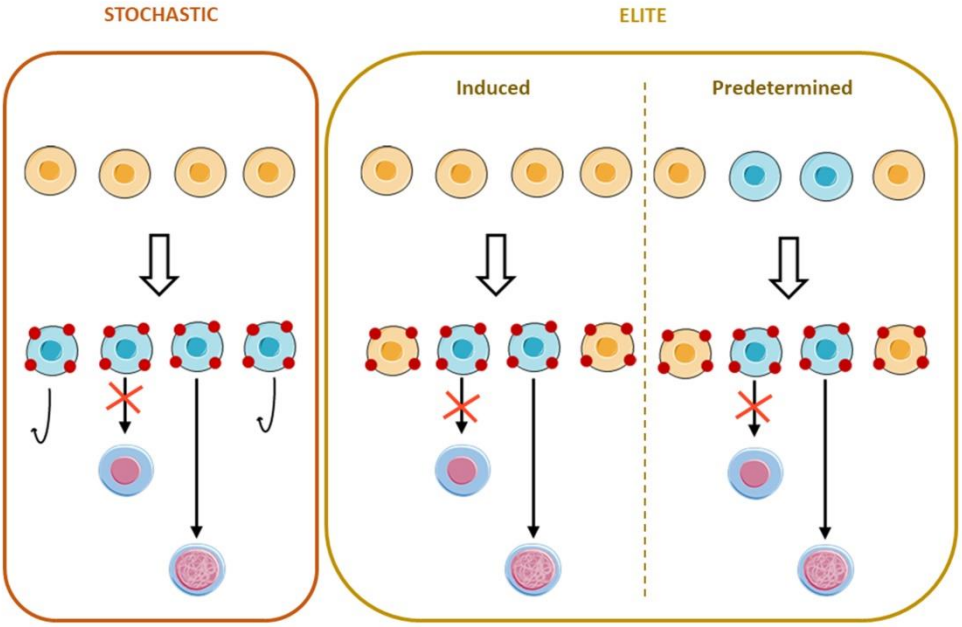

Figure 10. Scheme with the two main hypothesis about reprogramming mechanisms. Small red dots represent viral vectors carrying the four Yamanaka´s factors. Arrows that turn back represent cells not propperly infected. Arrows with a red cross represent reprogrammings that do not succed in overcoming some of the reprogramming barriers. Blue cells in the predetermined elite model represen cells that would be predetermined to be successfully infected, although after that some of them could fail in overcoming reprogramming barriers. Self-created image (using elements with Creative Common license).

2.4. Disease approaches with iPSCs

2.4.1. DISEASE MODELLING

Over time, it is widely known that many animal models are failing at the time of transferring the knowledge acquired by studying them to the clinic. Mice represent one of the most animal models used worldwide, and we share the 97.5% of our DNA with them. However, the difference of 2.5% supposes a huge phylogenetic gap impossible to overcome. This phylogenetic gap translates into differences in physiology, immune

system or inflammation; and these differences are critical when assaying new drugs in clinical trials since they mostly lose their pre-clinically proven effectiveness[67]. Besides of the effectiveness issue, these "small" but huge differences also contribute to the failure in the identification of toxic side effects in clinical trials, since they do not appear when performing toxicity assays in animal models.

To this regard, hiPSCs supposed a new and unexplored world full of potential and promising applications that could be transferred to clinic. After thirteen years, many researchers and research centers produce hiPSCs routinely in order to study and model diseases by differentiating these hiPSCs into the affected cell types for each disease[67]. Furthermore, for this differentiation, commercial providers but also researchers all over the world have developed and provide/share optimized differentiation protocols for almost every cell type.

Thus, although bringing hiPSCs to clinic is yet a mid/long-term goal that still has to prove its feasibility, an important part of the international scientific community has turned his eyes into hiPSCs as a tool to replace animal models to understand the mechanisms underlying diseases. In the so called "disease-in-a-dish" method, easily obtainable somatic cells (fibroblasts, peripheral blood mononuclear cells [PBMCs]) may be reprogrammed to hiPSCs and further differentiated into the affected cell type in a given disease. Once achieved the hiPSCs-based cell model, the possibility of assaying drug screening techniques and genetic editing tools highly enhance the possibilities offered by this cell modeling technique (Fig. 11):

- **Drug testing**: the estimated average out-of-pocket cost for the main pharmaceuticals to develop a new drug is currently exceeding 2.6$ billion[68]. In fact, of the 2.6$ billion spent to achieve a regulatory approval of a single new drug, 2.4$ billion is spent on candidate drugs that failed along the way, meanwhile just about 200$ million is spent on the compound that is actually approved. Furthermore, apart from the economic cost, there are thousands of person-years of scientific researchers' time that could be redeployed against compounds that still have the potential to change the health of the world. The challenge then would be to identify earlier, during the development process, drugs that will fail in clinical trials. Strategies to bridge studies between preclinical testing and clinical trials are needed to reduce the knowledge gap prior to first human exposures, and to allow earlier decisions to be made on the continuation or discontinuation of further development of drugs[69].

  To this regard, the discovery and development of hiPSCs have opened up new avenues that support the concept of screening for cell-based safety and toxicity at the level of a population, with the potential to reduce attrition of drugs in clinical development. Indeed, the noninvasive nature and unlimited supply of this patient-derived approach now allows performing surrogate clinical trials *in vitro*, with consequences that extend well beyond the ability to reduce the attrition of drugs.
- **Genetic editing**: at the beginning, the goal of the first studies using hiPSCs for disease modeling was to prove that cells differentiated from patient-specific hiPSCs exhibited *in vitro* the same phenotype as *in vivo*. Once proved that this model was

suitable for disease modeling, hiPSCs-based cell models were used to investigate the molecular and cellular pathological mechanisms underlying the disease under study. The next logical step, as stated before, was to use these cell models for drug screening purposes. However, despite all the advantages of the iPSCs, there is still one critical challenge in the field of disease modeling using hiPSCs: to discriminate between abnormal in vitro phenotype resulting from the specific causative mutation versus the individual's genetic background. To overcome this issue, a good approach in the field is to correct mutations in a given patient-specific hiPSC clone, thereby generating isogenic paired hiPSCs. This way, in case of being any difference between phenotypes of the corrected hiPSC clone and the non-corrected ones, this difference could be associated to the mutation.

To summarize, with the development of this hiPSCs-based cell models, several hurdles concerning the successful development of new drugs and researchers may also study and model disease with cells from the own patient in combination with the genetic editing tools. In fact, this theory has already been put into practice successfully. There are already pre-existing drugs which has been repurposed for some diseases through a better understanding of their mechanism of action. This was due thanks to their study on patient-derived hiPSCs, resulting into their translation to clinical trials and avoiding their previous test in animal models[70-72]. Nonetheless, these features have been made in "non-complex systems", this is, modeling diseases or just a part of complex diseases which just need monotypic cell cultures or which are caused by

specific single mutations. This facilitates to achieve an easier and more accurate model that mimics the disease.

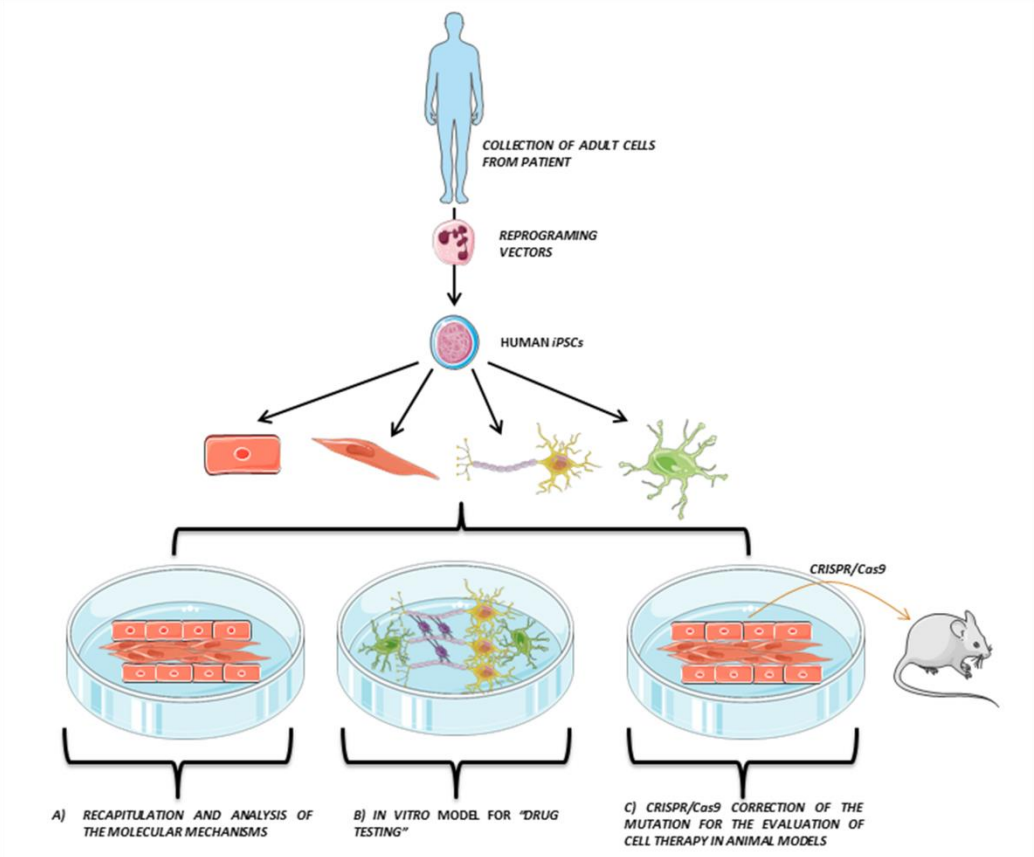

Figure 11. Fundamentals of the "disease-in-a-dish" process, with its potential applications. Self-created image (using elements with Creative Common license).

On the opposite, many diseases involve multiple cell types and/or include complex relationships between cell environment, tissue environment, multiple and/or different genetic alterations…that together make hiPSCs struggle at modelling them. There are three key factors that influence the amenability of complex diseases to *in vitro* modelling, which are: the onset of disease in patients, the cell-autonomous nature

of the disorder and the genetic complexity underlying disease. Which of these factors is the one that most strongly influences when it comes to generate the relevant disease phenotype *in vitro* is yet unknown. For example, Parkinson´s disease generally occurs in late stages of life. Also, it has a strong environmental component and underlying complex genetic alterations. Together, these factors make really difficult to model this disease. Unfortunately, the majority of the diseases that have the greatest socio-economic impact worldwide are polygenic and with a strong environmental influence (Alzheimer's disease, diabetes, congestive heart failure, Parkinson's disease…), and whether their key phenotypes can be reproduced *in vitro* remains to be elucidated[73].

On this matter, a new generation of disease models has arisen to face the challenge of modelling complex diseases. They are based on heterotypic cell cultures, integrated in "organ-on-chip" formats or in "organoids". The first ones consist in microfluidic devices where the different cell types are inserted, simulating complex synthetic human tissues within a chip. The second ones are 3D structures of cell cultures where cells self-organized in subunits. Both models may allow the identification of drugs that could reverse the condition *in vivo*. Furthermore, with these models they can also be assayed several forms of tissue stress such as inflammation by cytokines or stress induced by bacterial or viral challenges. Finally, they are also able to hold microfluidic flow systems, simulating interactions with the circulatory system[67].

2.4.2. REGENERATIVE MEDICINE

The regenerative medicine field chases the repairing of injured or degenerated tissues/organs by replacing, engineering or regenerating them to establish their normal function again. However, important hurdles like availability of tissue/organ and immunorejection make hard to implement this technology in many cases. This leads to the fact, frequently, that a patient dies due to the lack of donors. This issue intensifies with the fact that a patient can only be transplanted with cells/tissues/organs that do not have any disease and whose physiological profile matches with the patient so he does not get immunorejected, diminishing the already small availability of tissues[22].

To this regard, hiPSCs offers a good approach on this field, as they offer, theoretically, an endless source of tissue by differentiation of the repaired hiPSCs generated from the somatic cells from patient's own body, overcoming both issues in one shot. Thus, the aim of hiPSCs in regenerative medicine would be to repair the damaged or deteriorated tissues by generating those same tissues *in vitro* and their posterior transplantation to the affected area. Nowadays, hiPSCs have already been successfully used for the treatment of several injuries and degenerative diseases at pre-clinical level. For example, spinal cord injury or musculoskeletal injuries are some of the cases where injuries have been submitted to regeneration by the use of hiPSCs, generating specific cells that replace the damaged tissues[74, 75].

But apart from accidental injuries where damaged but physiologically healthy tissues need to be repaired, the regenerative capabilities of the hiPSCs, together with more recent and more efficient methods of gene

editing/repairing tools that are in continuous development, present good opportunities to treat several degenerative diseases caused by different mutations. On this case, the mutation is first corrected, either before the reprogramming of the somatic cells or at the hiPSC stage. Once the mutation is fixed, hiPSCs are differentiated into the desired cell types. After these cells are obtained, they can be transplanted into the body of the patient from where initial cells were obtained.

In order to correct mutations, in gene therapy for regenerative medicine, different genome editing tools may be employed such as zinc finger nucleases, the CRISPR/Cas9 system, transcription activators-like effector nucleases (TALENs) or adeno-associated viruses providing an efficient way of deleting/inserting from single nucleotides to whole genes[76-78]. Of all of them, the CRISPR/Cas9 system is the most recent and most promising one since its underlying mechanism allow it to perform extremely precise editing. Nonetheless, like in disease modelling, the chances of successfully implement this technology go hand in hand with the genetic background complexity of the disease.

In brief, since its very beginning, the hiPSCs technology has always had its translation to clinical practice as one of its main objectives if not the most important one. The use of hiPSCs carries with it several advantages. The hiPSCs themselves present several inherent characteristics that, together with the advantages based on their potential applicability and on their exploitation as a technological tool, make them a promising tool to new regenerative medicine therapy approaches and to disease modelling.

However, in the same way that there are inherent advantages to hiPSCs, there are also several risks that should be taken into consideration when thinking about using this technology for a given experiment/project (Fig.12). As an example, it is not the same to use hiPSCs to model a monogenic disease with just one affected cell type to study its physiopathological mechanisms, that to use them to model a multigenic, complex disease, with several affected cell types and environmental factors involved.

Figure 12. Advantages and disadvantages of hiPSCs depending on their inherent properties, their applicability and their use as technology. Self-created image.

2.5. Risks and regulatory issues

Since the medicine has tried to bring human embryonic stem cells into clinic, debates about their use have always been around, as their use implies the destruction of human embryos. With the discovery of iPSCs, this concern was overpassed. However, although hiPSCs bypassed this ethical issue and seem to be a promising tool to treat diseases, there are still some main concerns that surround hiPSCs. These concerns are: abnormal reprogramming, risk of tumorigenicity, producing germ cells from hiPSCs and the elaboration and application of informed consent[79].

Abnormal reprogramming: The process of reprogramming is far from being 100% efficient. From a huge quantity of cells, it just arises a small percentage of stem cell colonies, and it does not guarantee that they are comprised of real iPSCs either. To this regard, there are highly strict characterizations tests that a new cell line needs to pass before registering it and needs to be an available source for any kind of experiment/trial that may require that cell line. The expression of markers and genes associated to pluripotency must be assessed, as well as the property of the new line to form teratomas *in vivo* or embryoid bodies (EBs) *in vitro* and their differentiation to the three embryonic germ layers[80]. Also, iPSCs must be submitted to several and strict contamination tests (*Mycoplasma*, fungi, bacteria) as well as to genetic evaluations in order to check for any undesirable genetic mutation (karyotyping, DNA sequencing…). And yet, even though they pass all these tests, the epigenetic profile of the iPSCs is different from the profile of the somatic cells and should be taken into account when designing experiments. As an example, it has been proved that iPSCs

present aberrant reprogramming of DNA methylation and may be different in regard to gene expression[81].

Risk of tumorigenicity: The risk of tumorigenicity is associated with the repression during reprogramming of some tumor repressor genes[82]. If hiPSCs are going to be transplanted, it is a key fact that they maintain a normal and sustained growth rate and development in the desired location in order to perform normal functions *in vivo*. If this order brakes, it would result in uncontrolled cell proliferation, with the possibility of tumors being generated. Keeping the stability of the genetic and epigenetic characteristics of hiPSCs is critical, and since this fact has not been completely ensured yet, an ethical concern about whether hiPSCs are ready to be employed or not must be taken into consideration.

Producing germ cells from hiPSCs: As soon as iPSCs discovery was made, scientists began to think in the possibility of differentiating these cells into germ cells to use them for artificial reproduction. In fact, this was done for the first time in 2007, proving the feasibility of the process[83]. As a consequence of this, humanity had for the first time the possibility of using germ cells derived from hiPSCs to produce offspring. This, at first glance, could seem a very valuable tool to meet the demands of infertile couples and homosexual couples who want to have genetically related children. But, with the current genetic modification tools, it also raises a more intricate situation that is the possibility of selecting particular types of germ cells for reproduction in order to obtain offspring with desired phenotypic traits. However, even before entering in the thorny field of artificial human selection, there are other more pressing problems. Techniques to produce artificial germ cells from

hiPSCs are still in an early stage of development, with many technical problems that need to be solved before even considering the possibility to translate them to reality. To improve these techniques to that point, many germ cell lines should be produced, and many of them should be used for fertilization to produce embryos. Obviously, while the full efficiency of these techniques is not achieved, many of those embryos would be discarded since they would be generated by defective germ cells, implying the destruction of embryos, that is exactly one of the most important ethical issues that is pretended to be avoided with the technology of hiPSCs[79].

Elaboration and understanding of informed consent: With the appearance of the hiPSCs, new ethical concerns arose regarding their future use in clinic. It has been always clear that patients/donors have the right to know the use in what their cells are going to be involved. Every little piece of information not mentioned may be an important point for the donor. The use of the cells in animal experimentation, the possibility of failure in the experiments/trials that may cause some harmful outcome, etc. may be a reason for the donor to rectify his decision of donating cells. In summary, the patients´ full understanding of the basics in the iPSCs field and the use that will be given to their cells is critical when elaborating an informed consent for a project that involves hiPSCs. There is an interesting work from 2016 where authors tried to elucidate the understanding in iPSCs of patients that were going to donate skin biopsies for hiPSC research. Surprisingly, 91.5% of participants believed they knew what a stem cell was, but only 16.1%[84] answered correctly to all the questions related to stem cell properties when they were asked about filling a questionnaire about them. This

reveals a quite important gap of ignorance about stem cells and iPSCs in the population in general. In light of these data, it is quite clear that easily understanding and comprehensive informed consent involving the use of hiPSCs must be elaborated to ensure ongoing ethical progress of hiPSCs trials and biobanking.

3. STEM CELLS AND CELL THERAPY IN STROKE

3.1. Introduction

From the beginning, since the capacity of differentiation and self-renewal of stem cells became known, their use as cell therapy for a wide range of diseases has always been considered. In the last decades, researchers all over the world have highly focused on translate all the potential benefits of the stem cells into clinics, starting a revolution that led to several important discoveries that step by step are paving the way to convert cell therapy into real[85]. As previously mentioned, in 2006, with the major discovery made by Yamanaka and Takahasi, it was possible for the first time to get iPSCs reprogrammed from adult somatic cells. With this achievement, not only the possibility of bypassing the ethical issues concerning hESCs was gained, but also the possibility of autotransplants of tissues formed from hiPSCs of each patient. This way, the immune rejection that occurs in allogenic transplants would be avoided[86, 87].

In the field of neurology, this discovery supposed a new promising approach to several neurological diseases. Alzheimer[88, 89], Parkinson[90, 91] or ALS[92] are some of the diseases that have seen progress in their study thanks to the use of iPSCs. In these pathologies, iPSCs have been used

to generate neuronal cell lines to recapitulate and study the mechanics of the disease in *in vitro* models or to evaluate their neurorecovery capability (see Fig. 11). In the field of stroke, like other stem cells, iPSCs have been used as a neuroprotective cell therapy (mainly based on their immunomodulatory capacity) or as a neuroreparative therapy (by inducing neurogenesis, angiogenesis, synaptogenesis, modulation of the immune response or transdifferentiation). Beside its neuroprotective or neuroreparative application, the use of iPSCs for stroke modeling has been poorly exploited mainly because this is a neurological pathology with multiple affected cells types and reduced genetic component, compared to other neurological diseases as Alzheimer´s or Parkinson´s. However, the use of hiPSCs has been recently explored to model neurovascular genetic diseases associated with risk of stroke[42, 93], opening a promising approach in the study of these neurovascular diseases.

Stroke, resulting from the interruption of blood supply to the brain, is the leading cause of disability and death in the world within neurological diseases despite a decrease in its mortality rate[94]. Regarding the infarcted area, it is differentiated into the lesion core (dead and unrecoverable tissue) and the area of ischemic penumbra (affected but potentially recoverable zone)[95]. The need of new therapies that may report some kind of benefit in this disease is becoming more and more pressing as global life expectancy continues to rise. Pharmacological or mechanical reperfusion therapies are the most effective treatments during the acute phase of ischemic stroke and it is associated with good outcome in 50–70% of cases. However, these treatments are only applicable to <20% of patients because of the short therapeutic window

and side effects[96]. Besides, in the last 20-25 years, barely a 4% of all the potential drugs that reported some benefit in preclinical experiments have reached the market, overcoming clinical trials[97]. This is due to two main reasons: bias and deficiencies on the design of experiments and reporting results[98] and above all, the already mentioned phylogenetic gap between the species (where the drugs are tested) and the humans. This last reason could be overcome by using hiPSCs or adult stem cells, directly obtained or derived from the hiPSCs of the own patient, like neural stem cells (NSCs) or mesenchymal stem cells (MSCs).

In the field of stroke, the main objective is to reduce the damage within the injured area, more than to repair certain types of cells. Because of this, the approach with hiPSCs is different than in other neurological diseases. On this case, the cell modeling is relegated to very specific cases, with diseases that include among their symptoms the occurrence of stroke and that have a strong genetic component[42]. Stem cell-based therapies have emerged as a promising tool for the treatment of both acute and delayed phases of stroke owing to their multipotentiality, ability to release growth factors, and immunomodulatory capacities (Fig. 13). Thus, this transdifferentiation is able to produce cells with a neural lineage, to induce neurogenesis, angiogenesis and synaptogenesis, and to activate endogenous restorative processes through the production of cytokines and trophic factors. This approach is done by direct administration through several routes of hiPSCs or adult stem cells.

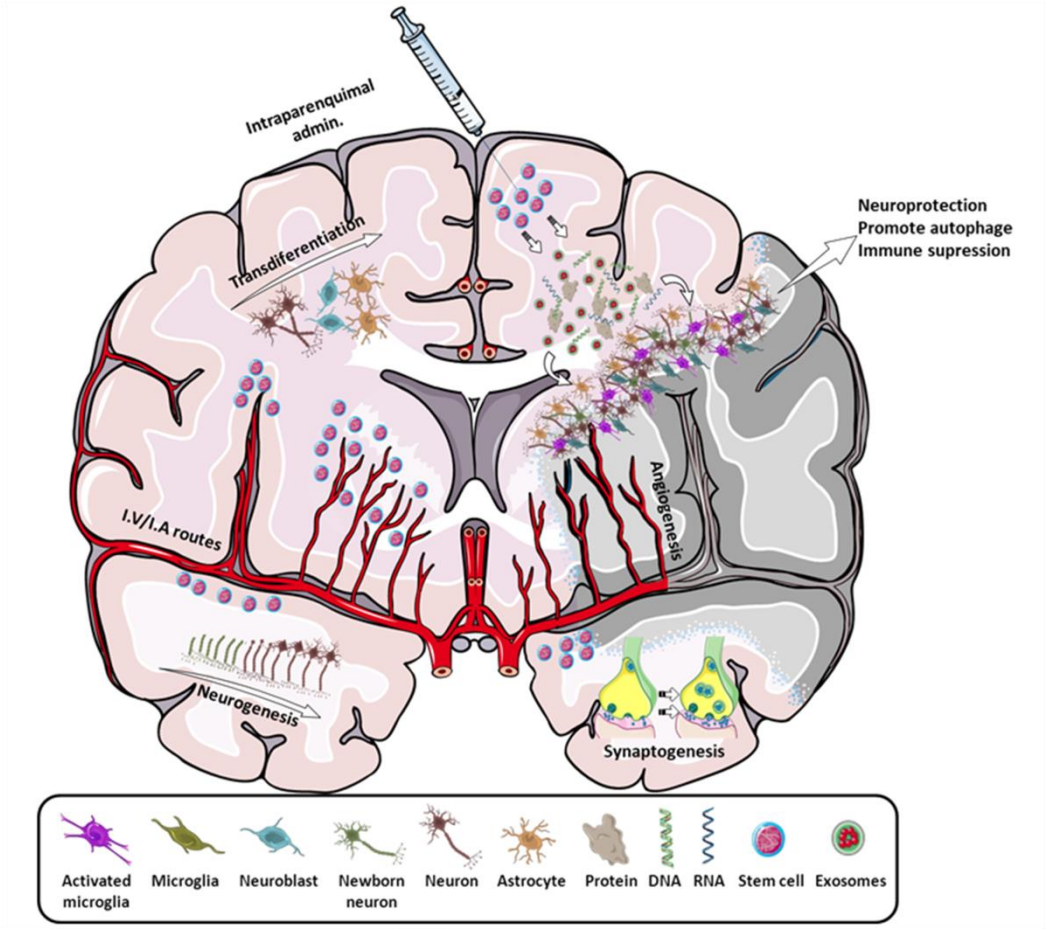

Figure 13. Scheme of all the main effects promoted by stem cells in stroke. By intraparenchymal injection or i.v/i.a routes, stem cells induce neurogenesis, transdifferentiation, angiogenesis, synaptogenesis and immune modulation by attracting or releasing trophic substances to the infarcted area. Self-created image (using elements with Creative Common license).

Nowadays, the therapy with hiPSCs is yet on preclinical experimentation. Year after year, more is known about their mechanisms and the ways to derive them to specific cell types[99-101]. There are a lot of diseases which would potentially benefit from the effective application of this technology. However, in part because it is a

relatively recent discovery, the use of hiPSCs and the establishment of consolidated cell therapies have been delayed due to several issues: the presence of an optimal time window for these therapies, possible adverse effects (tumorigenicity, stroke…) caused by the transplanted cells, a limited source of engraftable cells, and an inherited limitation of adult stem cell potential[102].

Regarding stroke, the main problems of the therapy with hiPSCs concern whether an authentic cell renewal and/or replacement occurs when the hiPSCs are transplanted[103], the disappearance of transplanted cells few weeks after their implantation in several cases,[104] and the possibility of tumorigenicity after reaching and engrafting within the brain[105]. These are the reasons why on the field of this disease, the use of hiPSCs has been replaced by the use of adult stem cells, whose action focuses more on a recovery by repairing damaged tissue, thanks to the release of various active substances and repairing molecules that enhance neurorepairing, angiogenesis, synaptogenesis and neurogenesis. This, added to the boom in the creation of several biomaterials is supposing an advance and maturation in the field of the stem cells as cell therapy. The biomaterials allow a higher efficiency in cell culture and hence a higher cell availability, and they also serve as a vehicle in the injection of cells[106].

In any case, independently of the stem cell chosen, all stem cell approaches share common walls to overcome before putting them into practice: cell dose, route of administration and cell fate and engraftment.

3.2. Methodology in stem cell administration.

Despite the special attention on stem cells as a promising therapeutic candidate for stroke, parameters such as administration route or cell dosage are still under discussion.

There are relatively few studies that have compared the different possible routes of administration of stem cells. The first studies that used stem cells for cerebrovascular diseases were looking for a neuronal replacement, so they chose an intraparenchymal injection as the most direct route for cell engraftment. These studies showed that the stem cells not only survived but they migrated to the affected zone[107, 108]. However, this choice is not the most suitable due to the need of opening a cranial window and also because it damages the brain parenchyma, which is not convenient for stroke patients.

The main alternative to this route of administration are the vascular routes, either intra-arterial (i.a.) or intravenous (i.v.), which are currently the most used for cell delivery. Intravenous injections are minimally invasive, and cell tracking studies following this route have shown that most administered cells remain trapped mainly in the lungs[109, 110] but also in liver[111] and spleen[112], indicating that a reduced number of cells reach the brain. On the other hand, i.a. administration is a promising strategy to direct the majority of injected cells to the brain, but this is a risky administration route and the fate of injected cells following this route remains unknown due to high variation in the reported results[113] (Fig. 14).

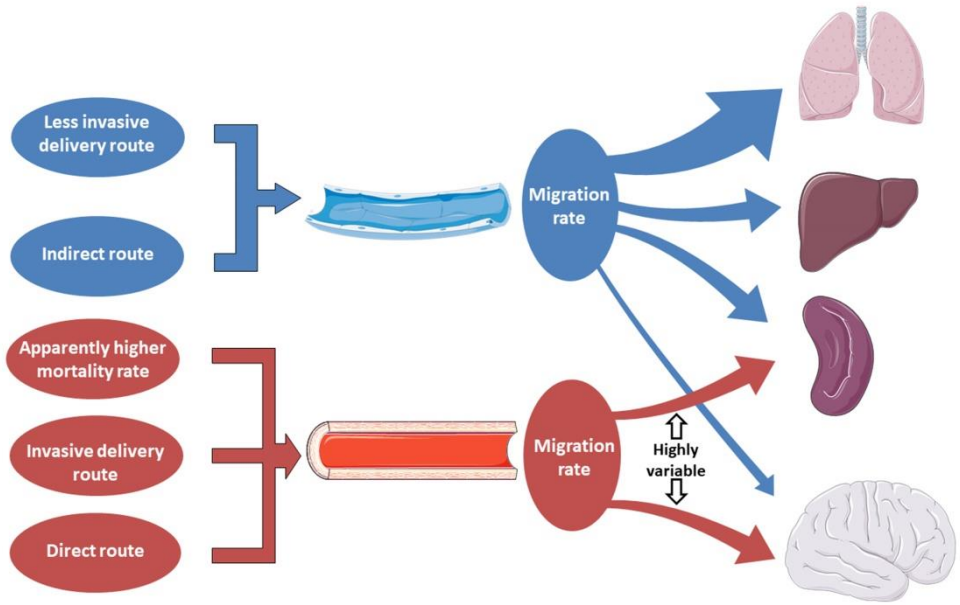

Figure 14. Scheme representing i.v (blue) and i.a (red) delivery main concerns. For migration rate, the thicker the arrow, the higher the migration rate. Self-created image (using elements with Creative Common license).

Whether one route is more efficient than the other is not clear and depends on the cell type used. Thus, in some studies it was found that the injection of neural progenitor cells (NPCs) by i.a. through the carotid artery presented a higher migration rate and a wider distribution pattern than i.v. administration. Nevertheless, the mortality rate for this i.a. delivery was significantly higher (41%) than in i.v. injection (8%)[114]. However, in other studies with bone marrow stem cells (BMSCs) and bone marrow mononuclear cells there was no greater mortality or greater recovery of infarct volume of one route respect to the other[115, 116].

The size of stem cells is also a critical parameter when passing through the lungs, and should be taken into consideration to decide the

best route of administration. As an example, when using MSCs, the majority of them get trapped in the lungs, while the NSCs have a pass-through rate two-fold higher[109].

Aimed to clarify the discrepancies about the best route for cell administration in stroke, there is a recent report that designed an experimental study to investigate whether MSCs were able to reach the brain following i.a. or i.v. administration after transient cerebral ischemia in rats, and to evaluate the therapeutic effects of both routes[113]. Based on its findings, the report concluded that MSCs were found in the brain following i.a. but not i.v. administration in ischemic rats. However, the i.a. route increased the risk of cerebral lesions (microstrokes) (Fig. 15), mainly because of the MSCs can get trapped inside blood vessels (Fig.16), and did not improve functional recovery, while the i.v. delivery produced functional recovery and was safe but MCSs did not reach the brain tissue. This fact implies that treatment benefits are not attributable to brain MCS engrafting after stroke[113].

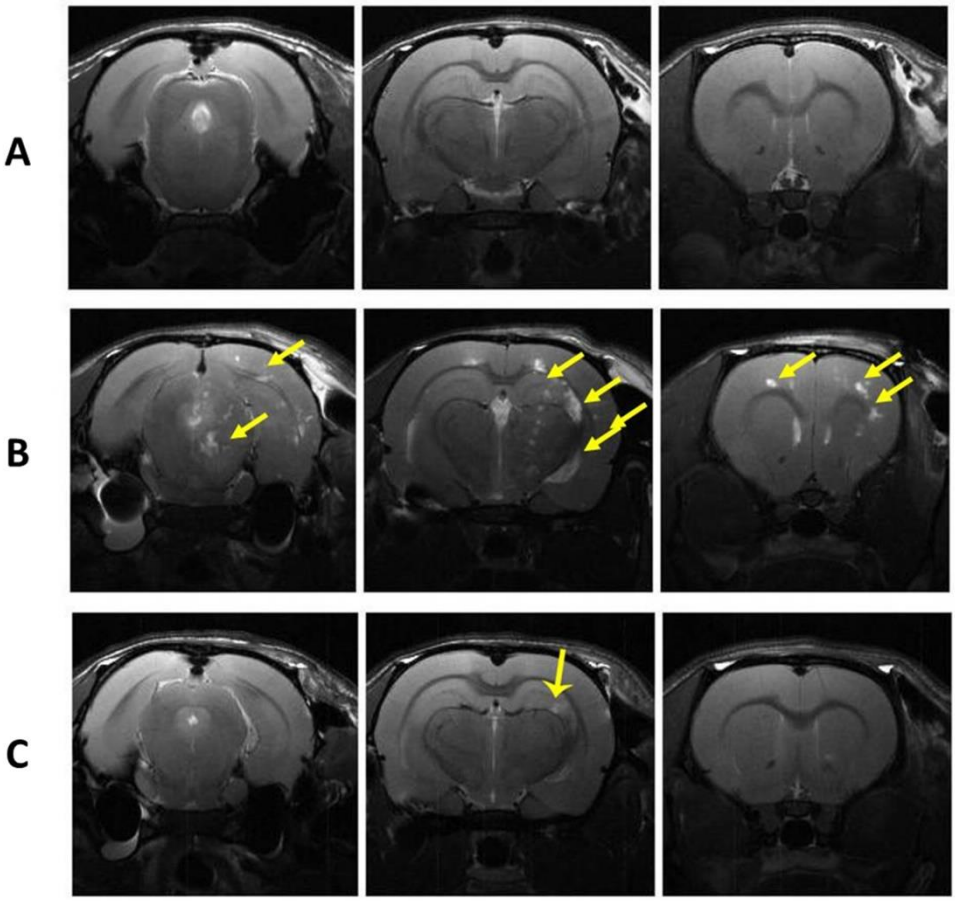

Fig. 15. MR T2-weighted images of several mouse brain slices 24 h after i.a PBS administration (A), $1x10^6$ MSCs i.a administration (B) and $0.25x10^6$ MSCs i.a administration. Multifocal ischemia (indicated with yellow arrows) is observed all along the brain after the administration of $1x10^6$ MSCs. For the administration of $0.25x10^6$ cells, the number of micro-ischemias is significantly reduced compared with the $1x10^6$ cell administration. Source: Argibay et al, *Sci Rep* (2017). Original images from the author´s laboratory.

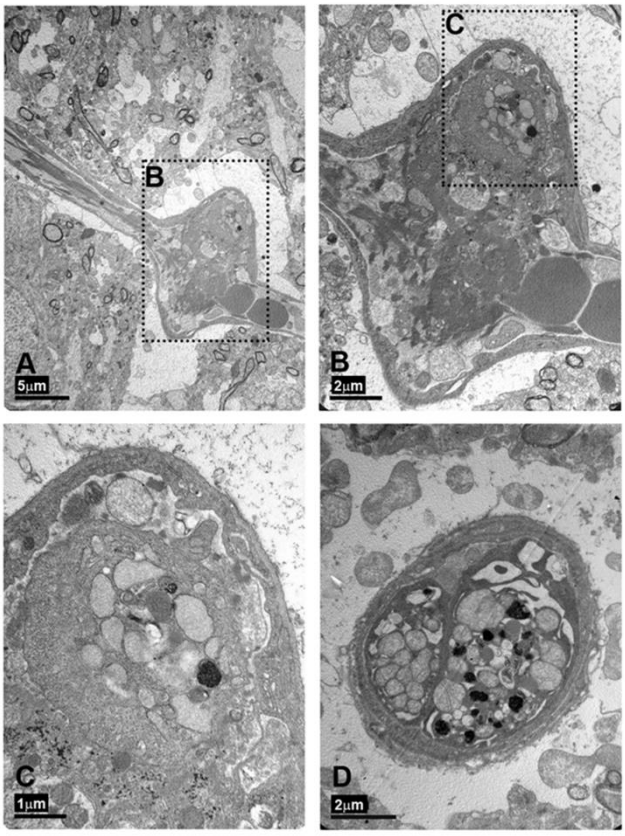

Fig. 16. Electron transmission micrograph of rat brain cortex after i.a delivery of dextran-coated labeled MSCs. A: Dilated brain vessel surrounded by neuropil. B: Magnification of vessel dilation in A. C: Magnification the upper vessel expansion in B. One well-defined MSC is identified by the encapsulated nanoparticles. D: Longitudinal section of a brain vesse where two labeled MSCs can be observed. Nanoparticles are noted by dark punctate patterns. Source: Argibay et al, *Sci Rep* (2017). Original images from the author´s laboratory.

Cell dose is another issue to take into account for both i.a. and i.v. administration which has not been very well elucidated yet. In line with other studies, we have estimated that doses higher than 10^5-$0.25x10^6$ cell/mL administered i.a. as bolus infusion increase significantly the risk of arterial occlusion[113, 117], while other studies have estimated that doses to $3x10^7$ cells are safe[115, 116].

3.3. Stem cell fate and engraftment

Together with the need of choosing properly the route of administration, it is equally important that cells reach the brain and graft successfully in the right place. Also, they need to be able to survive enough time to exert their repairing and healing properties. Indeed, this cellular engraftment and the cell fate suppose a key and controversial issue. It is critical in the sense that it has little value being able to vectorize cells to the brain if after that it is not possible to know what it is happening, where the cells go once they reach the brain or what is their behavior. And it is controversial since there are reports showing different results regarding these subjects[104, 118]. To this regard, there are some quite coherent researches that try to shed light to these issues. In 2012, Kokaia et al. performed a follow up of iPSCs-derived NSCs of up to 4 months transplanted into brain striatum and cortex of rats and mice subjected to stroke. They found a sensorimotor recovery after 1 week, and regarding cell fate and viability they found that engrafted cells survive for up to 4 months without forming tumors. Also, most of the cells had differentiated to neurons able to form axonal prolongations. In line with this, the proliferative capacity of these engrafted cells diminishes from 40% at 2 weeks to 8% and 0.5% at 2 and 4 months respectively, probably due to this NSCs differentiation to neurons[118].

On the other hand, other studies with MSCs have shown instead that the possibility of direct differentiation and/or direct replacement of the damaged tissue by these cells are less likely to occur, given that they do not present the voltage-gated ion channels that are present in the functional nerve cells[119]. Instead, their repairing effects are due more to their ability of attracting and releasing different trophic factors. Besides, it has been seen that BMSCs engraft at the ischemic penumbra an at the subventricular zone[120]. Also, they may be able to migrate to several regions under specific stimuli[121].

Nowadays, cell targeting with contrast agents for its follow-up by magnetic resonance imaging (MRI) it is being established as a powerful technology that is shedding light to the problem. In 2014, a research group reported the follow-up of NSCs by MRI for up to 1 year after cell transplantation, marking NSCs with the fluorescent dye PKH26[122]. Furthermore, they have also successfully tried the use of contrast agents such as fluorine-19[123] and gadolinium[124] without causing any kind of interference nor in cell viability nor in the migration capacity. Another research group labeled MSCs with dextrane-coated superparamagnetic nanoparticles (D-MNPs). Furthermore, they were able to deliver them to the brain and detect them by MRI imaging[113] (Fig. 17).

Fig. 17. MR T2* weighted image of one brain slice of a rat after i.a administration of $1x10^6$ MSCs labeled with D-MNPs. Labeled cells can be observed as punctate patterns in the right hemisphere of the animal. Source: Argibay et al, *Sci Rep* (2017). Original images from the author´s laboratory.

However, in order to achieve a correct implementation of this technology, a precise estimation of the cell quantity threshold needed to detect labeled cells at beginning and also over time, once the signal begin to fade due to cell divisions is critical. Also, another unsolved issue is the difficulty of discriminating between the initial labeled cells and the endogenous cells that may incorporate contrast agent molecules expelled by exocytosis by the initially labeled cells.

3.4. Stem cells in stroke

While the technology of the iPSCs is quite new and deeper studies are being carried out to know its real translationality, studies with adult stem cells have been performed for much longer, and there is more information about their use in cell therapy in stroke. Furthermore, there are already clinical trials going on and even closed and with results. Focusing on stroke, the stem cells most frequently used are the MSCs, due to their great trophic capabilities, and the NSCs, because of their lineage proximity to the affected cell types in stroke.

3.4.1. MESENCHYMAL STEM CELLS

The MSCs are pluripotent stem cells that are found, in small proportion, inside the bone marrow. These cells have the ability to differentiate into different cell type precursors (chondrocytes, osteocytes, myocytes…) but their use in cell therapy is based on their ability to release a wide range of bioactive molecules, with immunoregulatory and regenerative properties [125] (Fig. 18).

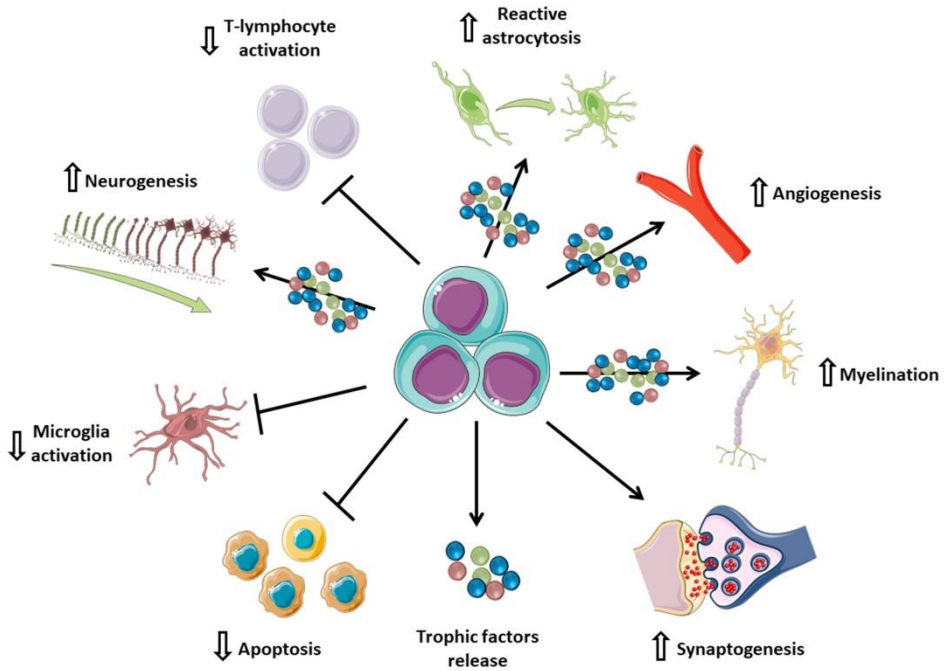

Fig. 18. MSCs properties.

MSCs are one of the most used stem cells in literature and of which more benefits have been reported in different stroke studies. MSCs are pluripotent stem cells that are found, in small proportion, inside the bone marrow. These cells have the ability to differentiate into different cell type precursors (chondrocytes, osteocytes, myocytes…) but their use in cell therapy is mainly based on their ability to release a wide range of bioactive molecules, with immunoregulatory and regenerative properties[125]. However, one of the main causes that has limited the advance of MSCs in stroke and other neurological diseases has been the arduous protocols that are sometimes required to obtain, expand and characterize human MSCs for clinical use[126].

Among the MSCs, due to their great regenerative potential and tissue engineering, the BMSCs are the most promising ones[125, 127]. It has been shown that the i.v. administration of BMSC 24 h after stroke induces angiogenesis within the surrounding lesion area in rats. This angiogenesis is mainly due to an increase in VEGF secretion by the BMSCs, and $VEGFR_2$ expression in cerebral endothelial cells[128]. Also, these BMSCs are able to induce the proliferation of endogenous neural stem cells[129]. BMSCs also have a neuroplasticity function, induced by the release of trophic factors within the affected region, enhancing restructuration processes[130]. Although the specific repairing mechanisms for all the aforementioned healing effects of the BMSCs (and MSCs in general) still remain quite unclear, it is well known that their ability of releasing high amounts of extracellular vesicles is the main pathway by which they exert these effects[131-133].

However, despite BMSCs seem an interesting tool for the treatment of stroke, these cells present ethical issues and difficulties in order to acquire them. Comparing to BMSCs, the adipose tissue-derived mesenchymal stem cells (ADMSCs) come from a more accessible source and they are more abundant. Also, they have already proved their effectiveness in stroke preclinical experiments, specifically as a promising treatment for stroke associated comorbidities[134].

Although the use of ADMSCs is less studied, there are works that show positive effects by using them. In a report from 2013, the effect of BMSCs versus ADMSCs was compared. Neither for BMSCs nor for ADMSCs there was reduction in infarct size or any cellular migration or engraftment. Still, for both cases, it was found a reduction in cell death and an increase in the proliferation rate with an increment in the levels

of VEGF, oligodendrocytes, synaptophysin and neurofilaments at day 14[135]. These results show that ADMSCs present the same regenerative abilities than BMSCs, but since the source of acquisition of the ADMSCs is better, maybe the use of these stem cells could be more suitable. Regarding the way ADMSCs exert their regenerative properties, it seems that it is due to the exosomes in the same way as it happens for BMSCs. In a study from 2016, it was proved that an intravenous injection of isolated exosomes from ADMSCs produced a greater infarct size reduction in rats subjected to 50' of middle cerebral artery occlusion than the injection of just ADMSCs[136]. Also, the safety of the ADMSCs has also been tested. A study in 2011 proved that an intravenous injection of ADMSCs in immunodeficient mice didn´t produce any toxicity effect all along 13 weeks, even at the highest cell dose ($2.5x10^8$cells/kg body weight). In the same way, they tested the possibility of tumor formation along 26 weeks, but they also didn´t find no evidence of tumorigenesis not even at the highest dose ($2x10^8$cells/kg). In a follow-up of 3 months to patients with spinal cord injury to which a single dose of hADMSCs ($4x10^8$cells) was administered, again no evidences of any adverse effect was found[137].

On the other side, the administration of MSCs in hemorrhagic stroke models seems to induce also neuroprotective effects during the acute phase of the lesion[138] and functional recovery when cells are administered at long term[139]. Moreover, MSCs has been tested in combination with recombinant tissue plasminogen activator to prevent the risk of hemorrhagic events thanks to the ability of the cells to inhibit endothelial dysfunction[140].

MSCs are also prone to cell engineering; for instance, excitatory amino acid transporter-2 (EAAT2) plays a pivotal role in glutamate clearance in the adult brain, thereby preventing excitotoxic effects after cerebral ischemic damage. Considering the high efficacy of EAAT2 for glutamate uptake, it exists the possibility of inducing the expression of this transporter in MSCs for systemic administration, combining the intrinsic properties of these cells with excitotoxic protection (Fig. 19)[141].

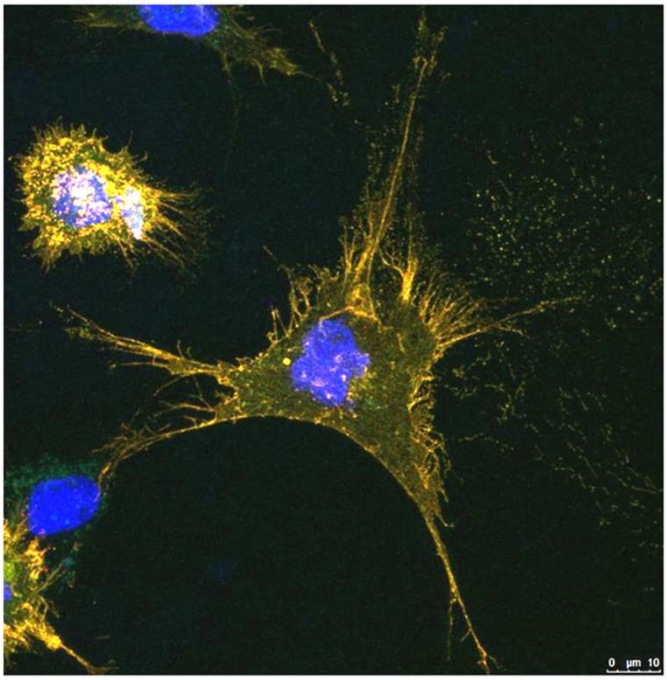

Fig. 19. MSC transfected with a yellow fluorescent protein-EAAT2 construct. Source: Pérez-Mato M et al, *EBioMedicine* (2019). Original images from the author´s laboratory.

3.4.2. NEURAL STEM CELLS

NSCs are adult stem cells present at the central nervous system that are able of self-renew and give birth to new neurons and glial cells, thus contributing to the plasticity and brain repair[142]. These processes are enhanced within ischemic brain as a neurorepairing mechanism[143, 144]. However, these processes do not occur at a rate high enough to be effective [145]. Because of that, several approaches in preclinical studies have been performed in order to compensate or supplement these endogenous mechanisms. The most used approach consists of the administration of exogenous NSCs[146, 147]. This approach has shown that i.a. administration of NSCs 24 h after stroke, in a mouse model, promotes a reduction on the inflammatory process and also reduces the BBB damage[148]. This reduction of the inflammatory process was also seen in a pig stroke model, also by intraparenchymal injection, but 5 days after stroke[149]. Nevertheless, the total percentage of NSCs that successfully migrate and engraft within the ischemic area is quite low. To this respect, genetic modifications that may make the cells more resistant to ischemic conditions[150, 151] would rise this percentage, such as the use of NSCs submitted to pre-conditioning conditions before administration[152, 153] or to release them with various biomaterials as vehicles[106, 154]. NSCs derived from hiPSCs have been also tested in rodent stroke models. The cells did not reduce stroke volume or improve behavioral recovery during the month following transplantation, but no tumor formation was observed[155]. Regarding intracerebral hemorrhages there are fewer studies, but they report improvements in functional performance after 2-8 weeks, independently of the administration route[156, 157].

3.4.3. CLINICAL TRIALS

Currently, there are no clinical trials for stroke with hiPSCs. This is due to the fact that the hiPSCs are yet in a relatively early stage of study, and that they present several problems yet to solve and previously described regarding their safety.

However, in the last decade different clinical trials have been carried out or are being carried out all over the world, mainly with mesenchymal stem cells (Table 1). These trials are shedding light about quantities, routes of administration and efficacy at different times with stem cells, as well as their safety. Nevertheless, they are in general small trials, waiting for their expansion or the creation of new and bigger ones, with a higher recruitment capacity, that may corroborate the results obtained by these pioneering trials. While these trials are not set up, the optimal conditions for the stem cell application in clinic (dosage, route of administration, therapeutic window, safety…) will be discussed.

Name of trial	Patient	Cells	Time	Dosage (cells)	Deliver	Efficacy
Intraarterial stem cells in subacute ischemic stroke (NCT00761982)	Subacute MCA stroke n=20 (n=10)	BM-MNCs	5-9 d	1.59x10⁶cells at 0.5 to 1mL/min	I.A.	Inconclusive
Stem cell therapy for acute ischemic stroke patients (InVeST) (NCT0150177)	Subacute stroke n=120 (n=58)	BMSCs	18.5 d	2.8x10⁸ cells	I.V	No
Reparative therapy for acute ischemic stroke with allogeneic mesenchymal stem cells from adipose tissue: a safety assessment (NCT01678534)	Acute stroke n=20 (n=10)	MSCs	≤2 w	1x10⁶ cells/kg at 4-6mL/min	I.V	↑Neurological outcomes
Safety/Feasibility of Autologous Mononuclear Bone Marrow Cells in Stroke Patients (NCT00859014)	Acute MCA stroke N=10	BM-MNCs	24-72 h	7x10⁶ to 1x10⁷ cells/kg over 30 min	I.V	Inconclusive
Intravenous transplantation of mesenchymal stem cells preconditioned with early phase stroke serum: current evidence and study protocol for a randomized trial STARTING-2 (NCT01716481)	Acute and chronic stroke n=60 (n=40)	MSCs	≤90 d	1x10⁶ cell/kg	I.V	Going on
Safety and efficacy of multipotent adult progenitor cells in acute ischaemic stroke (MASTERS): a randomised, double-blind, placebo-controlled, phase 2 trial (NCT01436487)	Acute stroke n=129 (n=67)	MAPC	24-48 h	4x10⁸ or 12x10⁸ cells	I.V	No
Intra-Arterial Immunoselected CD34+ Stem Cells for Acute Ischemic Stroke (NCT00535197)	Severe anterior circulation stroke n=5	Autologous immunoselected CD34+ stem/progenitor cells	≤7 d	1x10⁸ cells over 10 min	I.A	↑Clinical outcomes
Human neural stem cells in patients with chronic ischaemic stroke (PISCES): a phase 1, first-in-man study (NCT01151124)	Stable disability after stroke n=13 (n=11)	CTX0E03	6-60 m	2x10⁸, 5x10⁸, 10x10⁸, 20x10⁸ cells at 5µL/min	Putamen	↑NIHSS
Clinical outcomes of transplanted modified bone marrow-derived mesenchymal stem cells in stroke: a phase 1/2a trial (NCT01287936)	Stable, chronic stroke n=18	BMSCs	6-60 m	2.5x10⁸, 5x10⁸, 10x10⁸ cells. Deposits of 20µL of cells over 10 min each	Peri-infarct zone	↑Clinical outcomes endpoints

Table 1. Main clinical trials carried out in the last years. n= number of total patients. (n)= number of patients that received treatment. If there is no (n), all patients received tratment. Original table. Data collected from the web clinicaltrials.gov.

3.5. iPSCs in stroke

On the first years after Yamanaka and Takahashi iPSC research, the experiments and preclinical studies on stroke assayed the effect of a direct injection of iPSCs into the affected region. Several studies reported improvements both in infarct volume reduction and in functional recovery[158-160]. Also, improvements in the neurological function and survival rate in hemorrhagic stroke were reported[161]. However, most of these improvements attributed to the iPSCs were really due to a differentiation of these iPSCs into different adult stem cells on the affected region, which were the ones that really performed the repairing and beneficial effects[162, 163].

Moreover, one of the main problems of these studies in order to achieve a future translationality to the clinic was the formation of teratomas or tumorigenicity along the weeks. This is due to environmental effects of the niche where the iPSCs are implanted. These effects can induce a malignant transformation of this iPSCs. Formation of teratomas can also occur by transformation of residual iPSCs that remain on the area and that can become benign teratomas after some time[105, 164]. To this respect, there are some studies that tried to solve this issue. A study compared the formation of teratomas after the injection of iPSCs with and without fibrin glue as vehicular agent into the subdural region instead of its injection right into the cortex. In the injection of iPSCs by themselves, there was always formation of teratomas after 4 weeks whereas in the ones injected with fibrin glue there was not. The authors pointed that this was not only due to the fibrin glue, but also because the subdural region was not a niche appropriate enough to induce an uncontrolled growth of the iPSCs[159].

Besides, another study showed the possibility of inhibiting the formation of tumors due to this residual iPSCs by treatments with inhibitors of specific pro-apoptotic routes of stem cells, inducing their apoptosis and erasing them, while the derived differentiated cells survived and maintained their functionality[164].

However, a faster way to address these problems is the culture of iPSCs *in vitro* for their differentiation into the cell precursors needed (neuronal, epithelial…) and their administration.

4. CADASIL

4.1. Introduction

Within the field of stroke, 25-30% of them are caused by cerebral small vessel diseases (SVDs). Although stroke is a well-studied disease and its mechanisms and underlying processes are well known, there are some diseases that may be the cause of cerebral infarcts like SVDs, which present a lack of approaches and understanding[165]. Despite the impact that these SVDs have on the brain, nowadays there are no specific treatments for them. Furthermore, there are limited therapeutic options for secondary prevention compared with those other common causes of stroke. This causes that nowadays there are no solutions or treatments for them, even being a cause in many cases of the onset of stroke. The few studies that are carried out on these diseases focus on the study of monogenic variants of SVDs, in order to provide valuable insights into the molecular mechanisms underpinning idiopathic SVDs.

One of these variants is CADASIL, the most complex form of SVD. This disease presents degeneration of smooth muscle cells in the tunica

media, narrowing of the lumen and thickening of the vessel walls in small vessels, which leads to leukoencephalopathies that can be observed and used as diagnosis by several imaging techniques (Fig. 20-21), microbleeds due to microangiopathies (Fig. 22), narrowing of the lumen, dilated perivascular spaces and subcortical and cortical atrophy[166]. In consequence, CADASIL patients develop leukoencephalopathy, migraines with aura, recurrent ischemic strokes, motor disability and dementia as main symptoms (Fig. 23).

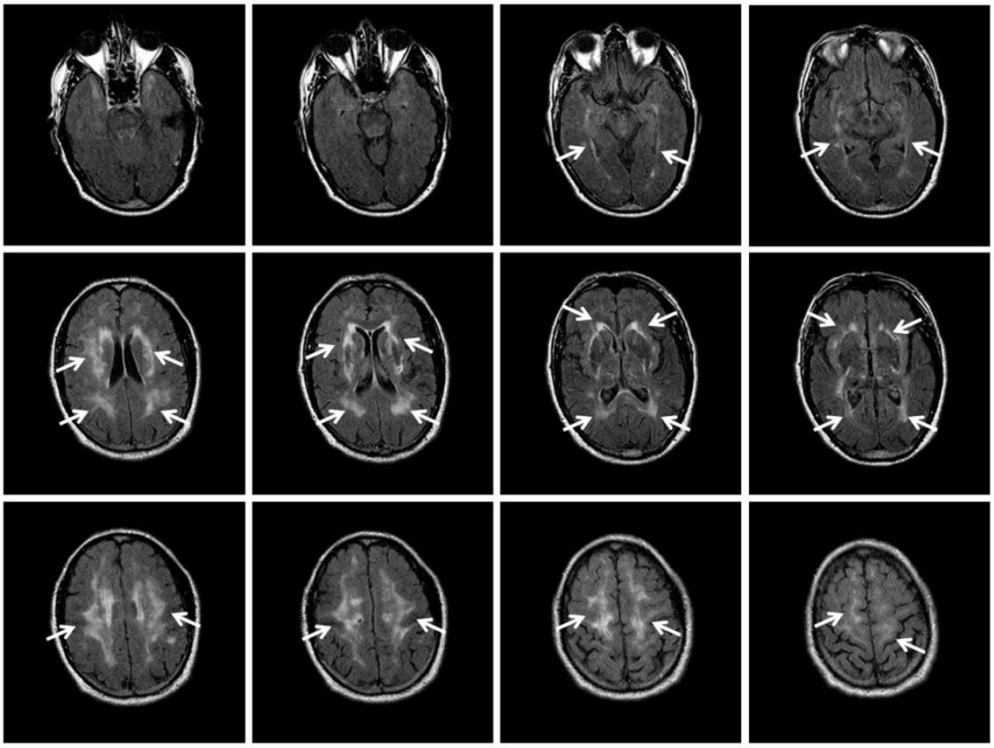

Fig. 20. FLAIR-weighted axial MRI images from the brain of a patient diagnosed with CADASIL. White arrows indicate regions with white matter alterations. Images kindly provided by the Neurology Department of the Hospital La Princesa.

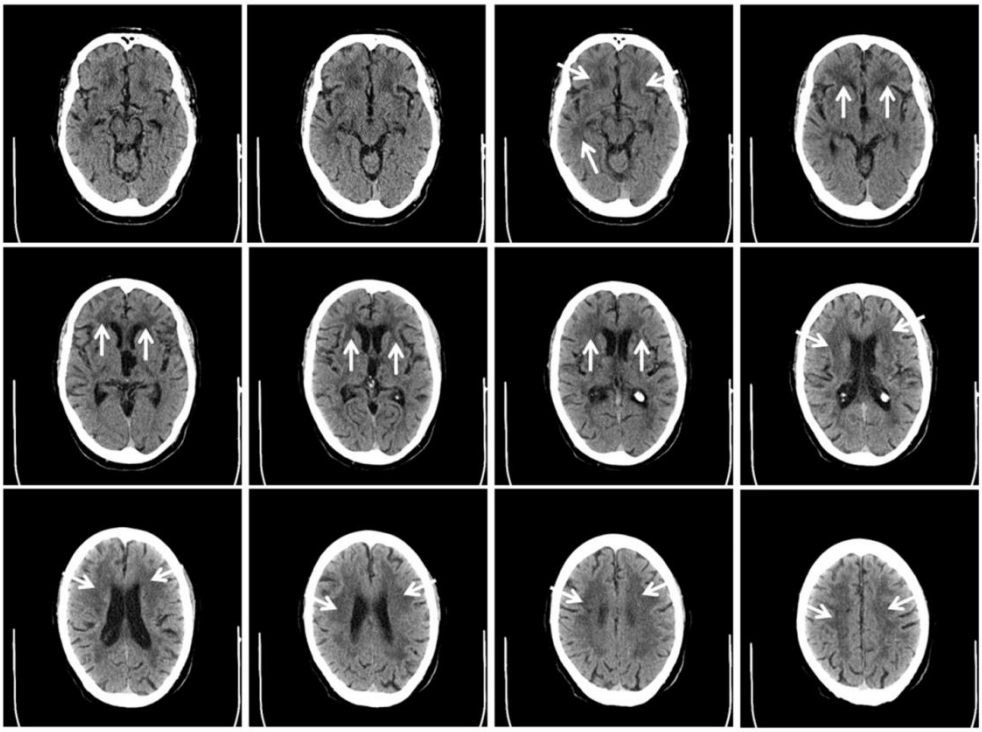

Fig. 21. CT axial images from the brain of a patient diagnosed with CADASIL. White arrows indicate regions with white matter alterations. Images kindly provided by the Neurology Department of the Hospital La Princesa.

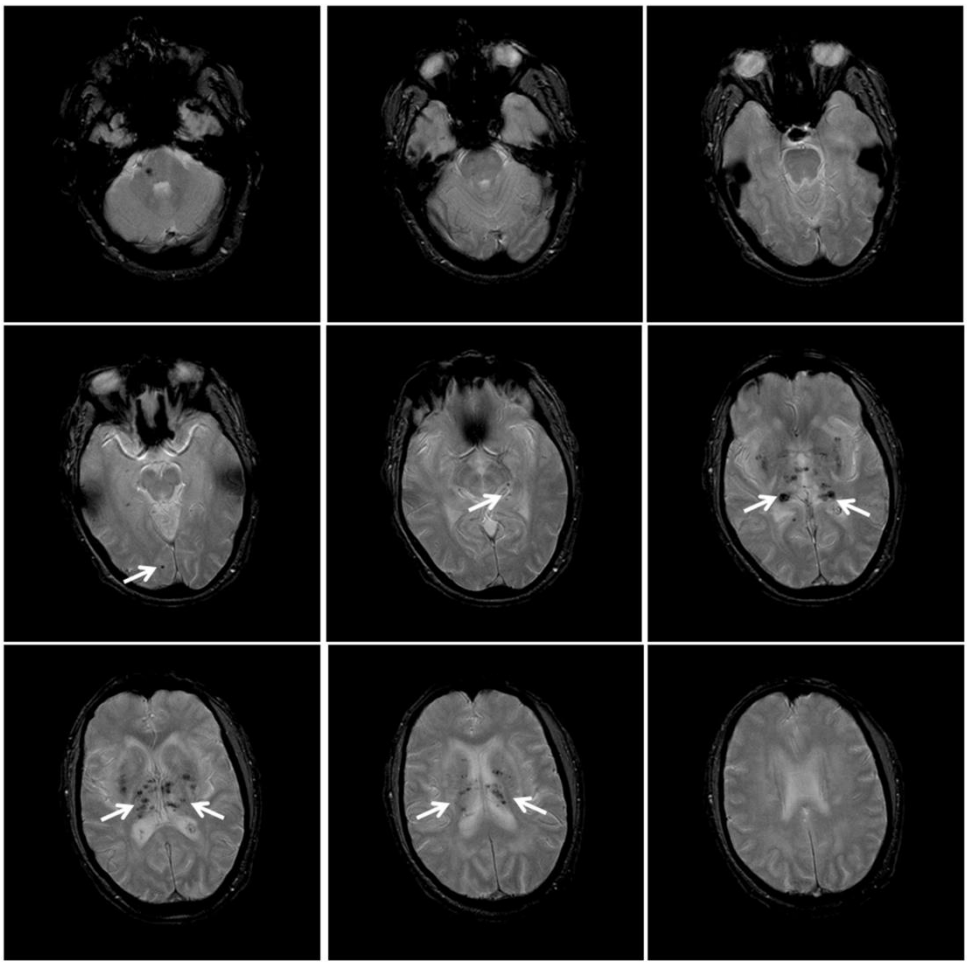

Fig. 22. T2-weighted MRI axial images from the brain of a patient diagnosed with CADASIL. White arrows indicate microangiopathies. Images kindly provided by the Neurology Department of the Hospital La Princesa.

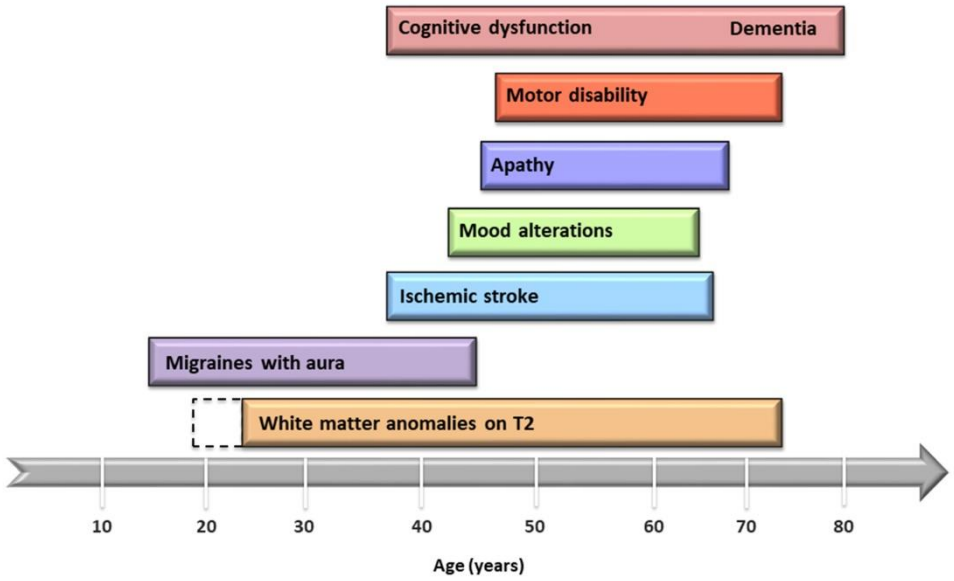

Figure 23. Approximate timeline with CADASIL symptoms appearance. Self-created image adapted from Chabriath et al, *Lancet Neurol* (2009)[167].

In CADASIL, the *NOTCH3* gene, located at the short arm of the chromosome 19(19p13.2-p13.1), presents a mutation in one of its exons, a loss or a gain of a cysteine residue. This mutation leads to an incorrect process of the metabolic pathway when the signal is triggered, which ends with the accumulation of the extracellular domain of the protein in deposits of granular osmiophilic material (GOM)[168, 169]. Thus, as the progressive weakness of the small brain vessels coincides spatially with GOM accumulation, some studies point that the continuous aberrant accumulation of the extracellular component of the NOTCH3 protein at the membrane is the main cause of the formation of this GOM, causing the vessel weakness[168]. However, as it will be further discussed, it is not so clear whether this accumulation is what really causes this weakness and progressively the disease or if it is the

aberrant NOTCH3 signaling which causes it, through this GOM accumulation as one of the pathways.

Regarding to the NOTCH3 protein, it is constituted by 2321 amino acids. This protein is a transmembrane protein that belongs to a family of highly conserved NOTCH receptors[170]. On this family there are four NOTCH receptor variants (NOTCH1 to NOTCH4), all of them sharing the same structure: an extracellular domain that binds non-covalently to an intracellular domain through a transmembrane domain, where it is also located a negative regulatory region (NRR). The ligands of these receptors vary between them, but they are always a combination of this five: Jagged 1-2 and Delta-like 1, 3 and 4[171, 172]. In the case of NOTCH3, these are Jagged 1 and Delta-like 4.

Although there are several mouse models of CADASIL[169] (knockouts for several and different mutations), it has been impossible to find any solution to the progressive accumulation of the NOTCH3 extracellular domain (NECD). The affected cell type in CADASIL is the vascular smooth muscle cell (vSMC). Nowadays it is well known that this cell type is the one that suffers the consequences of the NOTCH3 mutation. However, in the vessels, vSMCs and vascular endothelial cells (vECs) do not function independently in arteries and the possibility that there could be some disruption in the communication between these two cell types has not been studied yet. With cell modeling, it would be possible to generate these cell types from hiPSCs reprogrammed from adult somatic cells of a CADASIL patient and perform mono and co-cultures that would allow to study and understand better the molecular mechanisms of this disease and clarify the confusing and sometimes contradictory information that the mouse models provide[169].

4.2. CADASIL in clinic

CADASIL has a relatively short clinical history. In 1991 the clinical picture associated to this disease was first defined[173] and in 1993 the name of CADASIL was coined when mutations were mapped for the first time to chromosome 19[174]. Three years later, in 1996, *NOTCH3* mutation was associated with the disease[175].

CADASIL has no treatment nowadays, and the life expectancy of the patients is 64.6 years in men and 70.7 years in women. Currently, research is being directed towards the search of possible disease modifying strategies in order to mitigate clinical manifestations. At the moment, the very few studies that have already reported results are focused mainly on symptomatic outcomes and in cerebral and peripheral blood flow changes[176].

As a preventive approach, it is important to control vascular risk factors, specially smoking and hypertension. It is also common to use antiplatelet drugs such as clopidogrel or aspirin. To this regard, when treating CADASIL with antiplatelet drugs, the majority of neurologists apply the guidelines followed for sporadic stroke, although whether this application is appropriate or not is yet to determine. In fact, the thrombotic origin of ischemic stroke in this disease has not been proven yet. Also, in many cases, the presence of microhemorrhages (see Fig.22) in an important percentage of CADASIL patients have been reported, so the prescription of antiplatelet drugs in this disease may be risky and has to be clarified[176, 177].

In CADASIL, migraine is quite often the earliest symptom of the disease. It has been reported in about 55-75% of the cases. The age of

the onset is variable, but is generally around 30 years. It is important to remark that in CADASIL there is a high rate of patients suffering migraine with aura, and around half of them present atypical auras, such as prolonged visual auras, confusion or focal neurologic deficits[178]. The etiopathological reasons leading to increased aura prevalence in CADASIL remain unknown, being the main candidates an increased susceptibility to cortical spreading depression or the possibility that the gene *NOTCH3* itself may act as a migraine with aura susceptibility gene[176].

Another frequent clinical aspect in CADASIL patients (around 85% of symptomatic patients) is the occurrence of transient ischemic attacks and/or stroke, related mainly to cerebral small vessel disease (strokes that involve a large artery have been reported but it is not been clarified if these are co-incidental or related to the CADASIL disease itself)[179]. Less frequent but also important are acute encephalopathies, which have been described in 10% of CADASIL patients, being the first major symptom in most of them. It can be misdiagnosed as encephalitis[180].

Also, although the clinical manifestations of CADASIL are mainly neurological, this disease also presents psychiatric disturbances (around 20-41% of the patients)[181]. Among these disturbances, apathy and major depression are the most common.

Due to the characteristics involving CADASIL (autosomic, dominant mutation, no treatment), genetic counseling should be always offered to all patients diagnosed with CADASIL and subsequent genetic testing to all family members must be done. Genetic counseling must play an

important role in family planning, options for prenatal diagnosis, and pre-implantation of genetic diagnosis.

4.3. NOTCH3 signaling

The common name used to nominate all the variants of this gene (NOTCH1, NOTCH2…) comes from the genetic studies carried out by John Dexter and Thomas Hunt Morgan in *Drosophila melanogaster*, when they suppressed this gene and found that flies developed with notched wings. Later in the 80's, researchers began to unravel the molecular pathway of NOTCH by combining genetic and biochemistry techniques[171]. Although there are several NOTCH variants, all of them function through the same signaling pathway. The variants tend to differ in their contribution to different outcomes in some cell and disease context[182].

NOTCH receptors are large transmembrane proteins which contain an extracellular domain conformed by 34 epidermal growth factor-like protein (EGF) repeats, the NRR, and a intracellular portion made of a RAM domain, six tandem ankyrin repeats and a praline-, glutamate-, serine, threonine-rich sequence (PEST domain)[172] (Fig. 24).

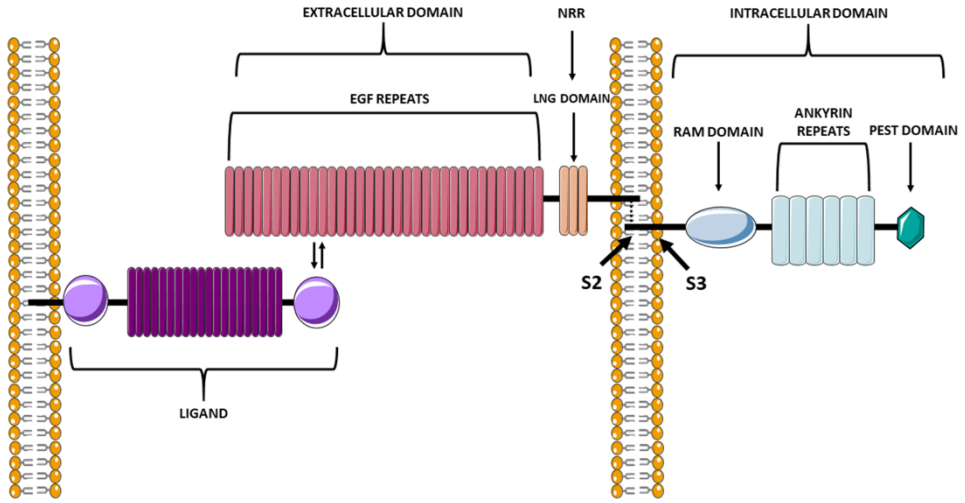

Figure 24. NOTCH3 structure. This protein is composed by an extracellular domain, which contains 34 EGF repeats, a negative regulatory region made of three cysteine-rich Notch/LIN-12 repeats and by an intracellular domain, which contains a RAM domain, sixtandem ankyrin repeats and the PEST domain. This intracellular domain is the one that will be internalize towards the nucleus once the ligand-receptor signal is triggered and the S2 and S3 cleavages are done. Self-created image (using elements with Creative Common license).

Nowadays the main components and steps in the signaling transduction cascade are already quite clear, (Fig. 25). NOTCH3 receptor is generated in the endoplasmic reticulum. From there, it is carried to the Golgi compartment, where it suffers the first cleavage (S1), carried out by furin-like convertases, becoming a bipartite receptor on its way to the cell membrane. Also, several O-glycans are added by different enzymes to the NECD before leaving the Golgi compartment. These modifications will enhance the ability of NOTCH3 to be cleaved when ligand interaction and also the sensing of the ligand binding itself[171]. Once the protein is placed in the cell membrane and the ligand interacts with NOTCH3, the NOTCH3-ligand complex is conformed, exposing the NRR of NOTCH3 to the second (S2) and third (S3) proteolytic cleavage,

carried out by ADAM metalloproteases and by a γ-secretase complex respectively. It is not clear where this S3 occurs; some reports support that this cleavage takes place at cell surface, but other ones support the idea that it happens inside endosomes. It is important to say that depending on whether S3 happens at cell membrane or after internalization, the position where the γ-secretase complex will do the cleavage may vary, yielding different NOTCH3 intracellular domains (NICDs). In any case, although the mechanism by which the cleavage sites get exposed are not definitely clear, it is a predominant view that the formation of the complex NOTCH-ligand exerts a pulling force that alters the structure of the negative regulatory region, making it accessible to enzymes[183].

After the final proteolytic step, two different NOTCH domains emerge, the NECD and the NICD. About the fate of NECD after S3, it is beginning to be understood, though it is not as well studied as NICD by far. Thus, it is believed that NECD is trans-endocytosed into ligand-expressing cells, where it is degraded in the lysosomes[184]. Regarding NICD, after S3 it travels to the cell nucleus inside endosomes. This step and the release of NICD inside the nucleus are highly regulated by a variety of molecules and enzymes. Also, it exists the possibility that the NICD inside the late endosome goes to a lysosome, where it is degraded, lowering NOTCH3 signaling[171, 185]. Apart from NOTCH3 receptor, all ligands present an intracellular routing. Although the biological sense still remains unclear, ligands are endocytosed from the cell membrane and recycled back to it to become mature and functional. These recycling steps are guided by several ubiquitylations at their COOH-termini[186].

Once in the nucleus, NICD interacts with a DNA-binding protein CSL. As a result of this union, the complex NICD-CSL recruits the transcriptional activator MAML forming a ternary complex. When CSL is not attached to NICD, it acts as a repressor, binding to and enhancing the expression of more co-repressors. On the other hand, the recruitment of NICD to CSL leads to a replacement of the co-repressors with activators[171, 187].

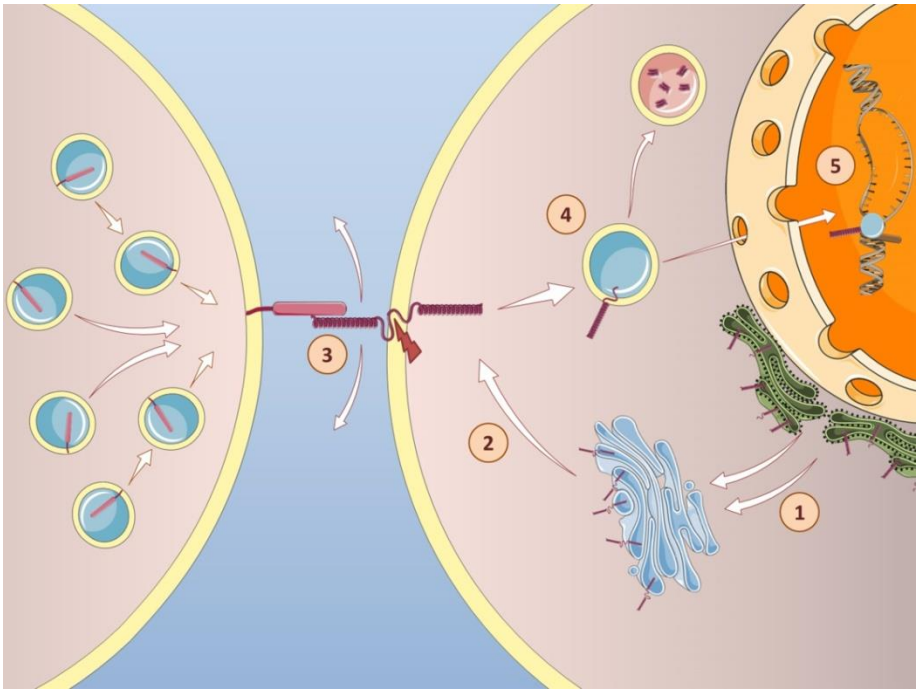

Figure 25. Summary of the NOTCH3 signaling cascade. 1) NOTCH3 is generated in the endoplasmic reticulum, from where it is sent to the Golgi apparatus. At the *cis* face of the Golgi apparatus, the protein suffers its first cleavage, S1. 2) NOTCH3 is fully packaged at the *trans* face of the Golgi apparatus and it is sent to the cell membrane. 3) At the cell membrane, NOTCH3 ligands interact with it, inducing the S2 and S3 cleavage (red lightning). NECD is released to extracellular space and endocytosed by the ligand-expressing cells. 4) NICD is endocytosed inside endosomes, which may release NICD inside the nucleus or turn into a lysosome where NICD is degraded. 5) If NICD goes inside the nucleus, it attaches to specific transcriptional factors in order to transcript NOTCH3-induced genes. Self-created image (using elements with Creative Common license).

4.4. Role of NOTCH3 in vasculature

The pattern expression of *NOTCH3* has been quite studied mainly during rodent development. What is been found is that *NOTCH3* is highly expressed during gastrulation and in the developing central nervous system. During the postnatal period, this expression seems to be downregulated. In adults, *NOTCH3* is expressed ubiquitously in all adult tissues but at low levels. Furthermore, it appears to be restricted to vascular smooth muscle cells[170, 172].

In general, NOTCH signaling is involved in multiple and crucial aspects of the vascular metabolism, such as angiogenesis, vasculogenesis, differentiation and remodeling vSMCs[172].

For the study of NOTCH3 role in vasculature, several *Notch3*-null mice have been generated by different approaches[188, 189]. Since *Notch1*-null mice have been impossible to generate due to the key role of *Notch1* during early embryogenesis there were doubts whether it would be possible to generate these *Notch3*-null mice. Thus, the fact that it was, supports the idea that *Notch3* is not so critical in the developmental stage[190]. Although the role of the NOTCH receptors family in vasculature is quite well established, the specific role of NOTCH3 is not so well studied. To this respect, there is one report from Domenga et al.[191] that studied the effect of suppressing and overexpressing *Notch3* in arterial identity and maturation of vSMCs. Their findings, summarized, were:

- For perinatal stages (P0.5) they did not find any differences between arterial vessels in *Notch3* -/- mice and vessels from control littermates, while in adult mice they found that *Notch3*-/-

mice presented structural abnormalities on their arteries (enlargement, thinner vSMCs coat). Also, they found that these abnormalities were more acute in the small arteries than in the major elastic arteries. Together, these facts suggest an important role of NOTCH3 in the maintenance and maturation of small arteries, which would agree with the fact that CADASIL patients manifest the physiological symptoms in the vSMCs of the brain small arteries.

- The remodeling process that undergo in arterial maturation was highly impaired in *Notch3*-/- mice. In fact, they say that vSMCs follow a maturation process more related to the one that happens in vessels, with a more elongated cell shape and formation of clusters with cells poorly oriented around the lumen. These correlated with the fact that *Notch3*-/- arteries have a positive staining for specific vSMCs markers such as α-smooth muscle actin at birth, but later they stained as abnormal aggregation, suggesting a key role of NOTCH3 in postnatal arterial maturation.

- Over-expression of a constitutively active form of NOTCH3, this is, the intracellular domain, resulted in an increase of actin stress fibers and steady-state levels of polymerized actin. This suggests a role of NOTCH3 in the rearrangement of actin cytoskeleton.

Interestingly, the authors also found that the expression of most of the immediate downstream genes in NOTCH pathway was not altered in *Notch3*-/- mice compared with their control littermates. Here the authors suggested that we could be in the presence of a NOTCH3-mediated signaling pathway different from the canonical one, and

through which it controls the maturation and development of arterial vSMCs. For the moment, this novel and hypothetical signaling pathway has not been proven. However, another possibility would be that *Notch3* and *Notch1* may have genetic redundancy. To this respect, although it is proved that *Notch3* does not substitute the *Notch1* function[189] it is not yet demonstrated that NOTCH1 is not able to replace *Notch3* functions.

4.5. *NOTCH3* mutations in CADASIL

As previously mentioned, NOTCH3 presents an intracellular domain, a transmembrane domain and an extracellular domain. This extracellular domain, constituted by 34 EGF repeats and encoded by exons 2-24, is where the mutations are typically located. The vast majority of disease-causing variants involve the loss or gain of a cysteine residue in 1 of the 34 EGF repeats (Fig. 26). This leads to an unpaired cysteine residue that impede the correct formation of the EGF repeat, affecting the protein tertiary structure[169, 192].

Nevertheless, there are also reports suggesting the existence of the so-called cysteine-sparing mutations, which do not affect the number of cysteine residues[192]. However, the link between these cysteine-sparing mutations and CADASIL is less robust and more information should be collected, since in most cases, assessment of the full spectrum of clinical markers of CADASIL disease has not been performed. It has been reported that some of these cysteine-sparing mutations present several clinical criteria for CADASIL, and specifically one of them (p.R75P) has already been reported in different families, generating a CADASIL-like phenotype[193]. Until now, the prevalence of CADASIL was considered to be around 2 to 5 of 100.000. This was always assumed to be an

underestimation of the prevalence due to two main reasons: the variability on the spectrum of the symptoms, making the disease to be diagnosed as another disease, and that CADASIL has a rather short clinical history. Also, a recent report increased the prevalence of CADASIL to 3.4/1000, almost a 100-fold higher frequency. The explanation that the authors give to this surprising but long suspected result lays on the idea that this disease is not fully penetrant. In this report, the authors found that CADASIL mutations found by clinical analysis resided in most of the cases in the EGF repeats 1-6, whereas the non-clinical mutations tend to locate in EGF repeats 7-34. Accompanying these results, the authors also found that mutations in EGF 7-34 cursed with lower white matter lesion compared with patients carrying a mutation in the EGF 1-6. However, the mechanisms underlying this difference in the severity of the disease depending on the position of the mutations remain unraveled[194].

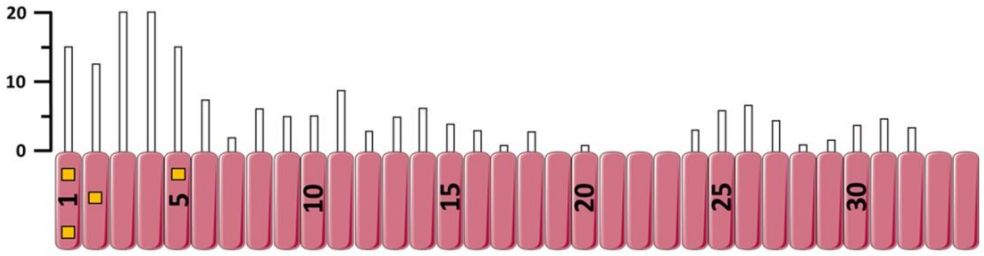

Figure 26. Map of NECD mutations (white bars). Each orange square represents a cysteine-sparing mutation. Bar at the left represents the number of mutation variants per EGF repeat. Self-created image adapted from Coupland et al, *Stroke* (2018)[169].

4.6. CADASIL ethiopatogeny

Although the clinical picture and symptoms of CADASIL are well known as well as the genetic aspects regarding the several mutations already reported over the years in the literature, the primary cause of the disease remains elusive. This uncertainty pivots around whether this disease may be caused by the aberrant aggregation of GOM or if the given mutation in *NOTCH3* is the origin of the disease development (including the aberrant GOM accumulation)[169].

To date, what it is thought is that all the mutations reporting CADASIL present the accumulation of the NECD in GOM deposits[170]. Why this accumulation happens is not clear at all. Although one of the main hypothesis is that mutations in exons coding for the EGF repeats may affect the release of the NECD once the ligand interaction and the cleavage of the NICD is done, there could also be wrong interactions during the metabolic pathway of NOTCH3 along its transport to cell membrane or even at the S1 state that affects the posterior fate of the NECD (Fig. 27). To this regard, works in *Drosophila* CADASIL-like model *Notchoid3*, which present mutations in the first EGF repeats (N-terminal region), showed an impaired endocytosis and trafficking of NOTCH3, with the consequent abnormal accumulation, suggesting that this region, apart from influence in the accumulation of NECD, also regulates NOTCH3 trafficking[195]. In fact, there are some studies reporting cases of mutations that do not affect NECD signaling but that show a delayed S1-processing, suggesting that trafficking and localization could be affected by some mutations[196, 197]. To summarize, although there are studies reporting both possibilities (mutations implicated in NECD accumulation and wrong signaling, and mutations apparently implicated in receptor

trafficking, processing and maturation), more studies should be performed to understand processing and maturation of NOTCH3 bot in wild type cases and mutations in order to understand the pathological change of CADASIL as well as the role of NOTCH3 in vSMCs.

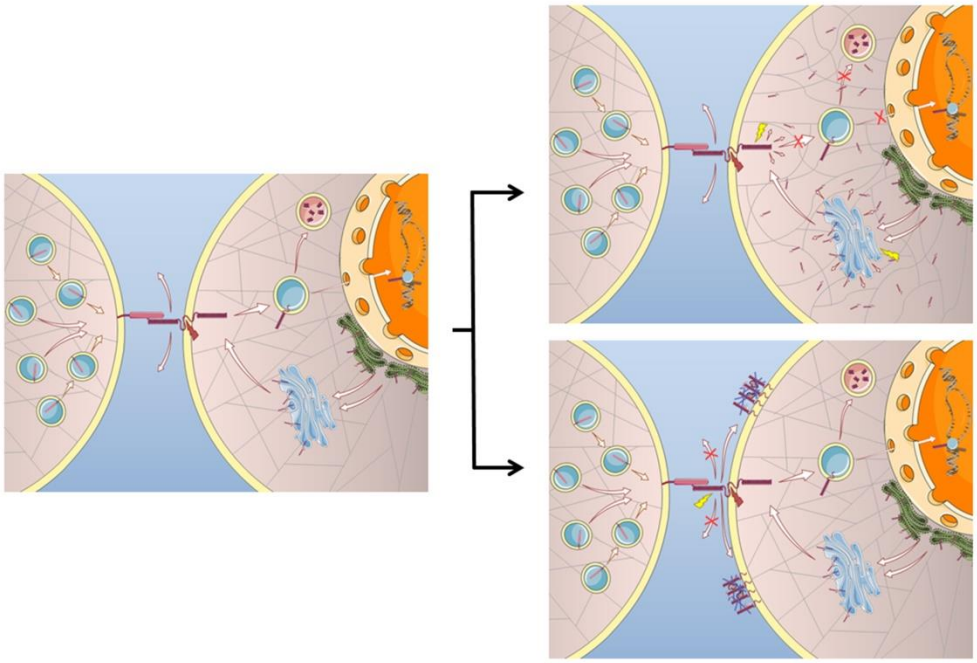

Figure 27. Representation of the two main hypothesis regarding CADASIL pathophysiology. Points where the alteration is thought to be produced are highlighted with yellow lightnings. Red lightnings represent S2 and S3 cleavages. On the one hand, the mutation of NOTCH3 would give rise to a cellular trafick disturbance due to wrong interactions at S1, causing an increase in NICD that could affect the cytoskeletal structure of the cell. Also, this altered intarcellular traficking could intefere in the NICD transport to the nucleus, incresing the NICD intracellular levels too. On the other hand, the common alteration relies in the NECD not being released once the S2 and S3 cleavage are done. This results in the NECD accumulation at the membrane, being the initial step of the GOM formations. Self-created image (using elements with Creative Common license).

As previously mentioned, it remains unclear whether CADASIL disease is due to an indirect consequence of the abnormal accumulation of the NECD, as a consequence of a disrupted or altered NOTCH signal

regulation or whether it is due to a combination of both. However, since it is common to see the presence of aggregated NECD in GOM deposits in the vasculature of most of the patients with CADASIL, it would be logical to ask if CADASIL is an aggregation disease and if GOM deposits are the cause of it. GOM deposits are composed not only by NECD but by other molecules, recruited by the NECD accumulation that, put together, constitute this GOM deposits. Observations that point to GOM deposits as the cause of CADASIL disease are based on that GOM deposits are very often associated with CADASIL cases. Also, NECD from mutated *Notch3* tend to aggregation in a higher frequency than NECD from wild-type *Notch3 in vitro*[198]. The presence of the metalloproteinase inhibitor TIMP3 in GOM deposits has also been reported in a mouse mutant for *Notch3* (R169C). This is relevant since TIMP3 was also found in 4 different cases of CADASIL patients. This enzyme regulates the density of voltage-gated potassium channels (Kv1) on vSMC membranes, affecting the myogenic tone and dilatation of the lumen of the small vessels[199]. On the opposite, there is a study in a mouse model expressing *Notch3* R90C mutation where vSMCs lost anchorage and exhibited functional impairment already before GOM deposition starts to happen[169]. This would suggest that there is an event prior to GOM accumulation that would discard it as one of the causes of CADASIL disease.

However, despite the seemingly importance of GOM deposits for CADASIL, there are studies questioning the need of NOTCH3 to take part in GOM composition. There are several mouse models expressing human *NOTCH3* mutations or knockout mouse models for *Notch3* that present GOM deposits but no immunoreactivity for NOTCH3 in those

aggregates, pointing in the direction that maybe GOM can arise in the absence of mutated *Notch3*[200, 201]. It is starting to be believed that GOM deposits may affect the glymphatic system. This glymphatic system serves as a fluid exchange system between fluid and interstitial fluid within the brain and operates in the perivascular space[202]; this perivascular space has been observed to get dilated and disrupted in patients with CADASIL[203].

For the study of CADASIL only mouse models with different mutations and knockout *Notch3* mice have been employed. Despite their value as studying tools for CADASIL, nowadays there is a lack of more translational studies and studies focused on the development of potential treatments for this disease. To this regard, animal models involve an already mentioned phylogenetic gap against which the drugs stumble. Because of this, hiPSCs technology arises as a possible solution to this problem. The modelling of a well-defined, monogenetic disease like CADASIL by the reprogramming of somatic cells from patients with CADASIL and their posterior differentiation to the affected cell types (smooth muscle cells mainly, and also endothelial cells) may suppose an appropriate *in vivo* platform for the study of this disease and for the testing of potential drugs, since the phylogenetic gap would be overcome. Also, it would also be possible, by genetic editing, to repair the mutation within the hiPSCs and, once differentiated into vSMCs, administer them in *Notch3* knockouts mice to see if the healthy vSMCs replace the damaged, endogenous ones. Last, the development of such a platform would also set the basis for the study of endothelial degeneration in cerebrovascular SVDs and neurodegenerative diseases.

USC
UNIVERSIDADE
DE SANTIAGO
DE COMPOSTELA

INTRODUCTION

HYPOTHESIS

OBJECTIVES

MATERIALS & METHODS

RESULTS

DISCUSSION

CONCLUSIONS

USC
UNIVERSIDADE
DE SANTIAGO
DE COMPOSTELA

Approximately 25-30% of stroke events are due to SVDs. Of these, CADASIL is probably the most aggressive form of SVD. It has been 15 years since *NOTCH3* was found to be the causative gene for CADASIL. However, the molecular mechanisms by which the mutant NOTCH3 results in the pathological changes of arteries are still largely unknown. Despite interesting insights into the disease pathology uncovered using transgenic mouse models, no specific and effective treatment is available. CADASIL disease exhibits a well-defined monogenetic profile, whose mutation triggers an accumulation of the NECD in the vSMCs membrane. However, vECs and vSMCs do not function independently in arteries and the possibility that there could be some disruption in the communication between these two cell types has not been studied yet.

The recent advance in stem cell biology has made it possible to obtain hiPSCs from somatic cells of patients to generate patient-specific disease cell models.

Keeping these ideas in mind, in this Thesis the following hypothesis are postulated:

A. A CADASIL *in vitro* cell model could be generated by differentiation of PBMCs-derived hiPSCs from patients with CADASIL into vSMCs and vECs.

B. The CADASIL cell model could be a valuable tool for the NICD and NECD study in both vSMCs and vECs.

USC
UNIVERSIDADE
DE SANTIAGO
DE COMPOSTELA

INTRODUCTION

HYPOTHESIS

OBJECTIVES

MATERIALS & METHODS

RESULTS

DISCUSSION

CONCLUSIONS

USC
UNIVERSIDADE
DE SANTIAGO
DE COMPOSTELA

The **main objective** of this project is the achievement of a cell model based on the induced pluripotent stem cell technology for CADASIL disease that allows the study, among others, of the NOTCH3 extracellular domain pathogenic accumulation in vascular smooth muscle cells and vascular endothelial cells.

Due to the extension of the objective set on this project, several sequential objectives are established, each subjected to the previous one. These objectives are:

1. The generation of a human induced pluripotent stem cell line from peripheral blood mononuclear cells of a patient with a previously diagnosed mutation associated with CADASIL disease.

    1.1. To perform all the characterization tests requested by the international research community in order to register it in several institutions.

    1.2. The generation of a second human induced pluripotent stem cell line from a second patient with the same mutation.

2. The achievement of CADASIL-human induced pluripotent stem cell-derived vascular smooth muscle cells and vascular endothelial cells from the first time created CADASIL-human induced pluripotent stem cell line by setting-up and implementing pre-existing protocols.

    2.1. The characterization of these cell lines by several techniques and its comparison with control cell lines: human aortic smooth muscle cells for CADASIL-human induced pluripotent stem cells-derived vascular smooth muscle cells; human aortic endothelial

cells for CADASIL-human induced pluripotent stem cells-derived vascular endothelial cells.

3. The study of NOTCH3 extracellular and intracellular domain levels and expression patterns both for CADASIL-human induced pluripotent stem cells-derived vascular smooth muscle cells and vascular endothelial cells. Also, to contrast the results with the same analysis in several control cell lines: human aortic smooth muscle cells and healthy-human induced pluripotent stem cells-derived vascular smooth muscle cells for CADASIL-human induced pluripotent stem cells-derived vascular smooth muscle cells; human aortic endothelial cells and healthy-human induced pluripotent stem cells-derived vascular endothelial cells for CADASIL-human induced pluripotent stem cells-derived vascular endothelial cells.

INTRODUCTION

HYPOTHESIS

OBJECTIVES

MATERIALS & METHODS

RESULTS

DISCUSSION

CONCLUSIONS

USC
UNIVERSIDADE
DE SANTIAGO
DE COMPOSTELA

Once given a view of the state of the art in CADASIL research, and the hypothesis and objectives set for this Thesis, on this section it will be described the initial approach followed in order to achieve them and that are reflected in Fig. 28.

Basically, a first step will consist on the generation and characterization of a first hiPSC line generated from PBMCs of a patient with CADASIL, and its subsequent registry in the "Banco Nacional de Líneas Celulares" at the "Instituto de Salud Carlos III" in Spain, and in the Human Pluripotent Stem Cell Registry. After that, on a second step, a second reprogramming from a second patient with CADASIL will be done in order to give strength and robustness to the project, demonstrating that reprogramming PBMCs from patients with CADASIL is possible. Finally, on a third step, differentiation protocols to the two affected cell lines in CADASIL, vSMCs and vECs, will be developed from the first reprogrammed cell line of hiPSCs. Once the protocols are achieved, analysis of the NICD and NECD will be performed. Because hiPSCs generation and cell differentiation are time-consuming protocols, vSMC differentiation and NOTCH3 analysis were considered a priority in this Thesis respect to ECs, as muscular cells are the ones with a critical role in this disease.

Also, the cell lines obtained over the differentiation processes will be compared with commercial control cell lines. For the differentiation to CADASIL-hiPSCs-derived vSMCs, the comparison will be done with a HAoSMC commercial line, and for the differentiation to CADASIL-hiPSCs-derived vECs, the comparison will be done with a HAoEC commercial line. Furthermore, we will compare the analysis of the NOTCH3 domains with two different control cell lines: in the case of CADASIL-hiPSCs-

derived vSMCs we will use a HAoSMCs commercial line and healthy vSMCs from a hiPSC line previously derived from a healthy patient. In the same way, the analysis of CADASIL-hiPSCs-derived vECs will be compared with a HAoECs commercial line and with healthy vECs from a hiPSC line previously derived from a healthy patient.

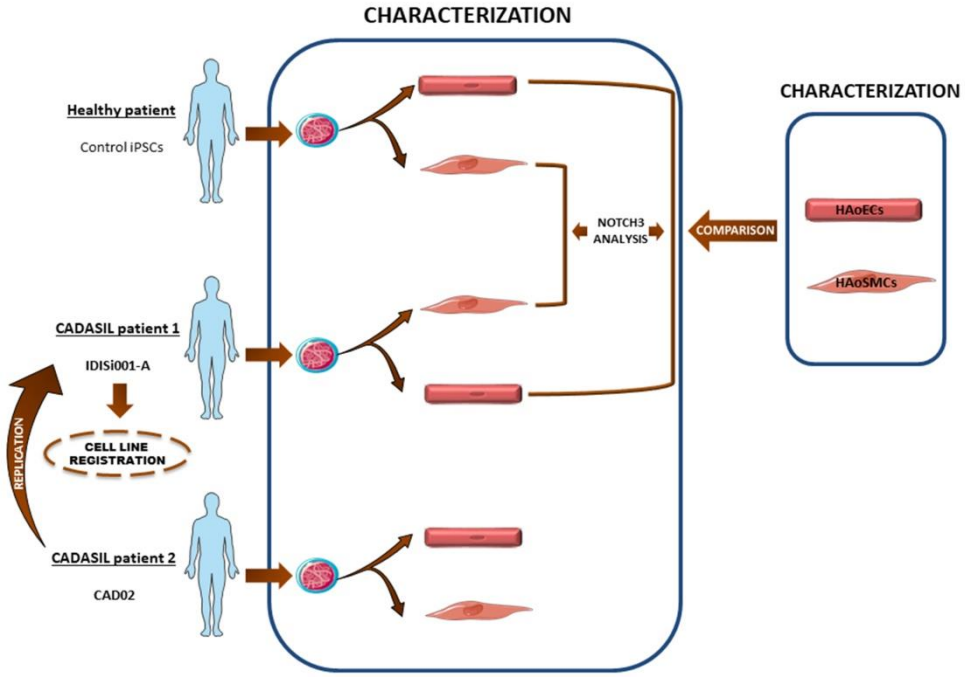

Figure 28. Graphical abstract summarizing the project design as it was conceived. Self-created image (using elements with Creative Common license).

5. Reprogramming of peripheral blood mononuclear cells from a patient with CADASIL

On this section, it will be described all the procedures from the initial diagnostic of the patients with CADASIL, going through the isolation of the PBMCs from the blood sample, to the viral transfection of these PBMCs. The procedures and protocols described for the reprogramming of the PBMCs were the same in the two patients.

5.1. Diagnostic

Mutation was found by new generation sequencing of the whole coding region of *NOTCH3* gene with a Solid 5500XL genetic analyzer (ThermoFisher, Massachusetts, USA). The first patient was a 67- year - old patient previously diagnosed with a white matter injury. This patient had a son with CADASIL as well.

Both patients had an Arg1242Cys/normal genotype due to a change from a cytosine to a thymine (c.3724C>T). Thus, both patients exhibited a change of an arginine for a cysteine at the exon 23 of the *NOTCH3* gene, located at the short arm of the chromosome 19. This mutation was reported for the first time for CADASIL disease. To note, this mutation at the exon 23 relates to the EGF repeat 31-32, which is a region with no previous mutations reported[204] (the anonymized genetic diagnosis can be found at Appendix 1).

5.2. Ethical and legal aspects

Before performing the blood extraction, the patients received an informed consent in which everything related to the project was explained. Once the doubts and questions asked were solved, both patients agreed to continue and signed the informed consent.

All the protocols and experiments performed during the development of this Thesis were approved by the Ethic Committee from the Santiago-Lugo Research (2016/450) (Appendix 2) and by the Guarantee Committee for the Donation and Utilization of Cells and Human Cells and Tissues from the Carlos III Health Institute (428 346 1) (Appendix 3).

5.3. Isolation and culture of peripheral blood mononuclear cells

A PBMC is any peripheral blood with a single round nucleus. These cells include lymphocytes (NK cells, T cells and B cells) and monocytes. In humans, lymphocytes comprise the vast majority of the PBMC population, followed by monocytes and just a small proportion is composed of dendritic cells[205]. To isolate these cells from the rest of the peripheral blood, a hydrophilic polysaccharide like ficoll was used. Ficoll separates, by centrifugation, the whole blood into two fractions above and below the density of 1.077 g/mL, obtaining a top layer of plasma, a cloudy, white layer where PBMCs are, and a bottom fraction of polymorphonucleated cells.

For the isolation of the PBMCs from the blood of both patient 1 and patient 2 samples, 12 mL out of 25 mL of the total peripheral blood extracted were used in a first round. The isolations were carried out

between 24 and 48 h after extraction in the case of patient 1 and less than 24 h after extraction in patient 2. To perform the isolation steps, SepMate™-50 tubes (StemCell™ Technologies, Vancouver, Canada) were used.

SepMate™ are tubes that facilitate the isolation of PBMCs by density gradient centrifugation. These tubes contain a septum that provides a barrier between the density gradient medium and blood, making easier to drop the blood over the density gradient medium (Fig. 29). Also, this septum separates the polymorphonucleated cells sediment from the plasma and the PBMCs.

At the beginning, the 12 mL of peripheral blood were mixed with PBS + FBS 2% (1:1 ratio). This 24 mL were then split into 2 SepMate™ of 50mL. Prior to this, 15 mL of Lymphoprep (StemCell™ Technologies, Vancouver, Canada) were added at the bottom of each SepMate™. The mix of peripheral blood plus PBS + FBS 2% has to be added carefully to avoid mixing with the Lymphoprep. Once ready, SepMates™ were centrifuged 10' at 1200g, RT and with the brake on. When the centrifugation finished, the plasma and the PBMCs (a white, thin, cloudy layer) were collected. After that, several washing (with PBS + FBS 2%) plus centrifugation steps were performed and finally PBMCs were counted in a Neubauer chamber (Brand Gmbh, Wertheim, Germany).

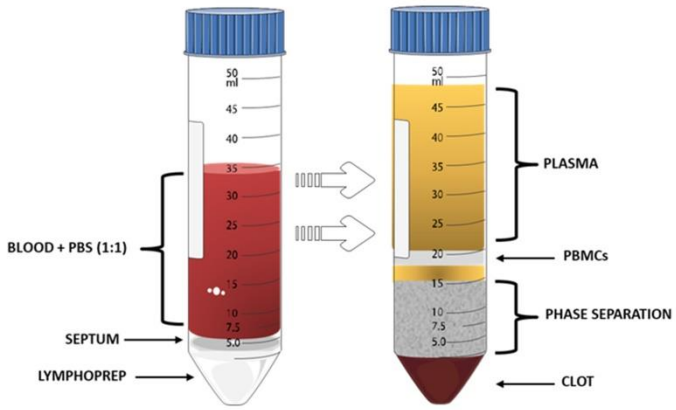

Figure 29. Schematic representation of the blood phases after Lymphoprep separation step. Self-created image (using elements with Creative Common license).

For culturing the PBMCs, these were seeded into 3 wells of a 12-multiwell plate (Corning, New York, USA), with $5x10^5$ cells into each one. PBMCs were cultured for 4 days before starting with the viral transfection to allow them to adapt to the medium. The medium for culturing the PBMCs consisted in StemPro-34 SFM (ThermoFisher, Massachussetts, USA) plus StemSpan™ CC100 at 1X (StemCell™ Technologies, Vancouver, Canada), which is a combination of 4 recombinant human cytokines (Flt3L, SCF, IL-3 and IL-6) formulated to support the proliferation of hematopoietic cells. Half of the medium (1mL out of the total 2 mL per well) was changed daily, tilting the plate for 5-7' to allow the cells to descend by gravity to the bottom of the well, so it became easier to aspire 1 mL of the medium without aspiring cells.

The rest of the PBMCs that were not seeded were frozen together with the PBMCs achieved on the isolation of the remaining 13mL of the

peripheral blood. A total of $2.5x10^6$ cells were frozen per cryovial (Simport, Quebec, Canada), using BAMBANKER (Nippon Genetics, Tokyo, Japan) as freezing medium (Fig. 30).

After 4 days, viral transfection was induced.

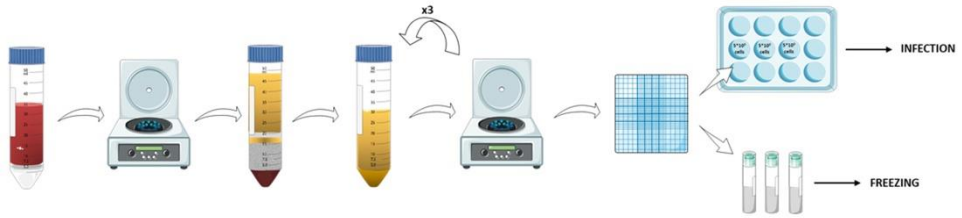

Figure 30. Schematic representation of the PBMCs isolation. Self-created image (using elements with Creative Common license).

5.4. Viral transfection

For the viral induction, Cytotune™-iPS 2.0 Sendai Reprogramming Kit (ThermoFisher, Massachussetts, USA) was employed. This kit is composed of three different viral vectors (each one provided in a different vial): a polycistronic vector containing *Klf4-Oct3/4-Sox2* (KOS), another one containing *c-Myc*, and the last one that contains more *Klf4* (Table 2). These Sendai Viruses are non-integrative, so they do not insert into the cell genome.

Cytotune Sendai™ Vector	Factor	GenBank ID
Cytotune™ 2.0 KOS	Human Klf4	BC029923.1
	Human Oct3/4	NM_002701.4
	Human Sox2	NM_003106.2
Cytotune™ hc-Myc	Human c-Myc	KO2276.1
Cytotune™ hKlf4	Human Klf4	BC029923.1

Table 2. All three viral vectors used for reprogramming and the human genes that carry inside.

After 4 days, all the PBMCs were collected into the same Falcon and counted. PBMCs were then passed into two polystyrene round-bottom tubes (Corning, New York, USA), $3x10^5$ cells per tube. One tube was committed for reprogramming and the other tube as a positive reprogramming control. The aim of this positive control was to check, by electrophoresis in an agarose gel, the presence of the virus, which would guarantee that a correct infection was made. Following the collection of the cells, two vials of each viral vector were thawed on ice and added to each tube, with a MOI of: KOS vial = 5; c-Myc vial = 5; Klf4 vial = 3. The equation to calculate the volume of each vial that had to be added was the following:

$$V_{Virus} = \frac{MOI\ (CIU/Cell) \times No.cells}{Viral\ Titer\ (CIU/mL) \times 10^{-3}(\mu L/mL)}$$

Thus, for each vial:

$$V_{KOS} = \frac{5\ (CIU/Cell) \times (3 \times 10^{-5})\ cells}{1.0 \times 10^{8}(CIU/mL) \times 10^{-3}(\mu L/mL)} = 15\mu L$$

$$V_{c-Myc} = \frac{5\,(CIU/Cell) \times (3 \times 10^{-5})\,cells}{0.84 \times 10^{8}(CIU/mL) \times 10^{-3}(\mu L/mL)} = 17.86 \mu L$$

$$V_{Klf4} = \frac{3\,(CIU/Cell) \times (3 \times 10^{-5})\,cells}{0.98 \times 10^{8}(CIU/mL) \times 10^{-3}(\mu L/mL)} = 9.18 \mu L$$

The viral titer was provided on the specific lot sheet of the kit.

The final volume of each polystyrene round-bottom tube was 1 mL. Thus, the tubes composition consisted of:

$$V_F = 600\ \mu L\ (\equiv 3 \times 10^{5} cells) + 42.04\ \mu L\ Virus + 357.56\ \mu L\ Medium$$

Prior to seed the cells, a 30' centrifugation step was done, at 1000 g, RT. This step increases the percentage of transfection by increasing the probability of each virus to attach to any cell. After that, the pellet was resuspended with the supernatant and an extra 1 mL was added, in order to seed the PBMCs in a total volume of 2 mL of complete medium (StemPro-34 SFM + StemSpan™ CC100 1X) into a well of a 12-multiwell plate (Fig. 31).

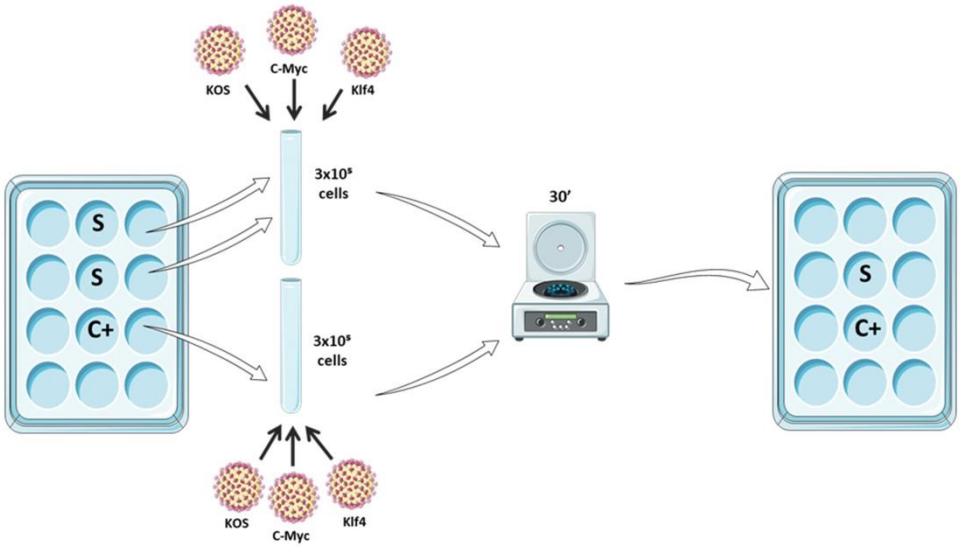

Figure 31. Schematic representation of the viral infection process. Self-created image (using elements with Creative Common license). S= sample to be reprogrammed; C+= positive control cells.

On the next day (Day 1), 17-18 h after transfecting the cells, each well was collected into a different Falcon of 15 mL. One of the Falcon tubes was centrifuged at 200g, 10', RT. This step helps to clear much of the virus from the cells. Then, the supernatant was aspired carefully, since the pellet can´t be seen, and the cells were resuspended with 500 µL of StemPro-34 SFM + StemSpan™ CC100 1X and seeded again into a well of a 24-multiwell plate (Corning, New York, USA).

The other Falcon, which had the positive control cells, was centrifuged at 200 g, 4', RT, and the pellet was used for RNA extraction in order to perform future retrotranscriptions and PCRs to check for the virus presence, which would guarantee that a correct infection was made (Fig. 32).

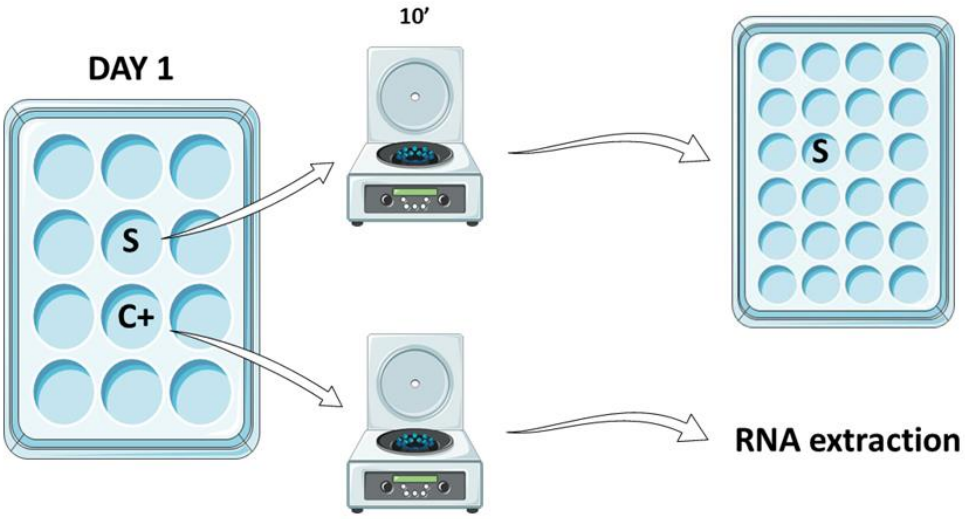

Figure 32. Day 1 after viral infection. One of the infected wells is subjected to a 10' centrifugation step in order to facilitate virus removal. The infected cell from the other well is collected for future RNA extraction to check whether the infection was correctly performed or not. Self-created image (using elements with Creative Common license).

6. Selection of hiPSCs colonies

On this section, the first four passages of the transfected PBMCs will be described in different subsections, since the methodology differs from each other. The methodology followed in the fourth passage will be the one used for the rest of the passages onwards. All the procedures and protocols described are valid for the culture of the two cell lines of hiPSCs generated.

At the beginning of the reprogramming process, once cells have been infected, it begins a period of approximately 2 months where the

emerging and potential hiPSC colonies appear and grow. During this period, a positive selection process was carried out, based on observing the emerging colonies every day under a microscope and isolating the colonies and/or parts of the colonies that present the typical morphological characteristics of a hiPSC colony.

Thus, on Day 2, cells were just observed under a Leica DMi1 microscope (Leica, Wetzlar, Germany) to check them. This microscope is also equipped with a 10" HDMI monitor MMT6 (Leica, Wetzlar, Germany) and a Universal Mounting Frame (PECON, Erbach, Germany). Groups of 3-4 cells starting to attach to the bottom of the plate were already seen at this point. Also, there were cells slightly more brilliant and bigger than others.

On day 3, cells were collected in a Falcon of 15 mL and centrifuged for 10', 200 g, RT. This step was done in order to remove the cytokines, since on this day cells are cultured just in StemPro-34 SFM. The supernatant was then removed and pellet resuspended with 1 mL of StemPro-34 SFM. Living cells were counted and after that, they were seeded into 3 Petri dishes of 35 mm^2 (Corning, New York, USA), at different densities: $15x10^3$, $30x10^3$ and $50x10^3$ cells. This way, the 3 Petri dishes had different growth rates and lab work did not accumulate overwhelmingly. The final volume of StemPro-34 SFM on the Petri dishes was 2 mL. At this point, cells were considered to be on passage 1. It takes 17-30 days to pass them to passage 2 depending on the growth of the colonies.

From Day 3 to Day 8, cells were submitted to a transition culture medium, from the PBMC medium StemPro-34 SFM, to the iPSC medium

mTeSR1 (StemCell™ Technologies, Vancouver, Canada). This transition was as follows: On Day 4, cells were just observed under the microscope. On Day 5, half of the medium was removed and replaced by StemPro-34 SFM without cytokines. On Day 6, cells were just observed under the microscope. On Day 7, half of the medium was replaced with mTeSR1 and, on Day 8, all the medium was replaced with mTeSR1. From Day 8 until all the colonies were selected, medium was changed daily. This selection process from the three initial Petri dishes (passage 1) to passage 2 begins at Day 15-17 approximately and finishes at Day 30-35. All over that period, the three Petri dishes were observed everyday under the microscope. Depending on several typical characteristics, emerging colonies were removed with a 200 µL sterile pipette tip, or selected (partially or the entire colony) for positive selection.

These characteristics used as a guide for a correct identification of good colonies are represented on Table 3:

MORFOLOGY OF THE COLONIES	MORFOLOGY OF THE CELLS
Round shaped colonies	Small rounded cells
Defined white and refractory borders	Compact growth, no spaces between them
Growth in 2D	High nucleus/cytoplasm ratio

Table 3. Summary of the main typical hiPSCs and hiPSC colonies that serve as a guide for the positive selection of the colonies.

As mentioned above, not always an entire emerging colony may have the characteristics of a good iPSC colony, but part of them. This would be the same case for colonies on passage 3. So, both to select an entire colony or just part of it, an Origio stripper (Origio, Copenhagen,

Denmark) was used to aspire them, with a 175 µm diameter stripper needle (Origio, Copenhagen, Denmark).

For positive selection, the needle was inserted into the stripper. This needle was then washed with ethanol 70% and next with DMEM-F12 (ThermoFisher, Massachusetts, USA). After that, a colony or part of the colony that presented the typical characteristics of pluripotency mentioned above was aspired carefully and the clusters were seeded into a well of a 12-multiwell plate (Fig. 33). Between colonies, the needle had to be washed with DMEM-F12 in order to prevent cells from different colonies from mixing inside the same well. Each colony or part of a colony selected was automatically assigned a number (#1, #2…) and each plate was assigned a letter (A, B, C…). Once the colonies were seeded they were considered to be in passage 2. At the end of the process (when all the colonies marked for that day had been selected) the needle was washed again with ethanol 70%.

Figure 33. Image from a typical positive selection step.

After 5-7 days in passage 2, emerging colonies started to reach confluence. During these days, colonies were observed everyday under the microscope in order to remove the colonies that clearly were not going to develop any pluripotency region. Medium was also changed every day. Thus, once the colonies reached a large size, a positive selection like the one described on passage 2 was performed.

On this case, each aspired colony or region of a colony from a same well was seeded into a different well of a 12-multiwell plate [named this time with numbers (1, 2, 3…)]. Each colony or part of a colony selected was automatically assigned the number of the colony from which it came plus a number corresponding to the order in which it was aspired from that well. As an example, if two colonies were aspired from the well #10, these colonies would be seeded into two different wells and would be named #10.1 and #10.2 respectively. Thus, each well of passage 3 would house a clone (for example #10.1) from a passage 2 colony (#10). This expansion process from passage 2 to passage 3 was performed in order to increase the possibilities of reaching stable hiPSCs colonies. Immediately after aspiring a colony or region, the small clusters that might remain on the well were removed with a 200 µL pipette tip, to prevent that in the future those clusters could grow again and be re-aspired.

Unlike the passage 2, on passage 3, when the emerging colonies start to grow and reach a proper size, is more usual to find entire colonies or even entire wells with fully hiPSCs colonies.

From passage 4 and next, the procedure to pass the colonies of hiPSCs changed and remained the same. It was assumed that all the

clones that passed through all the three first passages and reached the fourth passage presented relative pluripotent stability. The clones that still mostly continued to differentiate while growing in passage 3 were discarded. Finally, unlike from passage 2 to passage 3, entire wells that presented colonies that reached a quite stable state were entirely passaged at once into a 35mm^2 Petri dish by using dispase 1X and with the aid of a cell scraper (Thermofisher, Massachusetts, USA). These clones were cultured through passage 4 to passage 10 approximately and observed meticulously every day under the microscope in order to select the best clones to work with.

So, for passaging stable clones, mTeSR1 is replaced with 1 mL of DMEM-F12 and each Petri is placed under the microscope. Differentiating clones are removed with a 200 µL pipette tip and the medium is aspired and replaced with another 1 mL of DMEM-F12. After that, instead of performing the positive selection, all the clones are cut in a grid pattern with a 200 µL pipette tip (Fig. 34). Then, clones are detached with a cell lifter (Corning, New York, USA), aspired and put into a Falcon of 15 mL. The Petri dish is rinsed with an extra 1 mL of DMEM-F12. Next, the Falcon is centrifuged at 200 g, 4', RT. Once the centrifugation step is finished, depending on the pellet size, the clone is expanded in several Petri dishes, previously coated with Matrigel™ matrix (Corning, New York, USA) and placed inside an ICO105med incubator (Memmert, Bavaria, Germany) for 1 hour. The DMEM-F12 with the coating agent is removed and replaced with 1 mL of mTeSR1. Immediately, the DMEM-F12 of the centrifuged Falcon is removed and the pellet is resuspended with just 1-2 vigorously pipetting (if pipetted more than 1-2 times, clusters become too small) with 1 mL of mTeSR1. Then, that 1 mL

containing the clusters is distributed homogeneously among the new Petri dishes. These Petri dishes are properly labeled before placing them back into the ICO105med incubator. Each Petri is labeled in the cover with:

- Date when the coating was performed.
- Code that allows distinguishing clones from different sources (different patients for example).
- Split ratio
- Date of seeding

Regardless of how many Petri dishes the clone is expanded into, at least one of them is for freezing once it reached the confluence, in order to store it.

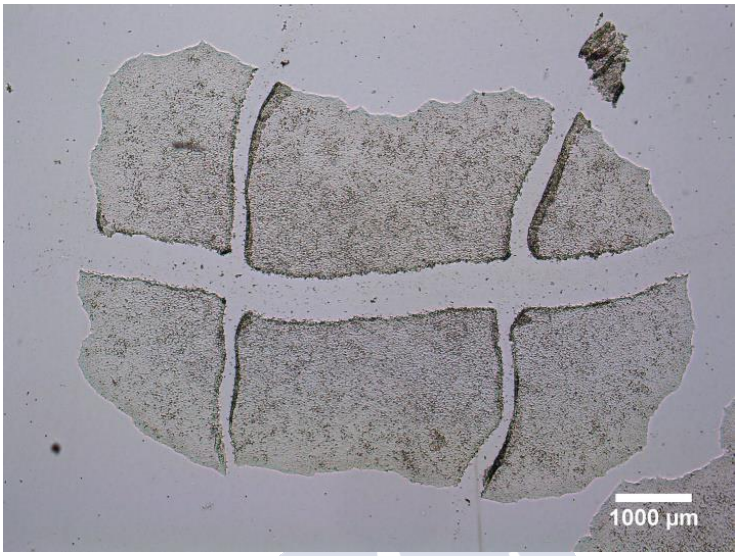

Figure 34. Image of the typical grid-pattern cut performed in some of the hiPSCs manipulation processes

7. Culture of hiPSCs colonies

Since the Yamanaka´s finding on 2006, multitude of different protocols for culturing and maintenance of hiPSCs under several different conditions have been reported all over the literature, until it could be said that every laboratory follows its own different protocols. The purpose of this section is to accurately describe all the protocols that were englobed inside the general handling of hiPSCs colonies all over this project. These protocols consist of: maintenance of hiPSCs colonies, expansion of hiPSCs colonies, freezing of hiPSCs colonies and thawing of hiPSCs colonies.

7.1. Maintenance of hiPSCs colonies

This subsection comprises several main considerations about the culture of the hiPSCs colonies on this project.

The first consideration to take into account is that every single clone of iPSC was cultured under *feeder-free* conditions; this is, with no fibroblast layer supporting the colonies below them. To achieve this, a Matrigel™ matrix was employed as covering for all the different culture plates used. This matrix consists of a solubilized basement membrane preparation extracted from the Engelbreth-Holm-Swarm mouse sarcoma. When the matrix arrives, it must be put immediately at -20ºC if stored, since this matrix turns into gel at room temperature, or at 4ºC overnight to make aliquots on the next day, so it slowly thaws and stay liquid at this temperature. On the next day, the matrix is aliquoted in cryovials, with a volume depending on the specific dilution factor (on this case, aliquots were of half of the volume indicated on the datasheet in order to prepare a more suitable quantity of plates once the aliquot is thawed) of each lot, and the aliquots are stored at -20ºC. Once an aliquot has to be used for covering plates, it has to be placed on ice inside a laminar flow hood to allow it to slowly thaw. Meanwhile, a methacrylate tray is placed over a flat tray. All the desired plates to be covered are placed over the methacrylate plate in order to cover them with the Matrigel™. This way, the plates get cold and the matrix gets distributed homogeneously all over the bottom of the plates. At the same time, a 50 mL Falcon tube is also placed on ice and once it gets cold, 12.5 mL of cold DMEM-F12 are added. This medium is previously filtered through a 0.10 µm Stericup® 1000 mL (EMD Millipore, Massachusetts, USA) with the help of a vacuum pump (Busch, Maulburg,

Germany) when performing the aliquots. Next, 1 mL of that DMEM-F12 is added to the aliquot of Matrigel™ and pipetted up and down until all the ice crystals become liquid, and then pipetted back to the 50 mL Falcon tube with the 12.5 mL of cold DMEM-F12. After properly mixing the Falcon tube (always keeping it on ice), different volumes of the mix are added to the plates, depending on their surface areas: 500 µL for wells of a 12-multiwell plates or 24-multiwell plates, and 1.1 mL for wells of a 6-multiwell plate and for 35 mm^2 Petri dishes. Once covered, still on ice, a thin parafilm layer is put all around the edge of the plates to ensure that nothing enters inside, and the plates are stored for up to 1 week at 4ºC. When needed, the plates have to stay at least an hour up to 3 h inside the ICO105med incubator to allow the Matrigel™ to adhere to the bottom of the plate, before removing the DMEM-F12. If the DMEM-F12 is removed, but the plate is not used, there is the possibility to add again 1.1 mL of new DMEM-F12, so that plate could be 24 h more inside the ICO105med incubator with its quality not being compromised (Fig. 35.A). In case that the matrix doesn´t adhere properly, either because it has turned into gel too soon or because it has not been distributed homogenously, the plate presents small clusters attached to its surface, and should be discarded.

The second consideration is the culture medium used for culturing the hiPSCs colonies. On this project, mTeSR1 was used as culture medium for all the plates with hiPSCs colonies because it is highly reported on the bibliography as a medium that supports *feeder-free* conditions[206-208]. This mTeSR1 consists of a basal medium plus a supplemental medium provided with the basal medium that has to be added when aliquoting. When culturing and maintaining the colonies, this medium has to be

changed daily, with a maximum threshold of 28-30 h when the plate reaches its confluence. When changing the medium, old medium is removed carefully and 1 mL of DMEM-F12 is added. Then the plate is placed under the microscope inside the hood. At the microscope, every single dish and well is observed in order to find colonies that might be differentiating. These differentiating colonies are removed with a 200 µL pipette tip. Once the cleaning step is finished, the DMEM-F12 is replaced with 1.5-2 mL (depending on the confluency and the size of the colonies) of new mTeSR1, and the plate is taken back into the ICO105med incubator (Fig. 35.B).

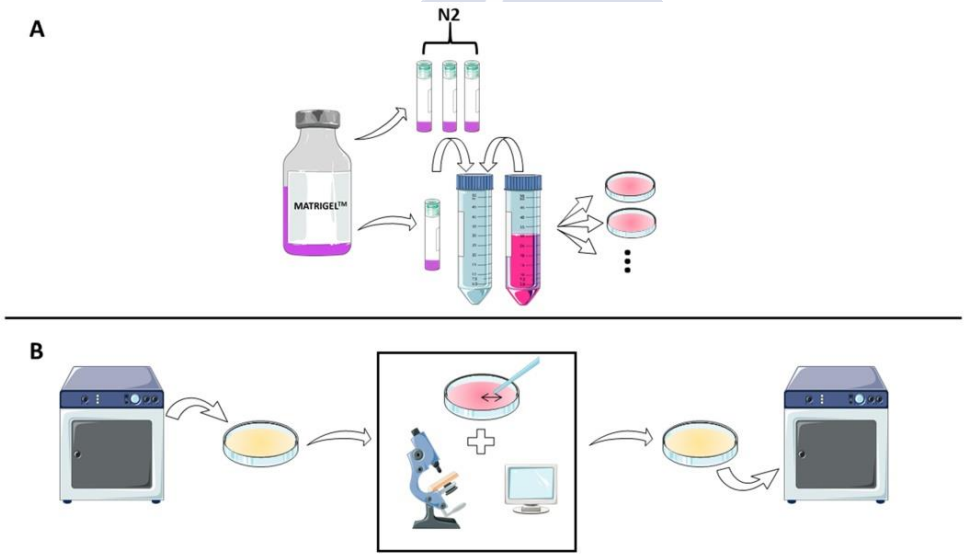

Figure 35. A) Representation of Matrigel™ preparation. B) Daily maintenance of a hiPSCs culture. Self-created image (using elements with Creative Common license).

7.2. Expansion of hiPSCs colonies

Regarding the growth of hiPSCs colonies, it takes up to 6-9 days within a 35 mm^2 Petri dish to reach the state at which is suitable to perform the expansion. This time frame depends on the initial size and number of the colonies. So, when it is time to expand a clone, first of all, the number of dishes in which the clone wants to be expanded must be taken out of the fridge and placed inside the ICO105med incubator for at least 1 hour, as explained on subsection 9.1, to allow the Matrigel™ to attach. Starting with the expansion, the clone is treated first as explained on the subsection 9.1, but when all the differentiating colonies are removed, the DMEM-F12 is replaced with 1 mL of new DMEM-F12 instead of mTeSR1. Then, the remaining colonies are cut in a grid-pattern with a 200 µL pipette tip (see Fig. 34). Next, with the help of a cell lifter, clusters are detached and transferred into a 15 mL Falcon tube, and the plate is rinsed with an extra 1 mL and checked under the microscope to be sure that all clusters have been aspired. After that, the tube is centrifuged at 200 g, 4', RT. Following this step, supernatant is aspired and pellet is resuspended with 1 mL of mTeSR1. At this point, is important to check for the size of the suspended clusters, as they can´t be not too big neither too small, or it will affect the correct growth of the attached colonies: if they too big, they will be stressed and if they are too small, they will not grow or will differentiate. If the clusters are too big, there is the possibility to make them smaller by pipetting up and down 2-3 times. So, having the clusters suspended and with the correct size, dishes with the matrix are taken out of the ICO105med incubator, DMEM-F12 is removed and, after checking by eye that no matrix clusters have been formed, it is replaced with 1 mL of mTeSR1. Then, hiPSCs

clusters are seeded depending on the ratio desired, and dishes are taken back to the ICO105med incubator (Fig.36).

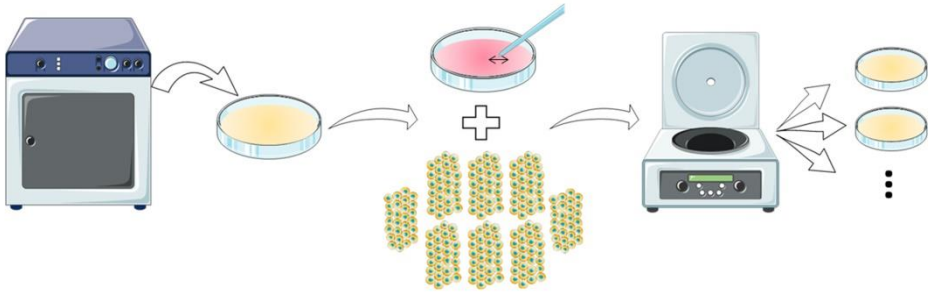

Figure 36. Schematic representation of hiPSCs expansion. Self-created image (using elements with Creative Common license).

7.3. Freezing of hiPSCs colonies

Freezing cells in a satisfactory way is highly dependent on the confluence. It is also a critical step that will affect the future thawing of the hiPSCs clusters. It is because of that, that when freezing hiPSCs, the dishes have to be more confluent than when they are going to be expanded. Also, when cutting the colonies in a grid-pattern, clusters have to be bigger than when performing an expansion. This is because when thawing the cryovial, the process breaks up the clusters a little, so they have to be a little bit bigger when freezing to counter this effect. This way, the clusters will have the correct size when thawing them. Briefly, the colonies are cut in a grid-pattern and lifted mechanically with a cell lifter. Then, they are centrifuged in a 15 mL Falcon tube at 200 g, 4', RT. After that, supernatant is aspired and the pellet is resuspended with 1 mL of freezing medium (BAMBANKER). With BAMBANKER, no sequential freezing steps are required, and also its use is consistently

reported throughout bibliography[209-211]. Once the clusters are resuspended on BAMBANKER and transferred into a cryovial, this cryovial is stored for 24 h in ultra-low temperature freezers (-80ºC) (Haier Biomedical, Middlesex, UK) inside a recipe with 2-methylbutane (Merck Millipore, Massachusetts, USA) (Fig.37). On the next day, cryovials are stored inside a liquid nitrogen container (Air Liquide, Paris, France) until their thawing.

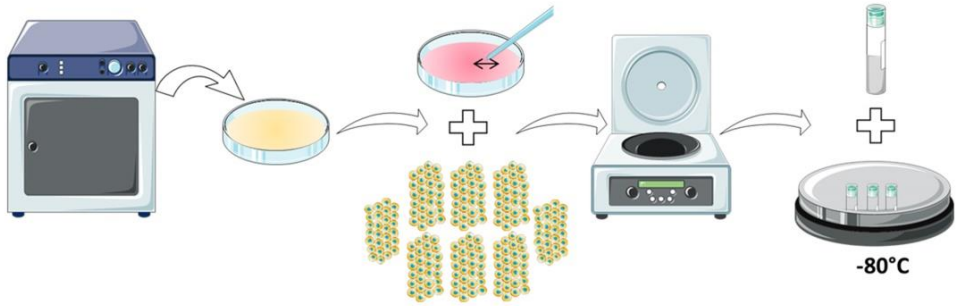

Fig. 37. hiPSCs freezing steps. Self-created image (using elements with Creative Common license).

7.4. Thawing of hiPSCs colonies

Thawing hiPSCs is a quite sensitive process, since the integrity of the frozen clusters gets compromised, so all the steps performed must be done really carefully.

When more than one vial wants to be thawed, they are always thawed one at a time. First of all, the desired vial is removed from the liquid nitrogen container and quickly put on ice, even if it is just to move it inside the culture hood. Then, inside the culture hood, the cap is twisted a quarter to turn to relieve pressure and then retighten. After that, the vial is immersed into a water bath (37ºC) just up to the screw cap for 1', paying attention that no water enters inside the vial (to

ensure this, wrapping the vial with parafilm is a good tip, although it doesn't allow to check the inside of the vial). Then, the vial is moved again inside the culture hood, transferred into a 50 mL Falcon tube and, drop by drop, 10 mL of mTeSR1 fresh medium (previously tempered at room temperature) is added. It is really important to do this drop by drop step, at least for the first 3-4 milliliters, and to slightly shake the Falcon while doing it, as this prevents the cells to die from an osmotic shock. Next, the Falcon is centrifuged at 200 g, 4', RT, and then the supernatant is removed. Pellet is resuspended with 1 mL of mTeSR1 and cells are seeded in a 35mm^2 Petri dish previously coated with Matrigel™, and filled with another 1 mL of mTeSR1. The content of the vials is never seeded in more than one Petri dish (as it can be done when expanding hiPSCs) because the attachment ratio of the clusters is too low to risk the success of this protocol by distributing the content in more than one vial (Fig. 38).

At this point it is important to note, as commented previously, that much of the success of this process comes from how well it has been carried out the freezing step. If the colonies were frozen in excessively small clusters, it doesn´t matter how carefully the thawing step is done, there will be really few clusters attached or even no clusters at all.

Figure 38. hiPSCs thawing process. The step where 10 mL of mTeSR1 medium is added drop by drop to the hiPSCs is critical in order to not induce an osmotic shock to the hiPSCs. Self-created image (using elements with Creative Common license).

8. Characterization of hiPSCs

On this section, all the experiments required for registering and validate a new line of hiPSCs will be described in two different subsections: cytological analysis and genetic analysis.

8.1. Cytological analysis

8.1.1. ANALYSIS OF ALKALINE PHOSPHATASE

The alkaline phosphatase (AP) is an enzyme that is highly related to pluripotent capacity. Although it is far from being a determinant test to validate an iPSC line by itself, it is a good first approach. The vast majority of the AP tests are carried out by previously fixing the cells. On this project, the Alkaline Phosphatase Live Staining test (ThermoFisher, Massachusetts, USA) was employed. This kit allows the Petri dishes used for these experiments to keep growing normally after performing the tests.

The stain was applied directly over the Petri dish with the hiPSCs colonies. The Petri dish was previously washed with pre-warmed DMEM-F12. Then, 3 µL of AP Live Stain 500X was diluted in 1.5 mL of DMEM-F12 and added to the Petri, which was incubated at RT for 30'. After that, the dilution was removed and after several washes of 5' each, the Petri was placed under an inverted Leica DMI 6000B fluorescence microscope (Leica, Wetzlar, Germany). Images were taken on the following 30 to 90' after the staining since the fluorescence vanishes quickly. Once the pictures were taken, DMEM-F12 was replaced with fresh mTeSR1 medium (Fig. 39).

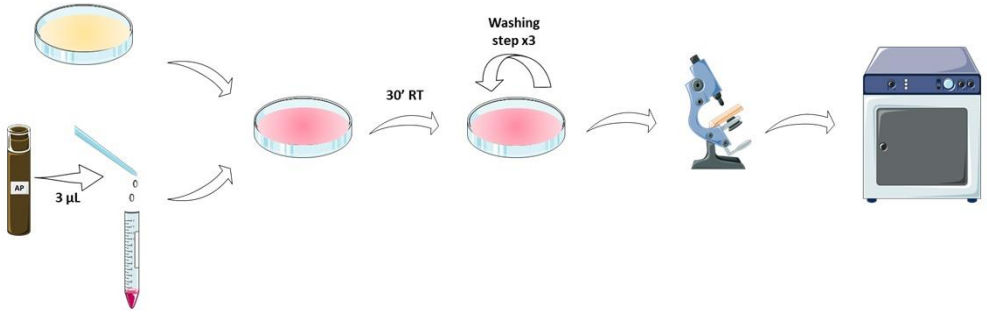

Figure 39. AP live stain representation. Self-created image (using elements with Creative Common license).

8.1.2. IMMUNOFLUORESCENCE ANALYSIS FOR MARKERS RELATED TO PLURIPOTENCY

Double immunofluorescences were carried out for SOX2 + TRA-1-60 and OCT4 + SSEA4 respectively, using the Pluripotent Stem Cell 4-Marker Immunocytochemistry Kit (ThermoFisher, Massachusetts, USA), being SOX2 and OCT4 nuclear pluripotency markers, and TRA-1-60 and SSEA4 cytoplasmic pluripotency markers. Moreover, an immunofluorescence for NANOG using a polyclonal RbαNANOG (Thermofisher, Massachusetts, USA) antibody was performed.

The combination of antibodies used on these immunofluorescences is shown on Table 4. Every immunofluorescence carried out on this project was performed in wells of 4-well culture chambers (Sarstedt, Nümbrecht, Germany). The procedure for the kit was the following:

1) mTeSR1 culture medium is removed and each well is washed twice with 500 µL of wash buffer (diluted as required with distilled H_2O), 3' each wash.

2) Wash buffer is removed and 200 µL of fixative solution is added and incubated for 15', RT.

3) Each well is washed twice with wash buffer. The first wash just for 30'' and the last one for 5'.

4) Wash buffer is removed and 200 µL of permeabilization solution is added and incubated for 15', RT.

5) Permeabilization solution is removed and 200 µL of blocking solution is added and incubated for 30', RT.

6) Blocking solution is removed and 200 µL of the corresponding and previously prepared aliquot is added into each well (see Table 4). After that, the chamber is wrapped with parafilm and foil and placed inside a fridge in order to incubate overnight at 4ºC.

7) On the next day, wells are washed three times with wash buffer for 15', RT.

8) Previously prepared aliquots with the different secondary antibodies (see Table 4) combinations are added into each well. Wells are incubated for 1 hour with the secondary antibodies at RT.

9) Wells are washed 3 times with wash buffer for 5', RT. On the last wash, 1-2 drops of DAPI (Thermofisher, Massachusetts, USA) per well are added.

10) DAPI is removed after 5' and wells are washed once with wash buffer. Then, this wash buffer is replaced with fresh wash buffer. At this point, the chamber is placed under the fluorescence microscope.

The procedure for the NANOG staining was the following:

1) mTeSR1 culture medium is removed and each well is washed with PBS twice, 5-10', RT.

2) Wash buffer is removed and the well is fixed with 200 µL of paraformaldehyde (PFA) (ThermoFisher, Massachusetts, USA) at 4%, 15', RT.

3) PFA is removed and the well is washed three times with PBS, 5-10', RT.

4) The well is blocked with 200 µL of a blocking solution for 1 hour, RT. The composition of the blocking solution is the following:

    - Serum of the animal in which the secondary antibody was made, at 3%.
    - TRITON™ 100X (Sigma-Aldrich, Missouri, USA) at 1X.
    - PBS, filling up to 200 µL.

5) Blocking solution is removed and the primary antibody aliquot is added and incubated over night at 4ºC. The aliquot composition was the following:

- Serum of the animal in which the secondary antibody was made, at 3%.
- TRITON™ 100X at 1X.
- RbαNANOG, 1:200.
- PBS, filling up to 200 µL.

6) The well is washed three times with PBS, 15', RT.
7) An aliquot with the secondary antibody is added and incubated for 1 hour, RT. The aliquot composition was the following:
    - Serum of the animal in which the secondary antibody was made, at 3%.
    - TRITON™ 100X at 1X.
    - DyLight 488 Goat α-Rb IgG (Vector Laboratories, California, USA), 1:200.
    - PBS, filling up to 200 µL.
8) The well is washed three times with PBS, 15', RT.
9) DAPI at 1:6000 diluted on PBS is added to the well and incubated for 5', RT.
10) The well is washed three times with PBS, 10', RT. At this point, the chamber is placed under the fluorescence microscope.

Primary antibody	Dilution	Secondary antibody	Dilution
SSEA4 Ms IgG3	1:100	Alexa fluor 488 Goat α-Ms IgG3	1:250
OCT4 Rb	1:100	Alexa fluor 594 Dk α-Rb	1:250
SOX2 Rat	1:100	Alexa fluor 488 Dk α-Rat	1:250
TRA-1-60 Ms IgM	1:100	Alexa fluor 594 Goat α-Ms IgM	1:250
NANOG Rb	1:200	DyLight 488 Goat α-Rb IgG	1:200

Table 4. Antibodies used against pluripotency-related markers for the immunofluorescence characterization of the generated hiPSC lines.

8.1.3. FORMATION AND DIFFERENTIATION OF EMBRYOID BODIES

Another key validation test for a new hiPSCs line is to prove that the colonies are able to form EBs (*in vitro*) or teratomas (*in vivo*). On this project we induced EBs formation and once they formed, we let them differentiate in order to check by immunofluorescence that they were able to differentiate into cells of the three different germ layers.

For the EBs formation, Petri dishes with large colonies (6-8 days) were washed with DMEM-F12 and the colonies cut in a grid pattern (forming clusters larger than when a passage is performed). Then, the DMEM-F12 was replaced with 1 mL of dispase 1X (StemCell™ Technologies, Vancouver, Canada) and incubated with it for 30-60''. Then, dispase was replaced with EBs medium (EBM 20%), clusters were detached with the aid of a cell lifter and transferred into a well of a 6-multiwell ultra-low attachment plate (Corning, New York, USA) and filled with a total of 2 mL of EBM 20%. This medium is homemade, and its composition consists of:

- DMEM-F12.
- FBS 20%.
- Penicillin/streptomycin (P/S) (Thermofisher, Massachusetts, USA) 1X.
- MEM (1X) + GlutaMAX™-I Minimum Essential Medium (MEM) (Thermofisher, Massachusetts, USA).
- 2-Mercaptoethanol (ThermoFisher, Massachusetts, USA).

Once the clusters were in the ultra-low attachment plate well, the compound Y-27632 (StemCell™ Technologies, Vancouver, Canada), also known as ROCK inhibitor was added to the well, at a concentration of 10μM. On the next day, EBs should be already formed. EBM 20% medium was changed on the next day of EBs formation and then every other day until day 5. To change the medium, EBs were aspired carefully with a serological pipette and transferred into a Falcon of 15 mL and placed inside the ICO105med incubator for 7-10' to allow the EBs to descend to the bottom of the Falcon by gravity. Meanwhile, the empty well was filled with 1 mL of EBM 20% and placed inside the ICO105med incubator too to maintain the medium tempered. Once the time passed, the supernatant of the Falcon was removed really carefully to not disturb the EBs at the bottom, and replaced with 1 mL of EBM 20%. After that, EBs were moved back to the well of the ultra-low attachment plate and inside the ICO105med incubator.

For the differentiation of the EBs, on day 5, these were transferred into a 4-well culture chamber, 5-7 EBs per well, and ROCK inhibitor was added at a concentration of 10 μM per well. The chamber wells were

previously coated with Matrigel™. The medium (EBM 20%) was changed on the next day and every other day from there, for 10-14 days. The wells were observed every day under the microscope to check for their differentiation and several photos were taken (Fig. 40).

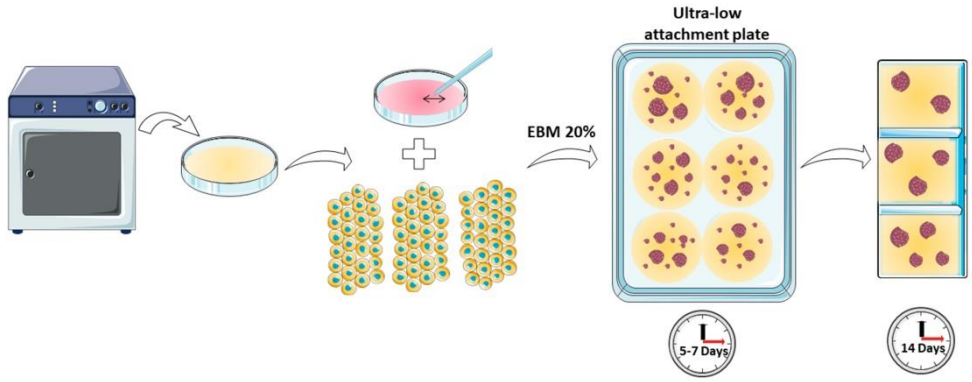

Figure 40. EBs formation and differentiation process. Self-created image (using elements with Creative Common license).

For the characterization of the three germ layers, the antibodies used on the immunofluorescences were: Rb α-FOXA2 (ThermoFisher, Massachusetts, USA) as a nuclear endodermal marker; Rb α-vimentin (BiossAntibodies, Massachusetts, USA) as a generic cytoplasmic mesodermal marker and Ms α-alpha-SMC actin (Sigma-Aldrich, Missouri, USA) as a more specific cytoplasmic mesodermal marker; Rb α-nestin (Abcam, Cambridge, UK) as an ectodermal marker (Table 5). The protocol used for the immunofluorescences were similar to those that were carried out for the pluripotency test for NANOG:

1) EBM 20% is removed and each well is washed with PBS twice, 5-10', RT.

2) Wash buffer is removed and the well is fixed with 200 µL of PFA at 4%, 5', RT and no shaking, as the EBs are less attached than most cells and they tend to detach.

3) PFA is removed and the well is washed two times with PBS, 5-10', RT.

4) The well is blocked with 200 µL of a blocking solution for 1 hour, RT. The composition of the blocking solution is the following:

    - Serum of the animal in which the secondary antibody was made, at 3%.
    - TRITON™ 100X at 1X.
    - PBS, filling up to 200 µL.

5) Blocking solution is removed and the primary antibody (see Table 5) aliquot is added and incubated over night at 4ºC. The aliquot composition is the following:

    - Serum of the animal in which the secondary antibody was made, at 3%.
    - TRITON™ 100X at 1X.
    - Primary antibody.
    - PBS, filling up to 200 µL.

6) The well is washed two times with PBS, 10', RT.

7) An aliquot with the secondary antibody (see Table 5) is added and incubated for 1 hour, RT. The aliquot composition is the following:

    - Serum of the animal in which the secondary antibody was made, at 3%.
    - TRITON™ 100X at 1X.
    - Secondary antibody.
    - PBS, filling up to 200 µL.

8) The well is washed two times with PBS, 10', RT.

9) DAPI at 1:6000 diluted on PBS is added to the well and incubated for 5', RT.

10) The well is washed three times with PBS, 10', RT. At this point, the chamber is placed under the fluorescence microscope.

Primary antibody	Dilution	Secondary antibody	Dilution
FOXA2 polyclonal Rb IgG	1:100	DyLight 488 Goat α-Rb IgG	1:200
Nestin polyclonal Rb IgG	1:200	DyLight 488 Goat α-Rb IgG	1:200
Vimentin polyclonal Rb IgG	1:100	DyLight 488 Goat α-Rb IgG	1:200
α-SMC actin monoclonal Ms IgG2A	1:100	DyLight 488 Goat α-Ms IgG	1:200

Table 5. Antibodies used against markers of cell types from the three different germ layers for the immunofluorescence characterization of the generated hiPSC-EBs after 10-14 days growing.

8.1.4. CELLULAR CONTAMINATION ANALYSIS

All Petri dishes were observed exhaustively every day under the microscope to check for fungal or bacterial contamination

For *Mycoplasma* contamination, all the clones used for characterization and differentiation processes were sent to an external service, where a PCR for *Mycoplasma* was carried out. For this test, an already confluent Petri dish for the specific clone was cultured for two days without changing the medium. After those two days, the colonies were detached and centrifuged, and the supernatant and the dry pellet were sent separately to the external service in order to check both samples.

8.2. Genetic analysis

In order to facilitate the lecture, a table of all the primers used (Table 6) and the schemes for retrotranscription, PCR and qPCR (Table 7) are provided.

Name	Sequence	Length (bp)	Concentration (mM)
SeV for	GGATCACTAGGTGATATCGAGC	22	100
SeV rev	ACCAGACAAGAGTTTAAGAGATATGTATC	29	100
Endo-OCT4 for	GGGTTTTTGGGATTAAGTTCTTCA	24	100
Endo-OCT4 rev	GCCCCCACCCTTTGTGTT	18	100
Endo-SOX2 for	CAAAAATGGCCATGCAGGTT	20	100
Endo-SOX2 rev	AGTTGGGATCGAACAAAAGCTATT	24	100
Endo-KLF4 for	AGCCTAAATGATGGTGCTTGGT	22	100
Endo-KLF4 rev	TTGAAAACTTTGGCTTCCTTGTT	23	100
Endo-c-MYC for	CGGGCGGGCACTTTG	15	100
Endo-c-MYC rev	GGAGAGTCGCGTCCTTGCT	19	100
Hs_Nanog for	AGGAAGACAAGGTCCCGGTCAA	22	100
Hs_Nanog rev	TCTGGAACCAGGTCTTCACCTGT	23	100
Hs_GAPDH for	GAAGGTCGGAGTCAACGGATT	21	100
Hs_GAPDH rev	TGACGGTGCCATGGAATTTG	20	100

Table 6. Primers used, when needed, for PCRs and qPCRs all over the project.

All the primers came lyophilized and reconstituted at 100 mM in RNAse-free H_2O. Then, 10 µL of the forward and reverse primer of each gene were mixed and diluted with 80 µL of RNAse-free H_2O so a final concentration of 10 mM was achieved for each primer within the mix.

RETROTRANSCRIPTION

5x Reaction Mix	Reverse transcriptase	RNA sample	H_2O RNAse free	Final volume
4µL	1µL	1µg	Fill up to the final volume	20µL

PCR

Red Taq polymerase	Primer mix (10mM)	cDNA sample	H_2O RNAse free	Final volume
10µL	1µL	20ng	Fill up to the final volume	20µL

qPCR

SYBR green	Primer mix (10mM)	cDNA sample	H_2O RNAse free	Final volume
10µL	1µL	10ng	Fill up to the final volume	20µL

Table 7. Reagent and sample quantities used for the retrotranscriptions, PCRs and qPCRs carried out throughout this Thesis.

8.2.1. EXPRESSION OF THE REPROGRAMMING FACTORS

The expression of the reprogramming factors was measured by qPCR. This was analyzed in the clones that were able to reach the passage 10. Their RNA was extracted and measured at the Nanodrop (ThermoFisher, Massachusetts, USA) (Fig. 41) and then, 1 µg of each sample was retrotranscribed to achieve 1 µg of cDNA.

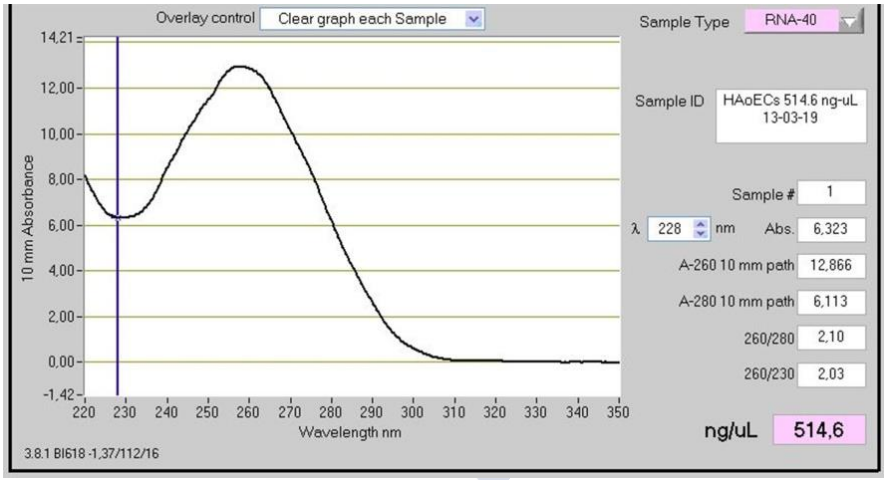

Figure 41. Example image of a NANODROP measurement, where it can be observed that 260/280 and 260/230 parameters fall into a correct interval.

RNA extraction

For the RNA extraction, the Quick-RNA™ MiniPrep Plus (Zymo Research, California, USA) was always used. The protocol was optimized based on the one provided with the kit. Briefly, the procedure is as follows:

- In order to homogenize the sample, cells are lifted and centrifuged (200 g, 4', RT) and then resuspended always with 300 µL of RNA Lysis Buffer, independently of the sample size.

- For sample clearing and removal of gDNA, the sample is centrifuged at 12000 g, 1', RT. The supernatant is then transferred to a yellow filter tube provided in the kit, and centrifuged again at 12000 g, 1', RT. On this case, the flow-through is saved and transferred into a green filter tube provided in the kit, for RNA purification.

- For RNA purification, a mix of 1 volume of ethanol 100% and 1 volume of RNA Lysis Buffer is added to the sample and centrifuged on the green filter tube at 12000 g, 30'', RT. Then 400 µL of RNA Prep. Buffer is added and the tube centrifuged again at 12000 g, 30'', RT.

- The final steps are for washing the sample. Several steps on which RNA wash buffer is added to the sample are done, centrifuging again at 12000 g, 1', RT on each washing step. Finally, 35 µL of DNAse/RNAse-free water is added directly over the filter matrix, and after a last centrifugation at 12000 g, 30'', RT, the flow-through is saved and 1 µL is measured at the Nanodrop to check for the RNA concentration and purity.

Retrotranscription

The objective of the retrotranscription is to retrotranscribe 1 µg of RNA to achieve 1 µg of cDNA. Thus, once the RNA concentration of the samples was measured, the different retrotranscription reagents were pipetted into a PCR Eppendorf tube (see Table 7).

The retrotranscription kit used for all the RNA samples was the iScript™ cDNA Synthesis Kit (BIO-RAD, California, USA), and the program used at the PCR device (Analytik-Jena, Jena, Germany) is shown at Fig. 42.

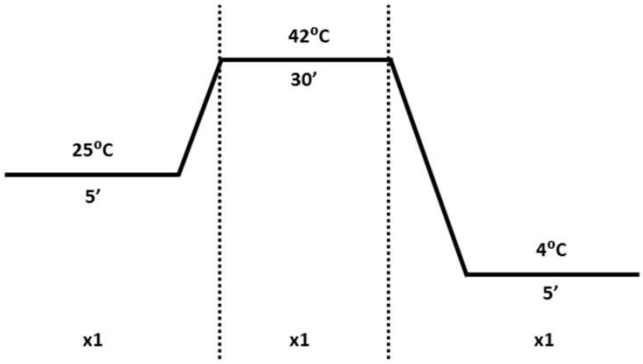

Figure 42. Program used for retrotranscription.

PCR

In order to check for a correct retrotranscription before beginning with the qPCR, a PCR for the housekeeping gene *GAPDH* was carried out.

At the end of the retrotranscription, the final cDNA concentration is 50 ng/µL. For PCRs, 20 ng of cDNA were amplified, so the cDNA sample was previously diluted to a concentration of 5 ng/µL to make easier to pipette the 20 ng. Thus, the several PCR reagents were mixed in a PCR Eppendorf tube as shown in Table 7.

Primers were designed using the guide provided by Sigma-Aldrich on its web. Primers came lyophilized and were reconstituted at 100 mM with nuclease-free H_2O, and then mixed together to a final concentration of 10 mM. While not used, primers were stored at 20ºC.

The PCR kit used for all the cDNA samples was the Ready Mix REDTaq PCR Reaction Mix (Sigma-Aldrich, Missouri, USA), and the program used at the PCR device is shown at Fig. 43.

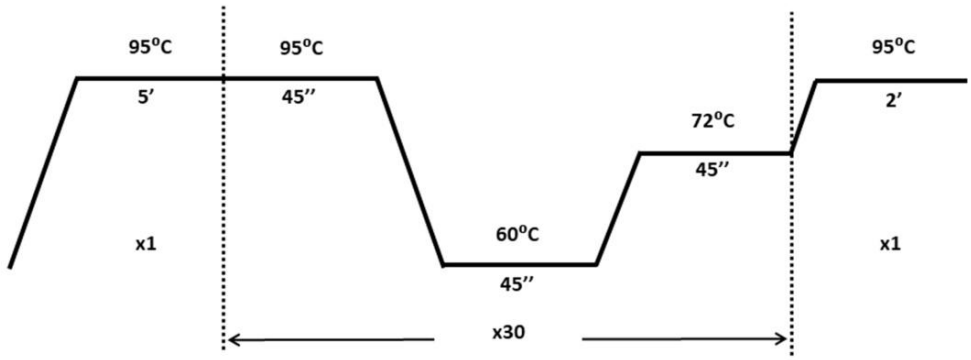

Figure 43. Program used for PCR.

Agarose gel preparation and DNA electrophoresis

In order to check the results of the PCR, DNA electrophoresis were carried out in a 2.5% agarose gel.

For the agarose gel preparation, the first step was to dilute 3 g of agarose (Sigma-Aldrich, Missouri, USA) in 120 mL of TAE buffer 1X (BIO-RAD, California, USA). Then it was heated in the microwave until the agarose was completely diluted. Right after heating and diluting the agarose, 6 µL of EuroSafe (Euroclone, Milan, Italy) was added and smoothly shaken until reaching the homogenization. The mix was carefully poured in a mold and a comb was placed to create the wells. The mix then was allowed to rest for 20-30' in order to let it solidify.

For the electrophoresis, 2.5 µL of the product of the PCR was pipetted into a well of the agarose gel. The ladder used was the Thermo Scientific GeneRuler DNA Ladder 100bp Plus (ThermoFisher, Massachussetts, USA). Finally, the agarose gel with the samples was run in a Sub-Cell® GT agarose gel electrophoresis system (BIO-RAD, California, USA) with TAE 1X, at 100 V, 2 A and the agarose gel was placed under a UV microscope for revelation.

qPCR

The concentration of the cDNA achieved was 50 ng/µL but it was diluted to 5 ng/µL. For the qPCR, the iTaq Universal SYBR Green Supermix (BIO-RAD, California, USA) was employed, and 10 ng of cDNA were used for each subclone sample. Each subclone sample was triplicated for each factor (Fig. 44).

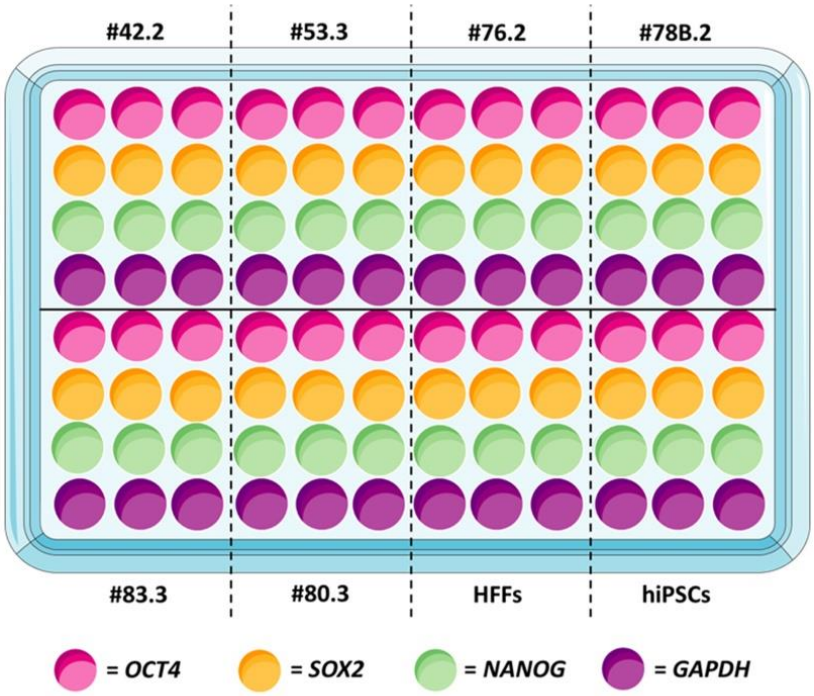

Figure 44. Scheme followed when analyzing pluripotency related genes in the stable clones achieved in first reprogramming process.

The program followed for the qPCR is represented at Fig. 45. The reprogramming factors measured both for the IDISi001-A and CAD02 cell line were SOX2 and OCT4.

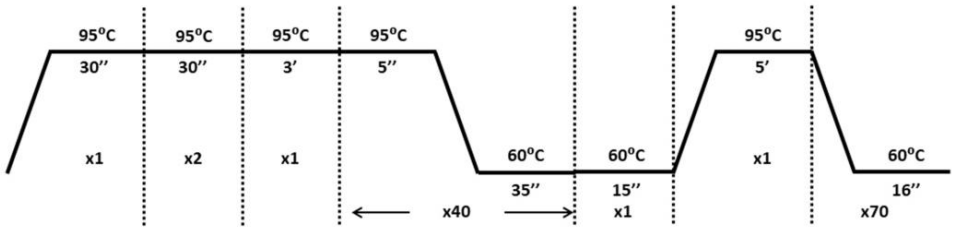

Figure 45. Program used for qPCR.

8.2.2. PRESENCE AND ABSENCE OF THE VIRUS

In order to check for a correct infection, the positive control cells were collected the day after the infection, and the RNA was extracted using the Quick-RNA™ MiniPrep Plus. After that, the RNA concentration was measured at the Nanodrop and a retrotranscription was performed using the iScript™ cDNA Synthesis Kit to achieve 1 µg of cDNA. Of this cDNA, 20 ng were amplified by PCR using the Ready Mix REDTaq PCR Reaction Mix. The final concentration of the cDNA was 50 ng/µL, but before performing the PCR it was diluted to a final concentration of 5ng/µL. Finally, 2.5 µL of the PCR product were pipetted into a well of an agarose gel (2.5%). The ladder used was the Thermo Scientific GeneRuler DNA Ladder 100bp Plus. The gel was run in the Sub-Cell® GT agarose gel electrophoresis system filled with TAE 1X, at 100 V, 2 A. Finally, the agarose gel was placed under a UV microscope for revelation. As a non-infected control, cDNA from a normal human foreskin fibroblast (HFF) cell line was charged.

In the same way that the correct infection must be checked, once several stable clones were achieved, they also had to be analyzed by

electrophoresis in order to check that the virus was completely removed from the cells. For this, one Petri dish of each of the clones that were able to reach the passage 5 was collected and the RNA was extracted and measured at the Nanodrop. Then, 1 µg was retrotranscribed and 20ng of cDNA were amplified for each subclone. After that, 2.5 µL of the product of the PCR for each subclone were charged into a well of an agarose gel (2.5%) and run at 100 V, 2 A. Finally, the agarose gel was placed under a UV microscope for revelation.

8.2.3. hiPSCs KARYOTYPING ANALYSIS

Karyotyping analyses were performed in order to check for possible chromosomal mutations in the two characterized hiPSCs cell lines. Karyotyping analyses were performed with samples at passage 10 for each cell line. The protocol for the karyotyping was the following:

1) First of all, a Petri dish with big and almost confluent hiPSCs colonies (5-7 days old) are incubated with KaryoMAX™ Colcemid™ Solution (ThermoFisher, Massachussetts, USA) for 3 h. What Colcemid does is to prevent spindle formation during cell division, thus causing metaphase arrest.

2) The next step is to detach cells by incubating them with trypsin-EDTA (0.25%) (ThermoFisher, Massachussetts, USA) for 8-10' and collected into a Falcon of 15 mL with 8 mL of washing medium (DMEM + PBS 5%).

3) Cells are centrifuged and then the supernatant is almost fully discarded and the pellet resuspended with the remaining supernatant. This step has to be done by pipetting up and down

several times and with emphasis, since the colonies are really hard to break up into a single-cell suspension.

4) After that, the single-cell suspension is exposed to a hypotonic KCl (0.075 M) solution for 10' at 37ºC. This KCl is added carefully drop by drop while the tube is being smoothly vortexing. What the KCl does is to disperse the chromosomes, making them distinguishable from each other.

5) The Falcon tube is centrifuged at 200 g, 5' at RT and the supernatant is almost fully removed. The remaining supernatant is used for resuspending the pellet.

6) For the fixation process, 5 mL of a Carnoy's fixative solution (methanol + glacial acetic acid in a 3:1 proportion) are added to the Falcon for 20', while smoothly vortexing. This step is repeated 2 more times.

7) After the third time of fixation, the supernatant is partially removed and the pellet resuspended with the remaining supernatant. Finally, 4-5 drops of the Falcon are placed on a preheated slide (44ºC), which evaporated the solution, remaining just the chromosomes on the slide. Once evaporated, the slide is stained with a KaryoMAX™ Giemsa Stain Solution (ThermoFisher, Massachussetts, USA). After that, the slide is able to dry. Once the slide is completely dry, it is cover slipped and ready to be placed under an inverted microscope for the searching and analysis of the metaphases.

9. Development and optimization of vascular smooth muscle and vascular endothelial cell differentiation protocols

On this section, it will be described all the procedures assayed for the differentiation of the hiPSCs into the two cell lines tested: CADASIL-hiPSCs-derived vSMCs and CADASIL-hiPSCs-derived vECs. The experiments regarding this section were only carried out on the IDISi001-A line.

9.1. Development and optimization of a vascular smooth muscle cell differentiation protocol

For the differentiation of CADASIL-hiPSCs into vSMCs, two different protocols were assayed. The first one, suggested by an external laboratory, consisted in exposing entire colonies within the same Petri dish to a culture medium composed of:

- FBS 10%.
- Ascorbic acid 30 µg/mL.
- P/S 1%.
- Dulbecco's modified eagle medium (DMEM) with L-glutamine (ThermoFisher, Massachusetts, USA).

For the second differentiation of hiPSCs into vSMCs, it was performed an adapted and optimized protocol taken from an article published at the *Biochemistry Journal* in January 2015[100] (Fig. 46).

On this case, the starting point is a suspension of small clusters of hiPSCs. To do so, a highly confluent Petri dish (6-7 days) of hiPSCs is cut following a grid-pattern, making small clusters. Then, 1 mL of dispase 1X per Petri dish is added for 30'' until the borders of the clusters begin to retract. After that, clusters are collected by using a cell lifter and placed into a 15 mL Flacon tube for centrifugation (200 g, 4', RT). Once the centrifugation is finished and the supernatant removed, the pellet is resuspended with 1 mL of differentiation medium 1 (DM1). This DM1 consists of:

- α-MEM with nucleosides (StemCell™ Technologies, Vancouver, Canada) as basal medium.
- FBS 10%.
- P/S 1%.
- Amphotericin B (ThermoFisher, Massachusetts, USA) 1%.
- 2-Mercaptoethanol, 0.1 mM.

Once resuspended, clusters are mechanically broken down by pipetting vigorously up and down until no clusters are seen by eye. The next step is to seed the cell suspension into a new 35 mm^2 Petri dish, previously coated with Matrigel™. Finally, prior to save the Petri dish inside the ICO105med incubator, ROCK inhibitor at 10 μM is added in order to promote the survival and attachment rate of the cells. To maintain these cells, medium is changed every day.

Between day 10 and day 14, depending on confluence, cells are lifted and split in a ratio 1:2, with differentiation medium 2 (DM2). This

medium contains the same as DM1 plus the addition of TGF-β (R&D Systems, Minneapolis, USA) at 1 ng/mL and PDGF-BB (R&D Systems, Minneapolis, USA) at 10 ng/mL. This medium is changed every two days, with fresh growth factors.

The preparation of the growth factors was as follows:

- **TGF-β**: TGF-β came lyophilized and it was initially dissolved at a final concentration of 20 µL/mL with HCl 4 mM with BSA (Sigma-Aldrich, Missouri, USA) at 1 mg/mL, as stated by the commercial company. After that, aliquots of 2 µg/mL with HCl 4 mM with BSA at 1 mg/mL were made so that the final volume to be added into Petri dishes was not too small in order to pipette it.
- **PDGF-BB**: It also came lyophilized. Following datasheet instructions, it was diluted to a final concentration of 100 µg/mL. Unlike TGF-β, PDGF-BB was diluted with HCl 4 mM without BSA. After that, aliquots of 10 µg/mL with HCl 4 mM without BSA were made so that, like for TGF-β, the final volume to be added into Petri dishes was not too small in order to pipette it.

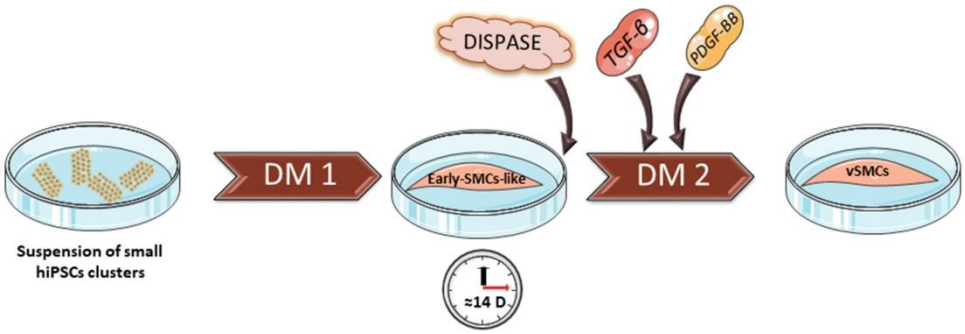

Figure 46. Differentiation protocol to vSMCs. Self-created image (using elements with Creative Common license).

9.2. Development and optimization of a vascular endothelial cell differentiation protocol

For the differentiation of hiPSCs into vECs, a protocol taken from an article published at the Stem Cells journal in April 2017[101] was followed (Fig. 47).

To begin with, hiPSCs from confluent 35 mm^2 Petri dishes are cut in a grid pattern to form clusters with a normal size. Clusters are then collected with a cell lifter after 30'' of incubation with dispase 1X. Once centrifuged, the resulting pellet is resuspended with STEMdiff™ APEL™2-LI Medium (StemCell™ Technologies, Vancouver, Canada) with P/S and amphotericin B at 1%. After the cells are seeded into Matrigel™ coated 35 mm^2 Petri dishes, they are supplemented with FGF2 (StemCell™ Technologies, Vancouver, Canada) at a concentration of 10 ng/mL. On the next day, medium is removed and fresh STEMdiff™ APEL™2-LI Medium is added and supplemented with 6 μM of CHIR99012 (StemCell™ Technologies, Vancouver, Canada). Next, on the second day after CHIR99012 is added, medium is changed again and replaced with fresh STEMdiff™ APEL™2-LI Medium, and this time cells are supplemented with FGF2 at 10 ng/mL, 25 ng/mL of BMP4 (StemCell™ Technologies, Vancouver, Canada) and 50 ng/mL of VEGF (StemCell™ Technologies, Vancouver, Canada). Again after 2 days, this time cells are lifted with the aim of dispase 1X, centrifuged at 200 g, 4' at RT and resuspended with EC Growth Medium MV2 (Promocell, Heidelberg, Germany). Then they are seeded in the desired number of 35 mm^2 Petri dishes without any kind of coating, and supplemented with an additional 50 ng/mL VEGF. After that, medium is changed every two days and without any kind of supplementation.

The preparation of the growth factors was as follows:

- **FGF2**: the vial was centrifuged previous to aliquot. Then it was diluted with distilled H_2O to a concentration of 0.1 mg/mL.
- **CHIR99012**: diluted with sterile DMSO to a final concentration of 5 mM.
- **BMP4**: diluted with 4 mM HCl with 0.1% of BSA to a concentration of 10 µg/mL.
- **VEGF**: the vial was centrifuged previous to aliquot. The vial was reconstituted with distilled H_2O to a concentration of 0.1 mg/mL.

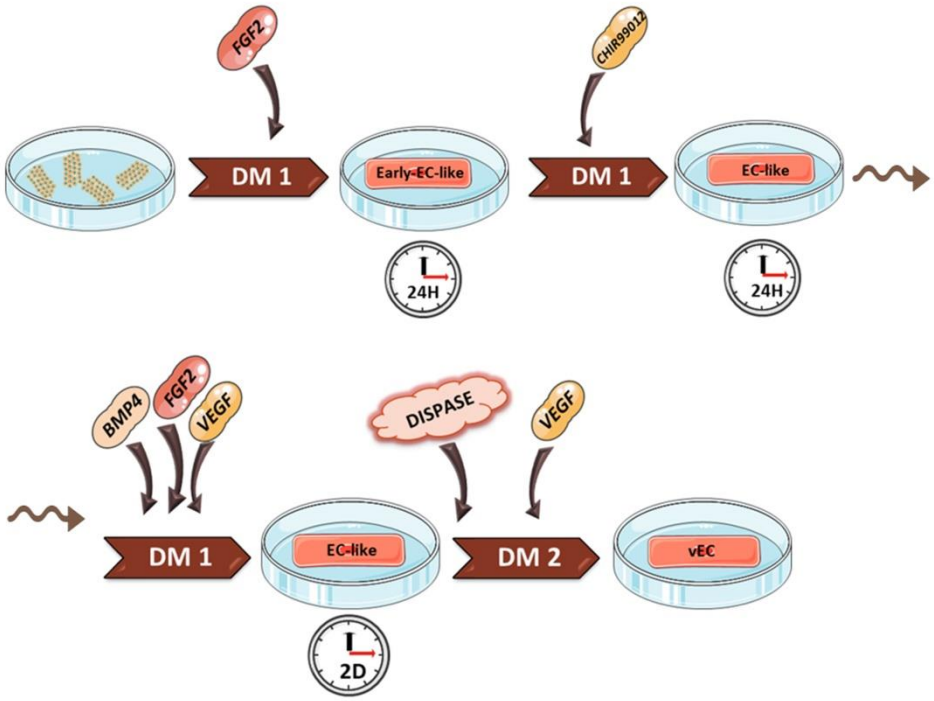

Figure 47 Differentiation protocol to vECs. Self-created image (using elements with Creative Common license).

10. Characterization of CADASIL-hiPSCs-derived vascular smooth muscle and vascular endothelial cell differentiation cell lines

10.1. Characterization of CADASIL-hiPSCs-derived vascular smooth muscle cells

Characterization of CADASIL-hiPSCs-derived vSMCs was assayed by immunofluorescence of several SMC markers and by the addition of carbachol (Sigma-Aldrich, Missouri, USA) in order to test their contractility.

Immunofluorescences using Rb α-Vimentin (1:100), Rb α-Desmin (1:200) (Abcam, Cambridge, UK) and Ms α-alpha-SMC actin (1:100) were performed separately as follows (Table 8):

1) SMC medium is removed and each well is washed with PBS twice, 5-10', RT.

2) Wash buffer is removed and the well is fixed with 200 µL of PFA at 4%, 5', RT.

3) PFA is removed and the well is washed three times with PBS, 5-10', RT.

4) Wells are blocked with 200 µL of a blocking solution for 1 hour, RT. The composition of the blocking solution was the following:

    - Serum of the animal in which the secondary antibody was made, at 3%.
    - TRITON™ 100X at 1X.
    - PBS, filling up to 200 µL.

5) Blocking solution is removed and the primary antibody aliquot is added and incubated over night at 4ºC. The aliquot composition was the following:

    - Serum of the animal in which the secondary antibody was made, at 3%.
    - TRITON™ 100X at 1X.
    - Primary antibody at the desired concentration.

- PBS, filling up to 200 µL.

6) Wells are washed three times with PBS, 15', RT.

7) An aliquot with the secondary antibody is added and incubated for 1 hour, RT. The aliquot composition was the following:

    - Serum of the animal in which the secondary antibody was made, at 3%.
    - TRITON™ 100X at 1X.
    - Secondary antibody suitable for the primary antibody, 1:200.
    - PBS, filling up to 200 µL.

8) Wells are washed three times with PBS, 15', RT.

9) DAPI at 1:6000 diluted on PBS is added to wells and incubated for 5', RT.

10) Wells are washed three times with PBS, 10', RT. At this point, the chamber is placed under the fluorescence microscope.

Primary antibody	Dilution	Secondary antibody	Dilution
Vimentin polyclonal Rb IgG	1:100	DyLight 488 Goat α-Rb IgG	1:200
α-SMC actin monoclonal Ms IgG2A	1:100	DyLight 488 Goat α-Rb IgG	1:200
Desmin polyclonal Rb IgG	1:200	DyLight 488 Goat α-Rb IgG	1:200

Table 8. Antibodies used for vSMC and HAoSMC characterization.

For the contractility test, differentiated vSMCs of 21 days were used. Carbachol was diluted with distilled H_2O to a stock solution of 5mM. For contractility tests, differentiation medium was replaced with a fresh one and 10 µmol/L of carbachol was added to a 35 mm^2 Petri dish with differentiated vSMCs. Then, the Petri was placed under the culture hood microscope and, without moving it, images of the same cells were taken every 10' for 30'. Also, in case that being outside the incubator for so long exerts a contractility effect, contractility test was performed storing the Petri dish inside the incubator and just putting it out for taking the pictures. To do so, cells subjected to study were previously marked with a pen to easily find them once the Petri dish was placed under the microscope. Once the experiment was over, medium was replaced with new fresh SMC differentiation medium. Measurement of contractility was done with the ImageJ software (National Institute of Health, Maryland, USA).

10.2. Characterization of CADASIL-hiPSCs-derived vascular endothelial cells

Characterization of CADASIL-hiPSCs-derived vECs was assayed by immunofluorescence of several EC markers and by testing their ability to form vessels.

Immunofluorescences with Rb α-CD31 (1:50) (Abcam, Cambridge, UK) and Rb α-vWF (1:50) (Immunostep, Salamanca, Spain) were performed following the same steps described in the characterization of CADASIL-hiPSCs-derived vSMCs (Table 9).

Primary antibody	Dilution	Secondary antibody	Dilution
CD31 polyclonal Rb IgG	1:50	DyLight 488 Goat α-Rb IgG	1:200
vWF polyclonal Rb IgG	1:50	DyLight 488 Goat α-Rb IgG	1:200

Table 9. Antibodies used for vEC and HAoEC characterization.

In order to check for the ability to form vessels, derived CADASIL-hiPSCs-derived vECs were passaged into wells of a 12-well plate previously coated with Matrigel® Growth Factor Reduced (GFR) Basement Membrane Matrix, *LDEV-free (Corning, New York, USA) and with EC Growth Medium MV2. Cell density for well of a 12-well plate was $3x10^5$ cells/cm^2. Vessel formation process was monitored daily under the microscope.

11. Short-tandem repeats and *NOTCH3* mutation analysis

Short tandem repeats or "microsatellites", are tracks of tandemly repeated short (1 to 6 bps) DNA sequence motifs. STRs comprise about 3% of the total human genome. Each person in the world possesses a unique combination of STRs.

Because of this, on this project this technique has been carried out to prove that every cell line derived from the patient's original sample was in fact the same cell line, since the combination of 10-15 STRs would be the same for all cell lines. To do this, samples from the original cell line (CADASIL-PBMCs) and samples from the different derived cell lines (CADASIL-hiPSCs, CADASIL-hiPSCs-derived vSMCs and CADASIL-hiPSCs-derived vECs) were collected each time any of the cell lines were successfully derived. For the collection of samples, cells were collected mechanically and centrifuged (200 g, 4', RT) and supernatant was removed in order to be resuspended with saline. Then, a new centrifugation step was made (200 g, 4', RT) to form a pellet. Samples were analyzed in a genomics service external to the laboratory.

On the other hand, as different cell lines were being obtained, it was necessary to check whether the initial diagnosed mutation for each patient was still present in all of them. For this purpose, the samples from the IDISi001-A cell line that were used for the STR analysis were also used at the same external service to check the presence of the mutation.

STRs and mutation analysis for the CAD02 line were just made in CAD02-PBMCs and CAD02-hiPSCs, while for the first cell line, IDISi001-

A, all analysis were made in every derived cell line (CADASIL-PBMCs, CADASIL-hiPSCs, CADASIL-hiPSCs-derived vSMCs and CADASIL-hiPSCs-derived vECs).

12. Culture of the different cell type controls

On this section, the different culture methodologies and requirements of all the commercial cell lines (muscle and endothelial cells) used as controls for the several characterization and analysis experiments will be described.

12.1. Human embryonic kidney cells

Human embryonic kidney (Hek) cells were used as negative control in immunofluorescence and contractility experiments for the characterization of CADASIL-hiPSCs-derived vSMCs (Fig. 48). They were also used in immunofluorescence experiments for the intracellular domain of NOTCH3.

The medium used for culturing Hek cells is homemade and consists of:

- MEM + Glutamax (ThermoFisher, Massachusetts, USA) as basal medium
- FBS 10%
- P/S 1%
- Amphotericin B 1%

- Non-essential amino acids (ThermoFisher, Massachusetts, USA) 1X

Hek cells were cultured in T75 flasks (Corning, New York, USA) and the medium was changed every two days. Depending on the experiment that wanted to be performed, cells were passaged into 35 mm^2 Petri dishes for contractility tests and into 4-well culture chambers for immunofluorescences.

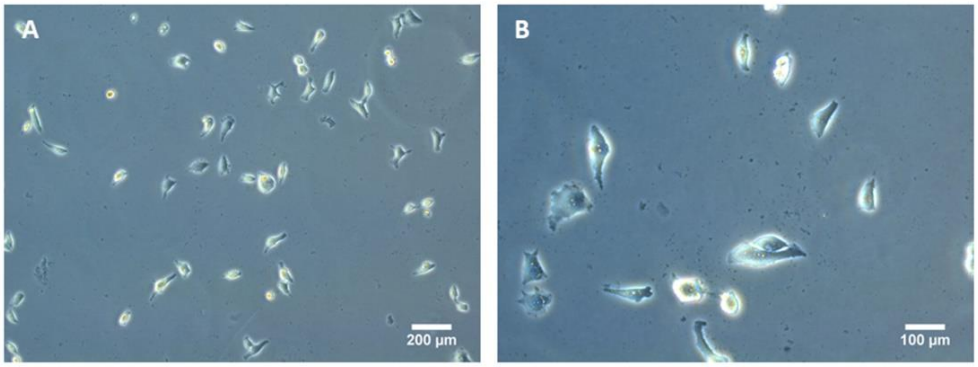

Figure 48. Images from a typical Hek cell culture at different magnifications (A=10X; B=20X**)**

12.2. Human aortic smooth muscle cells

As a positive control to compare with the obtained cell lines, for the characterization of CADASIL-hiPSCs-derived vSMCs, a commercial cell line of HAoSMCs (Promocell, Heidelberg, Germany) was cultured (Fig. 49). The medium used was Smooth Muscle Cell Growth Medium 2 (Promocell, Heidelberg, Germany). Upon arrival, cells were first thawed and seeded into two T25 flasks (Corning, New York, USA). Once they reached the confluence, cells were passaged into 35 mm^2 Petri dishes for contractility tests, 4-well culture chambers for immunofluorescence

and T25 flasks for maintenance and/or RNA or protein extraction. The passages were made mechanically, with a cell lifter, but with the aid of a previous incubation with dispase 1X for 30''.

Regarding HAoSMCs culture, it is important to point that the addition of amphotericin B to the culture had a negative impact, resulting in a non-proliferating culture. Once removed, cells began to grow normally. It is also important to remark that it should be understood as confluence the moment the cells start to line up in parallel. This happens 1-2 days after the dish/flask surface is almost fully covered by cells.

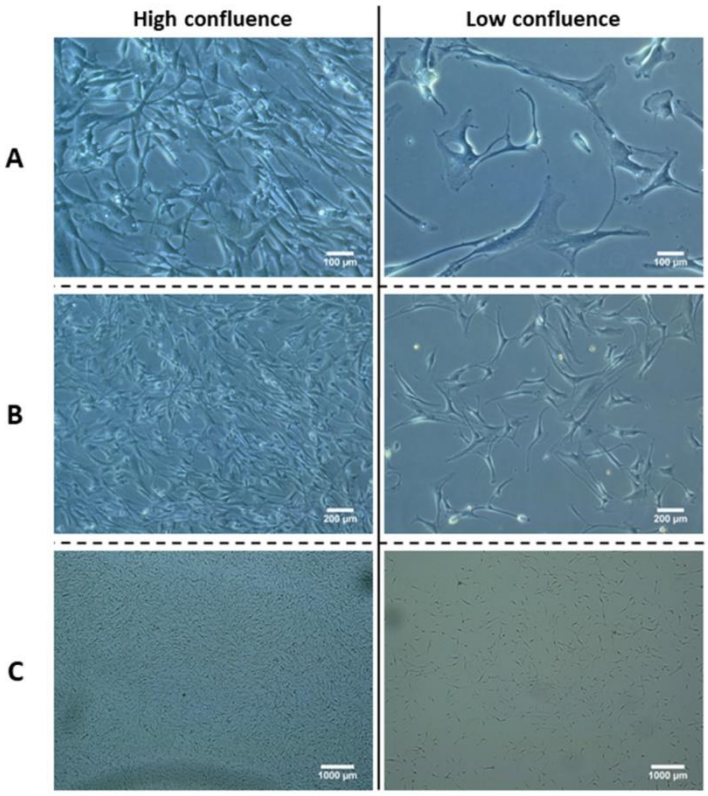

Figure 49. High and low confluence HAoSMC culture at 20X (A), 10X (B) and 2,5X (C) magnifications.

12.3. Human aortic endothelial cells

As a positive control for the characterization of CADASIL-hiPSCs-derived vECs, a commercial cell line of HAoECs (Promocell, Heidelberg, Germany) was cultured (Fig. 50). Upon arrival, cells were first thawed and seeded into two T25 flasks. Then, once they reached confluence, cells were passaged to 35 mm^2 Petri dishes in order to manipulate a proper volume of cells. Passages were always carried out mechanically, with the aid of dispase 1X to help the cells to easily detach.

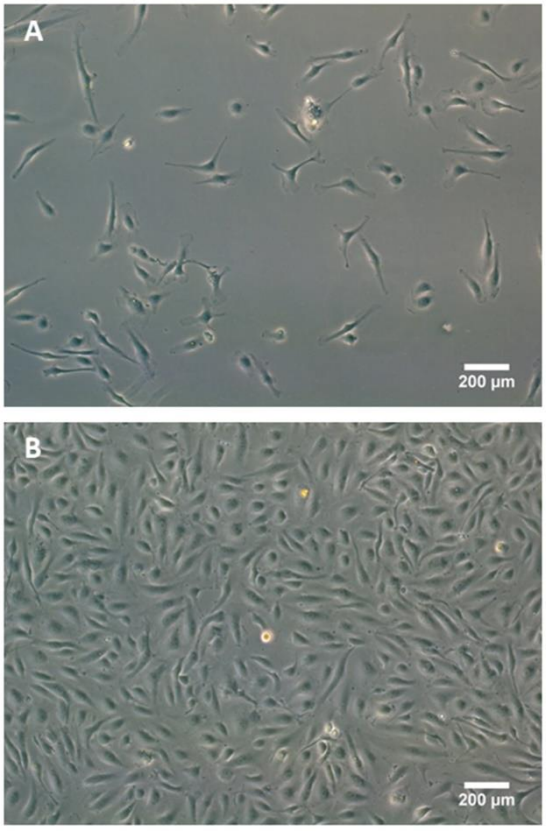

Figure 50. HAoECs typical culture at low (A) and high (B) confluence.

13. Expression analysis of NOTCH3 domains

On this section it will be described the procedures that were carried out in order to analyze the expression pattern of both NICD and NECD. All the derived cell lines used for the analysis were derived from the IDISi001-A-hiPSC line.

13.1. Expression pattern analysis

In order to analyze the expression pattern of both intra- and extracellular domain of NOTCH3, several immunofluorescences were performed in several cell lines. In both cases the idea was to be able to see the expression pattern of the NOTCH3 domains from the hiPSCs to different stages of differentiation for the derived CADASIL-hiPSCs-derived vSMCs and vECs.

13.1.1. NOTCH3 INTRACELLULAR DOMAIN

The antibody selected for the immunofluorescence was NICD polyclonal Rb IgG (ThermoFisher, Massachusetts, USA). The procedure was as follows:

1) Culture medium is removed and each well is washed with PBS twice, 5-10', RT.

2) Wash buffer is removed and the well is fixed with 200 µL of PFA at 4%, 5', RT.

3) PFA is removed and the well is washed three times with PBS, 5-10', RT.

4) Wells are blocked with 200 µL of a blocking solution for 1 hour, RT. The composition of the blocking solution was the following:

    - Rabbit serum at 3%.
    - TRITON™ 100X at 1X.
    - PBS, filling up to 200 µL.

5) Blocking solution is removed and the primary antibody aliquot is added and incubated over night at 4ºC. The aliquot composition is the following:

    - Rabbit serum at 3%.
    - TRITON™ 100X at 1X.
    - NICD polyclonal Rb IgG at 1:200.
    - PBS, filling up to 200 µL.

6) Wells are washed three times with PBS, 10', RT.

7) An aliquot with the secondary antibody is added and incubated for 1 hour, RT. The aliquot composition is the following:

    - Rabbit serum, at 3%.
    - TRITON™ 100X at 1X.
    - DyLight 488 Goat α-Rb IgG, 1:200.
    - PBS, filling up to 200 µL.

8) Wells are washed three times with PBS, 10', RT.

9) DAPI at 1:6000 diluted on PBS is added to wells and incubated for 5', RT.

10) Wells are washed three times with PBS, 10', RT. At this point, the chamber is placed under the fluorescence microscope.

13.1.2. NOTCH3 EXTRACELLULAR DOMAIN

The antibody selected for the immunofluorescence of NECD was NOTCH3/N3ECD monoclonal Ms IgG1, clone 1E4 (Merck Millipore, Massachusetts, USA). The procedure was as follows:

1) Culture medium is removed and each well is washed with PBS twice, 5-10', RT.

2) Wash buffer is removed and the well is fixed with 200 µL of PFA at 4%, 5', RT.

3) PFA is removed and the well is washed three times with PBS, 5-10', RT.

4) Wells are blocked with 200 µL of a blocking solution for 1 hour, RT. The composition of the blocking solution is the following:

    - Horse serum at 3%.
    - TRITON™ 100X at 1X.
    - PBS, filling up to 200 µL.

5) Blocking solution is removed and the primary antibody aliquot is added and incubated over night at 4ºC. The aliquot composition is the following:

- Rabbit serum at 3%.
- TRITON™ 100X at 1X.
- NOTCH3/N3ECD monoclonal Ms IgG1, clone 1E4 at 1:200.
- PBS, filling up to 200 µL.

6) Wells are washed three times with PBS, 10', RT.

7) An aliquot with the secondary antibody is added and incubated for 1 hour, RT. The aliquot composition is the following:

   - Rabbit serum, at 3%.
   - TRITON™ 100X at 1X.
   - DyLight 488 Hs α-Ms IgG (Vector Laboratories, California, USA), 1:200.
   - PBS, filling up to 200 µL.

8) Wells are washed three times with PBS, 10', RT.

9) DAPI at 1:6000 diluted on PBS is added to wells and incubated for 5', RT.

10) Wells are washed three times with PBS, 10', RT. At this point, the chamber is placed under the fluorescence microscope.

13.2. Western blot analysis of NOTCH3

In the same way as for the expression pattern analysis, both intra- and extracellular domains of NOTCH3 were subjected to western blotting in order to check for a possible anomalous accumulation of any of the domains. Samples of hiPSCs from the IDISi001-A cell line, HAoSMCs, HAoECs, IDISi001-A-hiPSCs-derived vSMCs at 16, 21 and 30 days after differentiation and IDISi001-A-hiPSCs-derived vECs were analyzed together on each western blot (WB) performed. As loading control, a GAPDH monoclonal Ms IgG1 antibody (ThermoFisher, Massachusetts, USA) was employed at a concentration of 1:2500. For NICD, the NICD polyclonal Rb IgG antibody already used for immunofluorescences and a different NICD polyclonal Rb IgG (ThermoFisher, Massachusetts, USA) were used at 1:2500. For NECD, a NECD monoclonal Ms IgG1, clon 5E1 (Creative Biolabs, New York, USA) was employed. WBs were revealed by chemiluminescence. Secondary antibodies were a polyclonal Goat α-Rb immunoglobulins/HRP (Dako, Hovedstaden, Denmark) and a polyclonal Rb α-Ms immunoglobulins/HRP (Dako, Hovedstaden, Denmark) specifically made for revelation with an ECL system, on this case, a Pierce™ ECL western blotting substrate (ThermoFisher, Massachusetts, USA).

But, prior to western blotting, protein had to be extracted and measured.

13.2.1. EXTRACTION OF PROTEIN

The protocol followed for the extraction of protein was as follows:

- As a result of different tests, it was found that the quantity of Petri dishes of 35 mm^2 that needed to be collected together in order to reach an appropriate quantity of protein for each cell line was:
    - hiPSCs: 2 confluent 35 mm^2 Petri dishes.
    - HAoSMCs: 3 confluent 35 mm^2 Petri dishes.
    - HAoECs: this cell line could be cultured both in 35 mm^2 Petri dishes and T25 flasks. For protein extraction, 1 confluent T25 flask was collected.
    - IDISi001-A-hiPSCs-derived vSMCs: 3 confluent 35 mm^2 Petri dishes.
    - IDISi001-A-hiPSCs-derived vECs: 3 confluent 35 mm^2 Petri dishes.
- After collecting the sample in a Falcon tube of 15 mL, cells are centrifuged at 200 g, 4' at 4ºC.
- Next, pellet is resuspended in 450 µL of cold RIPA buffer (Sigma-Aldrich, Missouri, USA) and 2 µL of protease inhibitor. The Falcon is then placed on ice and in medium and subjected to strong agitation for 15'.

- Once the agitation step is over, a small, floating pellet can be seen inside the Falcon. Both pellet and supernatant are pipetted to an Eppendorf tube of 1.5 mL. Sample is then centrifuged in a 5424R ultracentrifuge (Eppendorf, Hamburg, Germany) at 12000g, 45' at 4ºC.

- When the centrifugation is finished, everything but protein is sedimented as pellet, so the protein is in the supernatant, which is collected and stored at -20ºC.

13.2.2. PROTEIN MEASUREMENT BY BICINCHONINIC ACID ASSAY

Quantification of protein was performed following the instructions of a bicinchoninic acid assay kit (BCA) (ThermoFisher, Massachusetts, USA). The calibration pattern was performed with known concentrations of stock BSA at 2 mg/mL. The dilutions for the calibration pattern were: 200 µg/mL; 40 µg/mL; 20 µg/mL; 10 µg/mL; 5 µg/mL; 2.5 µg/mL; 1µg/mL; 0.5 µg/mL. These dilutions were made with RIPA buffer diluted 1:10 in H_2O_{mq}. The reason of this was because after several tests, the samples of the unknown proteins were always diluted 1:10 in H_2O_{mq}, so this way both calibration pattern dilutions and sample dilutions have RIPA in the same ratio so any interference effect due to RIPA is equalized. Samples had to be diluted 1:10 because after several tests, it was the dilution which best fit inside the calibration pattern.

After 105' of incubation, the plate was measured at 562 nm. Then, in an Excel, blank values were extracted to all values and after acquiring the calibration pattern, values for the unknown protein samples were obtained.

13.2.3. WESTERN BLOT

The procedure for all WBs was as follows:

- Prior to gel preparation, the WB glass plates (BIO-RAD, California, USA) are inserted within a casting frame (BIO-RAD, California, USA) (Fig. 51. A) and placed in a WB casting stand with a clamp (BIO-RAD, California, USA) (Fig. 51. B) and a pad at the bottom to not allow the liquid gel to drain off.

- Gel preparation: for running samples, they are loaded in a 10% acrylamide gel: 5 mL of resolving gel and 1 mL of stacking gel, with the composition reflected in (Table 10).

    - SDS (Sigma-Aldrich, Missouri, USA) at 10% and APS (GE-Healthcare, Chicago, USA) at 10% (both diluted in H_2O_{mq}) are prepared every time a WB is performed.

    - Resolving and stacking gel are prepared at the same time except for APS and TEMED (BIO-RAD, California, USA). These reagents are added to the stacking gel just once the resolving gel polymerizes.

    - Once the resolving gel polymerizes, APS and TEMED are added to the stacking gel preparation and 1 mL is added over the resolving gel. Quickly, a WB comb of 10 wells (BIO-RAD, California, USA) is inserted within the stacking gel. This way, once the stacking gel polymerizes and the comb is removed, the wells are formed.

	Resolving gel (mL)	Stacking gel (mL)
H_2O	4	2.7
30% acrylamide mix	3.3	0.67
1.5M Tris (pH 8.8)	2.5	0.5
10% SDS	0.1	0.04
10% ammonium persulfate	0.1	0.04
TEMED	0.004	0.004

Table 10. Resolving and stacking gel recipes for 2 acrylamide gels at 10%.

- Once the gel is ready, glass plates containing the gel can be removed from the casting frame and placed in a Mini-PROTEAN® Tetra Electrode Assembly (BIO-RAD, California, USA). This electrode assemblies with the plate glasses already clamped to it is placed inside the buffer tank (Fig. 51. C-E). The tank is filled with 500-600 mL of running buffer. In the same way, the WB gasket is also filled with running buffer. This buffer is prepared at 5X and diluted at 1X with H_2O_{mq}. (see Table 11 for composition)

	Running buffer 5X	Transfer buffer 25X
Glycine (g)	72	73
Tris base (g)	15	145
Sodium dodecyl sulfate (g)	5	9
H_2O (mL)	Fill up to 1L	Fill up to 1L

Table 11. Running buffer 5X and transfer buffer 25X recipes. Dilutions to 1X buffers are made with distilled H_2O.

- Before running the gel, samples have to be prepared and loaded,up to a maximum of 35 µL per well. Of this 35 µL, 7 µL are Laemmli buffer (Sigma-Aldrich, Missouri, USA); the other 28 µL are comprised of the same quantity of protein for each sample and the rest is filled up to 28 µL with distilled H_2O. For the protein, based on the results obtained on the BCA, the same quantity of protein must be loaded so the volume of protein for each sample has to be calculated. Once samples are prepared, they need to be placed at 99ºC for 10' in a Thermomixer (Eppendorf, Hamburg, Germany) in order to open them up. After that, samples are briefly spin and then loaded carefully inside the wells with gel-loading tips (BIO-RAD, California, USA). On the first well, 5 µL of Precision Plus Protein Dual Color Standards marker (BIO-RAD, California, USA) is loaded.

- Next, gel is run with a PowerPac Universal device (BIO-RAD, California, USA) at 140 V, 180 mA for 1h-1h15'.

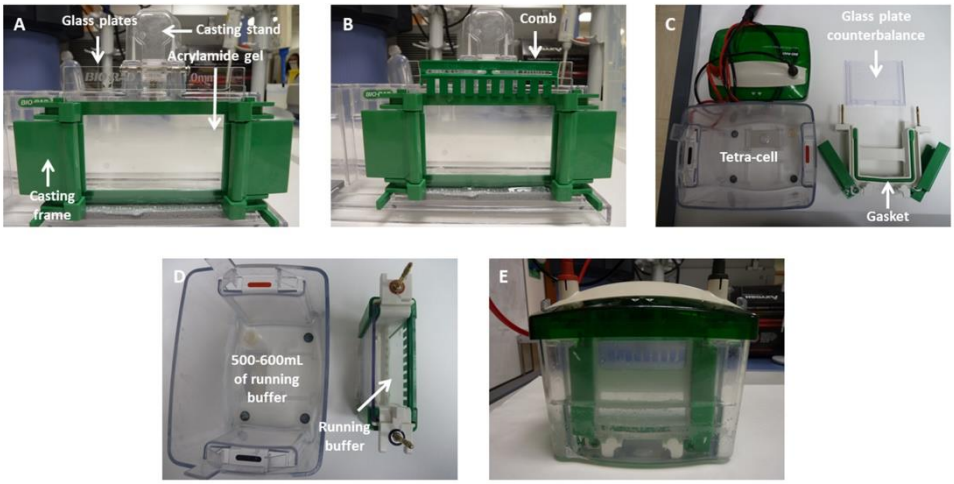

Figure 51. From A to E: chronologic sequence of the WB protocol until the running step.

- After running, a piece of transfer membrane (Merck Millipore, Massachusetts, USA) is cut with a size that fits the size of the gel. This membrane is incubated for 5' in a bucket filled with methanol (Scharlau, Barcelona, Spain). Then is washed inside a bucket filled with H_2O_{mq} for 5', and finally placed inside a bucket filled with transfer buffer 1X (Fig. 52). The composition of the transfer buffer 25X is shown in table 11. Transfer buffer 25X is diluted, for a 500 mL preparation, with 380 mL of H_2O_{mq} + 100 mL of methanol and 20 mL of transfer buffer 25X.

- Once the membrane is already inside the bucket with transfer buffer 1X, the glass plates containing the electrophoresis gel is placed in a crystal tray filled with transfer buffer 1X, together with 2 WB extra thick blot filter papers (BIO-RAD, California, USA). Then, with the aim of a gel releaser (BIO-RAD, California, USA), the thinner glass plate is separated from gel, and the

stacking part of the gel is cut. After that, one of the extra thick blot filter papers is placed in a Trans-Blot SD Semi-Dry Transfer Cell device (BIO-RAD, California, USA) already slightly humidified with transfer buffer 1X. Then the membrane is placed over the extra thick blot filter paper and carefully, the gel is placed over the membrane by letting it slide slowly over the thick glass plate to the membrane. Finally, the second extra thick blot filter paper is placed over the gel and Trans-Blot SD Semi-Dry Transfer Cell device is closed. The transference is done at 25 V, 180 mA for 1h45'.

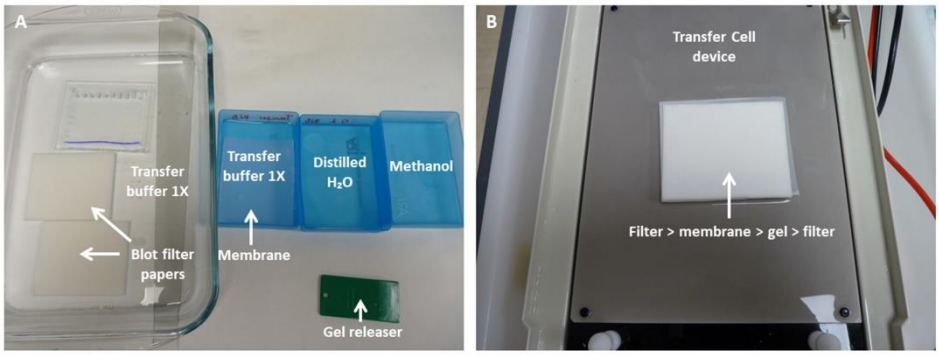

Figure 52. A to B: chronologic sequence of the transference steps in the WB protocol.

- When the transference is finished, the membrane is placed carefully inside a Falcon tube of 50 mL with 5 mL of BSA at 5% and incubated at RT in agitation for 1h as a blocking step. BSA is freshly prepared, diluting 2g of BSA with 36 mL of H_2O_{mq} + 4 mL of tris-buffered saline 10X (Sigma-Aldrich, Missouri, USA).

- After the blocking step, membrane is incubated overnight inside a different 50 mL Falcon with 5mL of BSA 5% and the desired

primary antibody against the protein whose quantity wants to be known.

- On the next day, the membrane is washed 3 times for 10' each in a bucket filled with TBS-T 1X, composed of TBS 10X diluted with distilled H_2O and Tween® 20 (Sigma-Aldrich, Missouri, USA) at 1%.

- After the washing step, membrane is incubated inside a 50 mL Falcon with 5 mL of BSA 5% and the desired primary antibody for the loading control protein for 1 hour at RT and in agitation. Once incubation is finished, another 3 washing steps are made.

- After the washing step, there are two possibilities. If both primary antibodies were made in the same host animal, the membrane can be incubated for 1h with the same secondary antibody inside a 50 mL Falcon with 5 mL of BSA and the secondary antibody. If the primary antibodies were made in different host animals, the membrane may be cut horizontally in two pieces, being careful not to cut along the region where any of the proteins are expected to be. This way, both pieces may be incubated separately for 1h inside a 50 mL Falcon with BSA 5% and the desired secondary antibody. After incubating with the secondary antibodies, other 3 washing steps are made.

- Finally, membrane was revealed by ECL system, in a ChemiDoc™ MP Imaging System (BIO-RAD, California, USA).

INTRODUCTION

HYPOTHESIS

OBJECTIVES

MATERIALS & METHODS

RESULTS

DISCUSSION

CONCLUSIONS

USC
UNIVERSIDADE
DE SANTIAGO
DE COMPOSTELA

14. Reprogramming of peripheral blood mononuclear cells from a patient with CADASIL

14.1. Isolation and culture of peripheral blood mononuclear cells

For the isolation of PBMCs, blood sample for the first reprogramming was manipulated 24 h after extraction, while blood sample from the second reprogramming and the reprogramming of healthy PBMCs extracted from a volunteer person was manipulated right after extraction. To this regard, no differences on cultures were found independently of the time passed between extraction and manipulation (Fig. 53).

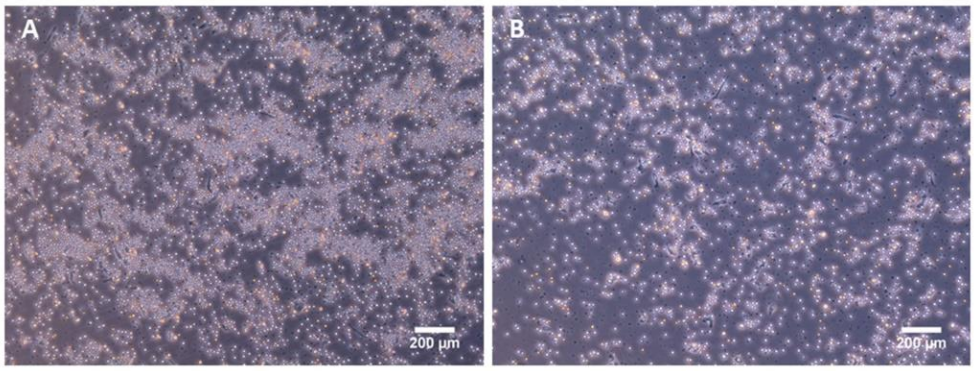

Figure 53. A) PBMC culture from the first patient. B) PBMC culture from the second patient.

14.2. Viral transfection

For viral transfection, the incidence of virus presence in cell survival was measured by comparing the number of living cells at day 3, when cells were collected for their seeding in the 3 starting Petri dishes. As seen in Table 12, a cell death rounding the 50% in all the reprogramming processes was found, probably due to the effect of the virus in cells.

Procedence	Number of infected cells	Number of cells at day 3 (cell/mL)	Percentage of cell death
Healthy patient	$3x10^5$	$1.55x10^5$	48.33%
First patient	$3x10^5$	$1.4x10^5$	53.33%
Second patient	$3x10^5$	$1.593x10^5$	46.9%

Table 12. Cell death 3 days after viral infection.

After viral transfection and cell seeding in a well of a 24-well plate, cells already started to present morphological changes. Some cells began to slightly adhere to the bottom of the well and to group up, forming small clusters of 3-10 cells at day 2-3. Also, on day 1 post-infection (p.i), it could also be seen that some cells get bigger and brighter than others (Fig. 54).

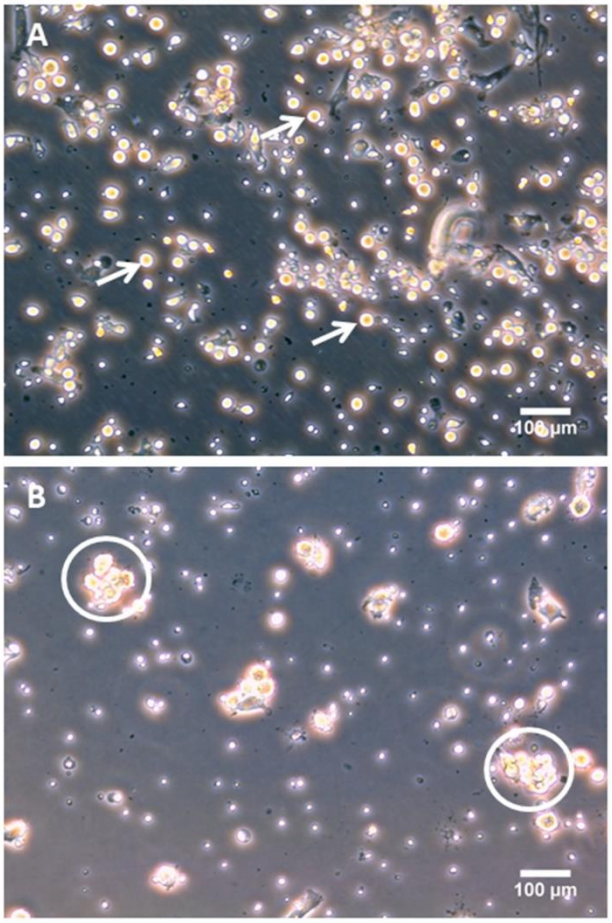

Figure 54. A) PBMCs 1 day after infection. White arrows point to bigger and brighter floating cells, probably infected ones already experiencing structural changes. B) PBMCs 3 days after infection. Aggrupation of cells can already be observed (white circles) because of the infection process.

14.3. Presence and absence of the virus

To check for the presence of the virus the day after infection, one of the 2 infected samples of $3x10^5$ cells was collected on the next day after infection and instead of performing the centrifugation step for removing the virus, their RNA was extracted. This RNA was retrotranscribed to cDNA. SeV virus cDNA sequence was amplified by PCR and run in a 2.5% agarose gel. As can be seen in Fig. 55.A, virus was cDNA present, so the reprogramming process with the other $3x10^5$ infected cells was allowed to continue. Prior to SeV virus cDNA amplification and running, the housekeeping gene *GAPDH* was also amplified and run in a 2.5% agarose gel to check for a correct retrotranscription (Fig 55.B).

On the other side, to check for the absence of the virus, 2 checkpoints were established, one at passage 5 and another one at passage 10 in case virus had not already removed from cells. Thus, the RNA of the 6 clones that achieved passage 5 was extracted. Their RNA was retrotranscribed and the SeV sequence of cDNA amplified and run in a 2.5% agarose electrophoresis gel. As seen in Fig. 57.C, SeV cDNA was not present at passage 5 in any of the clones, so the second checkpoint at passage 10 was unnecessary to do. Prior to SeV virus cDNA amplification and running, the housekeeping gene *GAPDH* was amplified for each sample by PCR and run in a 2.5% agarose electrophoresis gel to check for a correct retrotranscription (Fig. 57.D).

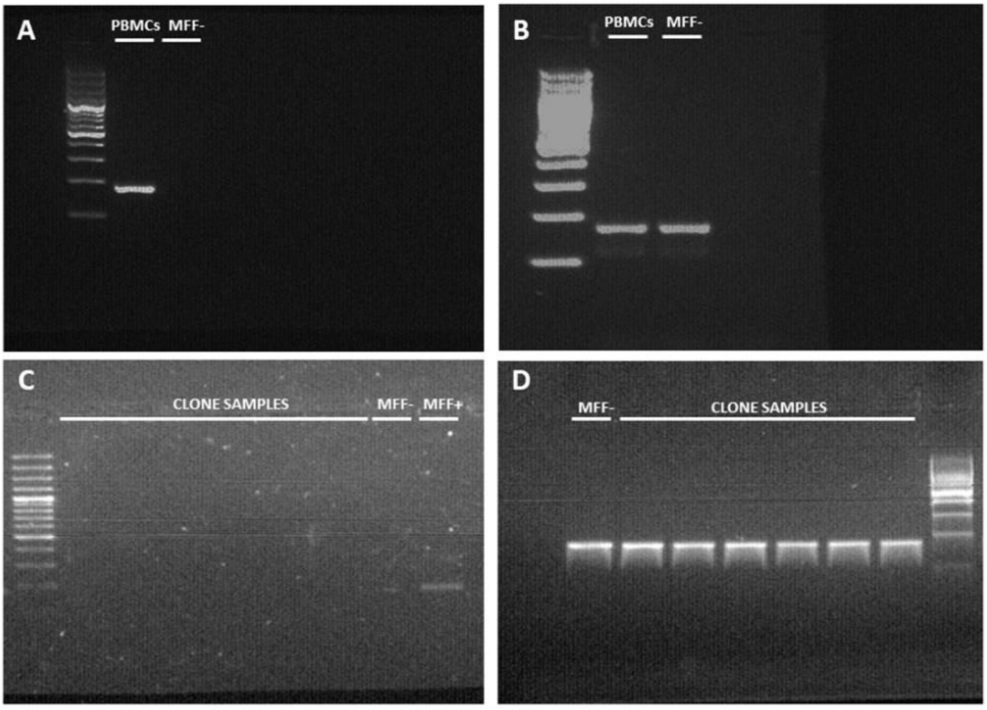

Figure 55. A) Agarose gel showing the presence of SeV cDNA. B) Agarose gel showing *GAPDH* cDNA of the previously infected PBMCs. C) Agarose gel showing the SeV cDNA absence at passage 5 for the analyzed stable clones of the first reprogramming process. D) Agarose gel showing the *GAPDH* cDNA presence at passage 5 for the analyzed stable clones of the first reprogramming process. MFF+: infected mouse foreskin fibroblast cell line. MFF-: non-infected mouse foreskin fibroblasts cell line.

15. Selection of hiPSCs colonies

After seeding the infected cells on Day 3 in the 3 starting Petri dishes, emerging colonies were monitored throughout the days, being able to remove the ones that were not growing properly (Fig. 56).

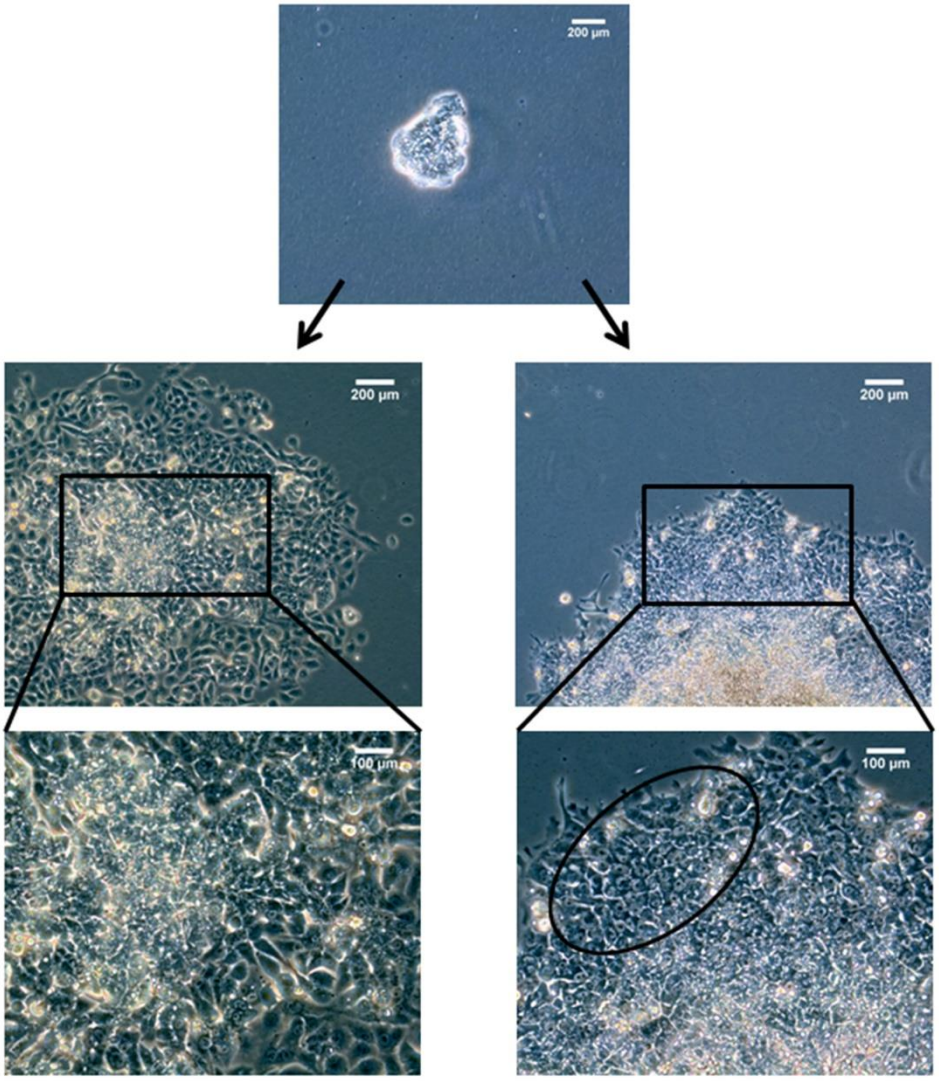

Figure 56. Diagram representing the correct (right column) and the wrong evolution (left column) of an emerging hiPSC colony. Black circle represents the region of the colony that should be positively selected.

As expected, the reprogramming process efficiency for both the first and the second reprogramming was quite low. For the first reprogramming, of the 83 colonies selected for further passages, just 6 of them gave rise to stable clones (Fig. 57), setting the efficiency of the reprogramming process in 7.22%. On the other side, for the second reprogramming, of the 26 colonies selected for further passages, just 1 colony gave rise to stable clones, setting the efficiency of the process in 3.84%.

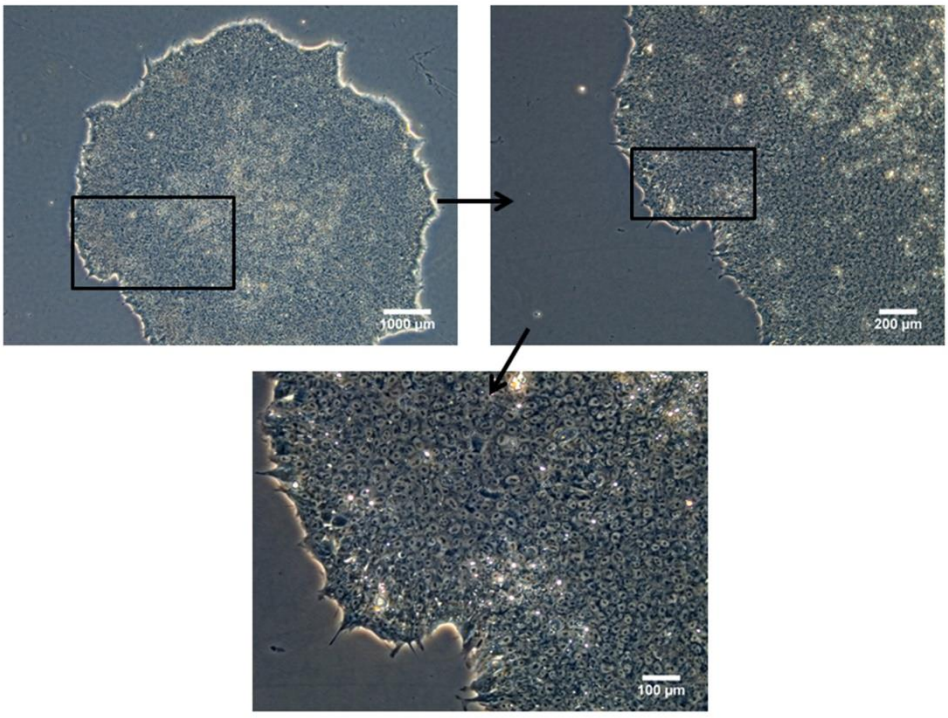

Figure 57. Sequencial magnification of a typical stable hiPSC colony obtained throughout one of the reprogramming process (first one on this case).

16. Characterization of hiPSCs

16.1. Alkaline phosphatase staining

The results obtained in the AP staining for both the first and second cell lines obtained from the two reprogramming processes showed that all colonies stained positive (Fig. 58). More specifically, at high magnification it could be seen how this enzyme accumulated in the extracellular space, more precisely in the plasma membrane, where it is reported its cellular location (Fig. 58.B and D).

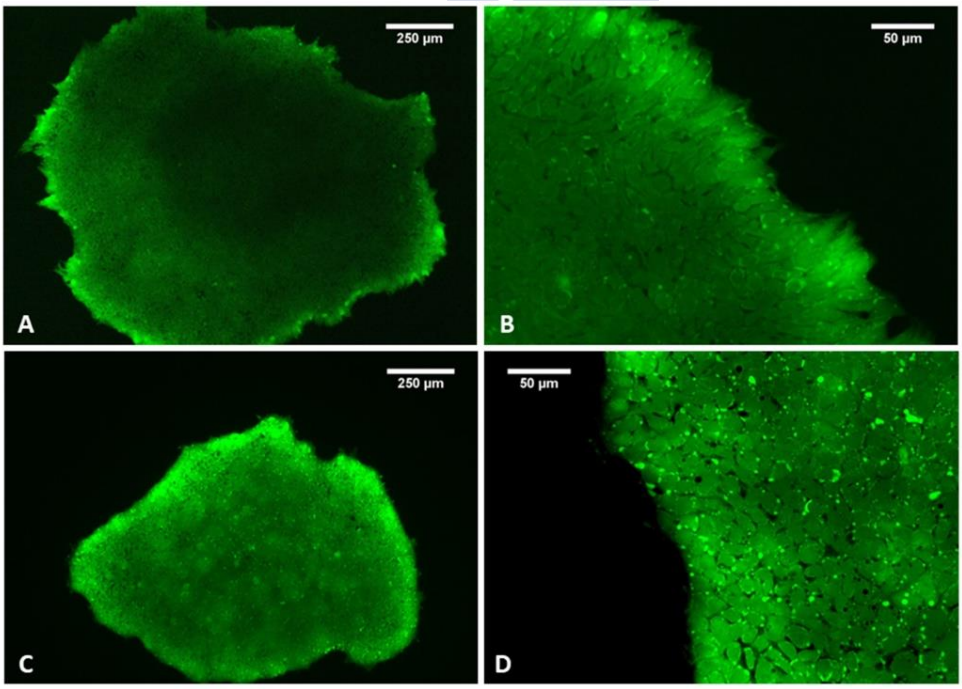

Figure 58. Alkaline phospatase live staining of the colonies obtained from the first (A-B) and second (C-D) reprogramming processes. D: non-compact colony showing AP staining.

16.2. Immunofluorescence test

For SOX2, OCT4, Tra-1-60 and SSEA4 combinations with the Pluripotent Stem Cell 4-Marker Immunocytochemistry Kit, no problems when performing the immunofluorescences were presented. The results obtained were positive for all the 5 markers both for the colonies obtained from the first (Fig. 59) and second reprogramming process (Fig. 60), although regarding the immunofluorescence for NANOG, at the beginning there were troubles with the fixation step probably because of an extreme sensitiveness of the hiPSCs to the PFA. Once the issue was solved, immunofluorescences were also positives for this pluripotency marker. It is important to point that the surface of the immunofluorescence chambers probably exerted some impact over the colonies since they tend to leave spaces between cells inside the colonies. But as it can be seen in Figure 59.B, it didn´t seem to affect the pluripotent phenotype of the cells. Also, in many cases it could be appreciate that cells located at the surface of the colonies were not pluripotent (Fig. 60. A-B).

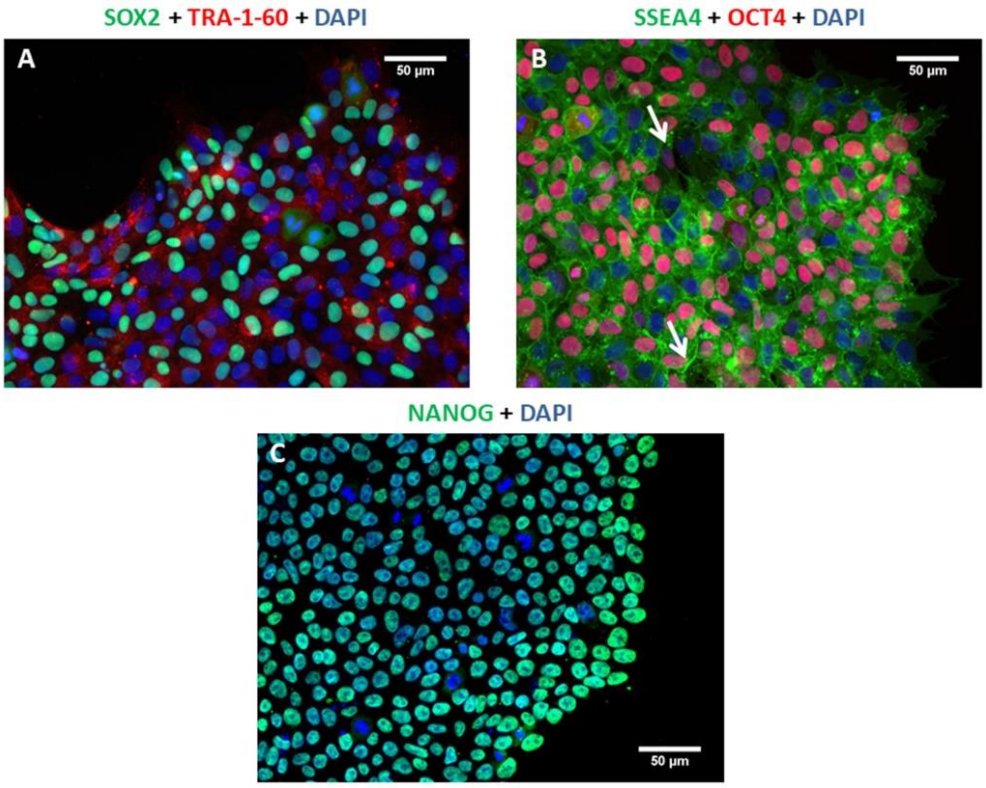

Figure 59. Immunofluorescences of colonies obtained from the first reprogramming process for several nuclear (SOX2, OCT4 and NANOG) and surface (TRA-1-60 and SSEA4) markers related to pluripotency. White arrows: gaps between inner cells inside the colonies.

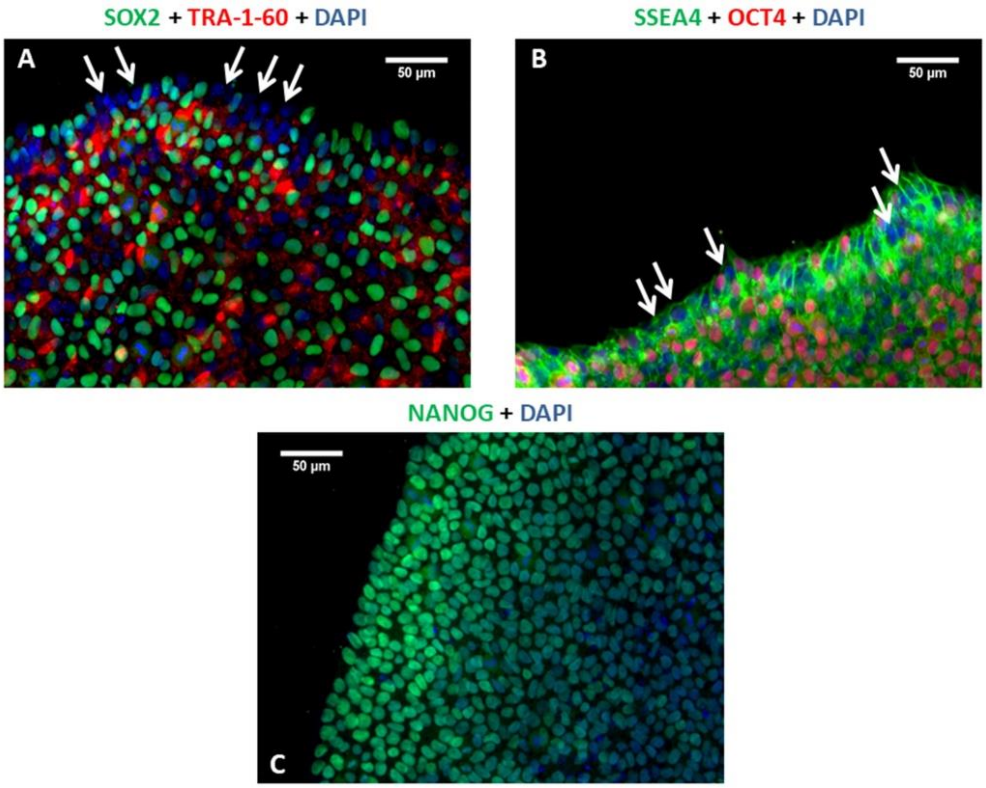

Figure 60. Immunofluorescences of colonies obtained from the second reprogramming process for several nuclear (SOX2, OCT4 and NANOG) and surface (TRA-1-60 and SSEA4) markers related to pluripotency. White arrows: peripheral cells without nuclear pluripotency factor staining.

16.3. hiPSCs-derived embryoid bodies analysis

16.3.1. FORMATION AND DIFFERENTIATION OF EMBRYOID BODIES

Formation and differentiation of EBs presented slightly different results depending on the source of reprogramming. The induction of EBs from a healthy iPSC cell line kindly provided by the Fibroblast Reprogramming Unit laboratory from Brescia, Italy, resulted in bigger and more round-shaped EBs than those from the reprogramming of the two different CADASIL-PBMCs cell lines. Also, with EBs from healthy-hiPSCs, there was almost no cell debris while for the EBs derived from the cell lines obtained from the first and second reprogramming process, it could be clearly seen a lot of cell debris/small clusters of cells that failed to form EBs (Fig. 61). In the differentiation process, healthy-hiPSCs-derived EBs expanded limitlessly, with a black core acting as a virtually infinite source of cells. On the other side, the EBs derived from the cell lines obtained from the first and second reprogramming process exhibited a limited growth potential, with the black core disappearing on the very first days (Fig. 61).

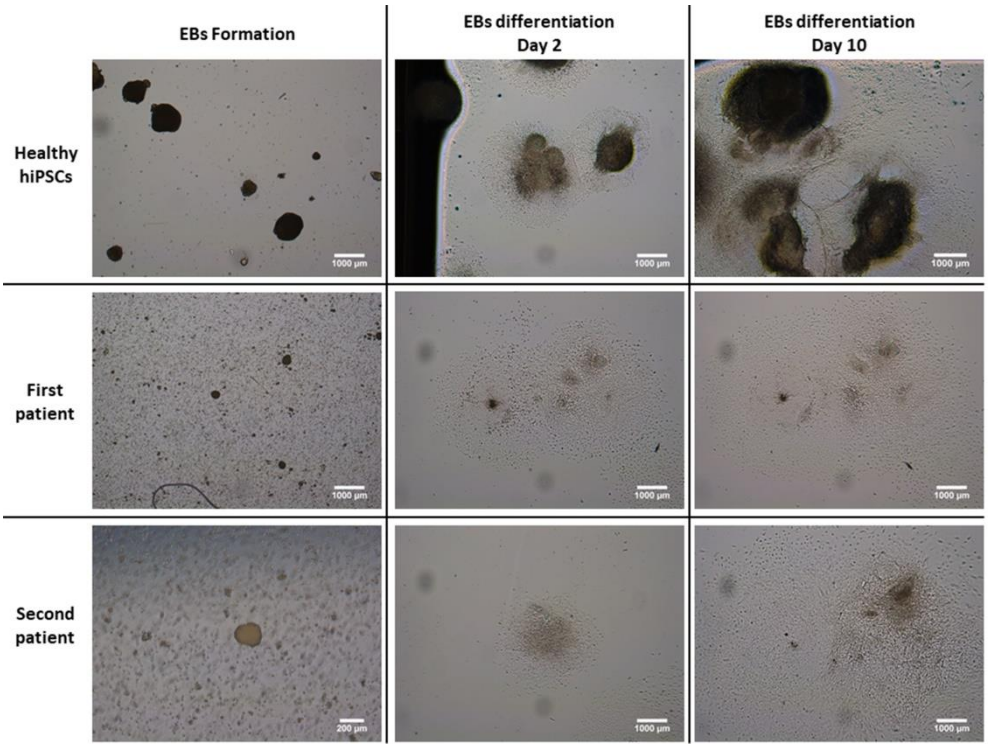

Figure 61. First colum. EBs formation and their differentiation for a healthy-hiPSC line, cells generated from the first reprogramming (IDISi001-A) and cells generated from the second reprogramming (CAD02).

16.3.2. IMMUNOFLUORESCENCE OF EMBRYOID BODIES

Staining for all markers used in immunofluorescence was positive both for colonies from the first (Fig.62) and second reprogramming process (Fig. 63). In Fig. 62, for FOXA2, α-SMC actin and vimentin, positive regions can be seen but also negative ones, indicating that those negative cells are other type of cells, probably from another germ layer.

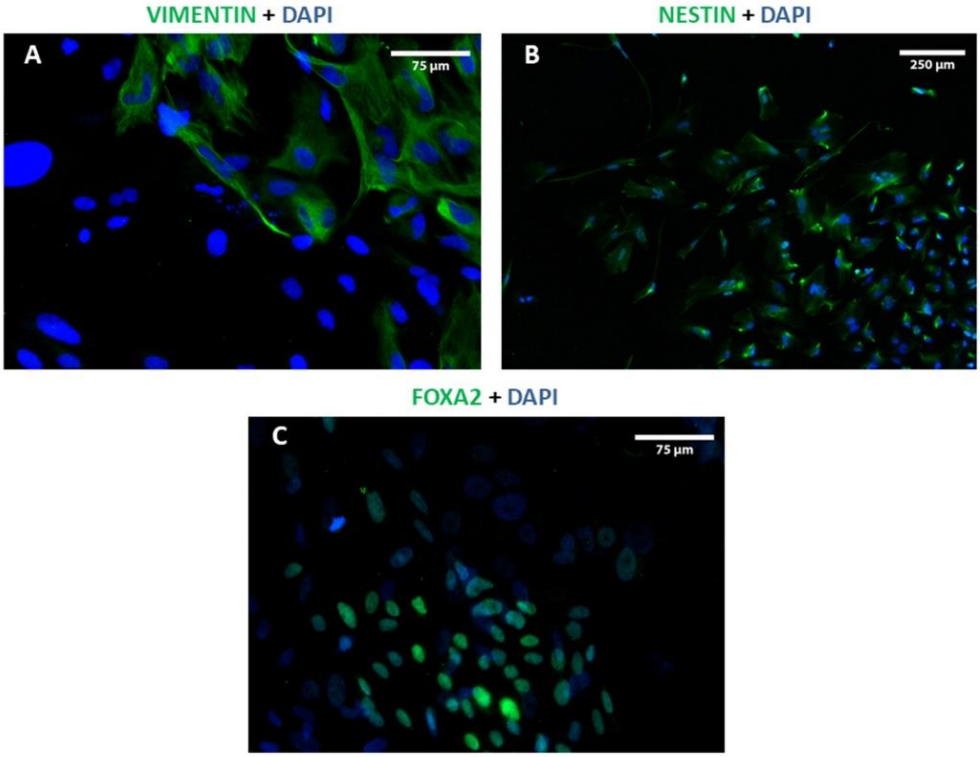

Figure 62. Immunofluorescences of EBs derived from the cells obtained from the first reprogramming for vimentin (mesoderm), nestin (ectoderm) and FOXA2 (endoderm) markers.

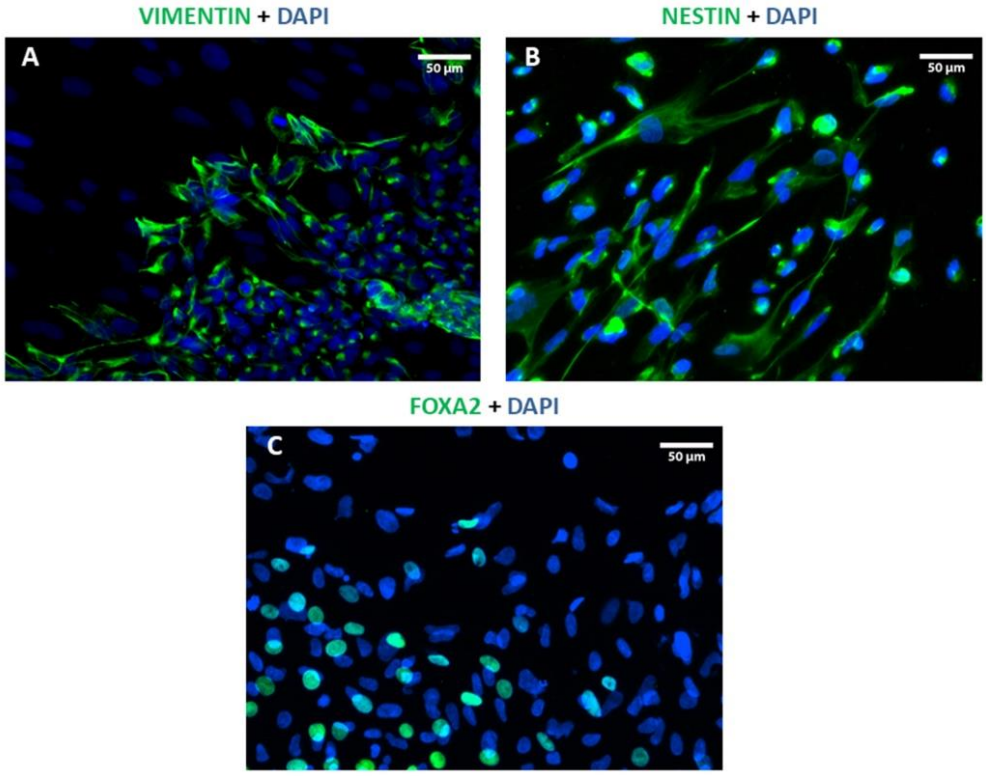

Figure 63. Immunofluorescences of EBs derived from the cells obtained from the second reprogramming for vimentin (mesoderm), nestin (ectoderm) and FOXA2 (endoderm) markers.

16.4. Cellular contamination analysis

As it can be seen in Fig. 64, at several points throughout the project there was yeast contamination. Specifically, 15-25 days after viral transfection, the three initial Petri dishes were prone to contamination. In fact, whereas there were no such cases in the first reprogramming, it happened twice in the second one. The typical round shaped structures forming chains of yeasts can be observed in Fig. 64.B, where contamination was starting, while in the Fig. 64.C, a fully contaminated Petri dish can be observed, being almost impossible to differentiate yeasts.

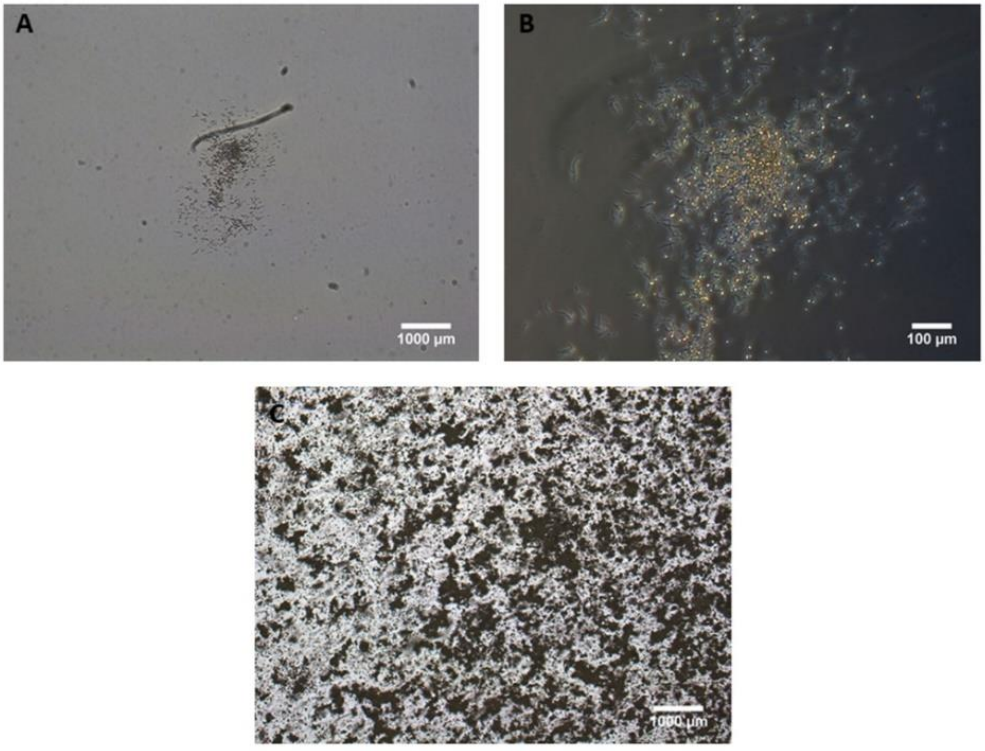

Figure 64. A) Beginning of yeast contamination. B) Amplification of image A. C) Yeast contamination 1-2 days after image A and B were taken.

Results for the external service were always negative for *Mycoplasma* contamination regarding cells from the first reprogramming (Fig. 65.A). However, we had a positive episode in cells from the second reprogramming when cells from both first and second reprogramming were being cultured (Fig. 65.B). After solving the problem several test were conducted in order to verify the contamination had been eliminated (Fig. 65.C). There were, though, structural changes in hiPSC colonies that led to the suspicion that they could be contaminated even before the confirmation by the external service: cells from the center of the colonies differentiating (Fig.65.D-E), driving the colonies to entire differentiation from inside to outside and, prior to this differentiation, black dots could be observed on the first days after passaging colonies (Fig. 65.F).

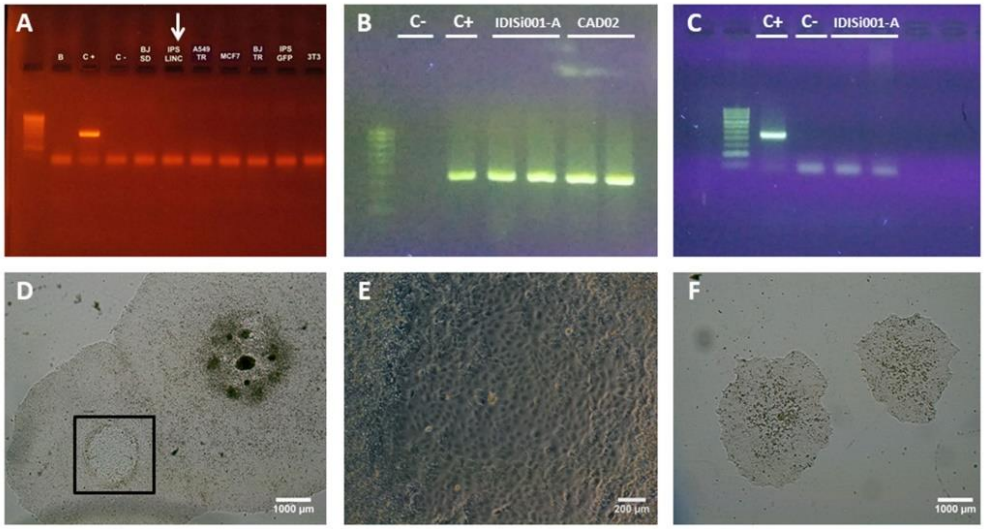

Figure 65. A**:** first *Mycoplasma* analysis. White arrow points to a sample from the first reprogramming. B: positive *Mycoplasma* analysis for samples from the first (IDISi001-A) and second (CAD02) reprogramming. C: *Mycoplasma* analysis for a sample from the first reprogramming. D-F: effects of *Mycoplasma* contamination on hiPSCs cultures. Black square: amplified region in E.

16.5. Expression of the reprogramming factors

Before showing the results of the PCRs and qPCRs, in Table 13 the values of each protein extraction for the clones analyzed can be observed.

Clon	A260/280	A260/230	[RNA]ng/µL	Final volume H_2O (µL)
#42.2	1.832	2.080	874.229	35
#53.3	1.803	2.121	533.954	35
#76.2	1.810	2.094	446.401	35
#78B.2	1.756	1.963	180.908	35
#83.3	1.807	1.953	543.311	35
#80.3	1.720	1.997	264.231	35

Table 13. RNA levels after RNA extraction of several stable clones from the IDISi001-A cell line.

Once the RNA levels were measured, retrotranscription and then PCR in order to check for a correct retrotranscription was be done. For that, *GAPDH* presence was assessed by PCR (Fig. 66).

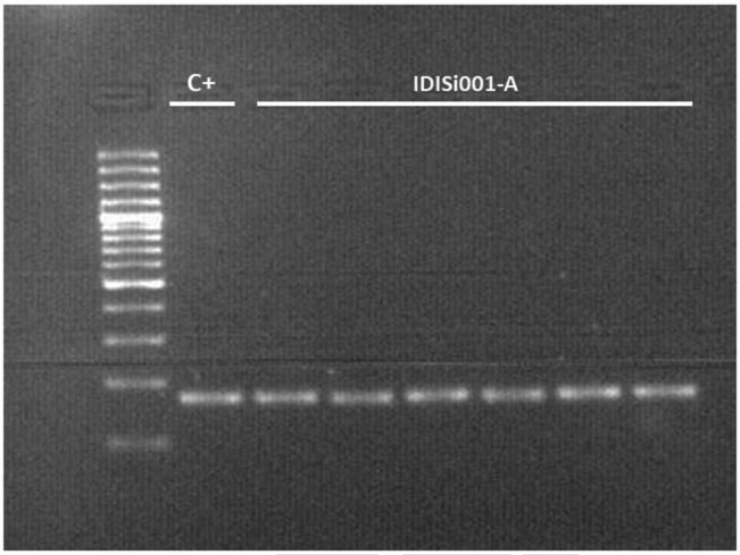

Figure 66. *GAPDH* PCR product of the 6 hiPSCs clones analyzed from the first reprogramming process (IDISi001-A) revealed by UV.

Finally, qPCR results for the clones from both the first reprogramming process and the second are shown in Fig. 67.

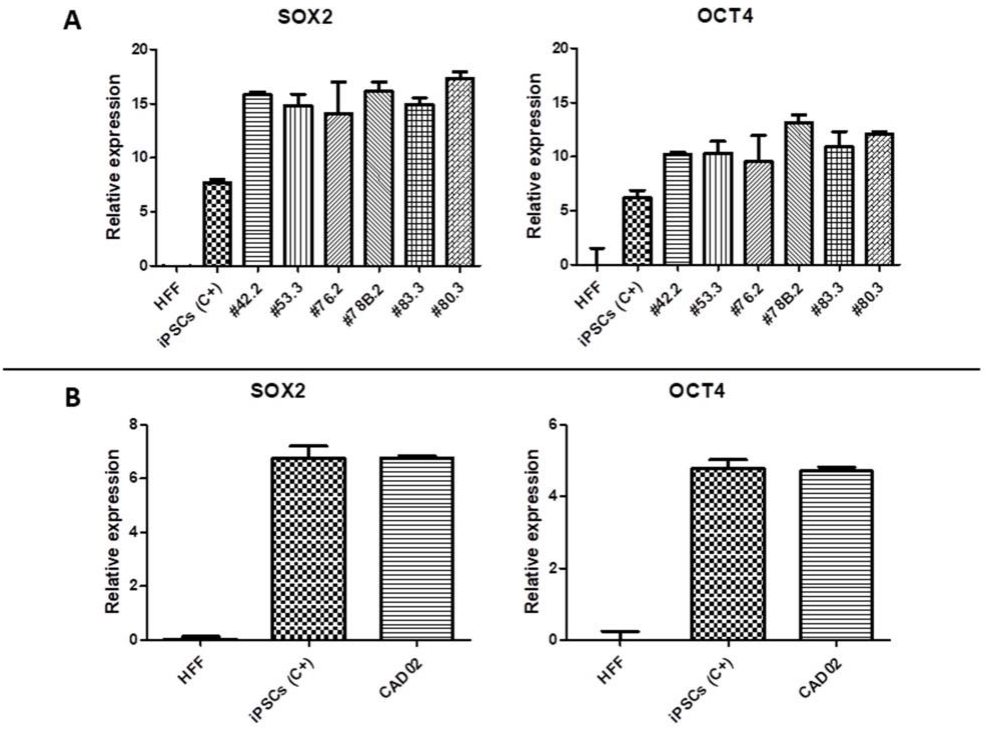

Figure 67. A: qPCR results from several stable clones generated in the first reprogramming. B: qPCR results from several stable clones generated in the second reprogramming. Each sample is normalized to its *GAPDH* expression values and at the same time to the *GAPDH* values of the negative control (HFF). iPSCs (C+)= healthy-hiPSC line that served as positive control. HFF= human foreskin fibroblast cell line that served as negative control. Both control lines were kindly ceded by the FRU laboratory from Brescia.

16.6. Karyotyping analysis

For both the first and the second reprogramming, no anomaly of any kind was found (Fig. 68). Up to 29 metaphases were analyzed in the case of the first reprogramming and up to 20 for the second one.

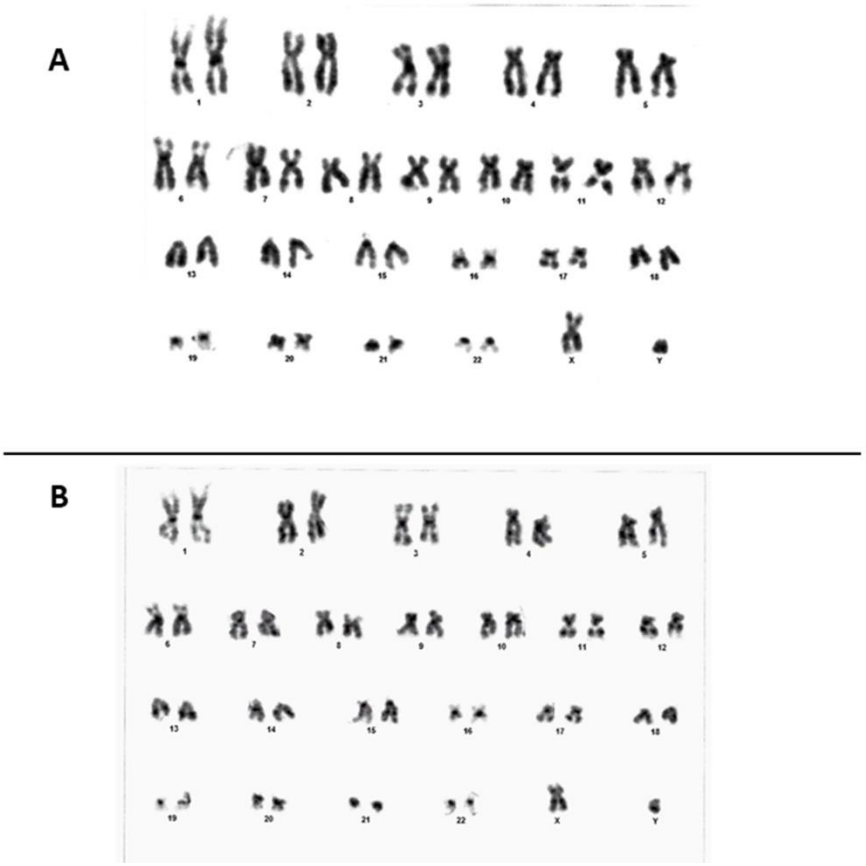

Fig. 68. Representative karyotipe image from samples of the first (A) and the second (B) reprogramming process.

Due to that all the analysis performed in order to characterize the stable clones obtained in the first reprogramming presented positive results and once proved that those cells still had the NOTCH3 mutation previously diagnosed on the PBMCs of the patient, the cell line was registered at the "Banco Nacional de Líneas Celulares del Instituto de Salud Carlos III" and at the Human Pluripotent Stem Cell Registry. Once done, the official IDISi001-A name was given to the cell line.

17. Development and optimization of vascular smooth muscle and vascular endothelial cell differentiation protocols

17.1. Differentiation into vascular smooth muscle cells

17.1.1. DIFFERENTIATION WITH ASCORBIC ACID

The generation of CADASIL-hiPSCs-derived vSMCs with ascorbic acid did not work. Colonies began to differentiate themselves by the periphery right on the next day after exposing them to the differentiating medium, but on the following days the morphology of the resulting cells didn't resemble to SMC morphology compared to the HAoSMCs cell line control (Fig. 69.A). Several variables were applied to the protocol: small clusters and single-cell suspension starting point and different concentrations of ascorbic acid. Only when the protocol started with the single-cell suspension, the resulting cells looked like SMCs, but not enough cells attached to the surface and they ended up dying (Fig. 69.C).

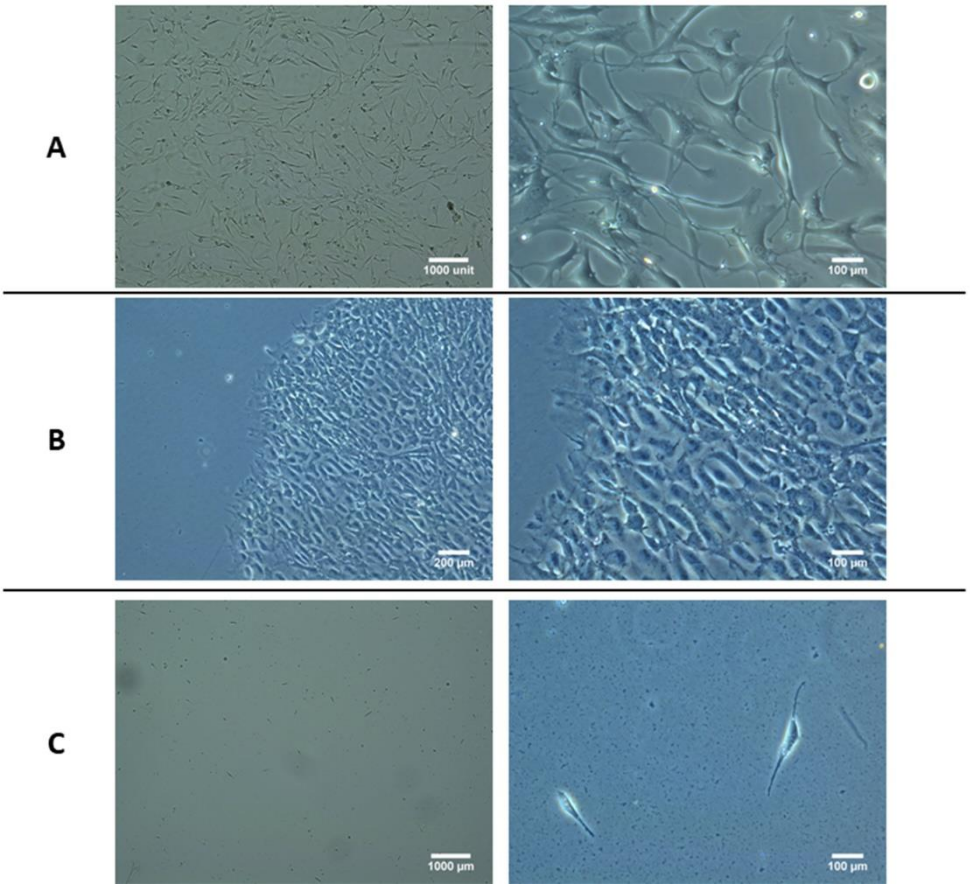

Fig. 69: A: control cell line (HAoSMCs) with which the cells obtained in the differentiation processes were compared. B: cells resulting from differentiation with ascorbic acid with small cluster suspension as starting point. C: cells resulting from differentiation with ascorbic acid with single-cell suspension as starting point.

17.1.2. DIFFERENTIATION WITH α-MEM WITH NUCLEOSIDES

With this protocol, CADASIL-hiPSCs-derived vSMCs were successfully achieved. In general, cell growth drove them to a final morphology quite similar to the HAoSMCs , giving a first impression of being working in the right direction. Briefly, on the next day after subjecting colonies to DM1, elongated cells can already be observed (Fig. 70.Day 1-3), and although on day 2 they seem to retract their prolongations, they proliferate over the days and recover the morphology of day 1 (Fig. 70.Day 5-7). By day 10-15 depending on the initial cell attaching rate, cells begin to reach confluence and they start to line up forming fibers (Fig.70 .Day 10-14).

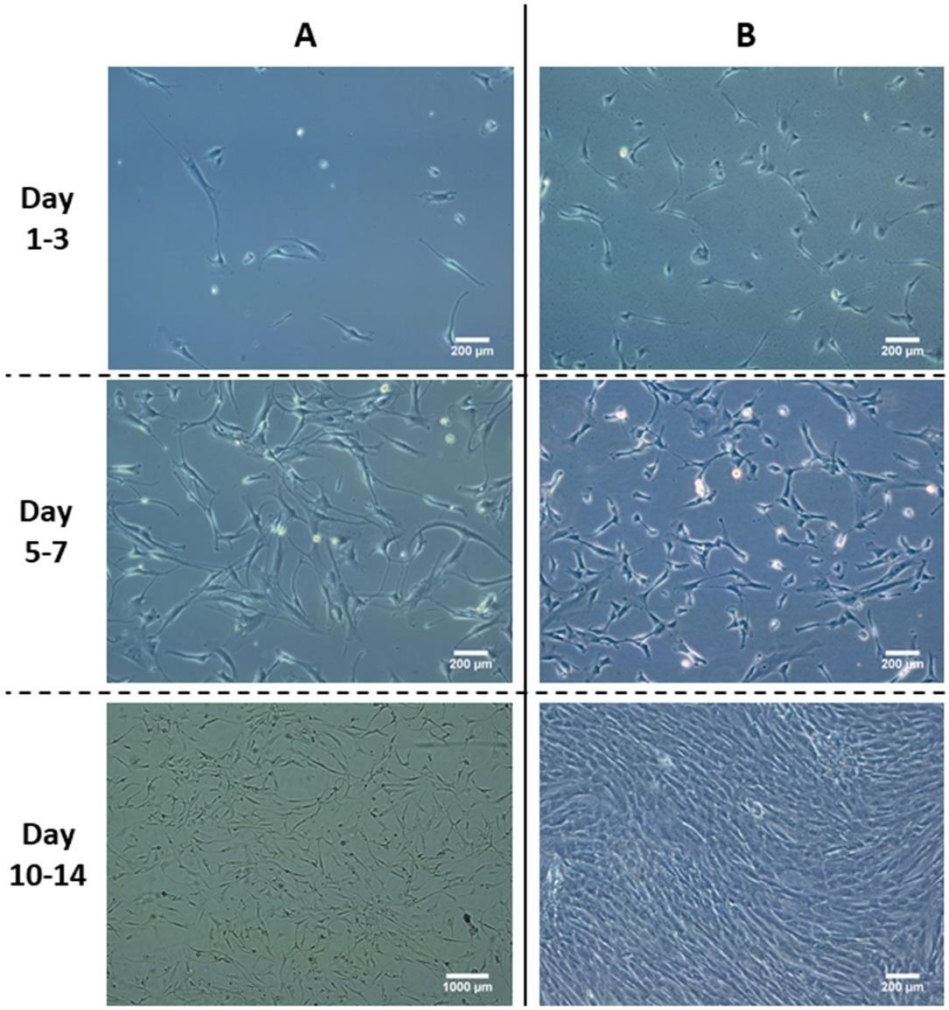

Figure 70. Comparison between HAoSMC cell line (A) and cells resulting from the second vSMC differentiation protocol (B) at different days.

After the protocol passaging step, when cells are subjected to DM2, cells kept their morphology but while they did not reach confluence, they tend to grow forming vessel-like structures (Fig. 71).

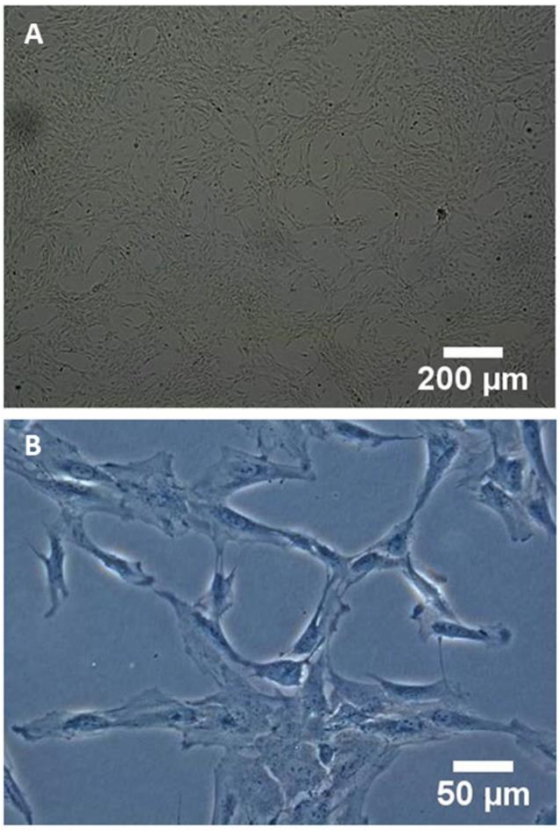

Figure 71. Vessel-like structures formed by CADASIL-hiPSCs-derived vSMCs when growing after the addition of the DM2.

17.2. Differentiation into vascular endothelial cells

The differentiation protocol resulted in cells with a morphology similar to the HAoEC control cell line already on the first attempts. In Fig. 72 it can be observed the several morphological changes that colonies suffer until reaching an endothelial morphology. Besides, although no data can be given, unlike CADASIL-hiPSCs-derived vSMCs, this CADASIL-hiPSCs-derived vECs were succefully frozen by means of BAMBANKER. When thawed, CADASIL-hiPSCs-derived vECs presented no problems on their proliferation. Also, they can be passaged, but after 3-4 passages they stop attaching.

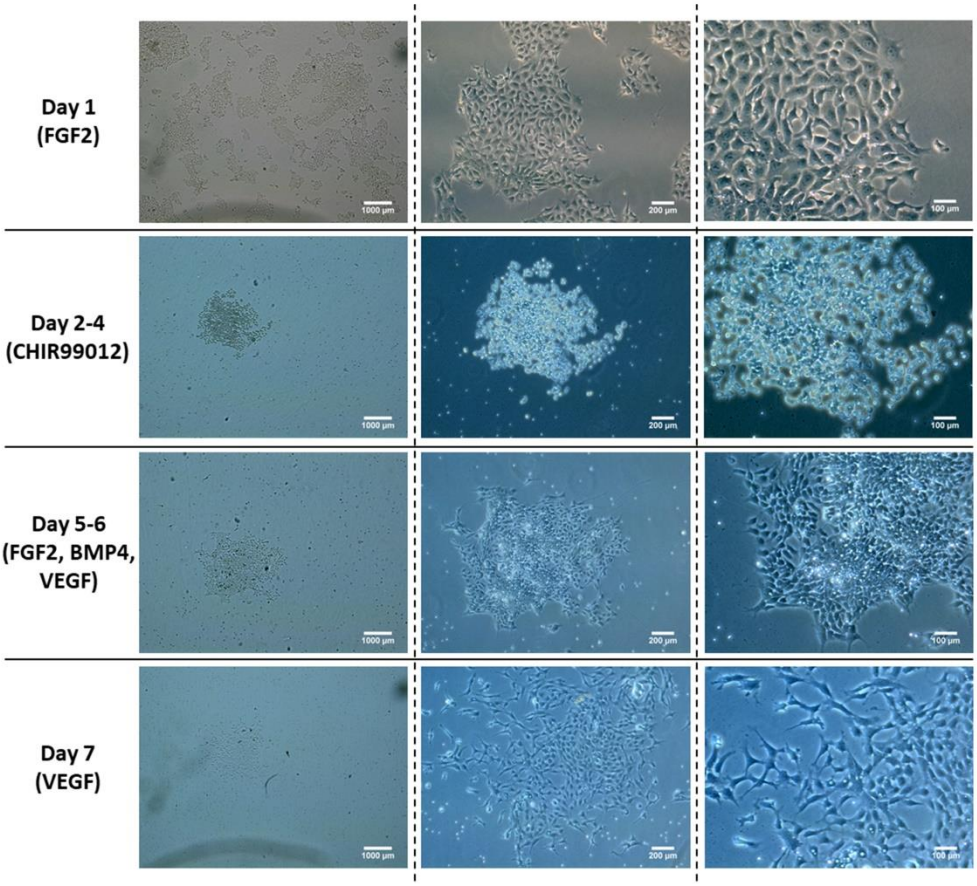

Figure 72. Sequential morphological changes that occur during differentiation to CADASIL-hiPSCs-derived vECs. Brackest: growth factor/s present in cell culture.

18. Characterization of derived vascular smooth muscle and vascular endothelial cells

18.1. Characterization of vascular smooth muscle cells

18.1.1. IMMUNOFLUORESCENCE ANALYSIS FOR VASCULAR SMOOTH MUSCLE CELL MARKERS

All the immunofluorescences performed with CADASIL-hiPSCs-derived vSMCs were positive for the SMCs markers used. Every immunofluorescence was contrasted with immunofluorescences in HAoSMCs (Fig. 73).

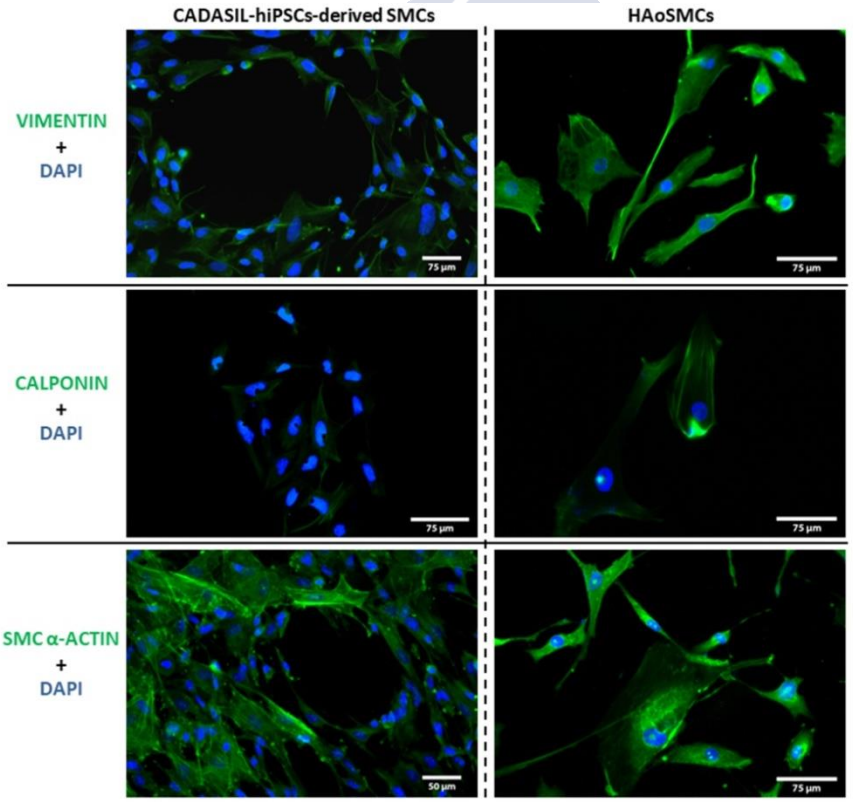

Figure 73. CADASIL-hiPSCs-derived vSMCs immunofluorescences (first column) for several SMC markers compared with a HAoSMC line (second column).

18.1.2. CONTRACTILITY TESTS

CADASIL-hiPSCs-derived vSMCs exhibited contraction capacity when exposed to carbachol 5mM. They exhibited an approximate contraction of 22% of their total area when they were under the microscope the whole time and exposed to carbachol, and an approximate contraction of 15% when they were placed inside the incubator and with carbachol. That difference may be probably due to the fact of being outside the incubator for so long. CADASIL-hiPSCs-derived vSMCs subjected to vehicle and Hek cells subjected to carbachol did not exhibit contraction (Fig. 74).

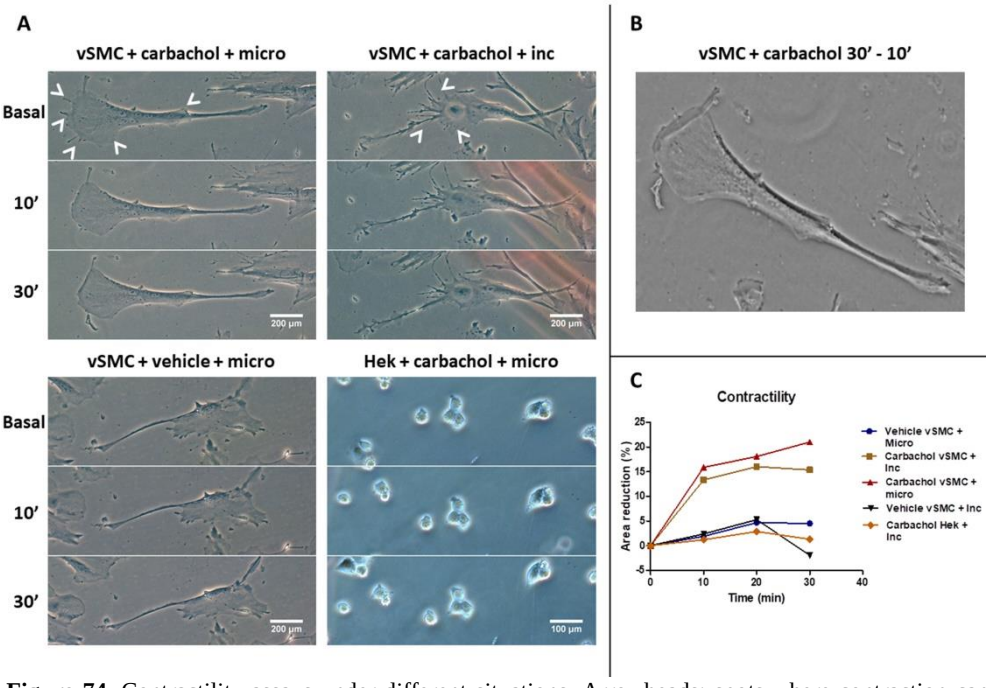

Figure 74. Contractility assays under different situations. Arrowheads: spots where contraction can be observed over time. B: overlay of the vSMC + carbachol + micro image at 30' over the same vSMC at 10'. C: graph showing the contraction capacity of the given cells under different conditions. Micro: culture placed under the microscope all the time. Inc: dish returned to the incubator while no photos are taken.

18.2. Characterization of vascular endothelial cells

18.2.1. IMMUNOFLUORESCENCE ANALYSIS FOR VASCULAR ENDOTHELIAL CELLS

All the immunofluorescences performed with CADASIL-hiPSCs-derived vECs were positive for the EC markers used. Every immunofluorescence was contrasted with immunofluorescences in HAoECs (Fig. 75).

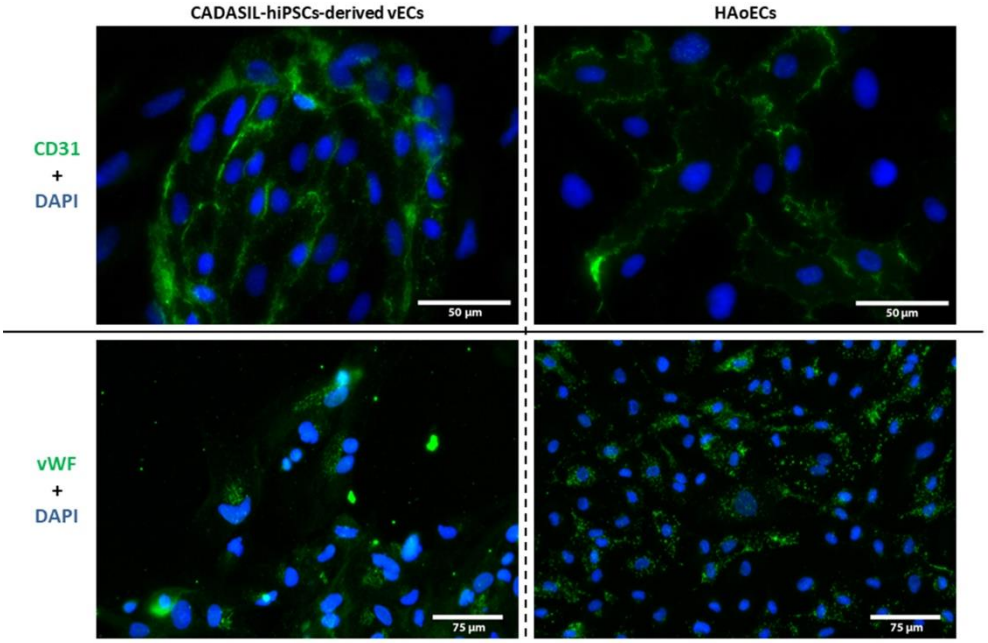

Figure 75. CADASIL-hiPSCs-derived vECs immunofluorescences (first column) for several EC markers compared with a HAoEC line (second column).

18.2.2. VESSEL FORMATION

For the vessel formation, after seeding the CADASIL-hiPSCs-derived vECs in a 12-well plate, the intention of forming vessels was already seen from the very first day after seeding the cells. However, it was not until day 6-8 that the vessel-like structures were not able to be seen in a clear manner (Fig. 76).

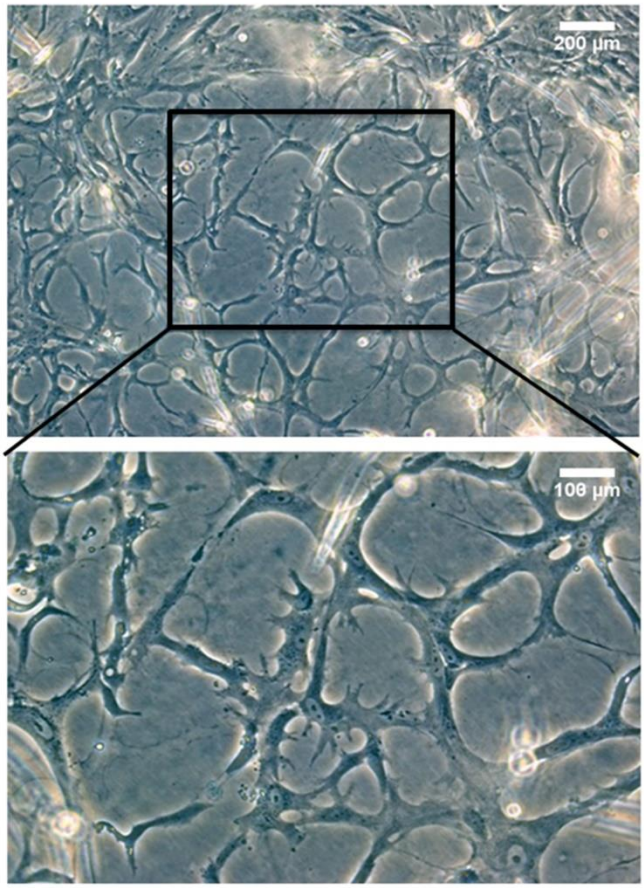

Figure 76. CADASIL-hiPSCs-derived vECs forming vessel-like structures.

19. Short-tandem repeats and NOTCH3 mutation analysis

19.1. Short tandem repeats analysis

As previously mentioned, a full STR analysis was made for all the derived cell lines from the IDISi001-A line (Table 14), while for CAD02, STR analysis were just made for the original CADASIL-PBMCs and the CADASIL-derived hiPSCs (Table 15), as CADASIL-hiPSCs-derived vSMCs and vECs were not generated from this line. For the CAD02 line, a combination of 8 alleles (some of them different from those analyzed in IDISi001-A line) was analyzed. As can be seen on Tables 14 and 15, for each patient, all the given cell lines had the same copies of each STR analyzed. There was an exception for CADASIL-IDISi001-A-vECs, since the allele D13S317 presented a variation of 1 repetition in one of its alleles, but probably due to a mistake during the analyzing process. In conclusion, with these results it can be said that for both patients, all the cell lines derived from each one all over this project had the same origin and belong to the same patient.

			PROFILE			
Allele	**Labelling**	**Range (bp)**	**CADASIL-IDISi001-A-PBMCs**	**CADASIL-IDISi001-A-iPSCs**	**CADASIL-IDISi001-A-vSMCs**	**CADASIL-IDISi001-A-vECs2**
Amelogenin	TMR	106(X), 112(Y)	X, Y	X, Y	X, Y	X, Y
CSF1PO	JOE	321-357	10, 11	10, 11	10, 11	10, 11
D13S317	JOE	176-208	10, 12	10, 12	10, 12	10, 11
D16S539	JOE	264-304	9, 11	9, 11	9, 11	9, 11
D21S11	FL	203-259	30, 33	30, 33	30, 33	30, 33
D5S818	JOE	119-155	11, 12	11, 12	11, 12	11, 12
D7S820	JOE	215-247	9, 10	9, 10	9, 10	9, 10
TH01	FL	156-195	9, 9	9, 9	9, 9	9, 9
TPOX	TMR	262-290	8, 11	8, 11	8, 11	8, 11
Vwa	TMR	123-171	17, 17	17, 17	17, 17	17, 17

Table 14. STR analysis for IDISi001-A PBMCs and all the derived cell lines obtained from them.

			PROFILE	
Allele	**Labelling**	**Range (bp)**	**CADASIL-CAD02-PBMCs**	**CADASIL-CAD02-iPSCs**
Amelogenin	TMR	106(X), 112(Y)	X,Y	X,Y
CSF1PO	JOE	321-357	11, 12	11, 12
D16S539	JOE	264-304	11, 12	11, 12
D7S820	JOE	215-247	10, 11	10, 11
TPOX	TMR	262-290	11, 11	11, 11
Penta E	FL	379-474	7, 14	7, 14
D18S51	FL	290-366	16, 17	16, 17
D3S1358	FL	115-147	16, 16	16, 16

Table 15. STR analysis for CAD02 PBMCs and all the derived cell lines obtained from them.

19.2. NOTCH3 mutation analysis

In the same way as for STRs, mutation analysis for the IDISi001-A patient were carried out in all of the generated cell lines (Fig. 77), while for the CAD02 patient just PBMCs and the reprogrammed hiPSCs were subjected to this analysis (Fig. 78), as CADASIL-hiPSCs-derived vSMCs and vECs were not generated from this line. In both cases, mutation was present all over the derived cell lines. For CAD02-derived hiPSCs, first analysis had some background noise right after the mutation spot, although mutation could be perfectly seen.

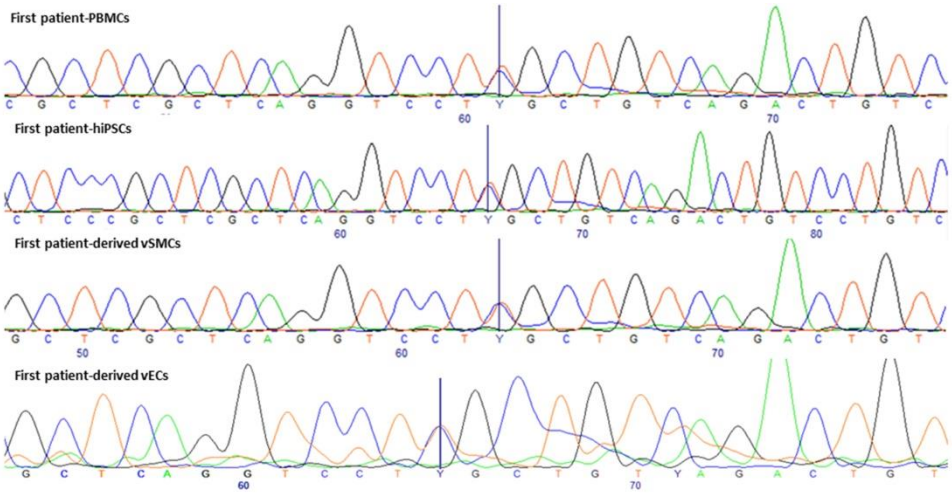

Figure 77. Mutation analysis of the *NOTCH3* segment where the mutation was diagnosed for the IDISi001-A-PBMC line and all the derived cell lines obtained from them.

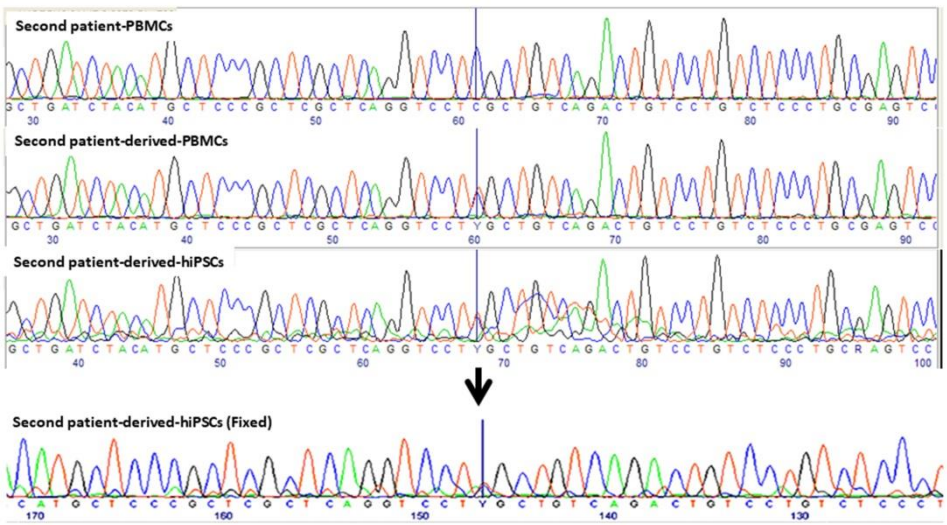

Figure 78. Mutation analysis of the *NOTCH3* segment where the mutation was diagnosed for the CAD02-PBMC line and the CAD02-hiPSC line compared with a healthy-hiPSC line. CAD02-hiPSCs analysis had to be repeated but in revers sense (black arrow) since there was some background noise on the first analysis.

20. Expression analysis of NOTCH3 domains

20.1. NOTCH 3 extracellular domain

Expression pattern of NECD can be seen in Fig. 79. NECD clearly expressed at the cell membrane. Specifically, it seemed to appear around day 10 after induction of CADASIL-hiPSCs-derived vSMCs differentiation. By day 16, this NECD seemed to accumulate at some points of the cell membrane, while by day 30, wells are so confluent that cells change their conformation and those "spots" changed into a net-pattern expression.

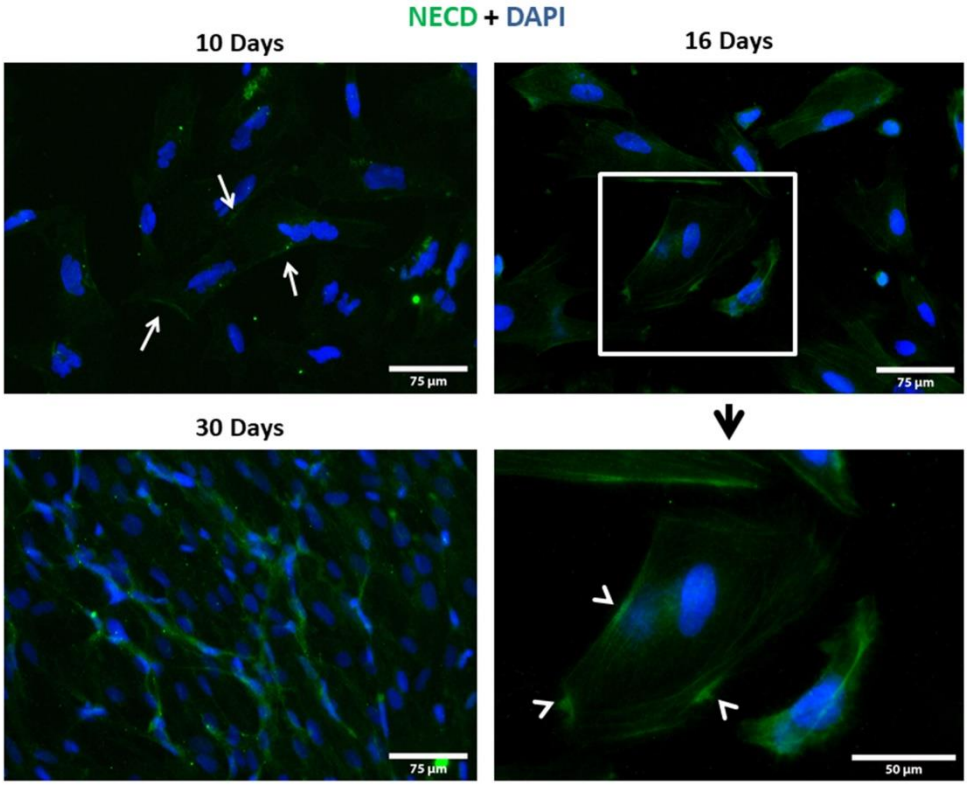

Figure 79. NECD staining in CADASIL-hiPSCs-derived vSMCs at different times. White arrows: NECD accumulation at cell surface. Arrowheads: possible GOM deposits.

When revealing WB, just one of the tested NECD antibodies had specific staining, but the stain was above 250 kDa, probably staining in the molecular weight of the entire NOTCH3 protein (280 kDa). This staining was present in IDISI001-A-derived vSMCs at days 20 and 35 with no differences between them, when at day 11 was absent. But more important, for the cell line control (HAoSMCs) there were no staining (Fig. 80). This suggests an accumulation of this molecule, whether it is the NECD or the entire NOTCH3.

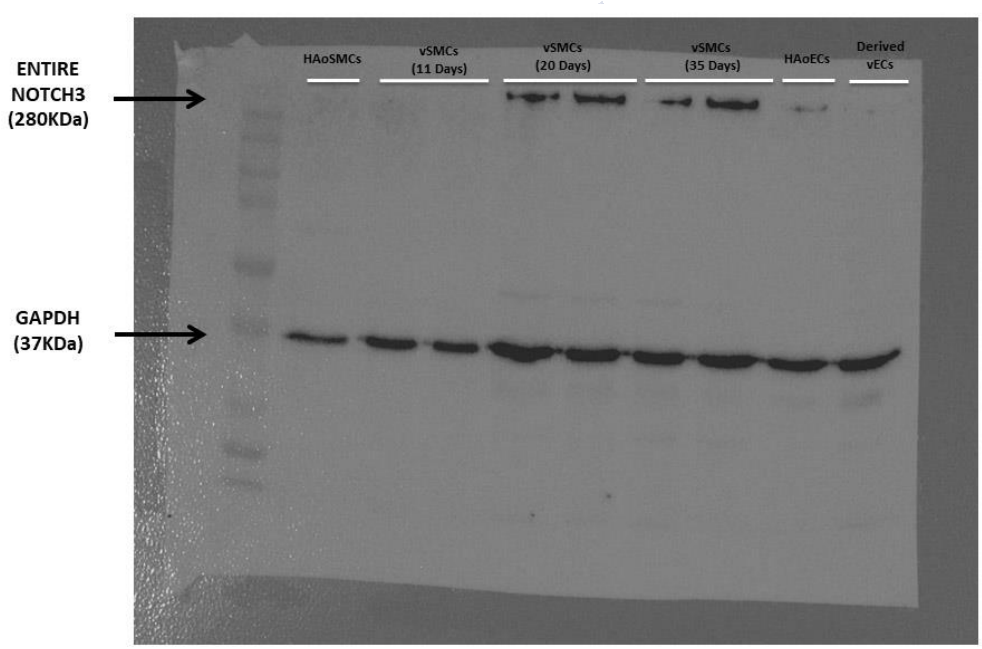

Figure 80. WB for NECD/NOTCH3 using the NECD/NOTCH3 monoclonal Ms antibody (5E1 clone).

20.2. NOTCH3 intracellular domain

Analysis in NECD in vSMCs hosed in Fig.81 reflects a pattern for hiPSCs, Hek cells, IDISi001-A-derived vECs and IDISi001-A-derived vSMCs. Curiously, while the staining for NICD in Hek cells was clearly at the membrane, for vSCMs, NICD appeared not only at the membrane but also at the cytoplasm level, staining in a filament-like manner in the same way as for vECs, but in this case the staining is not so intense in the cytoplasm. For hiPSCs, NICD stained all the cells in a diffuse way, maybe implying some role of NOTCH3 at this stage

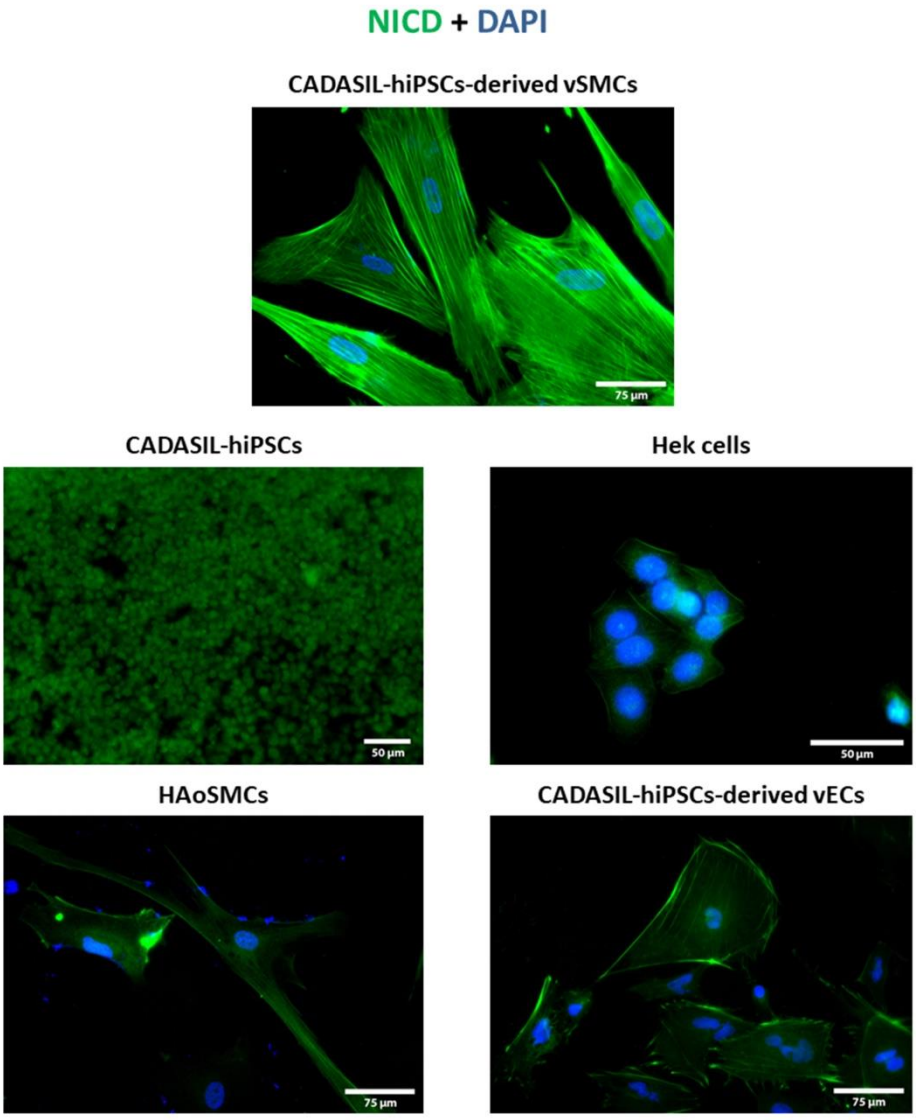

Figure 81. NICD staining in CADASIL-hiPSCs, Hek cells, HAoSMC line, CADASIL-hiPSCs-derived vSMCs and vECs.

Furthermore, while the membrane staining for the CADASIL-hiPSCs-derived vSMCs didn't seem to vary, the filament-like staining was progressive, increasing its intensity over the days (Fig. 82), suggesting some kind of accumulation at cytoplasmic level.

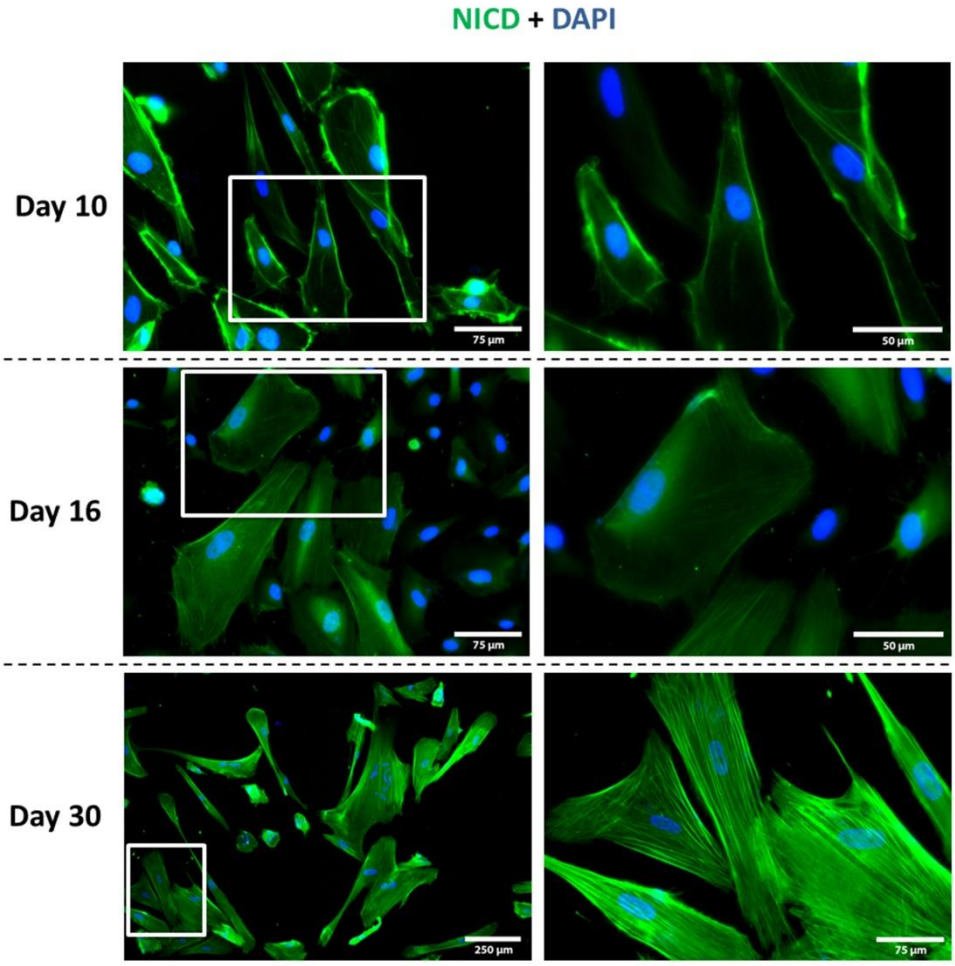

Figure 82. CADASIL-hiPSCs-derived vSMCs NICD staining at different days. NICD cytoplasmic accumulation throughout the days can be observed.

When analyzing NICD accumulation by western blotting, for the PA5-13203 antibody, higher levels of NICD were already seen in CADASIL-hiPSCs-derived vSMCs at day 10 compared to the HAoSMC line control (Fig. 83). It has to be said that the expected molecular weight of the NICD should be around 80-100 kDa. On the other hand, no difference in NICD accumulation between day 10 and day 35 was observed. However, two unexpected bands were also observed: One appeared at the same molecular weight as the band appearing at NECD WB, suggesting that probably the antibody used for NICD also reveal the entire NOTCH3 protein. The second one appeared really close to the NICD band but just in the CADASIL-hiPSCs-derived vSMCs samples. The implications of this band will be discussed later.

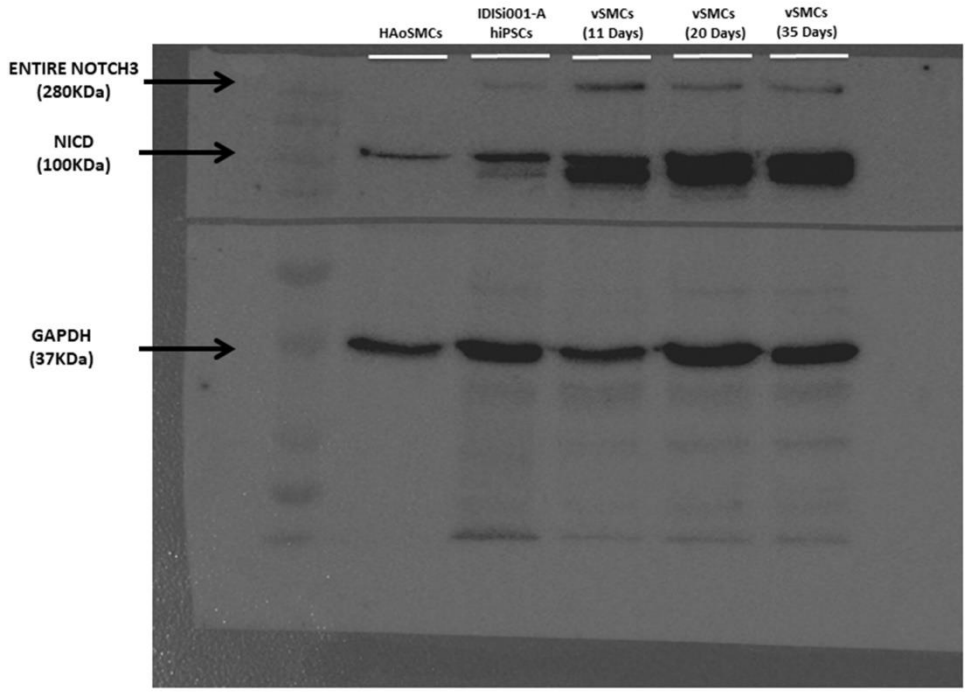

Figure 83. WB for NICD using the PA5-13203 NICD antibody.

For the PA5-19515 antibody, a WB with all the cell lines samples was done (Fig. 84). This figure represents a WB performed in the same membrane as the WB of the Fig. 80, but on the next day. In the same way as for PA5-13203 antibody, accumulation of the NICD was already higher at day 11 in CADASIL-hiPSCs-derived vSMCs compared to the HAoSMCs. Also, the band at day 35 in vSMCs seemed a bit more intense than the band at day 11. Regarding the mysterious second band that appeared in Fig. 83, it also appeared on this case. Interestingly, this band just appeared in the CADASIL-derived cell lines (vECs and vSMCs) but not in the control. But, for this antibody, it also appeared another band, which is the most intense of all, corresponding to 20 kDa or less. The implications of this band will be discussed later.

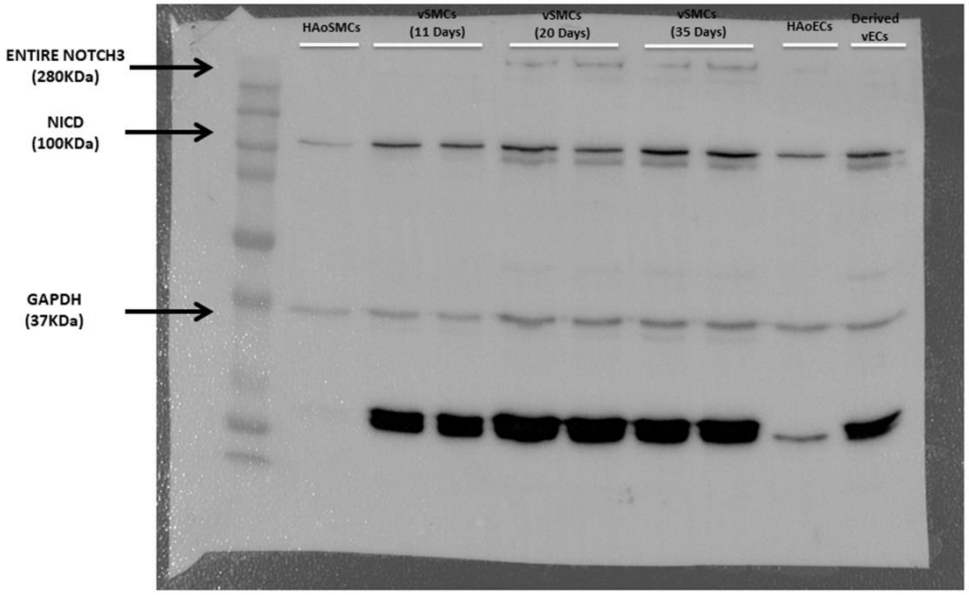

Figure 84. Western blot with all cell lines samples for NICD using the PA5-19515 antibody. Question mark: unknown band.

INTRODUCTION

HYPOTHESIS

OBJECTIVES

MATERIALS & METHODS

RESULTS

DISCUSSION

CONCLUSIONS

USC
UNIVERSIDADE
DE SANTIAGO
DE COMPOSTELA

In this is Thesis, a PBMCs-derived hiPSCs cell line from a patient carrying a mutation previously diagnosed and associated with CADASIL disease has been generated and registered for the first time. In addition, the two cell lines affected in the disease were obtained from this hiPSCs line: CADASIL-hiPSCs-derived vSMCs and vECs. The expression pattern of both NOTCH3 protein domains were analyzed, reflecting the molecular mechanisms that produces this pathology.

First of all, and as explained at the beginning of material and methods section, the initial idea of this project was to compare the expression pattern and accumulation levels of the two NOTCH3 domains in the CADASIL-hiPSCs-derived cell lines with the expression pattern of these domains in a commercial control cell line (HAoSMCs and HAoECs); and with the same derived cell line but derived from healthy hiPSCs, this is, with no mutation. Unfortunately, the comparison with these healthy-hiPSCs-derived cell lines was not possible due to the *Mycoplasma* contamination. This contamination forced that all the healthy-hiPSCs colonies had to be discarded. In an attempt to solve this issue, a new reprogramming of healthy PBMCs to hiPSCs was tried. Unluckily, it was not successful and a second intent, not included in this Thesis, is currently ongoing.

21. Reprogramming process and hiPSCs generation and characterization

On this project, PBMCs from two different patients with a previously diagnosed mutation and associated to CADASIL disease have been successfully reprogrammed to hiPSCs.

If we consider the reprogramming result in terms of final stable clones achieved, it can be said that both reprogramming processes were successful, specially the IDISi001-A cell line, with a 7.22% of efficiency (6 stable clones out of 83 selected). The reprogramming of the CAD02 cell line had lower efficiency and number of clones generated (3.84%; 1 stable clone out of 26 selected). These second values are in line with the reported values found throughout the bibliography, where they tend to be around 1% of efficiency for PBMCs reprogramming. These works use higher MOIs than the used for this project, and the same MOI for each vector[212-214]. In this Thesis the MOI used for each viral vector is known from the beginning, being a MOI of 5 for the *KLF4* + *SOX2* + *OCT4* viral vector and the *C-MYC* vector, and a MOI of 3 for the vector carrying extra *KLF4.* The differences found in the efficiency and generation of colonies between the two reprogramming processes could be due to several reasons: differences between reprogramming kit lots, cell counting errors when selecting $3x10^5$ cells for infection or even in the seeding process of the 3 initial Petri dishes, or just because of random variations within a stochastic process such as reprogramming. Besides, the reprogramming process during the initial 3 Petri dishes stage gave rise to cellular formations that were not counted as emerging colonies. It is very likely that, if they had been counted, the efficiency of the process would have fallen, but since they were not considered emerging colonies they were not quantified.

Once the hiPSCs cell lines were generated, they were submitted to several characterization processes in order to prove that the colonies obtained were indeed hiPSCs. In this project, one of the main objectives consisted on the registration, for the first time, of a hiPSC cell line with a

previously diagnosed mutation associated with CADASIL disease. For this reason, for the characterization of this cell line, all the tests required by the "Banco Nacional de Líneas Celulares del Instituto de Salud Carlos III" and the Human Pluripotent Stem Cell Registry in order to register the cell line were made. Besides, all these tests were also needed in order to publish in the *Stem Cell Research* journal[42]. Also, since it is a cell line with an associated mutation, the genetic sequencing was necessary in order to analyze the presence of the mutation throughout the several derived cell lines (CADASIL-PBMCs, CADASIL-hiPSCs, CADASIL-hiPSCs-derived vSMCs and vECs).

Regarding the characterization processes themselves, none of the generated cell lines showed special difficulties of any kind when generating them or differences among them. However, there were some small issues that deserve to be discussed.

For the characterization by immunofluorescences of the colonies, there was a certain tendency of the colonies to grow leaving gaps inside them (Fig. 59). In principle, this could mean some indications of differentiation and instability of the colonies, what could endanger their characterization. However, as it could be observed in the results, the presence of these gaps didn't seem to affect the pluripotency state of the colonies themselves. It is more likely that this growth was due to a change in the growing surface or to a change in the well size where the colonies are seeded for immunofluorescence assays (from a 35 mm^2 Petri dish to a well of 2 cm^2). Another fact that was observed during the immunofluorescence characterization of the colonies was the presence of a first superficial cell layer with no stain for nuclei related pluripotency markers (Fig. 60). A possible explanation for this, taking into account

that this superficial cell layer presents some prolongations quite often in cell culture, could be that this layer may be formed by some slightly specialized cells in charge of capturing nutrients for the rest of the colony, which could explain a partial loss of pluripotency, although there are no reports throughout bibliography reporting something similar.

To demonstrate that the new hiPSC lines were able to generate cell types belonging to the three germ layers, in this project, the generation and differentiation *in vitro* into EBs instead of the teratoma formation *in vivo* was chosen. The reason behind this is that for official registration of a new hiPSC line it is no longer mandatory the characterization by teratoma formation. For the EBs formation process, formation in ultra-low attachment plates was the one used, instead of other reported methods like the induction within conical-bottom wells that favors the formation of just one single EB per well at the bottom[215]. The results obtained from this experiment probably show the major differences between the healthy-hiPSCs line and the CADASIL-hiPSCs line observed all over the characterization process. The EBs generated from both CADASIL-hiPSC lines were clearly smaller than the EBs generated from healthy-hiPSCs and presented more single cells unable to form EBs floating in the culture. This issue didn't suppose a big problem, and after several tries the demonstration that the CADASIL-EBs were able to differentiate into cell type of all the three germ layers was already achieved. The markers used for each germ layer were FOXA2 (endoderm), nestin (ectoderm) and vimentin (mesoderm), based on the availability of the antibodies and because they also appeared throughout the bibliography as valid markers[80].

22. Differentiation to vascular smooth muscle and vascular endothelial cell

The next step once the generation, characterization and registration of a hiPSC generated from PBMCs from a patient with CADASIL were achieved was to differentiate this CADASIL-hiPSCs to vSMCs and vECs. On the one hand, the main goal was to obtain a CADASIL-hiPSCs-derived vSMC line as this cell type is the well-described one that suffers the degeneration and collapse in CADASIL due to the mutation. Because of that, this was the differentiation protocol addressed first. In addition, the differentiation protocol to CADASIL-hiPSCs-derived vECs was also wanted to be addressed as some studies have described that these vascular cells are also affected in this disease. The expression pattern and accumulation levels of both regions of NOTCH3 protein (NICD and NECD) were determined in the two differentiated cell types.

The first differentiation protocol to vSMCs, based on the addition of ascorbic acid[216], didn't work. Either trying from a single-cell suspension as starting point or from clusters and/or entire colonies as starting point, the protocol didn't result in vSMCs. By starting from a single-cell suspension it could seem that this protocol was going in the right path, given that the resulting cells seemed to have the typical elongated SMC morphology, but the attachment rate was so low that the attached cells were not able to grow.

Due to the low successful results obtained with the previous differentiation protocol, a second protocol was used based on α-MEM medium and the subsequent addition of TGF-β and PDGF-BB factors. This protocol showed positive stain for SMC markers in

immunofluorescences, and together with the contractility tests, indicated that the differentiated cells were SMCs, while the observed growth forming tubular structures once the TGF-β and the PDGF-BB were added pointed out to a more specific vSMC differentiation. Unfortunately, the success rate of this protocol was about 50%; barely half of the differentiation attempts to vSMCs progressed correctly, mainly because of the single-cell suspension[100, 217] used as starting point. In the same way as for the differentiation protocol with ascorbic acid, a single-cell suspension as starting point resulted in a very low attachment rate, which prevented the cell culture from growing, not even by adding rock inhibitor. However, with a small cluster suspension as starting point, the attachment rate increased, and the resulting cell culture was able to grow, with cells presenting the typical elongated SMC morphology. The limitation in this case was this small cluster suspension because both cluster size and cell density seeding were difficult to standardize.

To obtain vECs, the first protocol assessed allowed to achieve CADASIL-hiPSCs-derived vECs without remarkable issues[101]. Immunofluorescence tests and the induction of vessel formation proved that the achieved cells were vECs. Furthermore, unlike the differentiation protocol towards vSMCs, this protocol was completely standardized and its efficiency was 100%. Also, unlike differentiated vSMCs, these differentiated vECs can be frozen and may be driven to passage 3-4, which make them easier to manipulate.

Probably, the more important weakness regarding this protocol differentiation section is that no fluorescence-activated cell sorting (FACS) was done to determine the purity of the achieved cultures, since it is assumed that 100% purity is impossible to obtain when performing

iPSC differentiations. In fact, although not shown, the data of the immunofluorescences for both derived cell lines showed negative staining for specific SMCs and ECs marker in some regions.

23. NOTCH3 analysis

CADASIL is a disease whose etiopathological mechanisms are yet being unraveled. Many reports pointed to a NECD accumulation as the domain involved on its physiopathology, although accumulation of NICD was also associated as a potential mechanism related with this vascular disease. Indeed, a previous study from 2002 at PNAS journal[196] reported a case on which the mutation affected the intracellular trafficking of the NICD, which is in line with the results reported in this Thesis, mainly on vSMCs.

The results reported for the NECD analysis by western blotting revealed a band near the 280 kDa, which corresponds with the molecular weight of the entire NOTCH3 protein[170, 196]. This NOTCH3 accumulation in CADASIL-hiPSCs-derived vSMCs appeared at the second week after inducing differentiation, while HAoSMCs lacked of NOTCH3 band.

In the immunofluorescence assays, this protein accumulation at week 2 could also be observed. In CADASIL-hiPSCs-derived vSMCs, when not confluent, a greater intensity of signal was appreciated in concrete areas of the cellular membrane. This staining could correspond with GOM deposits. As it is reported in bibliography, these GOM deposits are formed mainly by NECDs[165, 170] due to the cell inability to remove the NECD because of the mutation. This data may indicate that for

immunofluorescence, the results reported on this project could be related to NECD. Another explanation, taking together both WB and immunofluorescence results, is that this mutation, being a cysteine-gaining mutation, may be producing undesirable multimerization of NOTCH3 proteins by the union of this extra-cysteine residues from different NOTCH3 proteins before the ligand-receptor signal interacts, thus impeding the S2 cleavage and the subsequent accumulation of NOTCH3 multimers. This would fit with the WB results, since no NECD band is found but an entire NOTCH3 accumulation appears. It would also fit with immunofluorescence results: no matter whether the staining is for the entire NOTCH3 protein or for NECD, if the mutation truly forces the multimerization of the NOTCH3 receptors, the entire NOTCH3 protein and the NECD domain would give signal at the same location.

To summarize, regarding NECD analysis, on this project it has been generated, for the first time, a CADASIL-hiPSCs-derived vSMC line that exhibits GOM deposits on cellular membranes and with accumulation of the entire NOTCH3 protein compared to a HAoSMC line.

About NICD, the reported results should be considered as preliminary data, mainly because of the almost null bibliography reporting physiopathological alterations concerning this domain, except for the already mentioned PNAS from 2002[196]. Nevertheless, WB results showed an approximate band of 100kDa, which fits with the estimated size of the NICD (97kDa)[218]. Thus, for CADASIL-hiPSCs-derived vSMCs, it could be said that there is an accumulation of the NICD with respect to the HAoSMC line. Furthermore, it seems to be also a slight accumulation in CADASIL-hiPSCs-derived vSMCs at day 35 with respect to those at day 11. This slight accumulation over the days appears to correlate with the

immunofluorescence results, where a greater intensity in the cytoplasm in form of cytoskeletal-like structures and an increment on their number can be seen over the days. This increasing in the signal intensity doesn't appear in the HAoSMC line. It must be said that this cytoskeletal-like structure staining for NICD in CADASIL-hiPSCs-derived vSMCs was strange and put in doubt whether this staining was truly for NICD or maybe for some structural filament, as it can be found in bibliography that in CADASIL-vSMCs an increasing in cytoskeletal filaments can be observed[93]. However, NICD staining for Hek cells, HAoSMCs and CADASIL-hiPSCs-derived vECs showed a membrane staining mainly. Together with the fact that this antibody was the same used for western blotting, whose band fit with the approximate NICD molecular weight, indicates that it is a truly NICD stain. So once this issue is clarified, this cytoskeletal-like structure could imply a role of NOTCH3 in cytoskeleton maintenance or that it travels attached to cytoskeletal filaments inside the cell. Paying attention to the wide bibliography on this field, it would be really surprising that the mutation reported on this project was the first one reporting a NICD accumulation. In any case, since the mutation is located in one of the nearest EGF repeats to the NRR, it would not be a crazy hypothesis that once the ligand-receptor interaction is triggered, the extra-cysteine residue somehow interacts altering the S2 cleavage process and subsequently the S3 cleavage. This could result in an incorrect NICD which could alter cellular trafficking. This hypothesis would be supported by the presence of the second ban near the main NICD band in WB, which could correspond with a different NICD variant, due to this interaction of the extra-cysteine residue with the NRR. However, it could also be due to a different S3 cleavage product that would depend on the cellular location where the γ-secretase performed

the cleavage (cellular surface or inside the endosome) as mentioned in the introduction of this Thesis[171]. On the other hand, NICD immunofluorescences show a clear increment in NICD staining inside the CADASIL-hiPSCs-derived vSMCs compared to the HAoSMCs, indicating that maybe there is something happening with the NICD on this mutation. Because of all the aforementioned contradictory facts, more specific and exhaustive experiments should be carried out in order to clarify what is really happening on this mutation regarding NICD, because if it truly is a mutation that alters both NECD and NICD pathways, it would be the first case being reported ever.

Finally, regarding NICD and NECD analysis for CADASIL-hiPSCs-vSMCs, it should be also mentioned the maximum day when protein from CADASIL-hiPSCs-derived vSMCs could be obtained. With the differentiation protocol employed for differentiation, it was impossible to maintain CADASIL-hiPSCs-derived vSMCs for more than 30-35 days in culture. This was mainly because these vSMCs were not able to survive to a second passage once they reached confluency. Thus, having in mind that the transition passage from DM1 to DM2 occurs approximately at day 10-15, cells tend to reach confluency at day 25-28, being able to survive in confluency until day 30-35. Maybe with a different differentiation protocol this barrier could be overcome. This fact together with the ones mentioned before when discussing the differentiation protocol to vSMCs are good reasons to look for a different, improved protocol in the future. Overcoming this 35-day barrier could be really important in order to perform a more extensive NECD and NICD accumulation profile.

So, to sum up, for NICD this project reports an apparent accumulation in a CADASIL-hiPSCs-derived vSMC line, which would be due to wrong interactions of the extra-cysteine residue from the mutated 31-32th EGF-repeat with the NRR domain. Nevertheless, further experiments should be assessed to prove this fact, since there are so many reports throughout bibliography that never mention this kind of mutation effect in CADASIL.

Regarding vECs, for WB, there is a tiny entire NOTCH3 band both in the HAoECs and CADASIL-hiPSCs-derived vECs; this band is clearly less intense than those for CADASIL-hiPSCs-derived vSMCs. CADASIL-hiPSCs-derived vECs present, also, a NICD band slightly more intense than the control and a second one near the NICD band that doesn't appear in the control. About these results, there are a few things to say: on the one side, there are works that say that NOTCH3 expression is restricted to vSMCs[170, 172]. On the other side, databases like Human Cell Atlas report that NOTCH3 is ubiquitously expressed in all tissues. If those works reporting a NOTCH3 expression restricted to vSMCs are right, the presence of a NICD and an entire NOTCH3 band in CADASIL-hiPSCs-derived vECs and HAoECs would not make any sense. However, both WB and immunofluorescence results shown in this Thesis clearly indicate that this protein is at least expressed in endothelial cell lines. This way, having the databases reports as accurate, the results obtained for NICD indicate that somehow this NOTCH3 accumulation happens exclusively in vSMCs, or that at least it happens at a higher speed (which would explain why vSMCs collapse first in CADASIL).

24. Considerations about the experimental work with iPSCs and future work guidelines

In this Thesis it is reported for the first time the generation of a time a non-integrative iPSC-based disease human model for CADASIL and obtained CADASIL-specific affected cells, muscular and endothelial cells, thereby. This achievement provides valuable clues for pathogenic analysis and therapeutic strategy development against CADASIL and potentially other neurovascular diseases related with vascular impairments.

It should be noted the relevance of this study being aware that researchers from this field have recently been awarded with the Brain Prize 2019, considered as the "Neuroscience Nobel". This reveals the increasing relevance that this disease is reaching and also suggests a "CADASIL race" among researchers to be the first ones in performing the next huge advance for this disease. Keeping this in mind, the work developed during this Thesis supposes an important step towards the understanding of CADASIL mechanisms. The development of a CADASIL cell human model with CADASIL-hiPSCs-derived vSMCs and vECS that allows the analysis of the NICD and NECD accumulation not only for vSMCs but for vECs too supposes a new platform for the study of this disease and the development of potential drugs directly in CADASIL-patient cells.

The creation of hiPSCs-based cell models is a really potent tool that has already proved its value not only for the disease that this Thesis focuses on but for many others[89, 90, 92] . Unfortunately, the development of an iPSCs-based technology has important limitations such as the long

protocol periods required to generate hiPSCs or the differentiation protocols to generate the required cell type. Besides, the iPSCs culturing protocols requires the iPSCs culture medium to be changed daily, which increases the risk of contamination and full-time dedication. Thus, this becomes another discouraging fact for small laboratories to work with this technology. Moreover, in addition to the hiPSCs time-consuming culturing, a disease cell modeling based on hiPSCs generates and implies to work with a lot of different cell lines, each one with its own requirements and its own experiments to be done. This fact, together with the hiPSCs culturing, makes the task even more impossible to be done by just one person.

On the other hand, iPSCs technology is a novel but potent tool that has already prove its value. It allows to translate the human disease to the laboratory by studying it directly in the own patient´s cells, which supposes a huge step towards more translational and efficient therapies. Moreover, in combination with the highly accurate genetic tools like CRISPR/Cas9, the iPSCs technology can become not only a tool to study diseases but a potent tool to fix genetic mutations in the iPSC stage and develop healthy cells that may be transplanted to the patient, avoiding immunorejection from allogenic transplants.

Personally, to work on the development of a hiPSCs-based disease cellular model like CADASIL, has been a rewarding work for this PhD student. From a professional point of view, work with such a novel technology opens up many possibilities for a scientific career, since there are many laboratories looking for people to start research lines based on the technology of iPSCs. Also, from the development of this Thesis several scientific papers have been published and several

presentations at different international and national scientific congresses have been made, which indicates that this field is very productive and has the attention of the scientific community. And from a more personal point of view, to work in hiPSCs-based disease modeling creates a feeling of being doing something important, of being working on something that could create advances in diseases that, as it is the case with this Thesis, has no treatment. And that is priceless, no matter how much time you have to devote to the task.

To finish, this Thesis is the first part of a wider project, and now that it has been demonstrated that it is possible to generate an *in vitro* model of CADASIL with vSMCs and vECs and to study the pathological features that occurs on this disease, new objectives will be pursued. Achieving these objectives is estimated to take about 4 years and suppose an estimated investment expense of 500.000€.

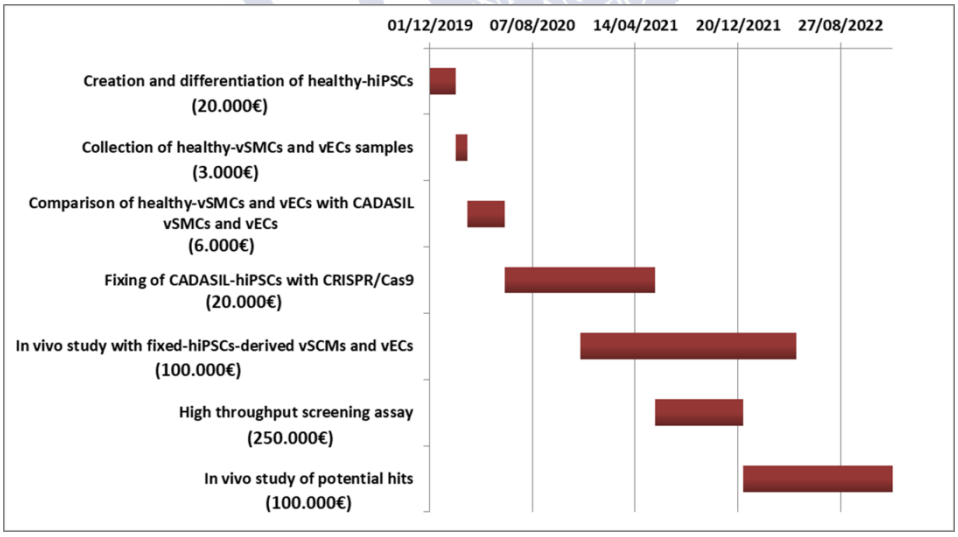

Fig. 85. Gantt diagram representing the next steps in the project and the estimated investment expense for each step.

Briefly, next year will be focused in strengthen the results obtained during this Thesis, with the creation and characterization of a healthy-hiPSCs cell line to differentiate it to vSMCs and vECs and compare the NECD and NICD accumulations with the CADASIL-hiPSCs-derived vSCMs and vECs.

Also, with the consolidation of this *in vitro* platform, two different paths to work in are open. One way will consist of learning and standardizing a protocol for the use of genetic editing tools, specifically the CRISPR/Cas9. Once this technology is implanted at the laboratory, next step will be to fix the mutation with the CRISPR/Cas9 system at the CADASIL-hiPSCs stage. Then, these fixed-CADASIL-hiPSCs will be differentiated into vSMCs and vECS to analyze, among other things, if the accumulation of NECD still happens in vSMCs. These studies are estimated to take another year. Finally, if it is proved that the fixed-CADASIL-hiPSCs-derived vSMCs and vECs do not exhibit abnormal accumulation of any of the NOTCH3 domains or any kind of phenotype abnormality, these cells will be injected into the brain of *Notch3-/-* knockout mice. The idea of this final step is to see if these cells are capable of substitute the endogenous, damaged ones within the vessel walls. As this step involves learning to handle laboratory animals and the surgery, it is estimated to take about 1-2 years.

The other way will consist in a drug screening assay. Using the high throughput screening technique will allow testing thousands of drugs to check for possible hits that reduce the accumulation of the NECD domain. If this happens, it will be necessary to prove these drugs in *in vivo* models, specifically in young *Notch3-/-* mice, and compare the accumulation levels of the NOTCH3 domains with healthy mice.

Another interesting possibility would be trying to create a specific mouse strain carrying the specific mutation reported on this Thesis. This will mimic more accurately than the *Notch3-/-* mice the specific phenotype reported on this Thesis and thus the reported results will be more reliable. However, the generation of a new strain is a long-time and expensive process to add to an already quite expensive and long-term project so to do or not this step should be thought carefully.

INTRODUCTION

HYPOTHESIS

OBJECTIVES

MATERIALS & METHODS

RESULTS

DISCUSSION

CONCLUSIONS

USC
UNIVERSIDADE
DE SANTIAGO
DE COMPOSTELA

CONCLUSIONS

For this project, the following conclusions have been reached:

1. It has been generated, for the first time ever, a human induced pluripotent stem cell line from peripheral blood mononuclear cells of a patient with a previously diagnosed mutation associated with CADASIL disease.

   1.1. This cell line (IDISi001-A) has been fully characterized and officially registered in several institutions: the "Banco Nacional de Líneas Celulares" at the "Instituto de Salud Carlos III" in Spain, and the Human Pluripotent Stem Cell Registry.

   1.2. In order to strengthen the consecution of this objective, a second human induced pluripotent stem cell line (CAD02) from a second patient with the same mutation has been successfully generated and characterized.

2. Both CADASIL-human induced pluripotent stem cells-derived vascular smooth muscle cells and vascular endothelial cells have been successfully achieved based on the implementation of pre-existing protocols.

   2.1. These cell lines have been successfully characterized and compared with characterized cell line controls.

3. NOTCH3 extracellular and intracellular domains have been studied in both CADASIL-human induced pluripotent stem cells-derived vascular smooth muscle cells and vascular endothelial cells. Thus, it can be said that a "disease-in-a-dish" model for CADASIL has been

achieved. Unfortunately, analysis of both NOTCH3 extracellular and intracellular domain could just be compared with the human aortic smooth muscle cells and human aortic endothelial cells but not in healthy-human induced pluripotent stem cells-derived vascular smooth muscle cells and vascular endothelial cells respectively. With this in mind, regarding the study of NOTCH3 extracellular and intracellular domain:

3.1. For NOTCH3 extracellular domain, no presence at western blot is observed, but for the entire NOTCH3 a clear accumulation, already at day 20 after differentiation in CADASIL-human induced pluripotent stem cells-vascular smooth muscle cells is observed compared with the human aortic smooth muscle cells line and both human aortic endothelial cells and CADASIL-human induced pluripotent stem cells-vascular endothelial cells. Also, it can be observed by immunofluorescence that, at day 20, these cells exhibit NOTCH3/NOTCH3 extracellular domain accumulation deposits in specific areas of the cell membrane. For CADASIL-human induced pluripotent stem cells-vascular endothelial cells, immunofluorescences for the NOTCH3 extracellular domain remained to be done, but in western blot it didn´t seem to be NOTCH3 extracellular domain accumulation.

3.2. For NOTCH3 intracellular domain, it seems to be a slight increase in CADASIL-human induced pluripotent stem cells-derived vascular smooth muscle cells and vascular endothelial cells compared with their cell line controls, and the presence of a possible second NOTCH3 intracellular domain variant. Also, it seems to be a slight increase in NOTCH3 intracellular domain

cytoplasmic levels in CADASIL-human induced pluripotent stem cells-derived vascular smooth muscle cells at day 35 after differentiation compared with CADASIL-human induced pluripotent stem cells-derived vascular smooth muscle cells at 11 days. Together, this suggests a possible alteration regarding the intracellular NOTCH3 domain levels, processing and/or cellular trafficking.

To summarize, this Thesis concludes that, for the first time, a CADASIL "disease-in-a-dish" model has been generated where at least NOTCH3/NOTCH3 extracellular domain accumulates in vascular smooth muscle cells, while for NOTCH3 intracellular domain, more analysis have to be carried out in order to better clarify what is going on with this domain.

CONCLUSIONES

Para este proyecto, se concluye que:

1. Se ha generado por primera vez una línea de células pluripotentes inducidas humanas a partir de células mononucleares de sangre periférica de un paciente con una mutación asociada a la enfermedad de CADASIL previamente diagnosticada.

   1.1. Esta línea generada (IDISi001-A) ha sido completamente caracterizada y registrada oficialmente en diversas instituciones: el "Banco Nacional de Líneas Celulares" en el "Instituto de Salud Carlos III" en España y al "Human Pluripotent Stem Cell Registry".

   1.2. Con el fin de reforzar la consecución de este objetivo, se generó y caracterizó con éxito una segunda línea de células pluripotentes inducidas humanas (CAD02) procedente de un segundo paciente con la misma mutación.

2. Se consiguió obtener tanto una línea celular de células musculares lisas vasculares derivada de células pluripotentes inducidas humanas procedentes de un paciente con CADASIL como una línea de células endoteliales vasculares a partir de la implementación de protocolos pre-existentes.

   2.1. Estas líneas celulares fueron caracterizadas y contrastadas con éxito al compararlas con la caracterización de las líneas celulares control.

3. Se pudo realizar con éxito el estudio tanto del dominio extracelular de NOTCH3 como del intracelular en células musculares lisas vasculares derivadas de células pluripotentes inducidas humanas procedentes de un paciente con CADASIL así como en las células endoteliales vasculares derivadas también de esta línea de células pluripotentes inducidas humanas. De ahí se desprende que se ha podido conseguir por primera vez un modelo de "disease-in-a-dish" para la enfermedad de CADASIL. Desgraciadamente, los análisis del dominio extracelular de NOTCH3 y del intracelular solo pudieron ser comparados con los análisis de células musculares lisas aórticas humanas y células endoteliales aórticas humanas, pero no pudieron ser comparados respecto a análisis con células musculares lisas vasculares y células endoteliales vasculares derivadas de células pluripotentes inducidas humanas sanas respectivamente. Teniendo esto en cuenta, respecto al estudio del dominio extracelular e intracelular de NOTCH3:

   3.1. Para el dominio extracelular de NOTCH3, no se encontró presencia de este dominio en western blot, pero sí se encontró acumulación de la proteína NOTCH3 entera en células musculares lisas vasculares derivadas de células pluripotentes inducidas humanas procedentes de un paciente con CADASIL a partir de los 20 días después de su diferenciación, en comparación con los niveles encontrados en las células musculares lisas aórticas humanas y las células endoteliales derivadas de esta misma línea celular. Además, por immunofluorescencia se observó acumulación de NOTCH3/dominio extracelular en forma de depósitos en zonas

concretas de la membrana celular de las células musculares lisas vasculares derivadas de células pluripotentes inducidas humanas procedentes de un paciente con CADASIL. Para las células endoteliales derivadas de células pluripotentes inducidas humanas procedentes de un paciente con CADASIL, es necesaria la realización de inmunofluorescencias para conocer su patrón de expresión. En western blot, no obstante, no se observó acumulación alguna del dominio extracelular de NOTCH3.

3.2. Para el dominio intracelular de NOTCH3, parece que se aprecia un ligero incremento en las células musculares lisas vasculares y células endoteliales vasculares derivadas de células pluripotentes inducidas humanas procedentes de un paciente con CADASIL en comparación con sus líneas celulares control, y también se observó la presencia de una posible variante del dominio intracelular de NOTCH3. Además, también parece observarse un ligero incremento del dominio intracelular de NOTCH3 en las células musculares lisas vasculares derivadas de células pluripotentes inducidas humanas procedentes de un paciente con CADASIL a los 35 días después de la diferenciación en comparación con esas mismas células musculares lisas vasculares a 11 días. Todos estos datos juntos sugieren una posible alteración de los niveles, el procesado y/o el tráfico celular del dominio intracelular de NOTCH3.

Para finalizar, en esta Tesis se concluye que se ha podido generar por primera vez un modelo de "disease-in-a-dish" para la enfermedad de CADASIL en el que, al menos, se observa una acumulación de NOTCH3/dominio extracelular de NOTCH3 en las células musculares lisas

vasculares. Para el dominio intracelular de NOTCH3, más experimentos son necesarios para poder aclarar qué es lo que está ocurriendo con este dominio exactamente.

APPENDIX 1

Genetic diagnosis of the two patients with CADASIL

MEDICINA MOLECULAR

Dirección: Dr. Ángel Carracedo Dr. Fernando Domínguez

XUNTA DE GALICIA
CONSELLERÍA DE SANIDADE
SERVICIO GALEGO DA SAÚDE

Caso: 1L240

PACIENTE: [redacted]
SERVICIO: Neurología
CENTRO: Hospital Clínico Universitario de Santiago
Dr./Dra.: Árias
TIPO DE MUESTRA: Sangre
PRUEBA SOLICITADA: CADASIL
FECHA DE RECEPCIÓN: 26/12/2011

ANALISIS: Búsqueda de mutacione en el gen NOTCH3 mediante secuenciación NGS (SOLID 5500XL) de toda la región codificante del gen.

INFORME:

Se remite muestra de paciente de 67 años, con enfermedad de sustancia blanca de varios años de evolución, para estudio genético de CADASIL.

Genotipo: Arg1242Cys / normal

Se ha encontrado una mutación en el codón 1242 del exón 23 de NOTCH3 que produce un cambio aminoacídico de Arg a Cys. Esta mutación no ha sido previamente descrita. Prácticamente todas las mutaciones responsables de la patología llevan a la ganancia o pérdida de un residuo Cys en el dominio GFR-like lo que probablemente afecta a la estructura terciaria de la proteína. Arg1242Cys presenta dichas características y consecuentemente muy probablemente es responsable de la clínica reportada en [redacted]

CADASIL es una enfermedad autosómica dominante y por tanto el riesgo de heredaria para cada descendiente de un individuo afecto es de un 50%. Se recomienda informar de este resultado en el contexto de un adecuado consejo genético.

UNIDAD DE MEDICINA MOLECULAR	FECHA
Dr. F. Barros	09/10/2012

Unidad de Medicina Molecular – FPGMX
Edificio de Consultas Planta -2. Hospital Clínico Universitario de Santiago
15706 SANTIAGO DE COMPOSTELA
Tlfn.: (981) 951490 Fax: (981) 951473

MEDICINA MOLECULAR

XUNTA DE GALICIA
CONSELLERÍA DE SANIDADE
SERVICIO GALEGO DA SAÚDE

Caso: 3F873

PACIENTE [redacted]
SERVICIO: Neurología
CENTRO: Hospital Clínico Universitario de Santiago
Dr./Dra.: Árias
TIPO DE MUESTRA: Sangre
PRUEBA SOLICITADA: CADASIL – Estudio de portador
FECHA DE RECEPCIÓN: 12/07/2013

ANALISIS: Análisis por secuenciación tras amplificación por PCR del exón 23 del gen NOTCH3.

INFORME:
Se remite muestra de varón de 32 años, con antecedentes familiares de CADASIL (padre afecto y con estudio genético positivo: portador de mutación Arg1242Cys en gen NOTCH3), asintomático, para estudio predictivo de la enfermedad.

Genotipo: Arg1242Cys / normal

Se ha detectado en heterocigosis la mutación Arg1242Cys en el exón 23 de NOTCH3. [redacted] ha heredado la mutación en NOTCH3 presente en su familia.

Prácticamente todas las mutaciones en NOTCH3 responsables de CADASIL llevan a la ganancia o pérdida de un residuo Cys en el dominio GFR-like de la proteína, lo que probablemente afecta a la estructura terciaria de la proteína. Arg1242Cys produce un cambio aminoacídico de Arg a Cys y aunque no ha sido previamente descrita, presenta las características antedichas y consecuentemente muy probablemente es responsable de la clínica reportada en el padre de [redacted].
Este resultado confirma en [redacted] el estado de portador de la patología y el riesgo de desarrollar la enfermedad, no pudiéndose predecir la edad de aparición de los síntomas, ni la severidad y el tipo de los mismos o el ritmo de progresión de la enfermedad.
El riesgo de transmisión de la mutación es de un 50% en su descendencia. Se recomienda informar de este resultado en el contexto de un adecuado consejo genético.

UNIDAD DE MEDICINA MOLECULAR	FECHA
Dr. F. Barros	24/02/2014

Unidad de Medicina Molecular – FPGMX
Edificio de Consultas Planta -2. Hospital Clínico Universitario de Santiago
15706 SANTIAGO DE COMPOSTELA
Tlfn.: (981) 951490 Fax: (981) 951473

APPENDIX 2

Authorization to work with human samples

XUNTA DE GALICIA
CONSELLERÍA DE SANIDADE
Secretaría Xeral Técnica

Secretaría Técnica
Comité Autonómico de Ética da Investigación de Galicia
Secretaría Xeral. Consellería de Sanidade
Edificio Administrativo San Lázaro
15703 SANTIAGO DE COMPOSTELA
Tel: 881546425. Correo-e: ceic@sergas.es

galicia

DICTAMEN DEL COMITÉ DE ÉTICA DE LA INVESTIGACIÓN DE SANTIAGO-LUGO

Guillermo José Prada Ramallal, Secretario del Comité de Ética de la Investigación de Santiago-Lugo,

CERTIFICA:

Que este Comité evaluó en su reunión del día 21 de septiembre de 2017 el estudio**:**

> **Título:** Xeración de células humanas inducidas pluripotentes (IPSC) a partir de células somáticas de enfermos con CADASIL. Unha nova estratexia para o estudo de CADASIL
> **Versión Enmienda**: Modificación: cambio de título
> **Tipo de estudio:**Outros
> **Promotor**: Francisco Campos Pérez
> **Código del Promotor**:
> **Código de Registro**: 2016/450

Y que este Comité acepta de conformidad con sus procedimientos normalizados de trabajo y tomando en cuenta los requisitos éticos, metodológicos y legales exigibles a los estudios de investigación con seres humanos, sus muestras o registros, que dicha enmienda sea incorporada al estudio de investigación mencionado.

NOTA: Francisco Campos Pérez se ausentó de la sala de reunión durante la evaluación de esta enmienda.

En Santiago de Compostela, a 27 de septiembre de 2017.

El Secretario del Comité Territorial de Ética de la Investigación de Santiago Lugo,

XUNTA DE GALICIA SECRETARÍA XERAL TÉCNICA SECRETARÍA DO COMITÉS DE ÉTICA DA INVESTIGACIÓN CONSELLERÍA DE SANIDADE

guillermo.jose.prada.ramallal@sergas.es
2017.09.27 09:14:18 +02'00'

Guillermo José Prada Ramallal

APPENDIX 3

Authorization to generate and use human pluripotent stem cells

MINISTERIO DE ECONOMÍA, INDUSTRIA Y COMPETITIVIDAD

REXISTRO XERAL DA XUNTA DE GALICIA
REX AXENCIA GALEGA PARA A XESTIÓN DO COÑECEMENTO EN SAÚDE
SANTIAGO DE COMPOSTELA
Data 23/10/2017 10:13:26
ENTRADA 522 / RX 2593583

Instituto de Salud Carlos III

Subdirección General de Investigación
en Terapia Celular y Medicina Regenerativa

MINISTERIO DE ECONOMÍA, INDUSTRIA Y COMPETITIVIDAD
INSTITUTO DE SALUD CARLOS III
17 OCT 2017
SALIDA
REGISTRO GENERAL
Núm. 8211

D. Luis León Mateo
Director Área de Planificación y Promoción de
la Investigación Sanitaria
Axencia de Coñecemento en Saúde
Avda. Fernando de Casas Novoa, 37
Santiago de Compostela
15707 A Coruña

Madrid, a 16 de octubre de 2017.

La Comisión de Garantías para la Donación y Utilización de Células y Tejidos Humanos, en base a lo acordado en la reunión de 19 de septiembre de 2017, bajo la presidencia del Director del Instituto de Salud Carlos III, acordó informar el siguiente proyecto:

428 346 1 Implementación de la medicina personalizada para el estudio y tratamiento de enfermedades cerebrovasculares CADASIL

Una vez recibida la documentación solicitada, se informa favorablemente

En el caso de que fueran a insertarse células humanas en ratón, el investigador deberá aportar el compromiso de evitar que los animales utilizados en el proyecto, portadores de células iPS humanas, se reproduzcan, debiendo comunicar esta circunstancia a la Comisión de Garantías.

Se le recuerda la obligación de remitir a esta Comisión un breve informe anual sobre la evolución del proyecto, indicando posibles publicaciones o comunicaciones a congresos.

Todo lo cual pongo en su conocimiento en cumplimiento de lo dispuesto en la Ley 14/2007 de 4 de julio de Investigación Biomédica.

Atentamente,

MINISTERIO DE ECONOMÍA, INDUSTRIA Y COMPETITIVIDAD
INSTITUTO DE SALUD CARLOS III

Emilia Sánchez Chamorro
Secretaria de la Comisión de Garantías para la Donación
Y Utilización de Células y Tejidos Humanos

Monforte de Lemos, 5 28029 Madrid Teléfono 91 8222103 / 86

APPENDIX 4

Reagents used throughout the PhD project and their references

- 1.5M Tris (pH 8.8) (BIO-RAD, cat. no. 1610798)
- 10" HDMI monitor MMT6 (Leica, cat. no. MC190)
- 10-well WB comb (BIO-RAD, cat. no. 1653365)
- 12-multiwell plate (Corning, cat. no. 3513)
- 175µm diameter stripper needle (Origio, cat. no. MXL3-175)
- 24-multiwell plate (Corning, cat. no. 353047)
- 2-Mercaptoethanol (ThermoFisher, cat. no. 21985023)
- 2-methylbutane (Merck Millipore, cat. no. 106056)
- 30% acrylamide (BIO-RAD, cat. no. 1610158)
- 35mm^2 Petri dishes (Corning, cat. no. 430165)
- 5424R ultracentrifuge (Eppendorf, cat. no. 5404000010)
- 6-multiwell ultra-low attachment plate (Corning, cat. no. 3471)
- Agarose (Sigma-Aldrich, cat. no. A2576)
- Alkaline Phosphatase Live Staining test (ThermoFisher, cat. no. A14353)
- Amphotericin B (ThermoFisher, cat. no. 15290018)
- APS (GE-Healthcare, cat. no. 17-1311-01)
- BAMBANKER (Nippon Genetics, cat. no. BB01)
- BCA kit (ThermoFisher, cat. no. 23235)
- BMP4 (StemCell™ Technologies, cat. no. 02524)
- BSA (Sigma-Aldrich, cat. no. A2058)
- Carbachol (Sigma-Aldrich, cat. no. Y0000113)
- Casting frame (BIO-RAD, cat. no. 1653304)
- Casting stand (BIO-RAD, cat. no. 1653303)
- CD31 polyclonal Rb IgG antibody (Abcam, cat. no. ab28364)

- Cell lifter (Corning, cat. no. 3008)
- Cell scraper (Thermofisher, cat. no. 179693)
- ChemiDoc™ MP Imaging System (BIO-RAD, cat. no. 17001402)
- CHIR99012 (StemCell™ Technologies, cat. no. 72052)
- Cryovials (Simport, cat. no. T311-1)
- Cytotune™-iPS 2.0 Sendai Reprogramming Kit (ThermoFisher, cat. no. A16517)
- DAPI (Thermofisher, cat. no. D1306)
- Desmin polyclonal Rb IgG antibody (Abcam, cat. no. ab15200)
- Dispase 1X (StemCell™ Technologies, cat. no. 07923)
- DMEM with L-glutamine (ThermoFisher, cat. no. 11966-025)
- DMEM-F12 (ThermoFisher, cat. no. 10565-018)
- DyLight 488 Goat α-Rb IgG (Vector Laboratories, cat. no. DI-1488)
- EC Growth Medium MV2 (Promocell, cat. no. C-22022)
- EuroSafe (Euroclone, cat. no. EMR440001)
- FGF2 (StemCell™ Technologies, cat. no. 78003.1)
- FOXA2 polyclonal Rb IgG antibody (ThermoFisher, cat. no. 720061)
- GAPDH monoclonal Ms IgG1 antibody (ThermoFisher, cat. no. 43700)
- Gel releaser (BIO-RAD, cat. no. 1653320)
- Gel-loading tips (BIO-RAD, cat. no. 2239915)
- Glycine (Sigma-Aldrich, cat. no. G7126)
- Goat α-Rb immunoglobulins/HRP (Dako, cat. no. P0488)
- HAoECs (Promocell, cat. no. C-12271)
- HAoSMCs (Promocell, cat. no. C-12533)
- ICO105med incubator (Memmert, cat. no. ICO105)
- iScript™ cDNA Synthesis Kit (BIO-RAD, cat. no. 1708890)
- iTaq Universal SYBR Green Supermix (BIO-RAD, cat. no. 172-5120)

- KaryoMAX™ Colcemid™ Solution (ThermoFisher, cat. no. 15212012)
- KaryoMAX™ Giemsa Stain Solution (ThermoFisher, cat. no. 10092013)
- Laemmli buffer (Sigma-Aldrich, cat. no. 38733)
- Leica DMI 6000B fluorescence microscope (Leica, cat. no. DMI6000B)
- Leica DMi1 microscope (Leica, cat. no. DMi1)
- Liquid nitrogen container (Air Liquide, cat. no. 082274)
- Lymphoprep (StemCell™ Technologies, cat. no. 07851)
- Matrigel® Growth Factor Reduced (GFR) Basement Membrane Matrix, *LDEV-free (Corning, cat. no. 356238)
- Matrigel™ matrix (Corning, cat. no. 354277)
- MEM (1X) + GlutaMAX™-I Minimum Essential Medium (Thermofisher, cat. no. 32561-029)
- MEM + Glutamax (ThermoFisher, cat. no. 41090-028)
- Methanol (Scharlau, cat. no. ME0306)
- Mini-PROTEAN® Tetra Electrode Assembly (BIO-RAD, cat. no. 1658037)
- mTeSR1 (StemCell™ Technologies, cat. no. 85850)
- Nanodrop (ThermoFisher, ND2000)
- NANOG polyclonal Rb IgG antibody (Thermofisher, cat. no. PA1-097)
- NECD monoclonal Ms IgG1, clon 5E1 (Creative Biolabs, cat. no. TAB-553MZ)
- NECD monoclonal Ms IgG1, clone 1E4 antibody (Merck Millipore, cat. no. MABC594)
- Nestin polyclonal Rb IgG antibody (Abcam, cat. no. ab27952)
- Neubauer chamber (Brand Gmbh, cat. no. 718605)

- NICD polyclonal Rb IgG antibodies (ThermoFisher, cat. no. PA5-13203 and PA5-19515)
- Non-essential amino acids (ThermoFisher, cat. no. 11140050)
- Origio stripper (Origio, cat. no. MXL3-STR)
- P/S (Thermofisher, cat. no. 15140122)
- PCR device (Analytik-Jena, cat. no. 846-x-070-301)
- PDGF-BB (R&D Systems, cat. no. 220-BB-010)
- PFA (ThermoFisher, cat. no. 28908)
- Pierce™ ECL western blotting substrate (ThermoFisher, cat. no. 32106)
- Pluripotent Stem Cell 4-Marker Immunocytochemistry Kit (ThermoFisher, cat. no. A24881)
- Polystyrene round-bottom tubes (Corning, cat. no. 352052)
- PowerPac Universal device (BIO-RAD, cat. no. 1645070)
- Precision Plus Protein Dual Color Standards (BIO-RAD, cat. no. 1610374)
- Quick-RNA™ MiniPrep Plus (Zymo Research, cat. no. R1057)
- Rb α-Ms immunoglobulins/HRP (Dako, cat. no. P0260)
- Ready Mix REDTaq PCR Reaction Mix (Sigma-Aldrich, cat. no. R2523)
- RIPA buffer (Sigma-Aldrich, cat. no. R0278)
- SDS (Sigma-Aldrich, cat. no. L3771)
- SepMate™-50 tubes (StemCell™ Technologies, cat. no. 85450)
- Smooth Muscle Cell Growth Medium 2 (Promocell, cat. no. C-22062)
- Solid 5500XL (ThermoFisher, cat. no. 4460730)
- STEMdiff™ APEL™2-LI Medium (StemCell™ Technologies, cat. no. 05271)
- StemPro-34 SFM (ThermoFisher, cat. no. 10639011)

- StemSpan™ CC100 (StemCell™ Technologies, cat. no. 02690)
- Stericup® 1000 mL (EMD Millipore, cat. no. SCGPU01RE)
- Sub-Cell® GT agarose gel electrophoresis system (BIO-RAD, cat. no. 170-4401 to 170-4486)
- T25 flasks (Corning, cat. no. 353109)
- T75 flasks (Corning, cat. no. 353136)
- TAE buffer 1X (BIO-RAD, cat. no. 1610773)
- TEMED (BIO-RAD, cat. no. 1610801)
- TGF-β (R&D Systems, cat. no. 240-B-002)
- Thermo Scientific GeneRuler DNA Ladder 100bp Plus (ThermoFisher, cat. no. SM0322)
- Thermomixer (Eppendorf, cat. no. 5382000015)
- Trans-Blot SD Semi-Dry Transfer Cell device (BIO-RAD, cat. no. 1703940)
- Transfer membrane (Merck Millipore, cat. no. IPFL00010)
- Tris base (GE-Healthcare, cat. no. 17-1321-01)
- Tris-buffered saline 10X (Sigma-Aldrich, cat. no. T5912)
- TRITON™ 100X (Sigma-Aldrich, cat. no. T9284)
- Trypsin-EDTA (0.25%) (ThermoFisher, cat. no. 25200056)
- Tween® 20 (Sigma-Aldrich, cat. no. P9416)
- Ultra-low temperature freezers (-80ºC) (Haier Biomedical, cat. no. DW-86L728J)
- Universal Mounting Frame (PECON, cat. no. Universal Mounting Frame AK)
- Vacuum pump (Busch, cat. no. RB0021 C)
- VEGF (StemCell™ Technologies, cat. no. 78202)
- Vimentin polyclonal Rb IgG antibody (BiossAntibodies, cat. no. bs-0756R)

- vWF polyclonal Rb IgG antibody (Immunostep, cat. no. VWFPU)
- WB extra thick blot filter papers (BIO-RAD, cat. no. 1703966)
- WB glass plates (BIO-RAD, cat. no. 1653308)
- Y-27632 (StemCell™ Technologies, cat. no. 72302)
- α-MEM with nucleosides (StemCell™ Technologies, cat. no. 36450)
- α-SMC actin monoclonal Ms IgG2A antibody (Sigma-Aldrich, cat. no. A5228)

BIBLIOGRAPHY

1. Wu J, Izpisua Belmonte JC. Stem cells: A renaissance in human biology research. *Cell*. 2016;165:1572-1585
2. Gearhart J, Hagan B, Melton D, Pedersen R, Thomas E, Thomson J. *Essentials of stem cell biology*. Academic Press (2nd Ed); 2009. Massachusetts.
3. Becker A, McCulloch E, Till J. Cytological demonstration of the clonal nature of spleen colonies derived from transplanted mouse marrow cells. *Nature*. 1963;197:452-454
4. Siminovitch E, McCulloch E, Till J. The distribution of colony-forming cells among spleen colonies. *Journal of cellular and comparative physiology*. 1963;62:327-336
5. Evans M, Kaufman M. Establishment in culture of pluripotential cells from mouse embryos. *Nature*. 1981;292:154-156
6. Bradley A, Hasty P, Davis A, Ramirez-Solis R. Modifying the mouse: Design and desire. *Biotechnology*. 1992;10:534-539
7. Czechanski A, Byers C, Greenstein I, Schrode N, Donahue LR, Hadjantonakis AK, Reinholdt LG. Derivation and characterization of mouse embryonic stem cells from permissive and nonpermissive strains. *Nature protocols*. 2014;9:559-574
8. Evans M. Discovering pluripotency: 30 years of mouse embryonic stem cells. *Nature reviews. Molecular cell biology*. 2011;12:680-686
9. Stevens L, Little C. Spontaneous testicular teratomas in an inbred strain of mice. *Proceedings of the National Academy of Sciences*. 1954;40:1080-1087
10. Kleinsmith L, Pierce G. Multipotentiality of singe embryonal carcinoma cells. *Cancer Research*. 1964;24:1544-1551
11. Brinster RL. The effect of cells transferred into the mouse blastocyst on subsequent development. *Journal of experimental medicine*. 1974;140:1049-1056
12. Thomson J, Itskovitz-Eldor J, Spahiro S, Waknitz M, Swiergiel J, Marshall V, Jones J. Embryonic stem cells derived from human blastocysts. *Science*. 1998;282:1145-1147
13. Horch E, Laurentius MP. *Regenerative medicine: From protocol to patient*. Springer (2nd Ed); 2013. New York.

14. Pennock R, Bray E, Pryor P, James S, McKeegan P, Sturmey R, Genever P. Human cell dedifferentiation in mesenchymal condensates through controlled autophagy. *Scientific Reports*. 2015;5:13113
15. Tata PR, Mou H, Pardo-Saganta A, Zhao R, Prabhu M, Law BM, Vinarsky V, Cho JL, Breton S, Sahay A, Medoff BD, Rajagopal J. Dedifferentiation of committed epithelial cells into stem cells in vivo. *Nature*. 2013;503:218-223
16. Tropepe V, Turksen K. The ontogeny of somatic stem cells. *Stem cell reviews*. 2012;8:548-550
17. Jones DL, Wagers AJ. No place like home: Anatomy and function of the stem cell niche. *Nature reviews. Molecular cell biology*. 2008;9:11-21
18. Takahashi K, Yamanaka S. Induction of pluripotent stem cells from mouse embryonic and adult fibroblast cultures by defined factors. *Cell*. 2006;126:663-676
19. Hockemeyer D, Jaenisch R. Induced pluripotent stem cells meet genome editing. *Cell stem cell*. 2016;18:573-586
20. Marei HE, Althani A, Lashen S, Cenciarelli C, Hasan A. Genetically unmatched human ipsc and esc exhibit equivalent gene expression and neuronal differentiation potential. *Scientific Reports*. 2017;7:17504
21. Cowan C, Klimanskaya I, McMahon J, Atienza J, Witmyer J, Zucker J, Wang S, Morton C, McMahon A, Powers D, Melton D. Derivation of embyonic stem cell lines from human blastocysts. *New England journal of Medicine*. 2004;350:1353-1356
22. Singh VK, Kalsan M, Kumar N, Saini A, Chandra R. Induced pluripotent stem cells: Applications in regenerative medicine, disease modeling, and drug discovery. *Frontiers in Cell and Developmental Biology*. 2015;3
23. Loh YH, Agarwal S, Park IH, Urbach A, Huo H, Heffner GC, Kim K, Miller JD, Ng K, Daley GQ. Generation of induced pluripotent stem cells from human blood. *Blood*. 2009;113:5476-5479
24. Cheng L, Lei Q, Yin C, Wang H-Y, Jin K, Xiang M. Generation of urine cell-derived non-integrative human ipscs and inscs: A step-by-step optimized protocol. *Frontiers in Molecular Neuroscience*. 2017;10
25. Kim K, Doi A, Wen B, Ng K, Zhao R, Cahan P, Kim J, Aryee MJ, Ji H, Ehrlich LIR, Yabuuchi A, Takeuchi A, Cunniff KC, Hongguang H, McKinney-Freeman S, Naveiras O, Yoon TJ, Irizarry RA, Jung N, Seita J, Hanna J, Murakami P, Jaenisch R, Weissleder R, Orkin SH, Weissman IL, Feinberg AP, Daley GQ. Epigenetic memory in induced pluripotent stem cells. *Nature*. 2010;467:285-290

26. Chin MH, Mason MJ, Xie W, Volinia S, Singer M, Peterson C, Ambartsumyan G, Aimiuwu O, Richter L, Zhang J, Khvorostov I, Ott V, Grunstein M, Lavon N, Benvenisty N, Croce CM, Clark AT, Baxter T, Pyle AD, Teitell MA, Pelegrini M, Plath K, Lowry WE. Induced pluripotent stem cells and embryonic stem cells are distinguished by gene expression signatures. *Cell stem cell*. 2009;5:111-123
27. Takahashi K, Tanabe K, Ohnuki M, Narita M, Ichisaka T, Tomoda K, Yamanaka S. Induction of pluripotent stem cells from adult human fibroblasts by defined factors. *Cell*. 2007;131:861-872
28. Bru T, Clarke C, McGrew MJ, Sang HM, Wilmut I, Blow JJ. Rapid induction of pluripotency genes after exposure of human somatic cells to mouse es cell extracts. *Experimental Cell Research*. 2008;314:2634-2642
29. Matoba S, Zhang Y. Somatic cell nuclear transfer reprogramming: Mechanisms and applications. *Cell stem cell*. 2018;23:471-485
30. Sparman M, Dighe V, Sritanaudomchai H, Ma H, Ramsey C, Pedersen D, Clepper L, Nighot P, Wolf D, Hennebold J, Mitalipov S. Epigenetic reprogramming by somatic cell nuclear transfer in primates. *Stem Cells*. 2009;27:1255-1264
31. No J, Choi M, Kwon D, Yoo J, Yang B, Park J, Kim D. Cell-free extract from porcine induced pluripotent stem cells can affect porcine somatic cell nuclear reprogramming. *The Journal of Reproduction and Development*. 2015;61:90-98
32. Kanherkar RR, Bhatia-Dey N, Makarev E, Csoka AB. Cellular reprogramming for understanding and treating human disease. *Frontiers in Cell and Developmental Biology*. 2014;2:67
33. Patel M, Yang S. Advances in reprogramming somatic cells to induced pluripotent stem cells. *Stem cell reviews*. 2010;6:367-380
34. Soza-Ried J, Fisher AG. Reprogramming somatic cells towards pluripotency by cellular fusion. *Current opinion in genetics & development*. 2012;22:459-465
35. Pomeranth J, Mukherjee S, Palermo A, Blau H. Reprogramming to a muscle fate by fusion recapitulates differentiation. *Journal of Cell Science*. 2009;122:1045-1053
36. Papapetrou EP, Tomishima MJ, Chambers SM, Mica Y, Reed E, Menon J, Tabar V, Mo Q, Studer L, Sadelain M. Stoichiometric and temporal requirements of oct4, sox2, klf4, and c-myc expression for efficient human ipsc induction and differentiation. *Proceedings of the National Academy of Sciences*. 2009;106:12759-12764

37. Soldner F, Hockemeyer D, Beard C, Gao Q, Bell GW, Cook EG, Hargus G, Blak A, Cooper O, Mitalipova M, Isacson O, Jaenisch R. Parkinson's disease patient-derived induced pluripotent stem cells free of viral reprogramming factors. *Cell*. 2009;136:964-977
38. Stadtfeld M, Nagaya M, Utikal J, Weir G, Hochedlinger K. Induced pluripotent stem cells generated without viral integration. *Science*. 2008;322:945-949
39. Zhou W, Freed CR. Adenoviral gene delivery can reprogram human fibroblasts to induced pluripotent stem cells. *Stem Cells*. 2009;27:2667-2674
40. Park A, Hong P, Won ST, Thibault PA, Vigant F, Oguntuyo KY, Taft JD, Lee B. Sendai virus, an rna virus with no risk of genomic integration, delivers crispr/cas9 for efficient gene editing. *Molecular therapy. Methods & clinical development*. 2016;3:16057
41. Malik N, Rao MS. A review of the methods for human ipsc derivation. *Methods in molecular biology*. 2013;997:23-33
42. Fernández-Susavila H, Mora C, Aramburu-Núñez M, Quintas-Rey R, Arias S, Collado M, López-Arias E, Sobrino T, Castillo J, Dell'Era P, Campos F. Generation and characterization of the human ipsc line idisi001-a isolated from blood cells of a cadasil patient carrying a notch3 mutation. *Stem Cell Research*. 2018;28:16-20
43. Warren L, Manos PD, Ahfeldt T, Loh YH, Li H, Lau F, Ebina W, Mandal PK, Smith ZD, Meissner A, Daley GQ, Brack AS, Collins JJ, Cowan C, Schlaeger TM, Rossi DJ. Highly efficient reprogramming to pluripotency and directed differentiation of human cells with synthetic modified mrna. *Cell stem cell*. 2010;7:618-630
44. Sandmaier SE, Telugu BP. Microrna-mediated reprogramming of somatic cells into induced pluripotent stem cells. *Methods in molecular biology*. 2015;1330:29-36
45. Anokye-Danso F, Trivedi CM, Juhr D, Gupta M, Cui Z, Tian Y, Zhang Y, Yang W, Gruber PJ, Epstein JA, Morrisey EE. Highly efficient mirna-mediated reprogramming of mouse and human somatic cells to pluripotency. *Cell stem cell*. 2011;8:376-388
46. Anokye-Danso F, Snitow M, Morrisey EE. How microrna facilitate reprogramming to pluripotency. *Journal of Cell Science*. 2012;125:4179-4187

47. Yu J, Hu K, Smuga-Otto K, Tian S, Stewart R, Slukvin, II, Thomson JA. Human induced pluripotent stem cells free of vector and transgene sequences. *Science*. 2009;324:797-801
48. Okita K, Matsumura Y, Sato Y, Okada A, Morizane A, Okamoto S, Hong H, Nakagawa M, Tanabe K, Tezuka K, Shibata T, Kunisada T, Takahashi M, Takahashi J, Saji H, Yamanaka S. A more efficient method to generate integration-free human ips cells. *Nature methods*. 2011;8:409-412
49. Shi Y, Do JT, Desponts C, Hahm HS, Scholer HR, Ding S. A combined chemical and genetic approach for the generation of induced pluripotent stem cells. *Cell stem cell*. 2008;2:525-528
50. Lyssiotis CA, Foreman RK, Staerk J, Garcia M, Mathur D, Markoulaki S, Hanna J, Lairson LL, Charette BD, Bouchez LC, Bollong M, Kunick C, Brinker A, Cho CY, Schultz PG, Jaenisch R. Reprogramming of murine fibroblasts to induced pluripotent stem cells with chemical complementation of klf4. *Proceedings of the National Academy of Sciences*. 2009;106:8912-8917
51. Ichida JK, Blanchard J, Lam K, Son EY, Chung JE, Egli D, Loh KM, Carter AC, Di Giorgio FP, Koszka K, Huangfu D, Akutsu H, Liu DR, Rubin LL, Eggan K. A small-molecule inhibitor of tgf-beta signaling replaces sox2 in reprogramming by inducing nanog. *Cell stem cell*. 2009;5:491-503
52. O'Doherty R, Greiser U, Wang W. Nonviral methods for inducing pluripotency to cells. *BioMed research international*. 2013;2013:705902
53. Gonzalez F, Huangfu D. Mechanisms underlying the formation of induced pluripotent stem cells. *Wiley interdisciplinary reviews. Developmental biology*. 2016;5:39-65
54. Stadtfeld M, Maherali N, Breault DT, Hochedlinger K. Defining molecular cornerstones during fibroblast to ips cell reprogramming in mouse. *Cell stem cell*. 2008;2:230-240
55. Brambrink T, Foreman R, Welstead G, Lengner C, Wernig M, Suh H, Jaenisch R. Sequential expression of pluripotency markers during direct reprogramming of mouse somatic cells. *Cell stem cell*. 2008;2:151-159
56. Buganim Y, Faddah DA, Jaenisch R. Mechanisms and models of somatic cell reprogramming. *Nature reviews. Genetics*. 2013;14:427-439
57. Soufi A, Donahue G, Zaret KS. Facilitators and impediments of the pluripotency reprogramming factors' initial engagement with the genome. *Cell*. 2012;151:994-1004
58. Nakagawa M, Koyanagi M, Tanabe K, Takahashi K, Ichisaka T, Aoi T, Okita K, Mochiduki Y, Takizawa N, Yamanaka S. Generation of induced

pluripotent stem cells without myc from mouse and human fibroblasts. *Nature Biotechnology*. 2008;26:101-106

59. Yamanaka S. Elite and stochastic models for induced pluripotent stem cell generation. *Nature*. 2009;460:49-52
60. Toma J, Akhavan M, Fernandes K, Barnabé-Heider F, Sadikot A, Kaplan D, Miller F. Isolation of multipotent adult stem cells from the dermis of mammalian skin. *Nature cell biology*. 2001;3:778-784
61. Hanna J, Markoulaki S, Schorderet P, Carey BW, Beard C, Wernig M, Creyghton MP, Steine EJ, Cassady JP, Foreman R, Lengner CJ, Dausman JA, Jaenisch R. Direct reprogramming of terminally differentiated mature b lymphocytes to pluripotency. *Cell*. 2008;133:250-264
62. Yunusova A, Fishman V, Vasiliev G, Battulin N. Deterministic versus stochastic model of reprogramming: New evidence from cellular barcoding technique. *Open biology*. 2017;7:160311
63. Guo S, Zi X, Schulz VP, Cheng J, Zhong M, Koochaki SH, Megyola CM, Pan X, Heydari K, Weissman SM, Gallagher PG, Krause DS, Fan R, Lu J. Nonstochastic reprogramming from a privileged somatic cell state. *Cell*. 2014;156:649-662
64. Di Stefano B, Collombet S, Jakobsen JS, Wierer M, Sardina JL, Lackner A, Stadhouders R, Segura-Morales C, Francesconi M, Limone F, Mann M, Porse B, Thieffry D, Graf T. C/ebpalpha creates elite cells for ipsc reprogramming by upregulating klf4 and increasing the levels of lsd1 and brd4. *Nature cell biology*. 2016;18:371-381
65. Hanna J, Saha K, Pando B, van Zon J, Lengner CJ, Creyghton MP, van Oudenaarden A, Jaenisch R. Direct cell reprogramming is a stochastic process amenable to acceleration. *Nature*. 2009;462:595-601
66. Buganim Y, Faddah DA, Cheng AW, Itskovich E, Markoulaki S, Ganz K, Klemm SL, van Oudenaarden A, Jaenisch R. Single-cell expression analyses during cellular reprogramming reveal an early stochastic and a late hierarchic phase. *Cell*. 2012;150:1209-1222
67. Passier R, Orlova V, Mummery C. Complex tissue and disease modeling using hipscs. *Cell stem cell*. 2016;18:309-321
68. DiMasi JA, Grabowski HG, Hansen RW. Innovation in the pharmaceutical industry: New estimates of r&d costs. *Journal of health economics*. 2016;47:20-33
69. Fermini B, Coyne ST, Coyne KP. Clinical trials in a dish: A perspective on the coming revolution in drug development. *SLAS discovery : advancing life sciences R & D*. 2018;23:765-776

70. Bright J, Hussain S, Dang V, Wright S, Cooper B, Byun T, Ramos C, Singh A, Parry G, Stagliano N, Griswold-Prenner I. Human secreted tau increases amyloid-beta production. *Neurobiology Aging*. 2015;36:693-709
71. Naryshkin NA, Weetall M, Dakka A, Narasimhan J, Zhao X, Feng Z, Ling KK, Karp GM, Qi H, Woll MG, Chen G, Zhang N, Gabbeta V, Vazirani P, Bhattacharyya A, Furia B, Risher N, Sheedy J, Kong R, Ma J, Turpoff A, Lee CS, Zhang X, Moon YC, Trifillis P, Welch EM, Colacino JM, Babiak J, Almstead NG, Peltz SW, Eng LA, Chen KS, Mull JL, Lynes MS, Rubin LL, Fontoura P, Santarelli L, Haehnke D, McCarthy KD, Schmucki R, Ebeling M, Sivaramakrishnan M, Ko CP, Paushkin SV, Ratni H, Gerlach I, Ghosh A, Metzger F. Motor neuron disease. Smn2 splicing modifiers improve motor function and longevity in mice with spinal muscular atrophy. *Science*. 2014;345:688-693
72. McNeish J, Gardner JP, Wainger BJ, Woolf CJ, Eggan K. From dish to bedside: Lessons learned while translating findings from a stem cell model of disease to a clinical trial. *Cell stem cell*. 2015;17:8-10
73. Wu SM, Hochedlinger K. Harnessing the potential of induced pluripotent stem cells for regenerative medicine. *Nature cell biology*. 2011;13:497-505
74. Nori S, Okada Y, Yasuda A, Tsuji O, Takahashi Y, Kobayashi Y, Fujiyoshi K, Koike M, Uchiyama Y, Ikeda E, Toyama Y, Yamanaka S, Nakamura M, Okano H. Grafted human-induced pluripotent stem-cell-derived neurospheres promote motor functional recovery after spinal cord injury in mice. *Proceedings of the National Academy of Sciences*. 2011;108:16825-16830
75. Tan Q, Lui PP, Rui YF, Wong YM. Comparison of potentials of stem cells isolated from tendon and bone marrow for musculoskeletal tissue engineering. *Tissue engineering. Part A*. 2012;18:840-851
76. Khan IF, Hirata RK, Wang PR, Li Y, Kho J, Nelson A, Huo Y, Zavaljevski M, Ware C, Russell DW. Engineering of human pluripotent stem cells by aav-mediated gene targeting. *Molecular therapy : the journal of the American Society of Gene Therapy*. 2010;18:1192-1199
77. Hockemeyer D, Wang H, Kiani S, Lai CS, Gao Q, Cassady JP, Cost GJ, Zhang L, Santiago Y, Miller JC, Zeitler B, Cherone JM, Meng X, Hinkley SJ, Rebar EJ, Gregory PD, Urnov FD, Jaenisch R. Genetic engineering of human pluripotent cells using tale nucleases. *Nature Biotechnology*. 2011;29:731-734

78. Hockemeyer D, Soldner F, Beard C, Gao Q, Mitalipova M, DeKelver RC, Katibah GE, Amora R, Boydston EA, Zeitler B, Meng X, Miller JC, Zhang L, Rebar EJ, Gregory PD, Urnov FD, Jaenisch R. Efficient targeting of expressed and silent genes in human escs and ipscs using zinc-finger nucleases. *Nature Biotechnology*. 2009;27:851-857
79. Zheng YL. Some ethical concerns about human induced pluripotent stem cells. *Science and engineering ethics*. 2016;22:1277-1284
80. Marti M, Mulero L, Pardo C, Morera C, Carrio M, Laricchia-Robbio L, Esteban CR, Izpisua Belmonte JC. Characterization of pluripotent stem cells. *Nature protocols*. 2013;8:223-253
81. Lister R, Pelizzola M, Kida YS, Hawkins RD, Nery JR, Hon G, Antosiewicz-Bourget J, O'Malley R, Castanon R, Klugman S, Downes M, Yu R, Stewart R, Ren B, Thomson JA, Evans RM, Ecker JR. Hotspots of aberrant epigenomic reprogramming in human induced pluripotent stem cells. *Nature*. 2011;471:68-73
82. Laurent LC, Ulitsky I, Slavin I, Tran H, Schork A, Morey R, Lynch C, Harness JV, Lee S, Barrero MJ, Ku S, Martynova M, Semechkin R, Galat V, Gottesfeld J, Izpisua Belmonte JC, Murry C, Keirstead HS, Park HS, Schmidt U, Laslett AL, Muller FJ, Nievergelt CM, Shamir R, Loring JF. Dynamic changes in the copy number of pluripotency and cell proliferation genes in human escs and ipscs during reprogramming and time in culture. *Cell stem cell*. 2011;8:106-118
83. Okita K, Ichisaka T, Yamanaka S. Generation of germline-competent induced pluripotent stem cells. *Nature*. 2007;448:313-317
84. Shaw R. *Bioethics beyond altruism: Donating and transforming human biological materials* Springer; 2017.
85. Watt FM, Driskell RR. The therapeutic potential of stem cells. *Philosophical transactions of the Royal Society of London. Series B, Biological sciences*. 2010;365:155-163
86. Bilic J, Izpisua Belmonte JC. Concise review: Induced pluripotent stem cells versus embryonic stem cells: Close enough or yet too far apart? *Stem Cells*. 2012;30:33-41
87. Halevy T, Urbach A. Comparing esc and ipsc-based models for human genetic disorders. *Journal of clinical medicine*. 2014;3:1146-1162
88. Israel MA, Yuan SH, Bardy C, Reyna SM, Mu Y, Herrera C, Hefferan MP, Van Gorp S, Nazor KL, Boscolo FS, Carson CT, Laurent LC, Marsala M, Gage FH, Remes AM, Koo EH, Goldstein LSB. Probing sporadic and familial

alzheimer's disease using induced pluripotent stem cells. *Nature*. 2012;482:216-220

89. Kondo T, Asai M, Tsukita K, Kutoku Y, Ohsawa Y, Sunada Y, Imamura K, Egawa N, Yahata N, Okita K, Takahashi K, Asaka I, Aoi T, Watanabe A, Watanabe K, Kadoya C, Nakano R, Watanabe D, Maruyama K, Hori O, Hibino S, Choshi T, Nakahata T, Hioki H, Kaneko T, Naitoh M, Yoshikawa K, Yamawaki S, Suzuki S, Hata R, Ueno S-i, Seki T, Kobayashi K, Toda T, Murakami K, Irie K, Klein William L, Mori H, Asada T, Takahashi R, Iwata N, Yamanaka S, Inoue H. Modeling alzheimer's disease with ipscs reveals stress phenotypes associated with intracellular aβ and differential drug responsiveness. *Cell stem cell*. 2013;12:487-496
90. Swistowski A, Peng J, Liu Q, Mali P, Rao MS, Cheng L, Zeng X. Efficient generation of functional dopaminergic neurons from human induced pluripotent stem cells under defined conditions. *Stem Cells*. 2010;28:1893-1904
91. Kikuchi T, Morizane A, Doi D, Magotani H, Onoe H, Hayashi T, Mizuma H, Takara S, Takahashi R, Inoue H, Morita S, Yamamoto M, Okita K, Nakagawa M, Parmar M, Takahashi J. Human ips cell-derived dopaminergic neurons function in a primate parkinson's disease model. *Nature*. 2017;548:592-596
92. Lee S, Huang EJ. Modeling als and ftd with ipsc-derived neurons. *Brain Research*. 2017;1656:88-97
93. Ling C, Liu Z, Song M, Zhang W, Wang S, Liu X, Ma S, Sun S, Fu L, Chu Q, Belmonte JCI, Wang Z, Qu J, Yuan Y, Liu GH. Modeling cadasil vascular pathologies with patient-derived induced pluripotent stem cells. *Protein & cell*. 2019;10:249-271
94. Feigin VL, Norrving B, Mensah GA. Global burden of stroke. *Circulation Research*. 2017;120:439-448
95. Ramos-Cabrer P, Campos F, Sobrino T, Castillo J. Targeting the ischemic penumbra. *Stroke*. 2010;42:S7-S11
96. Thiebaut AM, Gauberti M, Ali C, Martinez De Lizarrondo S, Vivien D, Yepes M, Roussel BD. The role of plasminogen activators in stroke treatment: Fibrinolysis and beyond. *The Lancet Neurology*. 2018;17:1121-1132
97. Chen X, Wang K. The fate of medications evaluated for ischemic stroke pharmacotherapy over the period 1995–2015. *Acta Pharmaceutica Sinica B*. 2016;6:522-530
98. Landis SC, Amara SG, Asadullah K, Austin CP, Blumenstein R, Bradley EW, Crystal RG, Darnell RB, Ferrante RJ, Fillit H, Finkelstein R, Fisher M,

Gendelman HE, Golub RM, Goudreau JL, Gross RA, Gubitz AK, Hesterlee SE, Howells DW, Huguenard J, Kelner K, Koroshetz W, Krainc D, Lazic SE, Levine MS, Macleod MR, McCall JM, Moxley Iii RT, Narasimhan K, Noble LJ, Perrin S, Porter JD, Steward O, Unger E, Utz U, Silberberg SD. A call for transparent reporting to optimize the predictive value of preclinical research. *Nature*. 2012;490:187-191

99. Chambers SM, Fasano CA, Papapetrou EP, Tomishima M, Sadelain M, Studer L. Highly efficient neural conversion of human es and ips cells by dual inhibition of smad signaling. *Nature Biotechnology*. 2009;27:275-280
100. Dash Biraja C, Jiang Z, Suh C, Qyang Y. Induced pluripotent stem cell-derived vascular smooth muscle cells: Methods and application. *Biochemical Journal*. 2015;465:185-194
101. Harding A, Cortez-Toledo E, Magner NL, Beegle JR, Coleal-Bergum DP, Hao D, Wang A, Nolta JA, Zhou P. Highly efficient differentiation of endothelial cells from pluripotent stem cells requires the mapk and the pi3k pathways. *Stem Cells*. 2017;35:909-919
102. Bang OY, Kim EH, Cha JM, Moon GJ. Adult stem cell therapy for stroke: Challenges and progress. *Journal of Stroke*. 2016;18:256-266
103. Dihné M, Hartung H-P, Seitz RJ. Restoring neuronal function after stroke by cell replacement. *Stroke*. 2011;42:2342-2350
104. Rosenblum S, Wang N, Smith TN, Pendharkar AV, Chua JY, Birk H, Guzman R. Timing of intra-arterial neural stem cell transplantation after hypoxia–ischemia influences cell engraftment, survival, and differentiation. *Stroke*. 2012;43:1624-1631
105. Lee AS, Tang C, Rao MS, Weissman IL, Wu JC. Tumorigenicity as a clinical hurdle for pluripotent stem cell therapies. *Nature Medicine*. 2013;19:998-1004
106. Chan HH, Wathen CA, Ni M, Zhuo S. Stem cell therapies for ischemic stroke: Current animal models, clinical trials and biomaterials. *RSC Advances*. 2017;7:18668-18680
107. Darsalia V, Kallur T, Kokaia Z. Survival, migration and neuronal differentiation of human fetal striatal and cortical neural stem cells grafted in stroke-damaged rat striatum. *European Journal of Neuroscience*. 2007;26:605-614
108. Kelly S, Bliss TM, Shah AK, Sun GH, Ma M, Foo WC, Masel J, Yenari MA, Weissman IL, Uchida N, Palmer T, Steinberg GK. Transplanted human fetal neural stem cells survive, migrate, and differentiate in ischemic rat

cerebral cortex. *Proceedings of the National Academy of Sciences*. 2004;101:11839-11844

109. Fischer UM, Harting MT, Jimenez F, Monzon-Posadas WO, Xue H, Savitz SI, Laine GA, Cox CS. Pulmonary passage is a major obstacle for intravenous stem cell delivery: The pulmonary first-pass effect. *Stem Cells and Development*. 2009;18:683-692
110. Eggenhofer E, Benseler V, Kroemer A, Popp FC, Geissler EK, Schlitt HJ, Baan CC, Dahlke MH, Hoogduijn MJ. Mesenchymal stem cells are short-lived and do not migrate beyond the lungs after intravenous infusion. *Frontiers in Immunology.* 2012;3
111. Ezquer F, Morales P, Quintanilla ME, Santapau D, Lespay-Rebolledo C, Ezquer M, Herrera-Marschitz M, Israel Y. Intravenous administration of anti-inflammatory mesenchymal stem cell spheroids reduces chronic alcohol intake and abolishes binge-drinking. *Scientific Reports.* 2018;8
112. Acosta SA, Tajiri N, Hoover J, Kaneko Y, Borlongan CV. Intravenous bone marrow stem cell grafts preferentially migrate to spleen and abrogate chronic inflammation in stroke. *Stroke*. 2015;46:2616-2627
113. Argibay B, Trekker J, Himmelreich U, Beiras A, Topete A, Taboada P, Pérez-Mato M, Vieites-Prado A, Iglesias-Rey R, Rivas J, Planas AM, Sobrino T, Castillo J, Campos F. Intraarterial route increases the risk of cerebral lesions after mesenchymal cell administration in animal model of ischemia. *Scientific Reports*. 2017;7
114. Li L, Jiang Q, Ding G, Zhang L, Zhang ZG, Li Q, Panda S, Lu M, Ewing JR, Chopp M. Effects of administration route on migration and distribution of neural progenitor cells transplanted into rats with focal cerebral ischemia, an mri study. *Journal of Cerebral Blood Flow & Metabolism*. 2009;30:653-662
115. Yang B, Migliati E, Parsha K, Schaar K, Xi X, Aronowski J, Savitz SI. Intra-arterial delivery is not superior to intravenous delivery of autologous bone marrow mononuclear cells in acute ischemic stroke. *Stroke*. 2013;44:3463-3472
116. Vasconcelos-dos-Santos A, Rosado-de-Castro PH, Lopes de Souza SA, da Costa Silva J, Ramos AB, Rodriguez de Freitas G, Barbosa da Fonseca LM, Gutfilen B, Mendez-Otero R. Intravenous and intra-arterial administration of bone marrow mononuclear cells after focal cerebral ischemia: Is there a difference in biodistribution and efficacy? *Stem Cell Research*. 2012;9:1-8

117. Hosoda T, Yavagal DR, Lin B, Raval AP, Garza PS, Dong C, Zhao W, Rangel EB, McNiece I, Rundek T, Sacco RL, Perez-Pinzon M, Hare JM. Efficacy and dose-dependent safety of intra-arterial delivery of mesenchymal stem cells in a rodent stroke model. *PLoS ONE*. 2014;9:e93735
118. Oki K, Tatarishvili J, Wood J, Koch P, Wattananit S, Mine Y, Monni E, Tornero D, Ahlenius H, Ladewig J, Brüstle O, Lindvall O, Kokaia Z. Human-induced pluripotent stem cells form functional neurons and improve recovery after grafting in stroke-damaged brain. *Stem Cells*. 2012;30:1120-1133
119. Hofstetter CP, Schwarz EJ, Hess D, Widenfalk J, El Manira A, Prockop DJ, Olson L. Marrow stromal cells form guiding strands in the injured spinal cord and promote recovery. *Proceedings of the National Academy of Sciences*. 2002;99:2199-2204
120. Park JW, Ku SH, Moon HH, Lee M, Choi D, Yang J, Huh YM, Jeong JH, Park TG, Mok H, Kim SH. Cross-linked iron oxide nanoparticles for therapeutic engineering and in vivo monitoring of mesenchymal stem cells in cerebral ischemia model. *Macromolecular bioscience*. 2014;14:380-389
121. Yu X, Chen D, Zhang Y, Wu X, Huang Z, Zhou H, Zhang Y, Zhang Z. Overexpression of cxcr4 in mesenchymal stem cells promotes migration, neuroprotection and angiogenesis in a rat model of stroke. *Journal of the Neurological Science*. 2012;316:141-149
122. Modo M, Beech JS, Meade TJ, Williams SCR, Price J. A chronic 1 year assessment of mri contrast agent-labelled neural stem cell transplants in stroke. *Neuroimage*. 2009;47:T133-T142
123. Bible E, Dell'Acqua F, Solanky B, Balducci A, Crapo PM, Badylak SF, Ahrens ET, Modo M. Non-invasive imaging of transplanted human neural stem cells and ecm scaffold remodeling in the stroke-damaged rat brain by 19f- and diffusion-mri. *Biomaterials*. 2012;33:2858-2871
124. Nicholls FJ, Rotz MW, Ghuman H, MacRenaris KW, Meade TJ, Modo M. DNA–gadolinium–gold nanoparticles for in vivo t1 mr imaging of transplanted human neural stem cells. *Biomaterials*. 2016;77:291-306
125. Caplan AI. Adult mesenchymal stem cells for tissue engineering versus regenerative medicine. *Journal of Cellular Physiology*. 2007;213:341-347
126. Ullah I, Subbarao Raghavendra B, Rho Gyu J. Human mesenchymal stem cells - current trends and future prospective. *Bioscience Reports*. 2015;35:1-18
127. Sobrino T, Arias S, Pérez-Mato M, Agulla J, Brea D, Rodríguez-Yáñez M, Castillo J. Cd34+progenitor cells likely are involved in the good functional

recovery after intracerebral hemorrhage in humans. *Journal of Neuroscience Research*. 2011;89:979-985

128. Chen J, Zhang ZG, Li Y, Wang L, Xu YX, Gautam SC, Lu M, Zhu Z, Chopp M. Intravenous administration of human bone marrow stromal cells induces angiogenesis in the ischemic boundary zone after stroke in rats. *Circulation Research*. 2003;92:692-699
129. Seung-Wan Y, Sung-Soo K, Soo-Yeol L, Hey-Sun L, Hyun-Soo K, Young-Don L, Haeyoung S-K. Mesenchimal stem cells promote proliferation of endogenous neural stem cells and survival of newborn cells in a rat stroke model. *Experimental and Molecular Medicine*. 2008;40:387-397
130. Andrews EM, Tsai SY, Johnson SC, Farrer JR, Wagner JP, Kopen GC, Kartje GL. Human adult bone marrow-derived somatic cell therapy results in functional recovery and axonal plasticity following stroke in the rat. *Experimental Neurology*. 2008;211:588-592
131. Zhang Y, Chopp M, Meng Y, Katakowski M, Xin H, Mahmood A, Xiong Y. Effect of exosomes derived from multipluripotent mesenchymal stromal cells on functional recovery and neurovascular plasticity in rats after traumatic brain injury. *Journal of Neurosurgery*. 2015;122:856-867
132. Zhang B, Yin Y, Lai RC, Tan SS, Choo ABH, Lim SK. Mesenchymal stem cells secrete immunologically active exosomes. *Stem Cells and Development*. 2014;23:1233-1244
133. Xin H, Li Y, Cui Y, Yang JJ, Zhang ZG, Chopp M. Systemic administration of exosomes released from mesenchymal stromal cells promote functional recovery and neurovascular plasticity after stroke in rats. *Journal of Cerebral Blood Flow & Metabolism*. 2013;33:1711-1715
134. Laso-García F, Diekhorst L, Gómez-de Frutos MC, Otero-Ortega L, Fuentes B, Ruiz-Ares G, Díez-Tejedor E, Gutiérrez-Fernández M. Cell-based therapies for stroke: Promising solution or dead end? Mesenchymal stem cells and comorbidities in preclinical stroke research. *Frontiers in Neurology*. 2019;10
135. Gutierrez-Fernandez M, Rodriguez-Frutos B, Ramos-Cejudo J, Teresa Vallejo-Cremades M, Fuentes B, Cerdan S, Diez-Tejedor E. Effects of intravenous administration of allogenic bone marrow- and adipose tissue-derived mesenchymal stem cells on functional recovery and brain repair markers in experimental ischemic stroke. *Stem Cell Research Therapy*. 2013;4:11
136. Chen K, Chen C, Wallace C, Yuen C, Kao G, Chen Y, Shao P, Chen Y, Chai H, Lin K, Liu C, Chang H, Lee M, Yip H. Intravenous administration of

xenogenic adipose-derived mesenchymal stem cells (admsc) and admsc-derived exosomes markedly reduced brain infarct volume and preserved neurological function in rat after acute ischemic stroke. *Oncotarget*. 2016;7:74537-74556

137. Ra JC, Shin IS, Kim SH, Kang SK, Kang BC, Lee HY, Kim YJ, Jo JY, Yoon EJ, Choi HJ, Kwon E. Safety of intravenous infusion of human adipose tissue-derived mesenchymal stem cells in animals and humans. *Stem Cells and Development*. 2011;20:1297-1308
138. Wang S-P, Wang Z-H, Peng D-Y, Li S-M, Wang H, Wang X-H. Therapeutic effect of mesenchymal stem cells in rats with intracerebral hemorrhage: Reduced apoptosis and enhanced neuroprotection. *Molecular Medicine Reports*. 2012;6:848-854
139. Vaquero J, Otero L, Bonilla C, Aguayo C, Rico MA, Rodriguez A, Zurita M. Cell therapy with bone marrow stromal cells after intracerebral hemorrhage: Impact of platelet-rich plasma scaffolds. *Cytotherapy*. 2013;15:33-43
140. Nakazaki M, Sasaki M, Kataoka-Sasaki Y, Oka S, Namioka T, Namioka A, Onodera R, Suzuki J, Sasaki Y, Nagahama H, Mikami T, Wanibuchi M, Kocsis JD, Honmou O. Intravenous infusion of mesenchymal stem cells inhibits intracranial hemorrhage after recombinant tissue plasminogen activator therapy for transient middle cerebral artery occlusion in rats. *Journal of Neurosurgery*. 2017;127:917-926
141. Pérez-Mato M, Iglesias-Rey R, Vieites-Prado A, Dopico-López A, Argibay B, Fernández-Susavila H, da Silva-Candal A, Pérez-Díaz A, Correa-Paz C, Günther A, Ávila-Gómez P, Isabel Loza M, Baumann A, Castillo J, Sobrino T, Campos F. Blood glutamate eaat2-cell grabbing therapy in cerebral ischemia. *EBioMedicine*. 2018
142. Bond Allison M, Ming G-l, Song H. Adult mammalian neural stem cells and neurogenesis: Five decades later. *Cell stem cell*. 2015;17:385-395
143. Jin K, Wang X, Xie L, Mao XO, Zhu W, Wang Y, Shen J, Mao Y, Banwait S, Greenberg DA. Evidence for stroke-induced neurogenesis in the human brain. *Proceedings of the National Academy of Sciences*. 2006;103:13198-13202
144. Thored P, Arvidsson A, Cacci E, Ahlenius H, Kallur T, Darsalia V, Ekdahl CT, Kokaia Z, Lindvall O. Persistent production of neurons from adult brain stem cells during recovery after stroke. *Stem Cells*. 2006;24:739-747
145. Schaapsmeerders P, Maaijwee NAM, van Dijk EJ, Rutten-Jacobs LCA, Arntz RM, Schoonderwaldt HC, Dorresteijn LDA, Kessels RPC, de Leeuw F-E.

Long-term cognitive impairment after first-ever ischemic stroke in young adults. *Stroke*. 2013;44:1621-1628

146. Bacigaluppi M, Russo GL, Peruzzotti-Jametti L, Rossi S, Sandrone S, Butti E, De Ceglia R, Bergamaschi A, Motta C, Gallizioli M, Studer V, Colombo E, Farina C, Comi G, Politi LS, Muzio L, Villani C, Invernizzi RW, Hermann DM, Centonze D, Martino G. Neural stem cell transplantation induces stroke recovery by upregulating glutamate transporter glt-1 in astrocytes. *Journal of Neuroscience*. 2016;36:10529-10544
147. Bacigaluppi M, Pluchino S, Jametti LP, Kilic E, Kilic Ü, Salani G, Brambilla E, West MJ, Comi G, Martino G, Hermann DM. Delayed post-ischaemic neuroprotection following systemic neural stem cell transplantation involves multiple mechanisms. *Brain*. 2009;132:2239-2251
148. Eckert A, Huang L, Gonzalez R, Kim H-S, Hamblin MH, Lee J-P. Bystander effect fuels human induced pluripotent stem cell-derived neural stem cells to quickly attenuate early stage neurological deficits after stroke. *STEM CELLS Translational Medicine*. 2015;4:841-851
149. Baker EW, Platt SR, Lau VW, Grace HE, Holmes SP, Wang L, Duberstein KJ, Howerth EW, Kinder HA, Stice SL, Hess DC, Mao H, West FD. Induced pluripotent stem cell-derived neural stem cell therapy enhances recovery in an ischemic stroke pig model. *Scientific Reports*. 2017;7
150. Sakata H, Niizuma K, Wakai T, Narasimhan P, Maier CM, Chan PH. Neural stem cells genetically modified to overexpress cu/zn-superoxide dismutase enhance amelioration of ischemic stroke in mice. *Stroke*. 2012;43:2423-2429
151. Wakai T, Sakata H, Narasimhan P, Yoshioka H, Kinouchi H, Chan PH. Transplantation of neural stem cells that overexpress sod1 enhances amelioration of intracerebral hemorrhage in mice. *Journal of Cerebral Blood Flow & Metabolism*. 2013;34:441-449
152. Sakata H, Niizuma K, Yoshioka H, Kim GS, Jung JE, Katsu M, Narasimhan P, Maier CM, Nishiyama Y, Chan PH. Minocycline-preconditioned neural stem cells enhance neuroprotection after ischemic stroke in rats. *Journal of Neuroscience*. 2012;32:3462-3473
153. Theus MH, Wei L, Cui L, Francis K, Hu X, Keogh C, Yu SP. In vitro hypoxic preconditioning of embryonic stem cells as a strategy of promoting cell survival and functional benefits after transplantation into the ischemic rat brain. *Experimental Neurology*. 2008;210:656-670

154. Zhong J, Chan A, Morad L, Kornblum HI, Guoping F, Carmichael ST. Hydrogel matrix to support stem cell survival after brain transplantation in stroke. *Neurorehabilitation and Neural Repair*. 2010;24:636-644
155. Jensen MB, Yan H, Krishnaney-Davison R, Al Sawaf A, Zhang S-C. Survival and differentiation of transplanted neural stem cells derived from human induced pluripotent stem cells in a rat stroke model. *Journal of Stroke and Cerebrovascular Diseases*. 2013;22:304-308
156. Lee HJ, Kim KS, Kim EJ, Choi HB, Lee KH, Park IH, Ko Y, Jeong SW, Kim SU. Brain transplantation of immortalized human neural stem cells promotes functional recovery in mouse intracerebral hemorrhage stroke model. *Stem Cells*. 2007;25:1204-1212
157. Jeong S-W, Chu K, Jung K-H, Kim SU, Kim M, Roh J-K. Human neural stem cell transplantation promotes functional recovery in rats with experimental intracerebral hemorrhage. *Stroke*. 2003;34:2258-2263
158. Jiang M, Lv L, Ji H, Yang X, Zhu W, Cai L, Gu X, Chai C, Huang S, Sun J, Dong Q. Induction of pluripotent stem cells transplantation therapy for ischemic stroke. *Molecular and Cellular Biochemistry*. 2011;354:67-75
159. Chen S-J, Chang C-M, Tsai S-K, Chang Y-L, Chou S-J, Huang S-S, Tai L-K, Chen Y-C, Ku H-H, Li H-Y, Chiou S-H. Functional improvement of focal cerebral ischemia injury by subdural transplantation of induced pluripotent stem cells with fibrin glue. *Stem Cells and Development*. 2010;19:1757-1767
160. Tornero D, Wattananit S, Grønning Madsen M, Koch P, Wood J, Tatarishvili J, Mine Y, Ge R, Monni E, Devaraju K, Hevner RF, Brüstle O, Lindvall O, Kokaia Z. Human induced pluripotent stem cell-derived cortical neurons integrate in stroke-injured cortex and improve functional recovery. *Brain*. 2013;136:3561-3577
161. Arumugam TV, Qin J, Ma X, Qi H, Song B, Wang Y, Wen X, Wang QM, Sun S, Li Y, Zhang R, Liu X, Hou H, Gong G, Xu Y. Transplantation of induced pluripotent stem cells alleviates cerebral inflammation and neural damage in hemorrhagic stroke. *PLoS ONE*. 2015;10:e0129881
162. Buhnemann C, Scholz A, Bernreuther C, Malik CY, Braun H, Schachner M, Reymann KG, Dihne M. Neuronal differentiation of transplanted embryonic stem cell-derived precursors in stroke lesions of adult rats. *Brain*. 2006;129:3238-3248
163. Takagi Y, Nishimura M, Morizane A, Takahashi J, Nozaki K, Hayashi J, N H. Survival and differentiation of neural progenitor cells derived from

embryonic stem cells and transplanted into ischemic brain. *Journal of Neurosurgery*. 2005;103:304-310

164. Lee MO, Moon SH, Jeong HC, Yi JY, Lee TH, Shim SH, Rhee YH, Lee SH, Oh SJ, Lee MY, Han MJ, Cho YS, Chung HM, Kim KS, Cha HJ. Inhibition of pluripotent stem cell-derived teratoma formation by small molecules. *Proceedings of the National Academy of Sciences*. 2013;110:E3281-E3290
165. Joutel A, Faraci FM. Cerebral small vessel disease: Insights and opportunities from mouse models of collagen iv-related small vessel disease and cerebral autosomal dominant arteriopathy with subcortical infarcts and leukoencephalopathy. *Stroke*. 2014;45:1215-1221
166. Yao M, Hervé D, Jouvent E, Duering M, Reyes S, Godin O, Guichard JP, Dichgans M, Chabriat H. Dilated perivascular spaces in small-vessel disease: A study in cadasil. *Cerebrovascular Diseases*. 2014;37:155-163
167. Chabriat H, Joutel A, Dichgans M, Tournier-Lasserve E, Bousser M. Cadasil. *The Lancet Neurology*. 2009;8:643-653
168. Ayata C. Cadasil: Experimental insights from animal models. *Stroke*. 2010;41:S129-S134
169. Coupland K, Lendahl U, Karlström H. Role of notch3 mutations in the cerebral small vessel disease cerebral autosomal dominant arteriopathy with subcortical infarcts and leukoencephalopathy. *Stroke*. 2018;49:2793-2800
170. Joutel A, Andreux F, Gaulis S, Domenga V, Cecillon M, Battail N, Piga N, Chapon F, Godfrain C, Tournier-Lasserve E. The ectodomain of the notch3 receptor accumulates within the cerebrovasculature of cadasil patients. *Journal of Clinical Investigation*. 1999;105:597-605
171. Siebel C, Lendahl U. Notch signaling in development, tissue homeostasis, and disease. *Physiological Reviews*. 2017;97:1235-1294
172. Wang T, Baron M, Trump D. An overview of notch3 function in vascular smooth muscle cells. *Progress in Biophysics and Molecular Biology*. 2008;96:499-509
173. Tournier-Lasserve E, Iba-Zizen M, Romero N, Bousser M. Autosomal dominant syndrome with strokelike episodes and leukoencephalopathy. *Stroke*. 1991;22:1297-1302
174. Tournier-Lasserve E, Joutel A, Melki J, Weissenbach J, Lathrop G, Chabriat H, Mas J, Cabanis E, Baudrimont M, Maciazek J. Cerebral autosomal dominant arteriopathy with subcortical infarcts and leukoencephalopathy maps to chromosome 19q12. *Nature Genetics*. 1993;3:256-259

175. Joutel A, Corpechot C, Ducros A, Vahedi K, Chabriat H, Mouton P, Alamowitch S, Domenga V, Cécillion M, Maréchal E, Maciazek J, Vayssière C, Cruaud C, Cabanis E, Ruchoux M, Weissenbach J, Bach J-F, Bousser M-G, Tournier-Lasserve E. Notch3 mutations in cadasil, a hereditary adult-onset condition causing stroke and dementia. *Nature*. 1996;383:707-710
176. Di Donato I, Bianchi S, De Stefano N, Dichgans M, Dotti MT, Duering M, Jouvent E, Korczyn AD, Lesnik-Oberstein SAJ, Malandrini A, Markus HS, Pantoni L, Penco S, Rufa A, Sinanović O, Stojanov D, Federico A. Cerebral autosomal dominant arteriopathy with subcortical infarcts and leukoencephalopathy (cadasil) as a model of small vessel disease: Update on clinical, diagnostic, and management aspects. *BMC Medicine*. 2017;15
177. Keverne JS, Low WC, Ziabreva I, Court JA, Oakley AE, Kalaria RN. Cholinergic neuronal deficits in cadasil. *Stroke*. 2007;38:188-191
178. Guey S, Mawet J, Herve D, Duering M, Godin O, Jouvent E, Opherk C, Alili N, Dichgans M, Chabriat H. Prevalence and characteristics of migraine in cadasil. *Cephalalgia : an international journal of headache*. 2016;36:1038-1047
179. Opherk C. Long-term prognosis and causes of death in cadasil: A retrospective study in 411 patients. *Brain*. 2004;127:2533-2539
180. Adib-Samii P, Brice G, Martin RJ, Markus HS. Clinical spectrum of cadasil and the effect of cardiovascular risk factors on phenotype: Study in 200 consecutively recruited individuals. *Stroke*. 2010;41:630-634
181. Valenti R, Poggesi A, Pescini F, Inzitari D, Pantoni L. Psychiatric disturbances in cadasil: A brief review. *Acta neurologica Scandinavica*. 2008;118:291-295
182. Liu Z, Brunskill E, Varnum-Finney B, Zhang C, Zhang A, Jay PY, Bernstein I, Morimoto M, Kopan R. The intracellular domains of notch1 and notch2 are functionally equivalent during development and carcinogenesis. *Development*. 2015;142:2452-2463
183. Chowdhury F, Li ITS, Ngo TTM, Leslie BJ, Kim BC, Sokoloski JE, Weiland E, Wang X, Chemla YR, Lohman TM, Ha T. Defining single molecular forces required for notch activation using nano yoyo. *Nano Letters*. 2016;16:3892-3897
184. Hansson EM, Lanner F, Das D, Mutvei A, Marklund U, Ericson J, Farnebo F, Stumm G, Stenmark H, Andersson ER, Lendahl U. Control of notch-ligand endocytosis by ligand-receptor interaction. *Journal of Cell Science*. 2010;123:2931-2942

185. Conner SD. Regulation of notch signaling through intracellular transport. *International review of cell and molecular biology*. 2016;323:107-127
186. Itoh M, Kim C, Palardy G, Oda T, Jiang Y, Maust D, Yeo S, Lorick K, Wright G, Ariza-McNaughton L, Weissman A, Lewis J, Chandrasekharappa S, Chitnis A. Mind bomb is a ubiquitin ligase that is essential for efficient acivation of notch signaling by delta. *Developmental cell*. 2003;4:67-82
187. Yatim A, Benne C, Sobhian B, Laurent-Chabalier S, Deas O, Judde J-G, Lelievre J-D, Levy Y, Benkirane M. Notch1 nuclear interactome reveals key regulators of its transcriptional activity and oncogenic function. *Molecular Cell*. 2012;48:445-458
188. Kitamoto T, Takahashi K, Takimoto H, Tomizuka K, Hayasaka M, Tabira T, Hanaoka K. Functional redundancy of the notch gene family during mouse embryogenesis: Analysis of notch gene expression in notch3-deficient mice. *Biochemical and biophysical research communications*. 2005;331:1154-1162
189. Krebs LT, Xue Y, Norton CR, Sundberg JP, Beatus P, Lendahl U, Joutel A, Gridley T. Characterization of notch3-deficient mice: Normal embryonic development and absence of genetic interactions with a notch1 mutation. *Genesis*. 2003;37:139-143
190. Conlon R, Reaume A, Rossant J. Notch1 is required for the coordinate segmentation of somites. *Development*. 1995;121:1533-1545
191. Domenga V, Fardoux P, Lacombe P, Monet M, Maciazek J, Krebs L, Klonjkowski B, Berrou E, Mericskay M, Li Z, Tournier-Lasserve E, Gridley T, Joutel A. Notch3 is required for arterial identity and maturation of vascular smooth muscle cells. *Genes & Development*. 2004;18:2730-2735
192. Muiño E, Gallego-Fabrega C, Cullell N, Carrera C, Torres N, Krupinski J, Roquer J, Montaner J, Fernández-Cadenas I. Systematic review of cysteine-sparing notch3 missense mutations in patients with clinical suspicion of cadasil. *International Journal of Molecular Sciences*. 2017;18:1964
193. Kim Y, Choi E, Choi C, Kim G, Choi J, Yoo H, Kim J. Characteristics of cadasil in korea: A novel cysteine-sparing notch3 mutation. *Neurology*. 2006;66:1511-1516
194. Rutten JW, Dauwerse HG, Gravesteijn G, van Belzen MJ, van der Grond J, Polke JM, Bernal-Quiros M, Lesnik-Oberstein SAJ. Archetypal notch3 mutations frequent in public exome: Implications for cadasil. *Annals of Clinical and Translational Neurology*. 2016;3:844-853

195. Bardot B, Mok LP, Thayer T, Ahimou F, Wesley C. The notch amino terminus regulates protein levels and delta-induced clustering of drosophila notch receptors. *Experimental Cell Research*. 2005;304:202-223
196. Karlstrom H, Beatus P, Dannaeus K, Chapman G, Lendahl U, Lundkvist J. A cadasil-mutated notch 3 receptor exhibits impaired intracellular trafficking and maturation but normal ligand-induced signaling. *Proceedings of the National Academy of Sciences*. 2002;99:17119-17124
197. Peters N, Opherk C, Zacherle S, Capell A, Gempel P, Dichgans M. Cadasil-associated notch3 mutations have differential effects both on ligand binding and ligand-induced notch3 receptor signaling through rbp-jk. *Experimental Cell Research*. 2004;299:454-464
198. Duering M, Karpinska A, Rosner S, Hopfner F, Zechmeister M, Peters N, Kremmer E, Haffner C, Giese A, Dichgans M, Opherk C. Co-aggregate formation of cadasil-mutant notch3: A single-particle analysis. *Human Molecular Genetics*. 2011;20:3256-3265
199. Capone C, Cognat E, Ghezali L, Baron-Menguy C, Aubin D, Mesnard L, Stöhr H, Domenga-Denier V, Nelson MT, Joutel A. Reducing timp3 or vitronectin ameliorates disease manifestations in cadasil mice. *Annals of Neurology*. 2016;79:387-403
200. Arboleda-Velasquez J, Manent J, Lee J, Tikka S, Ospina C, Vanderburg C, Frosch M, Rodríguez-Falcón M, Villen J, Gygi S, Lopera F, Kalimo H, Moskowitz M, Ayata C, Louvi A, Artavanis-Tsakonas S. Hypomorphic notch 3 alleles link notch signaling to ischemic cerebral small-vessel disease. *Proceedings of the National Academy of Sciences*. 2011
201. Kofler NM, Cuervo H, Uh MK, Murtomaki A, Kitajewski J. Combined deficiency of notch1 and notch3 causes pericyte dysfunction, models cadasil, and results in arteriovenous malformations. *Scientific Reports*. 2015;5:16449
202. Jessen NA, Munk AS, Lundgaard I, Nedergaard M. The glymphatic system: A beginner's guide. *Neurochemical research*. 2015;40:2583-2599
203. Cumurciuc R, Guichard J, Reizine D, Gray F, Bousser M, Chabriat H. Dilation of virchow-robin spaces in cadasil. *European Journal of Neurology*. 2006;13:187-190
204. Joutel A, Vahedi K, Corpechot C, Troesch A, Chabriat H, Vayssière C, Cruaud C, Maciazek J, Weissenbach J, Bousser M-G, Bach J-F, Tournier-Lasserve E. Strong clustering and stereotyped nature of notch3 mutations in cadasil patients. *The Lancet*. 1997;350:1511-1515

205. Kleiveland C. Peripheral blood mononuclear cells. In: Verhoeckx Kea, ed. *The impact of food in bioactives on health*. Springer, Cham; 2015.
206. Leonard A, Bertero A, Powers JD, Beussman KM, Bhandari S, Regnier M, Murry CE, Sniadecki NJ. Afterload promotes maturation of human induced pluripotent stem cell derived cardiomyocytes in engineered heart tissues. *Journal of molecular and cellular cardiology*. 2018;118:147-158
207. Halaidych OV, Freund C, van den Hil F, Salvatori DCF, Riminucci M, Mummery CL, Orlova VV. Inflammatory responses and barrier function of endothelial cells derived from human induced pluripotent stem cells. *Stem cell reports*. 2018;10:1642-1656
208. Marinho PA, Chailangkarn T, Muotri AR. Systematic optimization of human pluripotent stem cells media using design of experiments. *Scientific Reports*. 2015;5:9834
209. Tamai Y, Hasegawa A, Takamori A, Sasada A, Tanosaki R, Choi I, Utsunomiya A, Maeda Y, Yamano Y, Eto T, Koh KR, Nakamae H, Suehiro Y, Kato K, Takemoto S, Okamura J, Uike N, Kannagi M. Potential contribution of a novel tax epitope-specific cd4+ t cells to graft-versus-tax effect in adult t cell leukemia patients after allogeneic hematopoietic stem cell transplantation. *Journal of immunology*. 2013;190:4382-4392
210. Mieno S, Boodhwani M, Robich MP, Clements RT, Sodha NR, Sellke FW. Effects of diabetes mellitus on vegf-induced proliferation response in bone marrow derived endothelial progenitor cells. *Journal of cardiac surgery*. 2010;25:618-625
211. Hikichi T, Wakayama S, Mizutani E, Takashima Y, Kishigami S, Van Thuan N, Ohta H, Bui HT, Nishikawa S, Wakayama T. Differentiation potential of parthenogenetic embryonic stem cells is improved by nuclear transfer. *Stem Cells*. 2007;25:46-53
212. Chen IP, Fukuda K, Fusaki N, Iida A, Hasegawa M, Lichtler A, Reichenberger EJ. Induced pluripotent stem cell reprogramming by integration-free sendai virus vectors from peripheral blood of patients with craniometaphyseal dysplasia. *Cellular reprogramming*. 2013;15:503-513
213. Seki T, Yuasa S, Oda M, Egashira T, Yae K, Kusumoto D, Nakata H, Tohyama S, Hashimoto H, Kodaira M, Okada Y, Seimiya H, Fusaki N, Hasegawa M, Fukuda K. Generation of induced pluripotent stem cells from human terminally differentiated circulating t cells. *Cell stem cell*. 2010;7:11-14

214. Zhou H, Martinez H, Sun B, Li A, Zimmer M, Katsanis N, Davis EE, Kurtzberg J, Lipnick S, Noggle S, Rao M, Chang S. Rapid and efficient generation of transgene-free ipsc from a small volume of cryopreserved blood. *Stem cell reviews*. 2015;11:652-665
215. Pettinato G, Wen X, Zhang N. Engineering strategies for the formation of embryoid bodies from human pluripotent stem cells. *Stem Cells and Development*. 2015;24:1595-1609
216. Luo J, Qin L, Kural MH, Schwan J, Li X, Bartulos O, Cong XQ, Ren Y, Gui L, Li G, Ellis MW, Li P, Kotton DN, Dardik A, Pober JS, Tellides G, Rolle M, Campbell S, Hawley RJ, Sachs DH, Niklason LE, Qyang Y. Vascular smooth muscle cells derived from inbred swine induced pluripotent stem cells for vascular tissue engineering. *Biomaterials*. 2017;147:116-132
217. Wanjare M, Kuo F, Gerecht S. Derivation and maturation of synthetic and contractile vascular smooth muscle cells from human pluripotent stem cells. *Cardiovascular research*. 2013;97:321-330
218. Joutel A, Andreux F, Gaulis S, Domenga V, Cecillon M, Battail N, Piga N, Chapon F, Godfrain C, Tournier-Lasserve E. The ectodomain of the notch3 receptor accumulates within the cerebrovasculature of cadasil patients. *Journal of Clinical Investigation*. 2000;105:597-605

USC
UNIVERSIDADE
DE SANTIAGO
DE COMPOSTELA

USC
UNIVERSIDADE
DE SANTIAGO
DE COMPOSTELA